5-9-2014

Comparison of Geophysically-derived and Surficial Sediment-based Estimates of Seismic Risk in Hartford County, Connecticut

Sarah L. C. Morton
University of Connecticut - Storrs, sarah.morton@uconn.edu

Comparison of Geophysically-derived and Surficial Sediment-based Estimates of Seismic Risk in Hartford County, Connecticut

Sarah Laura Catherine Morton

B.S. Geoscience, University of Connecticut, 2011

A Thesis

Submitted in Partial Fulfillment of the

Requirements for the Degree of

Master of Science

At the

University of Connecticut

2014

APPROVAL PAGE

Master of Science Thesis

Comparison of Geophysically-derived and Surficial Sediment-based Estimates of Seismic Risk in Hartford County, Connecticut

Presented by

Sarah Laura Catherine Morton, B.S.

Major Advisor_____
Dr. Lanbo Liu

Associate Advisor_____
Dr. John W. Lane Jr.

Associate Advisor_____
Dr. Amvrossios C. Bagtzoglou

Associate Advisor_____
Margaret A. Thomas

University of Connecticut

2014

ACKNOWLEDGEMENTS

First, I would like to thank my advisors, Dr. Lanbo Liu, Dr. John Lane Jr., and Margaret Thomas for their infinite wisdom, encouragement and enthusiasm over the last three years. Second, I'd like to acknowledge the U.S. Geological Survey and the Connecticut Department of Energy and Environmental Protection, Connecticut Geological Survey for their financial support and research assistance. To my colleagues at the U.S. Geological Survey, Office of Groundwater, Branch of Geophysics: thank you all for the continuous support and guidance; and to the Volunteers for Science, especially John McKenna and Cameron Mitchel, for their willingness to go into the field with me time and time again.

I would like to thank Dr. Rick Miller and the Kansas Geological Survey for lending me the Vertical Seismic Profiling equipment so that I could explore a new seismic technique for my thesis research. Also thank you Shelby Peterie for many days helping me analyze my collected data and for being so patient.

To Professor Kuo-Liang Wen and Dr. Chun-Hsiang "Petit" Kuo at the National Center for Research in Earthquake Engineering in Taipei, Taiwan and the National Science Foundation: thank you for the incredible opportunity to participate in the 2012 East Asia and Pacific Summer Institute graduate internship program. Although my time abroad was short, the experience and knowledge I gained was a great factor in the success of my research and aspiring an inspiration for my career in geophysics. To my adopted older siblings and band mates, my summer in Taiwan would not have been complete without you.

I would also like to thank my closest friends and their families for putting up with me and my wild obsession for rocks and soil over the last fifteen years (in alphabetical order): Will "Stretch" Borthwick, Chris Durkin, Susan Hamilla, Brian Miller, Dara Moss, Leah Pemberton,

Tom Rainey, Paul Runko, and Megan Truax; although I am fairly certain most are still convinced I have just been taking photos of rocks and playing in the mud this whole time. I also would like to thank Dave Mirakian for being my crutch and my graduate older brother throughout my thesis work. Lastly, my boyfriend, Yuri Rupert who not only put up with me and my frazzled manner, but insisted I write three pages each day before being able to see him after work; despite the fact we shared an office space.

Finally, I'd like to thank my siblings Mark, Sharon, Michael and my parents, Maureen and Steve, for helping me follow my dream of studying earthquakes and natural disasters since I was eleven and later for accepting the fact that I will never be able to sit still. It was difficult and although I continue to drive my mother crazy chasing seismic zones across the world, it has all been worth it. Thank you!

TABLE OF CONTENTS

ABSTRACT

Seismic hazard classifications developed for Hartford County, Connecticut are based primarily on surficial materials and depositional environment to estimate classifications specified by the National Earthquake Hazard Reduction Program (NEHRP). A study using near-surface seismic techniques to measure sediment shear-wave velocities (Vs) in Connecticut was conducted in support of broader seismic hazard mapping efforts undertaken by New England State Geologists. Thirty field sites in Hartford County representative of the range of mapped seismic hazard classes were chosen based on the availability of boring logs and adequate open space for geophysical surveys. Because it can be difficult to acquire multi-channel seismic data in urban areas due to unwanted noise and open space restrictions, the use of passive single-station seismometer measurements was also investigated as a compact supplement and potential alternative to long-offset multi-channel measurements.

Here the results of active-source multi-channel analysis of surface waves (MASW) and passive horizontal-to-vertical spectral ratio (HVSR) seismic methods are compared to determine shear-wave velocity profiles and seismic hazard classification based on Vs30 and the shear-wave velocity of glacial sediments throughout Hartford County, Connecticut where Vs30 refers to an averaged shear-wave velocity of the earth's uppermost thirty meters. For additional verification, active-source vertical seismic profiling (borehole-VSP) was used at sites in two of the five hazard classifications. HVSR-derived seismic resonances were used as a constraint during inversion of the MASW dispersion curve to reduce model misfit and improve model comparison to site lithology.

From the calculated Vs30 profiles, we observed that most sites fall under a C or D seismic hazard level where bedrock velocities are included in the Vs30 estimate. For the HVSR method, reliable results were obtained from surveys conducted at sites where the sediment profile met or exceeded the 2:1 velocity contrast between sediment and underlying layers (e.g. bedrock). We also observed that MASW surveys generated suitable velocity profiles when the active seismic source induced sufficient energy into the subsurface. When HVSR and MASW results were combined, a relationship between the observed resonance frequencies at each site corresponded to the dispersion curve fundamental mode. In favorable conditions, the VSP results determine average velocities that compare favorably with the HVSR and MASW results. The active and passive seismic methods used for this study provided the first field-derived shear-wave velocity values for sediments underlying Harford County, Connecticut, necessary for quantitative assessment of seismic hazard class.

1. PURPOSE AND INTRODUCTION

The goal of this study is to obtain velocity-depth profiles throughout Hartford County, Connecticut, in order to determine average shear-wave velocity (Vs) values for seismic hazard assessment. This Master's project is a continuation of previous efforts by Connecticut State Geologist, Margaret Thomas, and other New England State Geologists (Becker et al., 2013) to assess seismic hazard in New England states. The geophysical surveys allowed seismic hazard classifications to be assigned to thirty sites; the classifications were based on "Vs30 method" consistent with the National Earthquake Hazard Reduction Program (NEHRP) classification system based on average shear-wave velocity of the sediments above the bedrock interface (Table 1.1). Funding was provided by the U.S. Geological Survey, Office of Groundwater, Branch of Geophysics, the Department of Energy and Environmental Protection's Connecticut Geological Survey, and the Department of Civil and Environmental Engineering at the University of Connecticut.

NEHRP Seismic Hazard Classifications		
Site Class	**Soil Profile Type**	**Average Shear-wave Velocity of Top 30 meters, Vs30, in meters/second**
A	Hard Rock	$V_S > 1524$
B	Rock	$762 < V_S \leq 1524$
C	Very dense soil and soft rock	$366 < V_S \leq 762$
D	Stiff soil profile	$183 < V_S \leq 366$
E	Soft soil profile	$V_S < 183$

Table 1.1. NEHRP Seismic Hazard Site Classifications. The National Earthquake Hazard Reduction Program (NEHRP) seismic hazard site classifications, as published in the 2000 International Building Code, (Table 1615 1.1, page 350), use the average shear-wave velocity of the uppermost thirty meters (or 100 ft) known as Vs30. The five site classifications are differentiated by soil type and observed average shear-wave velocity ranging from hard rock, which has the lowest seismic hazard, to soft soil, which exhibits the greatest seismic hazard.

Currently, the 2008 seismic hazard map of Connecticut (Figure 1.1) only considers one soil type for classifying hazard; however, the surficial materials in Connecticut vary considerably from shallow crystalline rock to sand and gravel deposits, thick till, glacial clays, and fines (Figure 1.2).

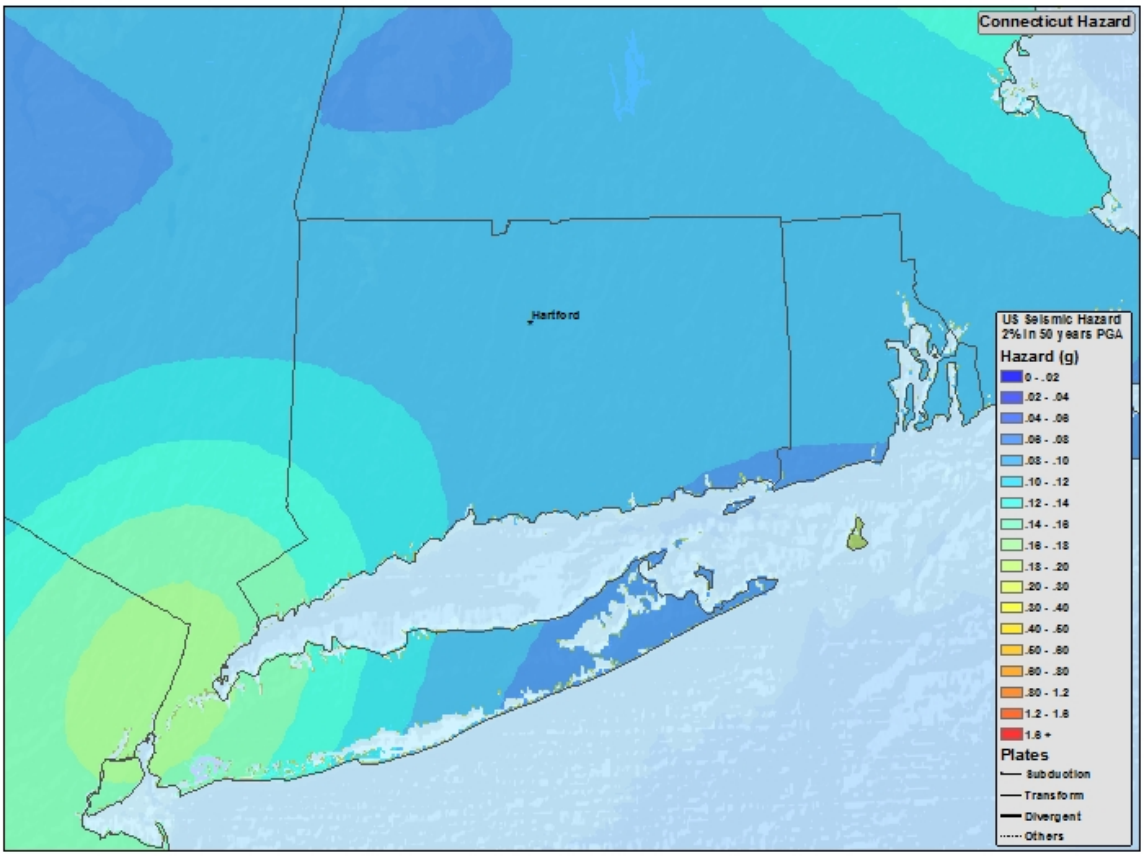

Figure 1.1. USGS Seismic Hazard Map of Connecticut. This map by Petersen *et al.* (2008) shows the current seismic hazard map of Connecticut which defines hazard by peak ground acceleration (PGA). PGA is the highest acceleration a particle can experience during an earthquake motion. This also relates to the allowable horizontal force a building should be able to endure during an earthquake according to current building codes (BSSC, 2000).

The National Earthquake Hazard Reduction Program (NEHRP), which was established by the Earthquake Hazards Reduction Act of 1977 (2008) uses the average shear-wave velocity of materials in the upper thirty meters (Vs30) for seismic hazard assessment (Table 1.1). This law was passed long before the Connecticut seismic hazard map was created and is yet to be updated.

In order to classify hazard consistent with NEHRP guidelines, average shear-wave velocities of the upper thirty meters must be determined, however, throughout a majority of Connecticut, hard crystalline bedrock lies within those thirty meters (Figure 2.2). These higher shear-wave bedrock velocities would then have to be incorporated into the averaged result, which in turn would decrease the seismic hazard classification.

One of the first initiatives to assess seismic hazard was untaken by New England State Geologists. A preliminary hazard map of Hartford County was created using a geospatial analysis of surficial materials data (Figure 1.3). The surficial materials of Hartford County, Connecticut, were categorized into five modified NEHRP classifications (Table 1.2). To explore these new classifications, it was necessary to collect actual field data measurements to profile the underlying sediment layers down to bedrock. After field data was collected and analyzed, these values were categorized using NEHRP classifications (Table 1.1) and then compared back to the surficial material-based site classes. Well log information was collected for thirty sites including all five hazard classes; at each site passive single-station, seismic surveys were performed. Within these thirty sites, an additional non-invasive active multi-channel seismic survey was done at ten sites as well as an invasive active seismic survey was done at three sites.

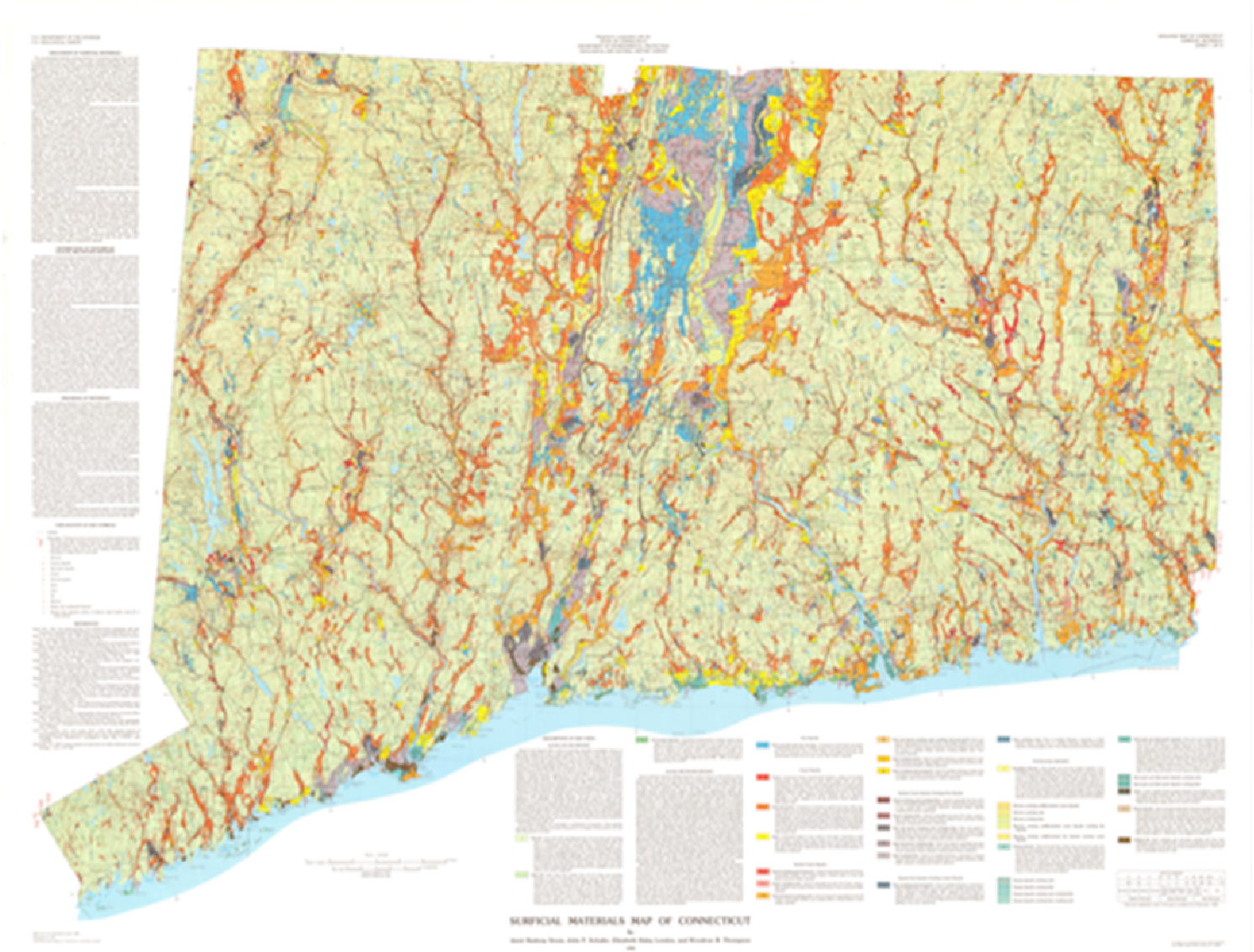

Figure 1.2. USGS Surficial Materials Map of Connecticut. This map displays the mapped surficial materials of Connecticut. It includes thirty-four different types of materials ranging from stiff till to soft clays (Stone *et al.*, 1992).

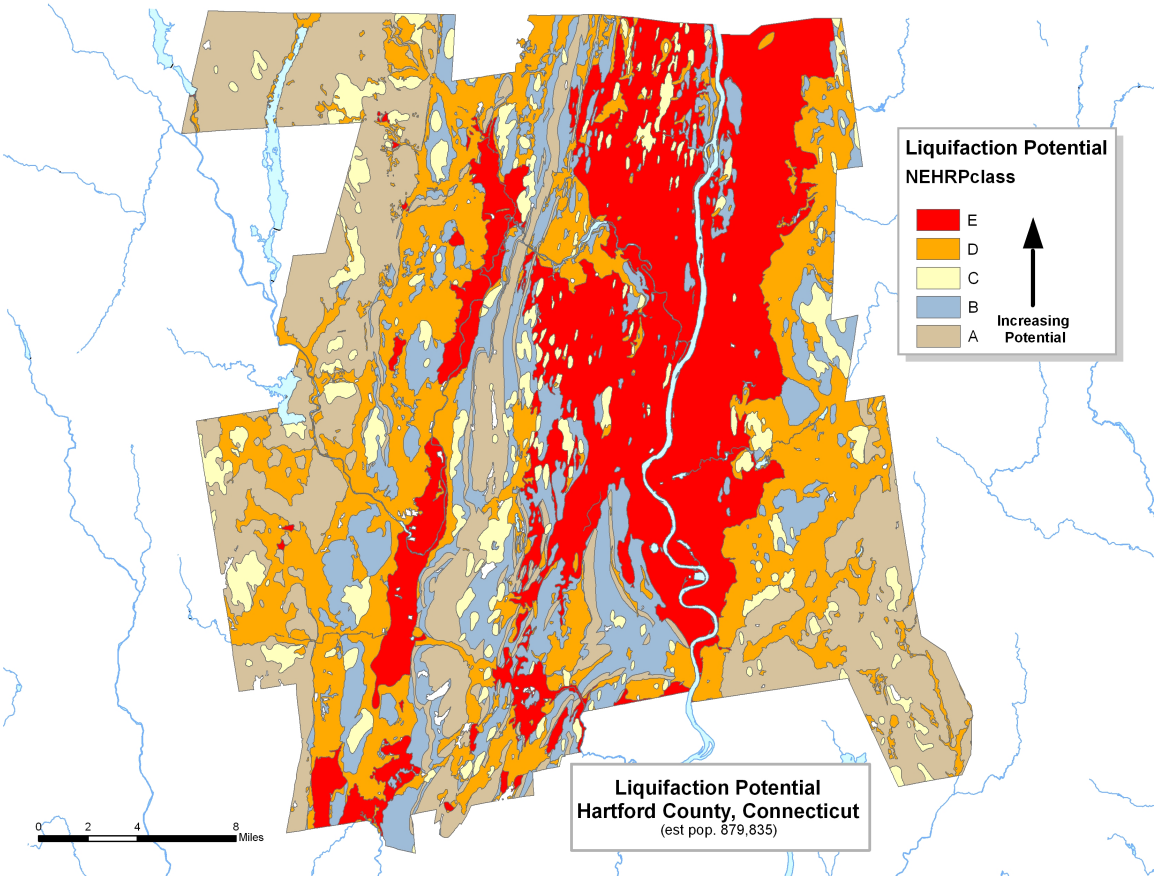

Figure 1.3. Liquifaction Potential of Hartford County, Connecticut. This surficial materials map of Hartford County displays five hazard classifications ranging from crystalline rock (Class A, tan) to glacial lake clays and fines (Class E, red). Class A is the location of materials with the lowest potential for liquifaction and Class E is the location of materials with the highest potential for liquifaction. Additional information about each class is described in Table 1.2. The greatest hazard is centralized around the Connecticut River, which is the main river that flows through New England. The lowest hazard materials are seen in the outermost regions of the map. This area is within the Connecticut River Valley (Becker et al., 2013).

NEHRP Classifications Hartford County, Connecticut*	
A	Crystalline Rock & Till (till < 15' thick)
B	Sedimentary Rock & Till (till < 15' thick)
C	Thick Till (> 15 ft thick)
D	Glacial outwash sand & gravel
E	Glacial lake clays and fines; stacked units involving fines c/f; f/c; s/f; postglacial deposits (saturation and subunit dependent); AF
*Classifications are Hartford County specific; geographically variable dependent on the geologic setting, degree of saturation, and environment of deposition. County and material specific shear wave velocity data is needed for more accurate prediction.	

Table 1.2. Northeast State Geologist Site Classifications for Hartford County, CT. These NEHRP classifications are a modified version of the site classes found in Table 1.1. The state geologist categorized each class by the mapped surficial materials rather than averaged shear-wave velocities in an effort to quickly determine a new seismic hazard classification system (Becker et al., 2013).

In the last five years, the eastern United States has experienced at least three earthquakes with recorded magnitudes greater than 4.0. Unlike earthquakes occurring in the western United States, these events were felt as far as 700 miles from their epicenter (Figure 1.4) due to the geologic makeup of the eastern states. The eastern US is centrally located on the North American tectonic plate, therefore the underlying geologic conditions differ from areas located directly along a plate boundary like California.

Both active and passive non-invasive seismic methods were used at thirty field sites in Hartford County in order to most efficiently examine the Hartford County field sites in a minimal amount of time. This data was used to test the classifications on the surficial materials-based hazard map. In addition, an active seismic borehole method was used at three sites to verify findings from the surface geophysical tests. Each test site was selected based on proximity to wells, field space large enough to conduct geophysical surveys, and known site characteristics such as depth to

rock. The Department of Energy and Environmental Protection's Connecticut Geological Survey and U.S. Geological Survey's Connecticut Water Science Center provided the well log information for this project.

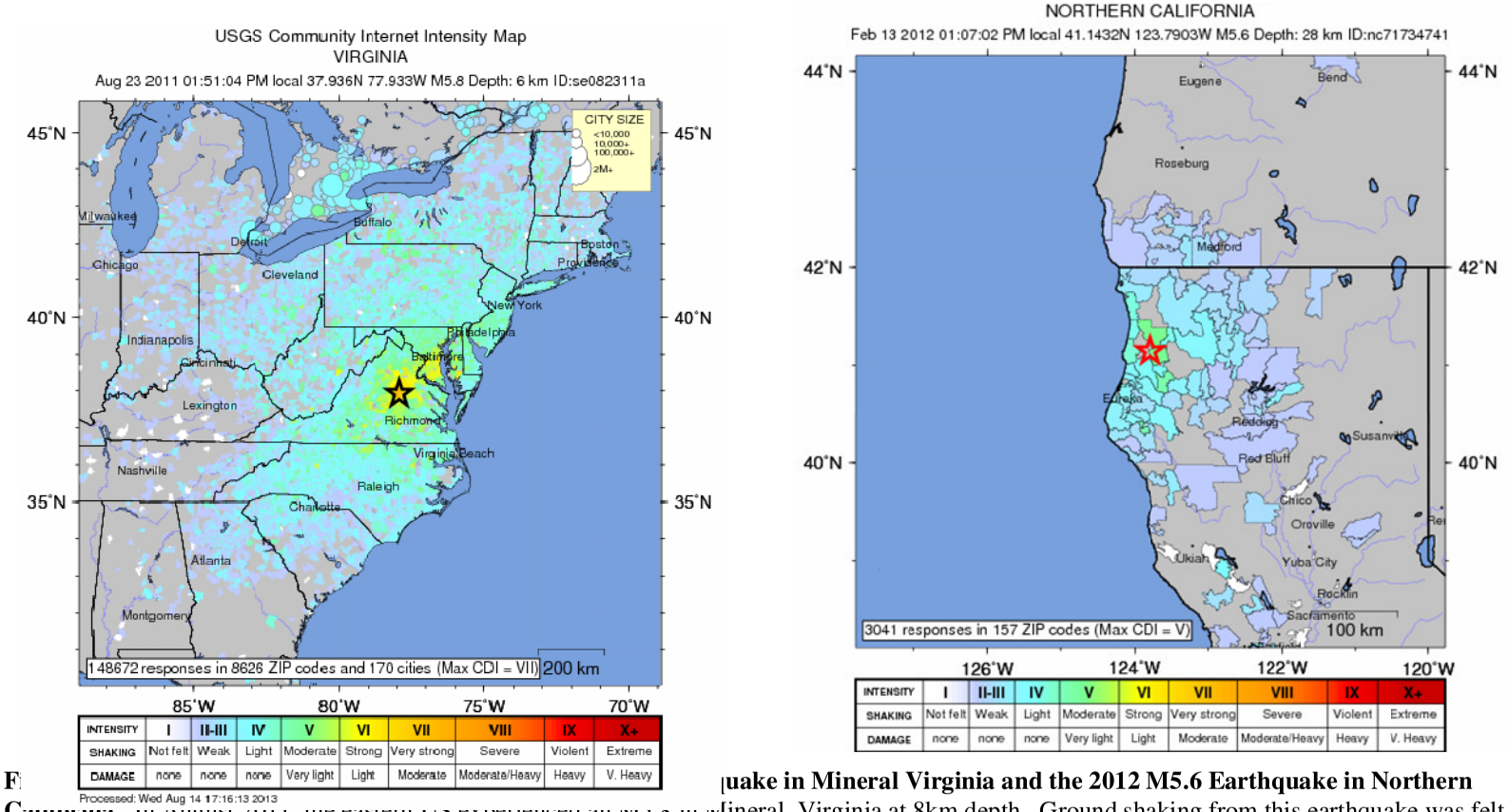

F **uake in Mineral Virginia and the 2012 M5.6 Earthquake in Northern California.** In August 2011, the eastern US experienced an M5.8 in Mineral, Virginia at 8km depth. Ground shaking from this earthquake was felt as far south as Alabama and north into Canada, extending almost 400 miles from the epicenter, which is designated on the map by a star. In 2012, northern California experienced an M5.6 earthquake at 28 km depth, however the radius of ground shaking was significantly shorter.

2. GEOLOGY OF CONNECTICUT

Active and passive seismic surveys were performed in Hartford County, Connecticut, located in the north central region of the state. With an estimated population of 894,014 people, Hartford County contains twenty-nine towns and cities including Hartford, the state capital. The county's total area is 1944.0 km^2 and is divided by the Connecticut River, the longest (655 km) and largest river in New England that flows south from New Hampshire through Connecticut into the Long Island Sound. Hartford County lies within the Hartford Rift Basin, which is mostly composed of Mesozoic age rift basin deposits of the Newark terrane. The bedrock consist mainly of clastic, sedimentary rocks with basalts and diabase trap rock that were deposited during Late Triassic and Early Jurassic events (McHone, 2004).

The geologic history of Connecticut can be divided into three major events. Eastern Connecticut during the Taconic Orogeny, 460-440 million years ago (mya) and western Connecticut throughout the Acadian, 440-350 mya, and Allegenian orogenies, 350-270 mya. After these three compressional events, the region began to rift as Gondwana and Avalonia started to separate to form the Atlantic Ocean. This extension and bedrock cooling caused the rock to become more brittle, yielding major fractures giving Connecticut the north-south bedrock fabric that still exists today. As a result, this rifting event in central Connecticut opened up what is known as the Hartford Rift Basin (Coleman, 2005).

This basin was later affected by two glaciations: the Illinoian (150-130,000 years ago) and the Wisconsinan (26-15,500 years ago). The Illinoian ice sheet removed most of the weathered Alleghenian sediments. The larger Wisconsinan ice sheet covered all of Connecticut and part of Long Island. As the glacier receded, a moraine formed off the coast of Connecticut creating a dam for Glacial Lake Connecticut. The Wisconsinan ice sheet continued to retreat northward

later forming glacial Lake Hitchcock, which dammed in present-day Rocky Hill of Hartford County (Stone *et al*., 2005).

Geologically, the Hartford Rift Valley is a half graben, which is characterized by the Eastern Border fault that separates the Newark Terrane from the Bronson Hill Anclinorium and other geologic terranes of eastern Connecticut (Figure 2.1). Although, this fault has been inactive for over 140 million years, there have still been over 1214 recorded seismic events in the New England area since 1568, many of which have originated in Moodus, CT (Ebel *et al*., 1982). Connecticut is also known as an intraplate earthquake area since it resides within the North American tectonic plate and not directly on a plate boundary like California (Grotzinger, 2007). This is due to the geologic properties of the underlying bedrock in this region compared to the west coast. The bedrock in Connecticut is more metamophosed, meaning it has undergone high pressures and temperatures, which has caused it to become stiffer. This allows seismic waves to travel greater distances as exemplified by shake maps from East Coast earthquakes (Figure 1.3) (Alter, 1995). In contrast to earthquakes occurring on the West Coast where the ground shaking is relatively centralized, when an earthquake occurs on the East Coast, the ground amplification endangers states hundreds of miles away. Therefore, it is important to understand the local geology in Connecticut since any regional earthquake can create a hazard to the area.

Above the bedrock in Hartford County are large areas of fine deposits, coarse deposits, and stacked coarse deposits overlying fine deposits (Figure 1.2). Compared to the rest of Connecticut, Hartford County has a higher concentration of total sediment thickness greater than 30 m (Figure 2.2). These thicker sediments are distributed throughout the Connecticut River Valley in the eastern half of the county. However, these thicker sediments consist primarily of fines such as very fine sand, silt and clay, and sands overlying fines, which are more susceptible

to seismic wave amplification. The rigid bedrock, varying sediment thicknesses and their susceptibility to ground shaking create motivation for this research project.

Seismic hazard, in contrast to seismic risk, defines the intensity of ground shaking for a given area. Seismic risk pertains to the amount of damage or loss caused by an earthquake, which is dependent on an area's seismic hazard. This hazard has been quantified by the NEHRP site classes (Table 1.1) and has been used in various building codes in the form of Vs30 (eq. 2.1), the average shear-wave velocity of the upper 30 m.

$$Vs30 = \frac{30}{\sum_{i=1}^{n} \frac{H_i}{Vs_i}} \qquad \text{(Eq. 2.1)}$$

Vs30 uses the summation of layer i with thickness H_i and shear-wave velocity Vs_i where n is the number of layers within the 30 m (Aboye *et al*., 2011). In order to define seismic hazard throughout Hartford County, passive and active seismic experiments were used across various field sites to calculate Vs30. These field techniques and their results are described in the following chapters.

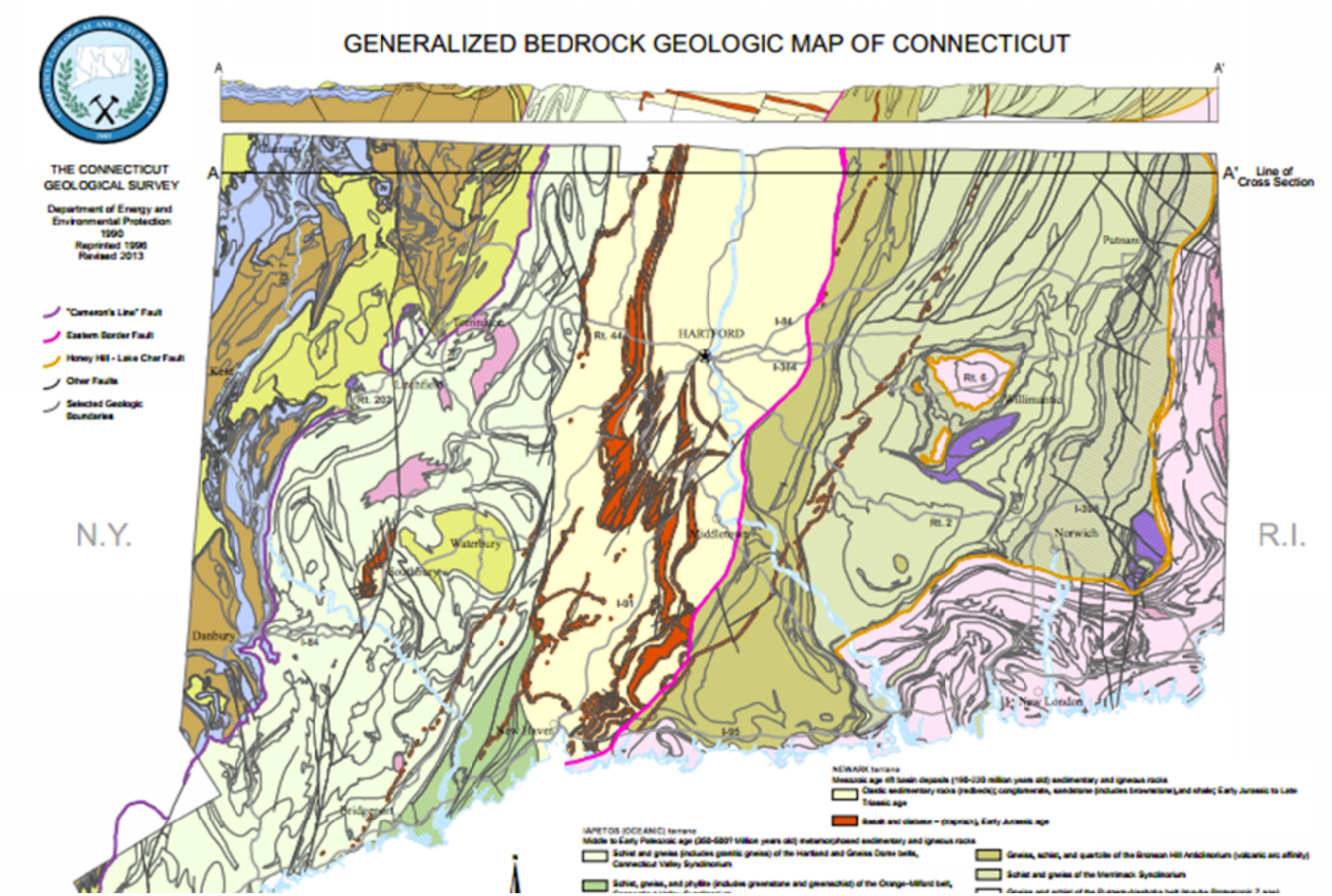

Figure 2.1. Bedrock Geologic Map of Connecticut. Connecticut is comprised of various rock types including igneous, sedimentary, and metamorphic rocks. The Mesozoic Hartford Rift Basin in Central Connecticut is illustrated in yellow. Within the basin are Jurassic age basaltic flows and sills shown in red. Hartford County is located in the Northern portion of the Hartford Rift Basin as indicated by the red square. The basin is bounded by the Eastern Border Fault (pink line), the most well-known fault in Connecticut (*Generalized Bedrock Geologic Map of Connecticut*, Rodgers, 1985).

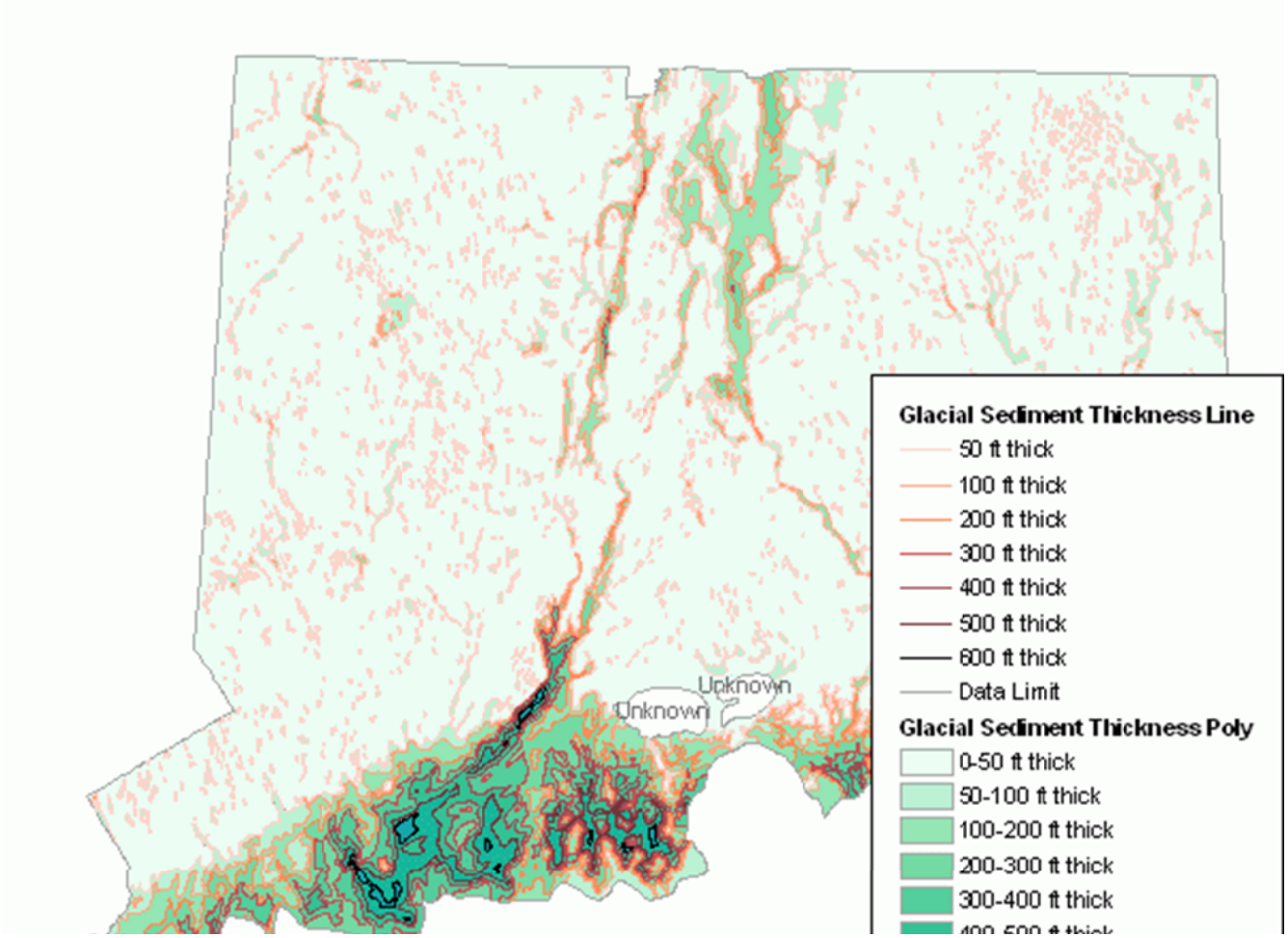

Figure 2.2. Thickness Map of Glacial Sediments in Connecticut and Long Island Sound Basin. The glacial sediment thicknesses are displayed by colored polygons. A majority of Connecticut has less than 50 ft of sediment thickness. Hartford County is located in North-Central Connecticut, where the sediments become thicker in the Hartford Rift Basin. The thick sediments along the southern coast of Connecticut are largely within the Long Island Sound (Stone *et al.*, 2005).

3. PASSIVE SEISMIC METHODS

3.1. BACKGROUND INFORMATION

Passive seismic surveys measure the ambient noise or microtremors of the ground surface in order to determine the natural resonance frequency and depth to bedrock. This method is time-efficient and inexpensive in comparison to other geophysical techniques such as borehole drilling or MASW. It is assumed that these ambient vibrations consist mainly of surface waves that propagate along a horizontally stratified surficial layer (Wathelet, 2007). The passive surveys discussed in this chapter were conducted using three-component, single-station seismometers; the two horizontal components (x, y) are influenced by both Rayleigh and Love waves whereas the vertical component (z) is seldom influenced by Rayleigh waves. Since Rayleigh wave particle motion utilizes both the horizontal and vertical directions with respect to the surface, it simulates a retrograde elliptic motion known as "ground roll." Love waves, however, are horizontally-polarized where the particle motion travels parallel to the surface, but at right angles (Reynolds, 1997). For this study, Love waves will not be discussed because analysis of Rayleigh wave motion is the main objective of the MASW method.

Unlike body waves, surface waves exhibit dispersive characteristics that enable the calculation of shear-wave velocity (Vs) as a function of depth (Wathelet, 2007). These dispersive characteristics can be identified by Fast Fourier Transform inversion algorithms used in part with the Horizontal-to-Vertical Spectral Ratio (HVSR). The HVSR method utilizes three-component single-station data to determine the ratio between the horizontal and vertical wave amplitude spectra. This method enables the observation of the fundamental resonant frequency (f_0) at the

measured location with implied amplification factors of the underlying sediments (Nakamura, 2008).

In order for a resonance frequency to be observed, there must be a 2:1 velocity contrast between the underlying layers (Costa, 2005). For example, if a fine sand layer, which has an average shear-wave velocity range 200-300m/s, is overlying a hard crystalline rock, which can have an average shear-wave velocity >1000m/s, this exceeds the 2:1 contrast and a resonance frequency peak can be observed. If a gradual grain-size increase with depth is present, a peak may not be observed because the velocity contrast is too small or the increase too gradual. However, layer thickness is also important; if a thin low velocity layer such as clay is present between two higher velocity layers such as sand or gravel, the low velocity layer can be masked by the surrounding layers. When the velocity contrast requirement is met and the observed sediment layers are non-gradational with depth, the HVSR will typically exhibit a clear, sharp peak.

The Time-Frequency Analysis (TFA) is a processing technique used to observe Rayleigh wave ellipticity; ellipticity is the ratio between horizontal and vertical particle motion. This technique uses a continuous wavelet transform (CWT) to remove the effects of unwanted body waves and Love waves that may alter the observed amplitude in the HVSR fundamental frequency peak; after this transform is applied, the Rayleigh Wave Ellipticity curve remains. Theoretically, if the wave field was composed of only Rayleigh waves, the HVSR and ellipticity curves would be identical, therefore the peak observed using the HVSR method is an overestimation of the Rayleigh wave ellipticity curve. The ellipticity curve is then used in an inversion algorithm to determine a shear-wave velocity profile; an immediate disadvantage of this method is that it cannot identify low-velocity zones. The observation of ellipticity dates back to 1969 by Boore and Toksöz, yet further investigations of the topic are still being determined. For the purpose of

this paper, TFA will be used as a supplement to the HVSR method in areas where depth to rock is known (Fah *et al*., 2008; Hobiger *et al*., 2012).

Sometimes multiple HVSR peaks appear within the observed frequency band; the shape and location of each infers changes in the underlying soil structure. The shape of a peak is influenced by the energy of the Rayleigh wave within the frequency band. With the elliptic motion of Rayleigh waves in mind, at the HVSR peak the amplitude of the vertical component Rayleigh wave approaches zero, but along the sides of the peak, Rayleigh wave energy approaches its maximum (Nakamura, 2008). If more than one peak or a "higher mode" is observed, there is more than one resonance source within the soil structure (Wathelet, 2005). This can be caused by a multi-layer system or in some situations effects of a mechanical noise source can give be observed especially if the peak has a very low and broad peak such as an underground pump or generator (Haghshenas, *et al*., 2008). These mechanical sources can be filtered out so that the rest of the curve is not disturbed. The fundamental frequency is the first peak observed within the spectra and exhibits the lowest frequency; in most situations, this peak represents the bedrock interface, however, if a shallower, sharp velocity contrast exists, this peak may be evidence of that shallower interface. Any peaks visible after the peak frequency, known as higher modes, can usually be identified as shallower layers or structures within the profile that exhibit a velocity contrast (Fah *et al*., 2001).

Passive seismic is recommended for use in areas that are considered to have low to moderate seismicity where this is a lack of significant earthquake recordings. It has also proved to be an adequate technique for geophysical exploration in urban areas where space is limited for larger array methods. Although it may not supply as detailed information of the subsurface as an invasive technique would, it has the advantage that it uses compact and inexpensive equipment

and requires less time for data acquisition than techniques previously mentioned. The end result is also stable given any measured time and season. Therefore, it is an ideal survey type for fast site characterization in Connecticut (Costa, 2005; Delgado *et al*., 2000a; Nakamura, 2008).

3.2. FIELD SETUP FOR PASSIVE SURVEYS

Passive seismic surveys were performed using broadband, three-component seismometers. Four seismometers were used to simultaneously collect single-station passive data at multiple locations within each field site and proximal to a known borehole. The instruments recorded at 128 Hz for 20-30 minutes depending on anticipated depth to bedrock. The instrument distribution at each site varied depending on the availability of open space; Photo 3.1. shows an example of seismometer field distribution. In Photo 3.1, four instruments are arranged surrounding a monitoring well for a Huddle Test; this data are used to calibrate other data taken further from the well within the same site.

Photo 3.1. Example of Passive Field Survey Setup. Four single-station seismometers arranged in a huddle test formation around a Church water-supple well in Canton, CT.

Data sheets were used at each site to record the field parameters of the instrument, assigned data files for each survey, weather conditions and other local observations of geologic conditions, see the Appendix for an example. In the event of unfavorable weather conditions, a bucket is placed over each seismometer to negate potential wind and rain resonance interference; however, surveys were not performed in heavy wind and rain events. When the instrument is installed in the field, the seismometer is oriented to true north and leveled using the three adjustable metal feet and bubble level located on the unit's top face. At most field sites, surveys were taken on cleared, grassy or earth material, which use long thin metal feet to couple the unit with the surface. However, at some sites measurements were taken on pavement, which require wider, short feet that do not penetrate the surface. After acquisition, the passive data was imported using software provided by the manufacturing designed specifically for the instrument. For analysis, the records were exported to a freeware signal-processing program, which is discussed in the following section.

3.3. DATA PROCESSING

3.3.1. Horizontal-to-Vertical Spectral Ratio

The HVSR method was originally proposed by Nogoshi and Igarashi (1971) as the ratio between the horizontal and vertical component Fourier spectra to estimate underlying soft soil characteristics (Bonnefoy-Claudet, 2006; Costa, 2005). This method was later popularized by Nakamura in 1989; however, this method still lacks a clear theoretical explanation. In the vertical component, Rayleigh waves are dominant; therefore, it can be assumed that the ratio is related to Rayleigh wave ellipticity. Based on the assumptions that the area being investigated is composed of a rigid bottom layer with soft overlying soil layers and that microtremors consist of Rayleigh waves, the layers will excite by these microtremors. The frequency observed from the HVSR method is then also related to the soil transfer function (Delgado *et al*., 2000a).

This transfer function exhibits a peak or maximum within the dominant resonance frequency of the soil given by:

$$Se(f) = H_S(f)/H_B(f) \qquad \text{Eq. 3.1}$$

Where H_S and H_B are the horizontal component spectral amplitudes in terms of frequency at the surface (S) and base (B) of the layer. The recording displays the combined effect of source perturbations, vibration trajectory, as well as characteristics of the site being investigated. However, these source effects must be removed in order to determine the effect of the microtremors on the soil. Therefore, Equation 3.1 is then divided by the spectral amplitudes, $S_s(f)$, of the microtremor's vertical component at the surface, $V_s(f)$, and base of the layer, $V_B(f)$:

$$S_s(f) = V_s(f)/V_B(f) \qquad \text{Eq. 3.2}$$

Assuming $HB/VB = 1$, the transfer function is defined as:

$$TF(f) = H_S(f)/V_S(f) \qquad \text{Eq. 3.3}$$

This resulting equation shows reveals that the soil transfer function is equal to the horizontal and vertical component spectral ratio at a given location with respect to frequency (Delgado *et al*., 2000a).

Since the HVSR method is controlled by shear-wave resonance, it is related to the soil transfer function and is determined using Equation 3.4, as written by Delgado *et al*. (2000b), which computes the average ratio at a site:

$$HVSR = \frac{\sqrt{S_{NS}^2 + S_{EW}^2}}{2S_Z^2} \qquad \text{Eq. 3.4}$$

S_{NS} and S_{EW} are the horizontal spectral amplitudes and S_z is the vertical spectral amplitude of the passive record; these three-component spectral amplitudes determine the sampling properties of the H*VSR*. This frequency dependent ellipticity appears as an amplitude peak known as the fundamental resonance frequency (Bonnefoy-Claudet *et al*., 2006; Nakamura, 2000).

Within the HVSR processing algorithm are the dispersion index q and relative error ε, which determine the ratio's relative accuracy. To reduce any potential artificial variability, these parameters need to be minimized; this can be achieved by increasing the total record length of the passive survey (Picozzi *et al*., 2005). Therefore, Picozzi *et al.* proposed recording for at least 20 min, where each time processing window is ~60 s since they found that q and ε decrease less dramatically when more than 20 signal windows are used.

In the field single-station, three-component seismometers were deployed within close proximity of a well with previously attained ground truth. Each survey records for 20-30 minutes at a sampling frequency of 128 Hz using high gain. If the depth to bedrock is known and the resonance frequency is determined, the shear-wave velocity value of a 1-dimensional model can be estimated using Equation 3.5 (Nakamura, 2008):

$$V_s = 4zf_0 \qquad \text{Eq. 3.5}$$

Where z is the sediment layer thickness, V_S is the calculated shear-wave velocity of the sediment layer, and f_0 is the observed resonance frequency. This 1-D propagation consists of vertically incident SH waves. However, if z is unknown, this equation is not adequate for calculating shear-wave velocities.

For the purpose of this explanation, passive data were collected near borehole JL-1 at Haddam Meadows State Park in East Haddam, Connecticut and processed as discussed; the borehole log for JL-1 is in Appendix. Please note this site is located outside the Hartford County focus area, but was selected as the exemplary site as it is a recognized study area by the U.S. Geological Survey. After data acquisition, each passive record was analyzed using a freeware signal-processing program developed by the SESAME European Project (2005). The software applies the HVSR algorithm to raw three-component data (Figure 3.1.) in order to determine a peak resonance frequency (f_0).

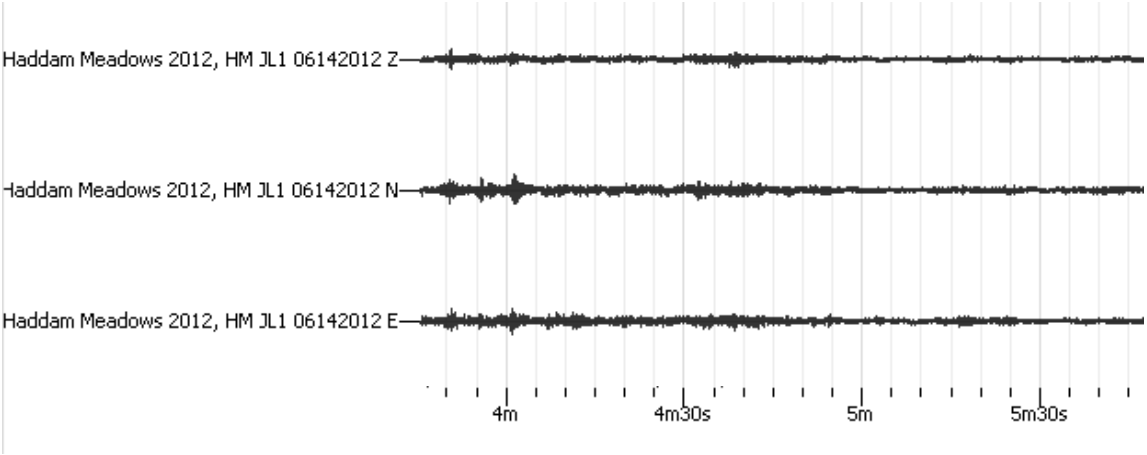

Figure 3.1. Example of Raw Three-Component Seismometer Data. Each passive record consists of three-component data represented here as the amplification of each component with respect to time. "Haddam Meadows 2012, HM JL1 06142012" is the unique filename for the trace record and *Z* is the vertical component, *N* is the north-south horizontal component and *E* is the east-west horizontal component. This data were taken at Haddam Meadows State Park in East Haddam, CT.

Before the fundamental frequency can be determined, processing parameters must be specified: for this record, 30 s time windows were used for the 28.5 min total record length, a Konno & Ohmachi (1998) smoothing type was applied with smoothing constant b=40 and 5% cosine taper and the frequency sampling range was 1-20 Hz. Once the HVSR algorithm was initiated, the total processing time took seconds and produced a strong resonance frequency peak ~2.14 Hz (Figure 3.2) which is displayed as the peak amplitude with respect to frequency. Although a second broader peak appears from 13-15 Hz, for simplicity, only the fundamental frequency will be discussed at this time to maintain the 1-D earth assumption with 1-layer over half-space.

In this case, multiple records taken around the same borehole location were processed at the same time; the resulting frequency peaks in each record are seen in Figure 3.3. In Figure 3.2, each colored line refers to a different time window within the record, the dotted lines represent the upper and lower bounds of the amplitude's standard deviations and the vertical, two-toned gray rectangle represents the standard deviation of the fundamental frequency; where the two rectangles meet is the average value of the fundamental mode. Some time windows were removed from the processing to reduce the standard deviation.

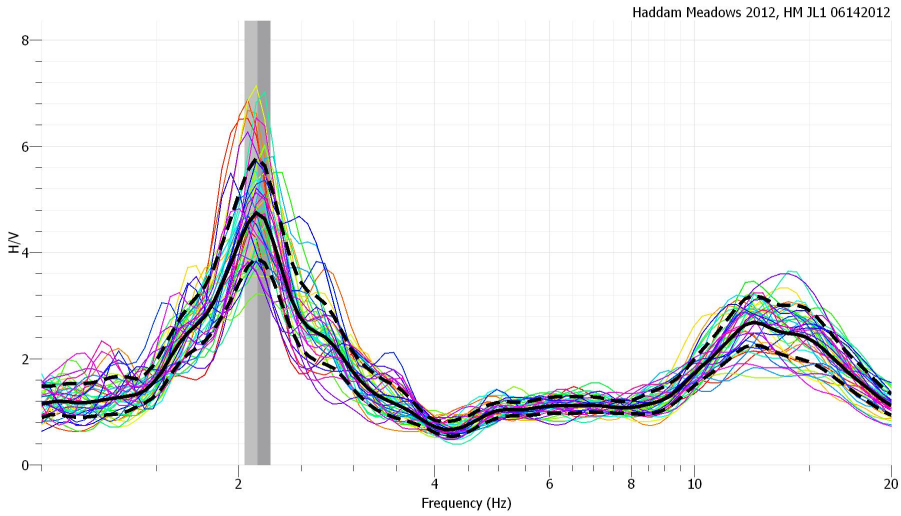

Figure 3.2. HVSR Result at JL-1. The fundamental mode or peak frequency can be clearly identified by the high amplitude peak at 2.14 Hz. The HVSR curve is plotted as amplitude with respect to frequency. The colored lines refer to different time windows used for processing within the signal trace, the solid black inner line represents the average HVSR curve, the two dotted outer lines represent the standard deviation bounds of that curve and the vertical, two-toned gray rectangle represents the standard deviations of the fundamental frequency. Where those two gray colors meet is the average value of the fundamental mode.

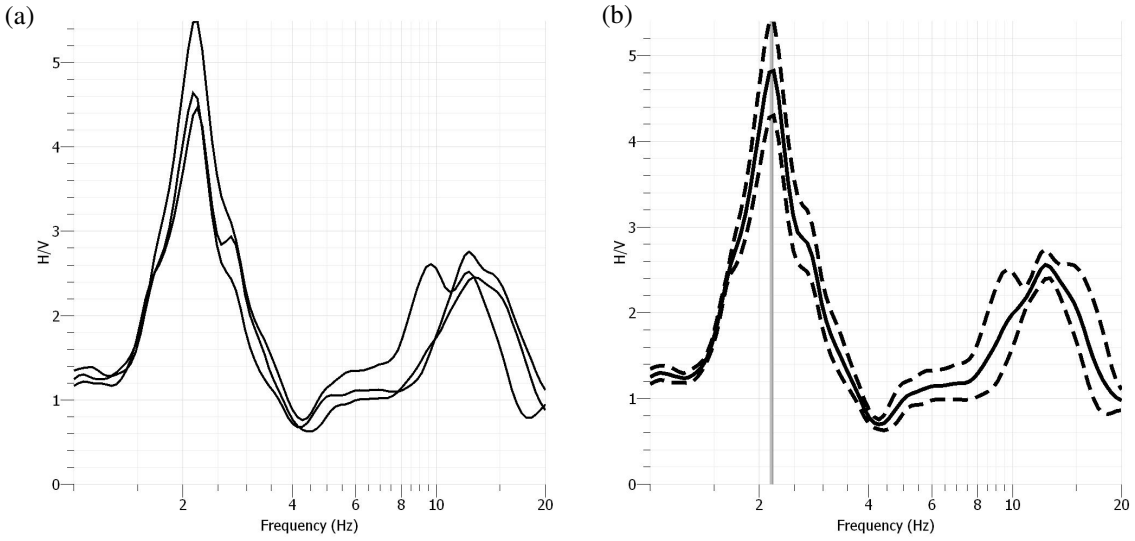

Figure 3.3. All Individual HVSR Results and Averaged HVSR Result. (a) All three records taken at the same location are combined in one plot to not only compare peak frequencies, but to ensure that the same peak is obtained by each instrument. Since each peak has the same frequency value, this confirms the 1-D earth model assumption. (b) All three records' HVSR curves are averaged and displayed as the solid black line and the associated standard deviations are represented as the dotted lines. The averaged peak frequency is indicated by the vertical gray rectangle.

From this observed HVSR resonance peak at 2.14 Hz and a known depth to bedrock from the JL-1 well log (38.1 m), the average Vs of the sediment layer overlying rock can be calculated using Equation 4.5; this is based on the assumption that the peak at 2.14 Hz represents the sediment and bedrock interface. As a result the average Vs of the sediments is ~326 m/s; based on average Vs values of known materials, these sediments are consistent with sand and gravel sediments. However, the NEHRP hazard class is based on Vs30, therefore, if the sediment type is uniform over the 38 m interval, the Vs30 would be ~257 m/s. Therefore, this site and the JL-1 site would be classified as a D class based on the NEHRP Seismic Hazard Classification standard.

3.3.2. Time-Frequency Analysis

In addition to determining the fundamental resonance mode, recent work utilizes the average HVSR curve to obtain shear-wave velocity profiles (e.g. Fah *et al*., 2001, 2008; Hobiger *et al*., 2013). In order to determine the Vs structure, the concept of Rayleigh wave ellipticity, which is embedded in the average HVSR curve is used. The shape of the Rayleigh wave ellipticity is sensitive to shear-wave velocity structure, although constraints need to be applied to the inversion to avoid ambiguous results (Hobiger *et al*, 2013).

Rayleigh wave ellipticity is the ratio between horizontal and vertical particle motion. Rayleigh wave ellipticity exhibits a peak at the resonance frequency, similar to that revealed by the HVSR curve. However, the HVSR curve is composed of both surface and body waves; if this curve is to be used to interpret Vs structure, the effects of Love wave (SH) and body waves must be minimized such that only Rayleigh wave energy (P-SV) remains (Fäh *et al*., 2003, 2008). Thus, the HVSR curve is a starting point for estimation of the Rayleigh wave ellipticity curve (Hobiger *et al*., 2013). The Vs structure can be retrieved from the ellipticity curve by inverting after adjusting the HVSR curve for love wave and body wave contribution (Fäh *et al*., 2001, 2003;

Poggi *et al*., 2012). Including HVSR peak frequency can improve estimation of the Rayleigh wave dispersion curve (Scherbaum *et al*., 2003), however, the addition of too many constraints can also bias the results.

An ellipticity curve exhibits a sharp peak and trough asymptotic with the resonance frequency; however, some parts of the curve are more stable than others. The amplitude of the peak and trough depends on the impedance contrast; the larger the impedance contrast, the sharper the peak. When the ellipticity is equal to 1, the contributions of the horizontal component are equal to the vertical component. Because the trough is influenced by horizontal components or Love waves, estimations taken from above the trough frequency can be misinterpreted. Therefore, the portion of the ellipticity peak to the high frequency side is the most reliable for measuring and modeling.

In order to remove these effects and observe the Rayleigh wave ellipticity within the HVSR curve, a Time-Frequency Analysis was performed on the raw passive single-station data discussed in 4.3.1 from Haddam Meadows State Park, near borehole JL-1. This analysis was also done in the same freeware software package; the following theoretical background and details about the processing software was provided by the Network of Research Infrastructures for European Seismology JRA4 report (Fäh *et al*., 2008).

The algorithm uses a Continuous Wavelet Transform (CWT) (Eq. 4.6) with the modified Morlet wavelet (Eq. 3.9):

$$CWT\{x\}_{(a,b)} = \frac{1}{\sqrt{|a|}} \int_{-\infty}^{\infty} x(t)\, \psi^* \left(\frac{t-b}{a}\right) dt \qquad \text{Eq. 3.6}$$

Where t is time, a is the scaling parameter that is inversely proportional to frequency and b is the translation in time. The wavelet $\psi(t)$ is scaled and translated in order to form analyzing wavelets; the width of the analyzing wavelets in the time domain is proportional to the scaling parameter a. The wavelet coefficient $CWT\{x\}_{(a,b)}$ measures the function of the wavelet at a and b is similar to the time-frequency signal structure. The wavelet $\psi(t)$ has to then fulfill the admissibility condition where $\Psi(\omega)$ is the Fourier transform of $\psi(t)$ (Eq. 3.7):

$$C_\psi = 2\pi \int_{-\infty}^{\infty} \frac{\Psi(\omega)^2}{|\omega|} d\omega < \infty \qquad \text{Eq. 3.7}$$

From the CWT (Eq. 3.6), the signal *f(t)* is reconstructed by Eq. 3.8:

$$x(t) = C_\psi^{-1} \iint_{-\infty}^{\infty} CWT\{x\}_{(a,b)} \psi(t)_{(a,b)} \frac{da\, db}{a^2} \qquad \text{Eq. 3.8}$$

The modified Morlet wavelet was used in this CWT analysis because it has a well-defined central frequency, displays the lowest amount of time and frequency uncertainties and allows signal phase information to be extracted. This complex wavelet is represented by Eq. 3.9:

$$\Psi(\omega) = \frac{1}{\sqrt[4]{\pi}} \exp(-(a\omega - \omega_0)^2 m), for\ \omega > 0 \qquad \text{Eq. 3.9}$$

Where the time domain $\Psi(t)$ is defined by Eq. 3.10:

$$\Psi(t) = \pi^{-\frac{1}{4}} e^{i\omega_0 t} e^{-\frac{t^2}{2}} \qquad \text{Eq. 3.10}$$

In the frequency domain, the modified Morlet wavelet is narrower than the common Morlet wavelet. Although this decreases the time resolution, the frequency resolution becomes more substantial.

The frequency domain is controlled by the *m* value in Eq. 3.9; the *m* value parameter is the Morlet wavelet parameter, as the width of the wavelet narrows the *m* value increases. For the JL-1 data, m was set to 2.

Within the TFA described by Fah *et al*. (2008), the resolution of time and frequency are given by equations 3.11 and 3.12, which change during processing. These equations control the parameters of the wavelet such as across what frequency range the wavelet is applied. For the JL-1 data, the selected frequency range is from 1-20Hz.

$$\Delta t_a(f) = a\Delta t_\psi = \frac{\omega_0}{\omega}\sqrt{m} = \frac{\omega_0}{2\pi f}\sqrt{m} \qquad \text{Eq. 3.11}$$

$$\Delta f_a = \frac{\Delta f_\psi}{a} = \frac{1}{4\pi\sqrt{m}}\frac{\omega}{\omega_0} = \frac{2\pi f}{4\pi\omega_0\sqrt{m}} = \frac{f}{2\omega_0\sqrt{m}} \qquad \text{Eq. 3.12}$$

In these equations, ω is the angular frequency and f is the corresponding frequency in Hertz which are estimated by Eq. 3.13 and 3.14:

$$\omega = \frac{\omega_0}{a} \qquad \text{Eq. 3.13}$$

$$f = \frac{\omega_0}{2\pi a} = \frac{f_0}{a} \qquad \text{Eq. 3.14}$$

In order to create the Rayleigh wave ellipticity curve, the CWT combines the horizontal components (Eq. 3.15) in order to identify peaks in the vertical component's absolute value. From these maxima, the corresponding $|CWT_H|$ are picked within the time domain at a ¼ period delay. This is repeated for all frequencies.

$$|CWT_H| = \sqrt{CWT_{NS}^2 + CWT_{EW}^2} \qquad \text{Eq. 3.15}$$

CWT_{NS} and CWT_{EW} are complex forms of the CWT horizontal components.

Once this is achieved, a log-scale histogram is created for each frequency. Within the histogram is the variable *nppm*, number of maxima used per minute. This assures that the histogram is an adequate representation of the average data characteristics; the smaller the *nppm*, the more rigid the selection. For the JL-1 data, *nppm* was set to 10. The ellipticity curve is then extracted from the histogram by estimating the geometrical mean. Similar to picking a dispersion curve, the highest values within the histogram at certain frequencies are picked; these correspond to the Rayleigh wave ellipticity (Figure 3.4). Dispersion curve theory is discussed at greater detail in the following chapter. As stated before, the effects of Love waves and other body waves will increase the overall amplitude of the curve, but the amount at which these affect the curve are reduced as *nppm* is decreased (Fah *et al*., 2008).

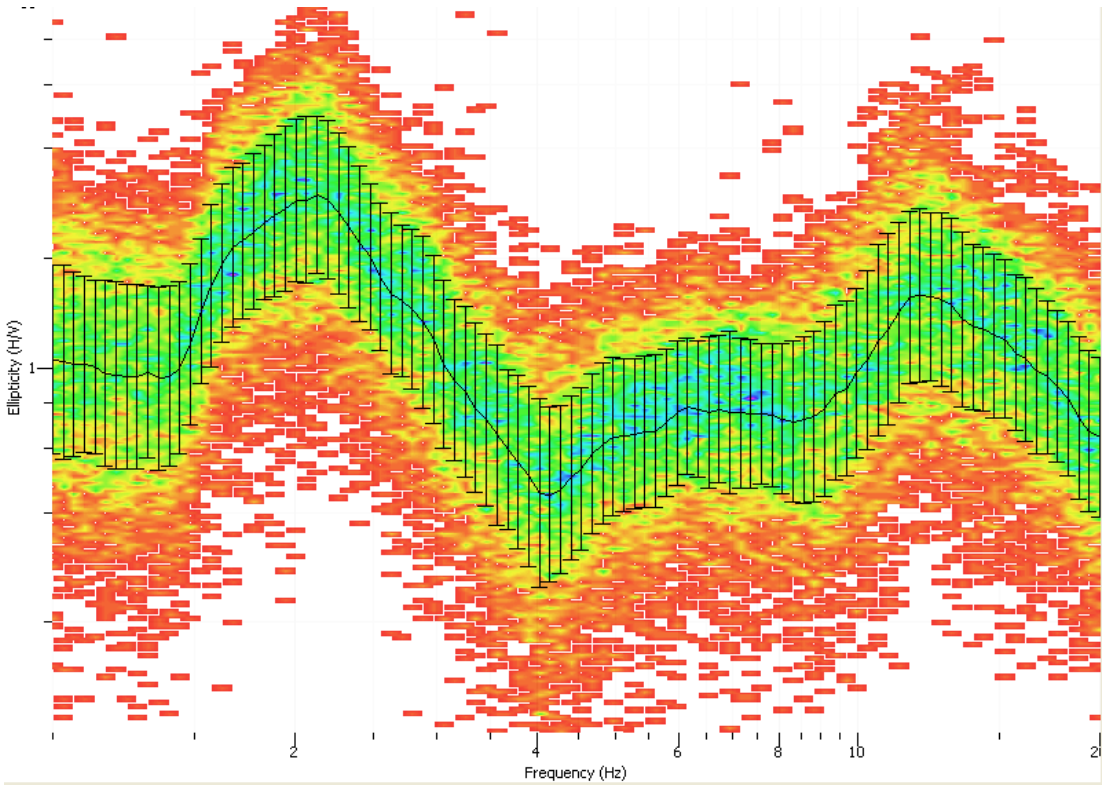

Figure 3.4. Histogram of JL-1 Data with Picked Dispersion Curve. The black line with error bars represents the picked dispersion curve of the histogram. The cooler colors refer to higher energy and the warmer colors are lower energy. In this data, the ellipticity peak is located at 2 Hz, similar to the HVSR peak in Figure 3.2; the ellipticity trough is located at 4 Hz. The elliptic structure is centered on an Ellipticity value of 1 (y-axis) with the peak and trough amplifying to 2.5.

Once the curve was picked, it was inverted to create a 1-layer over half-space model with constraints on depth to rock and the ellipticity peak. The inversion program uses a Monte-Carlo algorithm. The Monte-Carlo is favorable because it avoids linearity assumptions between the known and unknowns within the non-unique problem (Fah *et al.*, 2008). It has been used extensively in complex and difficult problems as well as retrieving velocity profiles (Socco *et al.*, 2008). For the inversion, five tests with 2550 models each were used; each test had a ~0.56 resulting minimum misfit value. The ellipticity models created from the inversion are displayed in Figure 3.5 with the original ellipticity curve. As previously stated, the right side of the ellipticity peak is the best to fit to the models produced since the trough is most affected by Love waves.

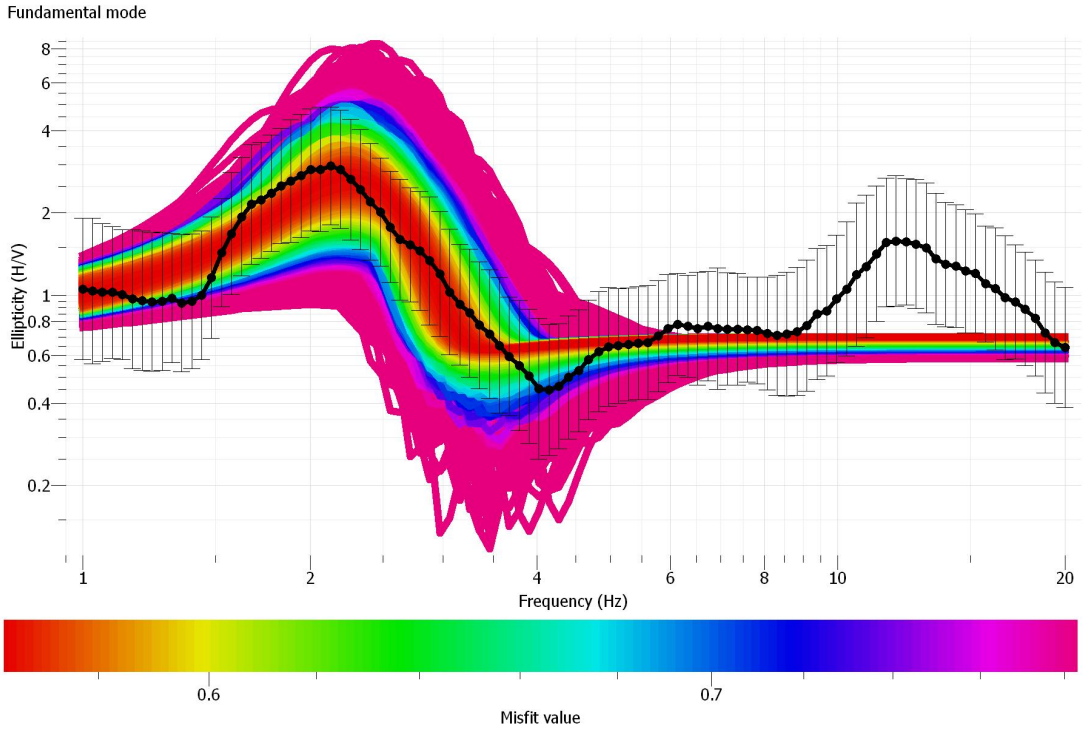

Figure 3.5. Ellipticity Curve Models of Haddam Meadows Well JL-1. The extracted ellipticity curve is represented by the dotted black line and standard deviation error bars. The colored lines represent ellipticity models with corresponding misfit values. In this figure, the peak and peak's right side of the extracted ellipticity curve are similar to the red ellipticity models; this part of the curve is observed as the most reliable part of the ellipticity curve (Hobiger *et al*., 2013). Therefore, the models that correspond with that part of the curve should be used for evaluating the Vs profile.

In Figure 3.5, the black dotted line is the extracted ellipticity curve from the histogram and the colored lines represent a different model; the color of each line refers to the misfit value of that model. The red lines, which represent the lowest misfit models, align with the ellipticity curve's right side. The associated Vs profiles are displayed in Figure 3.6. Again, the colored lines refer to the misfit value in the Vs profile where red is the lowest misfit; note that the misfit color value changes from the ellipticity to the Vs profile. This 1-layer model shows an obvious boundary around 38 m, which is the depth to bedrock as constrained in the inversion parameters. As a result, the average velocity of the first layer is ~350 m/s, which coincides with the average Vs of the sediments determined from the HVSR calculations in Section 3.2.

In order to assign a NEHRP site hazard classification, the Vs30 must be determined, however in this model our average Vs for the first layer is 350 m/s, which would classify the site as a Class D (stiff soil profile). Based on both the HVSR and Rayleigh wave ellipticity, this site is interpreted as a D seismic hazard class. The following section applies the two processing methods to field data collected in each hazard classification as originally assigned by the surficial materials hazard map. The results from these two processing techniques enabled real Vs profiles to be determined from field data for the first time in Hartford County, Connecticut. The classifications assigned from the field results were then compared to the surficial materials hazard classification. These classifications were then remapped where necessary.

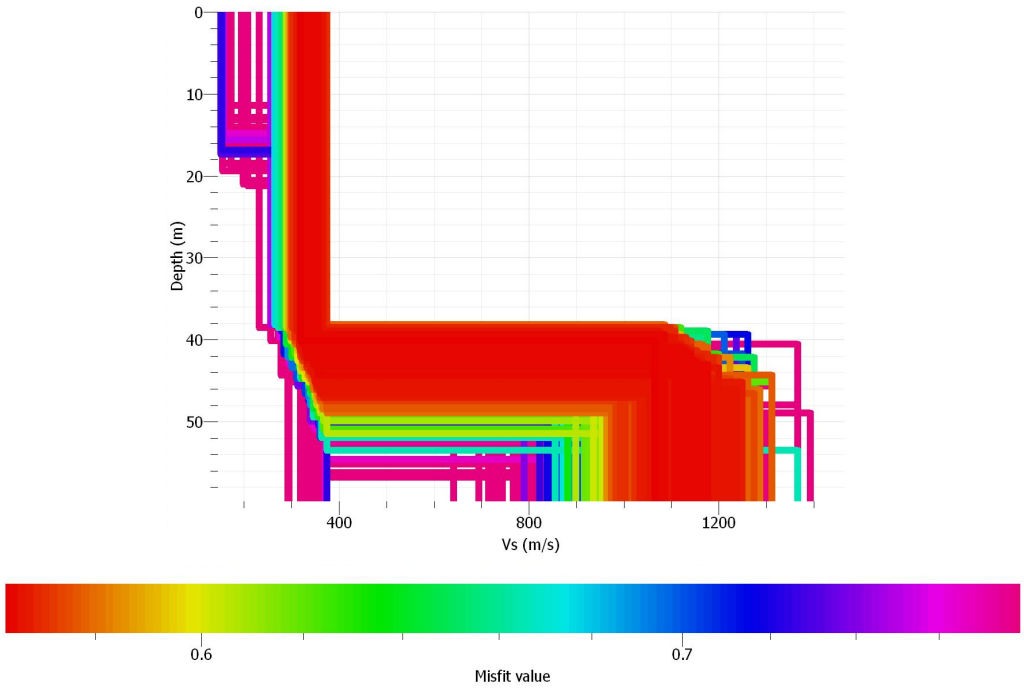

Figure 3.6. Velocity Profile from Rayleigh Wave Ellipticity of Haddam Meadows Well JL-1. From the s-wave profile, there is obvious agreement for a layer interface at 38 m, which is due to the depth constraint in the inversion parameters. The goal of this model was to determine an average s-wave velocity of the sediment layer over rock, which is ~350 m/s. Each line is a different model from the inversion and the color refers to the misfit value of that model.

3.4. RESULTS

At each field site, passive, single-station data were collected around the observed well similar to Photo 3.1. The data were processed using the HVSR technique in order to determine the resonance frequency of that site. Data were also processed using the Rayleigh Wave Ellipticity technique as a supplement to the HVSR in order to determine if additional field techniques were required to obtain an adequate shear-wave velocity profile. This procedure was repeated for each of the thirty specified sites, an example from each site class is discussed in this section. The remaining twenty-four results including HVSR and ground profiles are shown in the Appendix. Data acquisition parameters were kept constant for each site with record length > 20 minutes and sampling frequency = 128 Hz.

Passive seismic surveys were performed at a 4-H Camp in Marlborough, CT which was identified as a Class A site (shallow crystalline rock and till) on the. Three seismometers were used in a huddle test surrounding a 2-inch diameter, PVC casing well with a drilled depth 5 m (16.5 ft), note this well is not drilled to rock. The total record time was 30 minutes with a sampling frequency of 128 Hz.

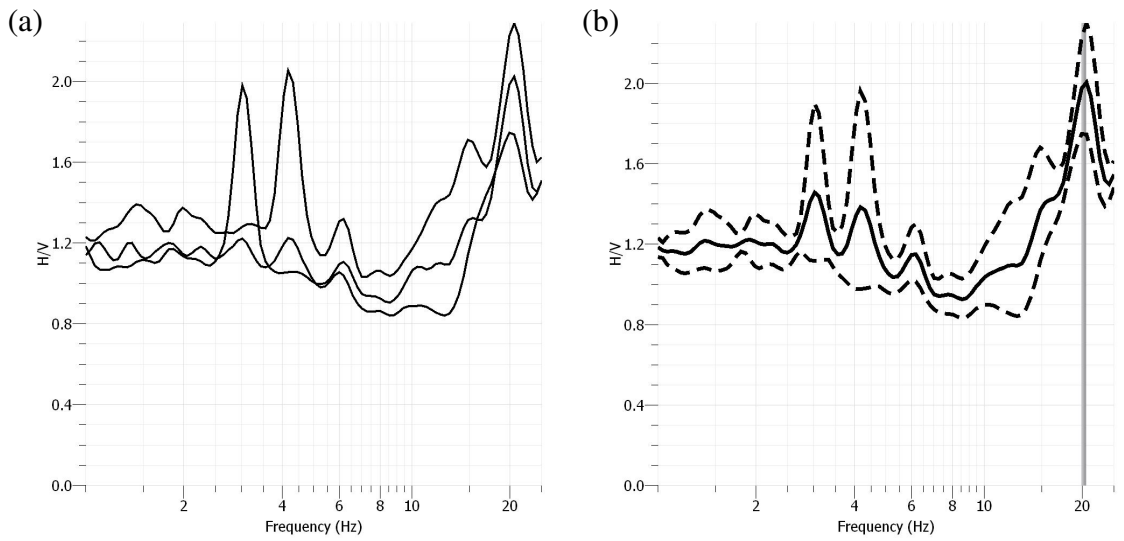

Figure 3.7a-b. Class A: HVSR Huddle Test Measurements from 4-H Camp in Marlborough, CT. (a) Each of the three single-station measurements are displayed as frequency vs. H/V amplitude. A common peak frequency is observed ~20.1 Hz, this peak is perceived as the fundamental frequency. However, other lower frequency peaks with similar amplitudes are seen on different HVSR curves. (b) The average HVSR curve from (a) is displayed as the solid black line with respect to frequency and H/V amplitude. The two dotted lines represent the upper and lower bounds of the standard deviation. The vertical gray line shows the location of the average fundamental frequency at 20.1 Hz.

All three HVSR curves from the huddle test show a common peak at 20.1 Hz, however, other peaks with similar amplitudes were observed between 3-5 Hz (Figure 3.7a-b). The peak at 20.1 Hz implies a shallow layer interface observed by all three seismometers, which could be assumed to be bedrock, but the lower frequency peaks imply that a deeper layer may be present. Without a borehole log that penetrates deeper, it is difficult to say which the bedrock peak is. The well may have not been drilled deeper because of refusal; this would coincide with the surficial material mapping classification that bedrock is near the surface.

From the TFA results, the 20.1 Hz peak was used to constrain the results seen in Figure 3.7c-d. The inversion models are represented by each colored line in Figure 3.7c and the dotted black line with error bars is the ellipticity curve obtained from the TFA algorithm. The ellipticity peak is observed at 3.2 Hz, which does not match the HVSR curve even though it was constrained.

There is also very little correlation between the models and the ellipticity curve. Another inconsistency can be seen in the Vs profile in Figure 3.7d which shows disagreement in locating the bedrock interface. Even though there lowest misfit models (red) indicate an interface at 76 m and 1500 m/s, these models cannot be considered reliable. From the literature, a high velocity contrast is necessary for the TFA and inversion method to perform. In these results, the amplitude is only 2. At this site, the HVSR method alone would not be sufficient for assigning a seismic hazard classification therefore additional geophysical techniques are necessary.

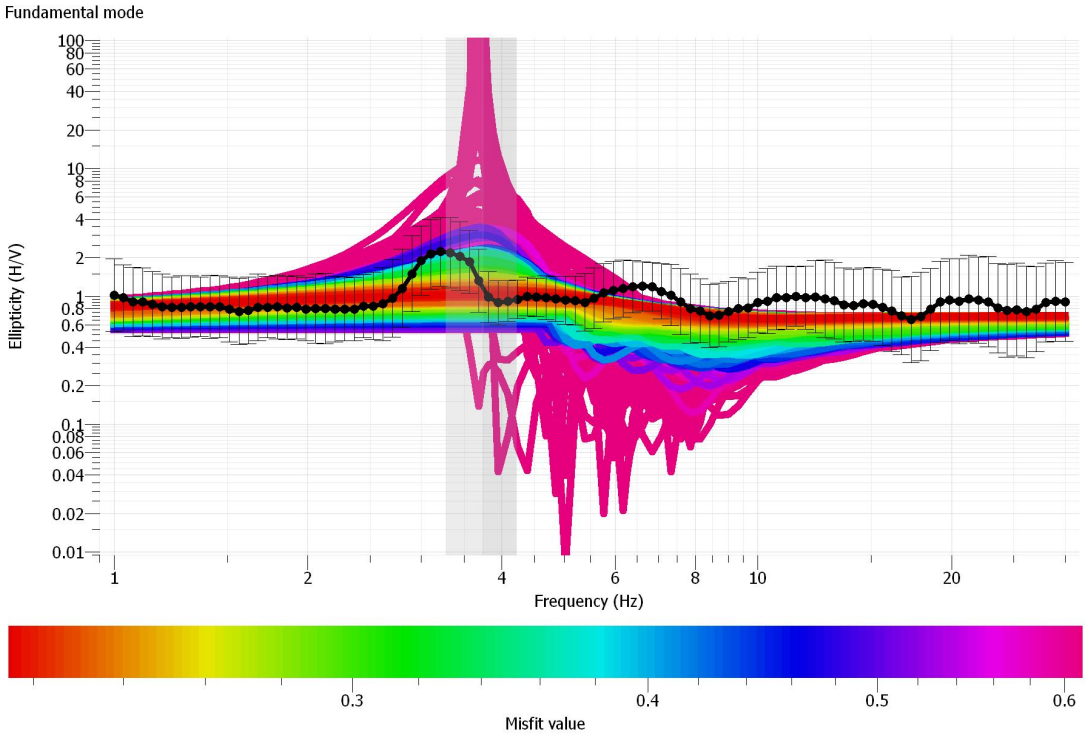

Figure 3.7c. Class A: 4-H Camp Field Site Rayleigh Wave Ellipticity Models. The extracted TFA ellipticity curve is shown as the dotted black line with error bars and the inversion models are shown as the colored lines. The vertical axis is the ellipticity ratio amplitude, the horizontal axis is frequency (Hz) and the vertical purple box is the ellipticity peak's standard deviation. The color refers to different misfit values as seen on the color bar below the figure. If the colored models aligned with the black ellipticity curve, they would be considered best fits; however, the models here do not.

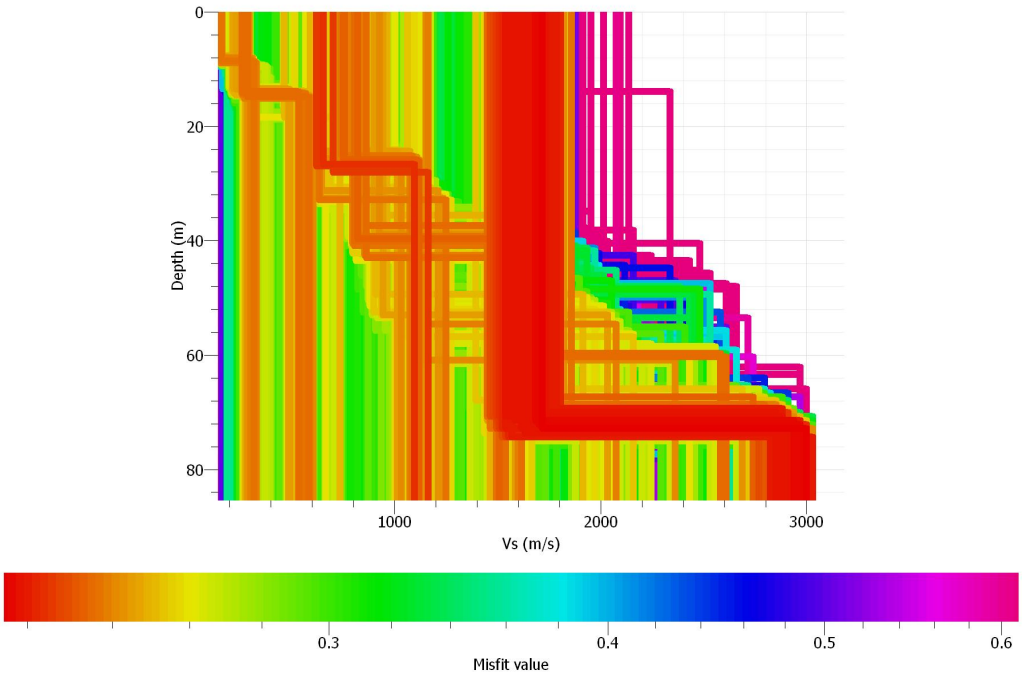

Figure 3.7d. Class A: 4-H Camp Field Site Shear-wave Velocity Profiles from Inversion. Each 2-layer Vs model is represented by each colored line where the color refers to the misfit value. The red models have the lowest misfit and the pink have the highest misfit, however, multiple models have a low misfit, but great variation in layer thickness. These inconsistencies may be due to the ellipticity curve's poor fit in Figure 4.7c. Without additional information, such as depth to rock, an adequate evaluation cannot be made for seismic hazard classification.

In Rocky Hill, CT, four passive seismic measurements were taken at Dinosaur State Park near the old barn's domestic well; this site was considered a B class by the surficial materials hazard map with sedimentary rock and till <4.6 m thick.. Figure 3.8a-b displays the HVSR results from the huddle test measurements with a clear, sharp peak at 3.78 Hz with minimal deviation from all four seismometers. This peak frequency agreement at 3.78 Hz confirms the 1-D earth assumption of the site. The depth to rock at this site is unknown because the original well log could not be found; therefore additional information is needed to calculate the actual Vs structure.

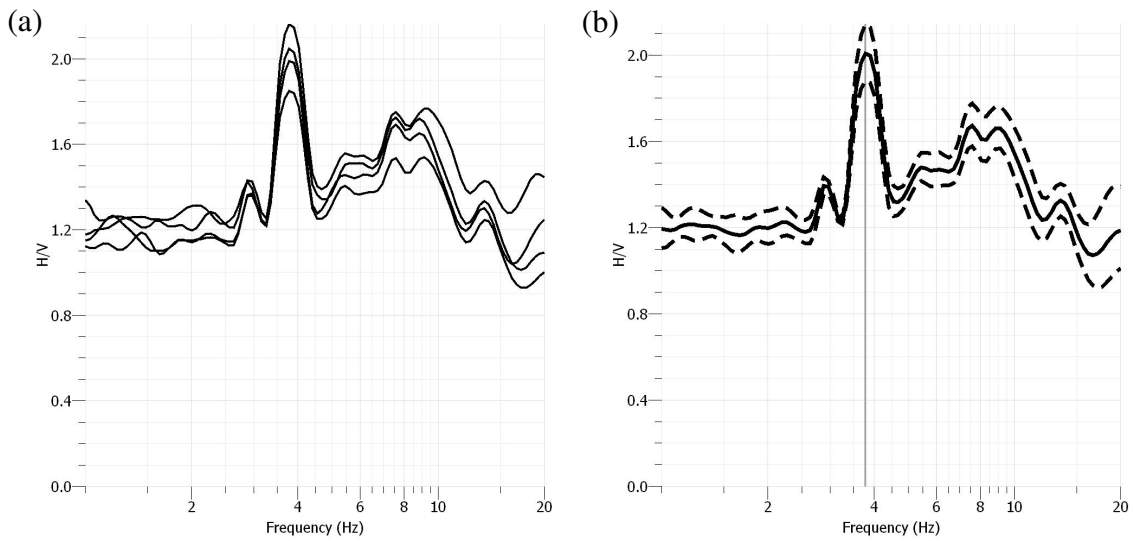

Figure 3.8a-b. Class B: HVSR Huddle Test Results from Dinosaur State Park in Rocky Hill, CT. (a) Each of the three single-station measurements is displayed with respect to frequency and H/V amplitude. A common peak is observed at 3.78 Hz, this is understood as the fundamental frequency. (b) The average HVSR curve is shown as a solid black line and the upper and lower standard deviations are the dotted black lines. The vertical gray line indicates the average peak frequency.

When this data were used in the TFA, poor ellipticity results were observed (Figure 4.8c) which shows little agreement between the extracted ellipticity curve (black dotted line) and inversion models (colored lines). Although the red lines have the lowest misfit value, the green lines show better agreement on the peak and right flank of the extracted ellipticity curve. From these selected green-colored models, the corresponding Vs profiles are shown in Figure 3.8d where an obvious layer interface is seen around 15 m with a 240 m/s average velocity. If the 240 m/s Vs and 15 m layer depth as used in Eq. 3.5, the resulting resonance frequency is 4 Hz, which corresponds to the HVSR results in Figure 3.8a-b. Based on average Vs, the sediment based site class is D, however, the NEHRP requires Vs30 which means the average velocity of the bedrock needs to be included in the Vs30 calculation. This increases the average Vs to 340 m/s, which would still be considered a D class, not a B class. For this site, additional field techniques should be considered for an improved hazard classification.

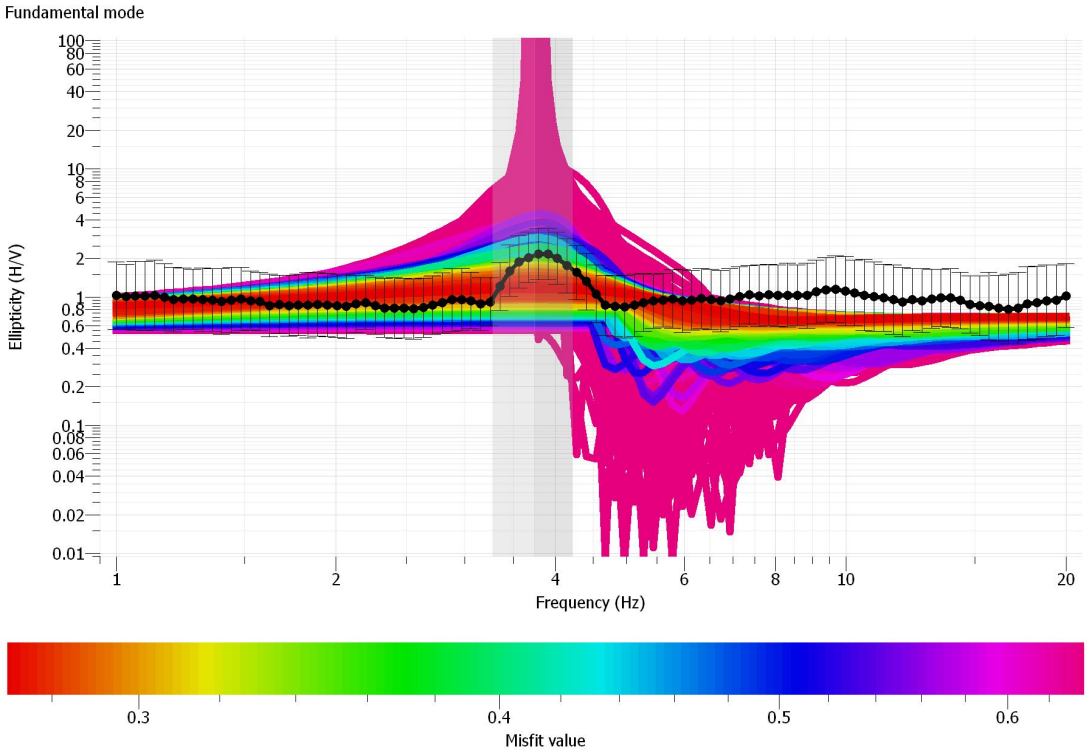

Figure 3.8c. Class B: Dinosaur State Park Field Site Rayleigh Wave Ellipticity Models. The extracted TFA ellipticity curve from the HVSR curve in Figure 4.8a is shown as the black dotted line with error bars. The models created from the inversion are the colored lines where red refers to a lower misfit and the pink refers to a higher misfit. The curves are plotted as frequency vs. ellipticity ratio with a vertical purple box to indicate the standard deviation of the ellipticity peak. A best fit model is defined to correlate the black dotted line with the models at the peak and right flank of the curve. This result shows a poor fit between the extracted curve and lowest misfit models. However, the green models exhibit a better fit to the extracted curve and were used for generating Vs profiles in Figure 3.8d.

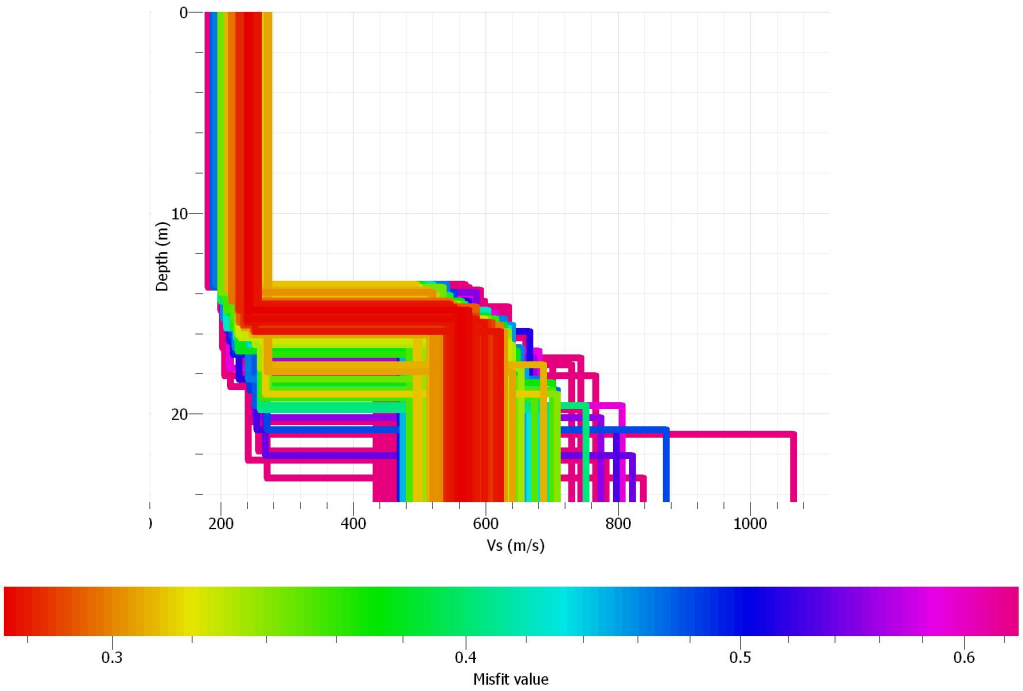

Figure 3.8d. Class B: Dinosaur State Park Field Site Shear-wave Velocity Profiles from Inversion. Each 2-layer Vs model is a colored line where color refers to the model's misfit value. The red models have the lowest misfit and the pink have the highest misfit. The models seen in this figure were selected from the best fitting ellipticity models in Figure 4.8c. The low-misfit models cluster around an interface at 15 m with average sediment Vs of 240 m/s.

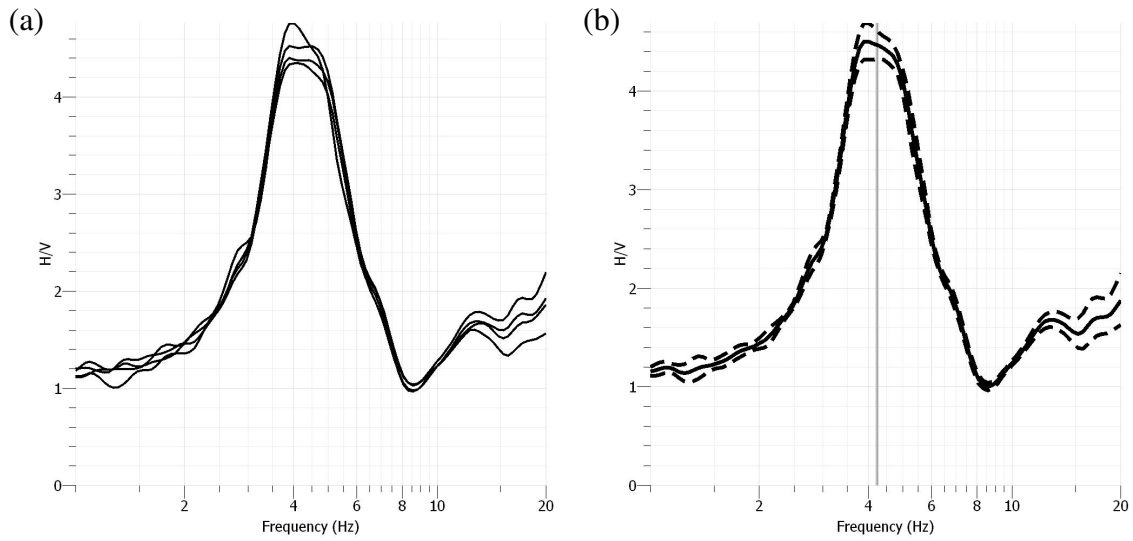

Figure 3.9a-b. Class C: HVSR Huddle Tests from a Department of Corrections facility in Enfield, CT. (a) Each of the four single-station HVSR measurements are displayed as frequency vs. H/V amplitude. The common peak observed is ~4.4 Hz. This peak is perceived as the fundamental frequency of the site. (b) The average HVSR curve from the curves in (a) is displayed as the solid black line with respect to frequency and H/V amplitude. The two dotted black lines represent the upper and lower standard deviations. The vertical gray line indicates the average fundamental frequency at 4.4 Hz.

A Department of Corrections facility in Enfield, CT was classified as a C class (thick till) by the surficial materials hazard map. Four seismometers were used in a huddle test outside the onsite well housing which observed a common peak ~4.4 Hz (Figure 3.9a-b). The depth to bedrock recorded by the well log is 41 m. Based on these values, the average Vs, as calculated by Eq. 3.5, is 721.6 m/s of the sediments. As previously stated, the NEHRP uses the Vs30, not the average Vs of the sediments. With an adjusted 30 m depth, the Vs30 at this site decreases to 528 m/s, C class which matches the original surficial materials site classification.

After the TFA, the extracted ellipticity curve (black line with error bars) is overlaid on the colored inversion models in Figure 3.9c. The ellipticity peak value correlates with the HVSR peak in Figure 4.9a-b and the lowest misfit models (red) fit the broad ellipticity peak; however, the right flank does not align with any models. The Vs profile generated from each ellipticity model is shown in Figure 3.9d. Three 2-layer Vs models stand out with depths ranging from 25

to 56 m, but none shown a layer interface at 41 m. Based on Eq. 3.5 again, with a 25 m depth and 400 m/s, the resulting resonance frequency is 4 Hz; a 45 m depth and 750 m/s, the resonance frequency is 4.2 Hz; a 56 m depth and 950 m/s, the resonance frequency is also 4.2 Hz. These calculations coincide with the peak frequency observed on the HVSR curve, which was also used as a constraint in the inversion model. However, based on the well log, the sediments recorded include a till layer above bedrock around the modeled 25 m depth. This till layer could be masking the bedrock interface because the impedance contrast between till and rock does not meet the 2:1 requirement. Therefore based on this information, the new estimated Vs30 at this site is 452 m/s, which still classifies as C.

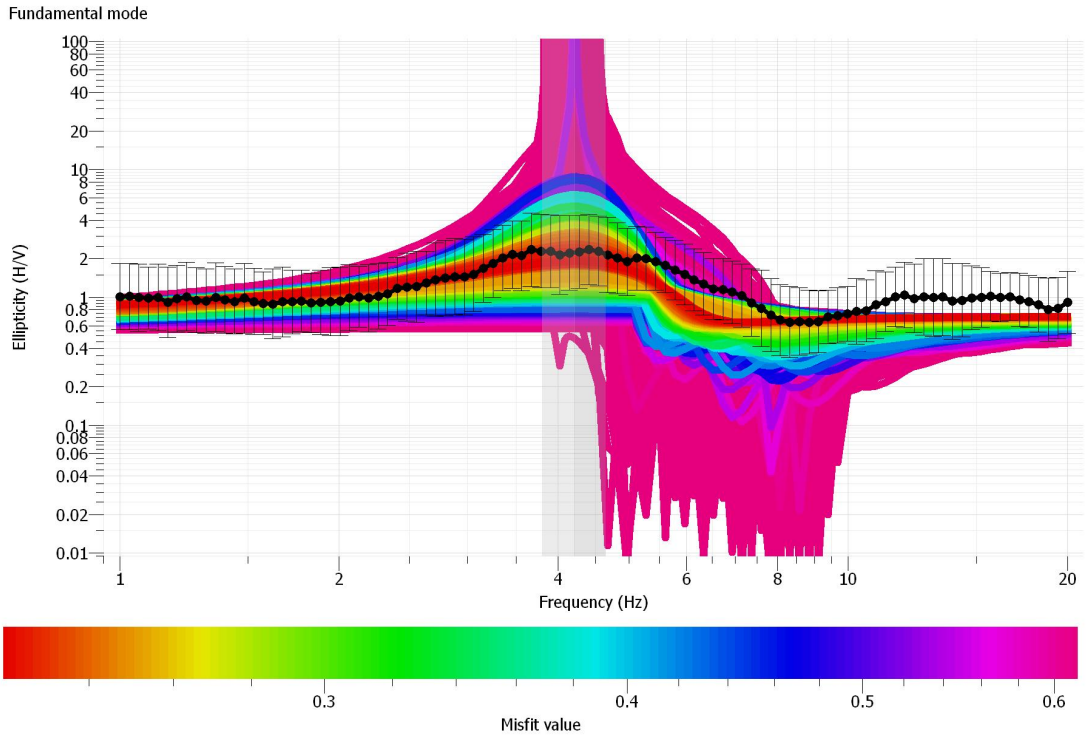

Figure 3.9c Class C: Department of Corrections Facility Field Site Rayleigh Wave Ellipticity Models. The extracted TFA ellipticity curve from the HVSR curve in Figure 3.9a is shown as the dotted black line with error bars. The inversion models are shown as the colored lines where red has a lower misfit and pink as a higher misfit value. The vertical purple box is the ellipticity peak's standard deviation. If the colored models correlate to the black ellipticity curve's peak and right flank, the models are considered a best fit. In this figure, only the peaks align with the red colored models. These models are used for generating Vs profiles from inversion (Figure 3.9d).

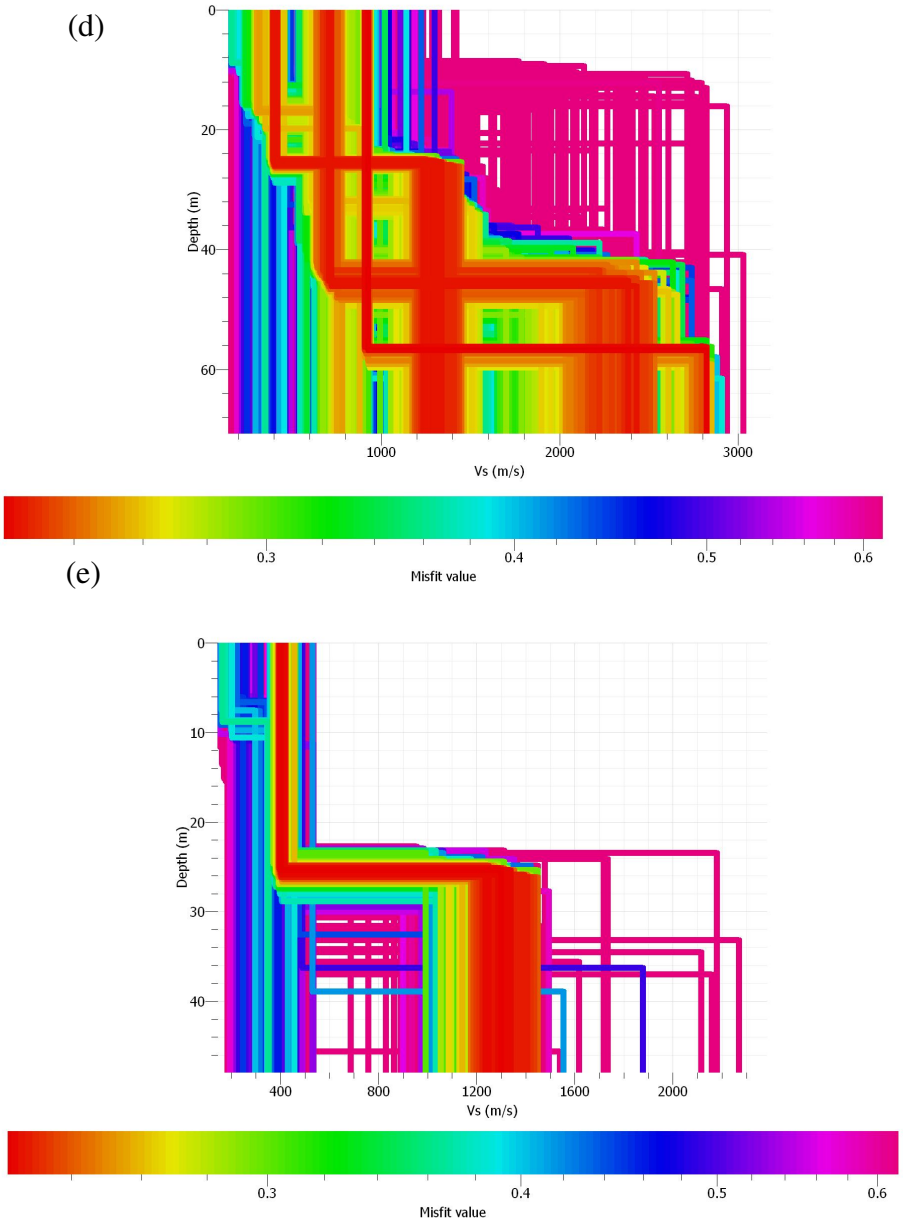

Figure 3.9d-e. Class C: Department of Corrections Field Site Shear-wave Velocity Profiles from Inversion. Each colored line represents a different 2-layer model generated by the ellipticity models in Figure 3.9c; red colored models have a lower misfit and pink models have a higher misfit value. (d) Three obvious 2-layer models are displayed with varying interface depths. However, the recorded depth to rock is 41 m, which none of these models correspond, but the well log does indicate a till layer overlying the bedrock around 25 m. Considering this 25 m depth and associated Vs, the observed fundamental frequency in Figure 4.9a agrees with these model parameters. (e) The assumed till layer model is separated from the other models.

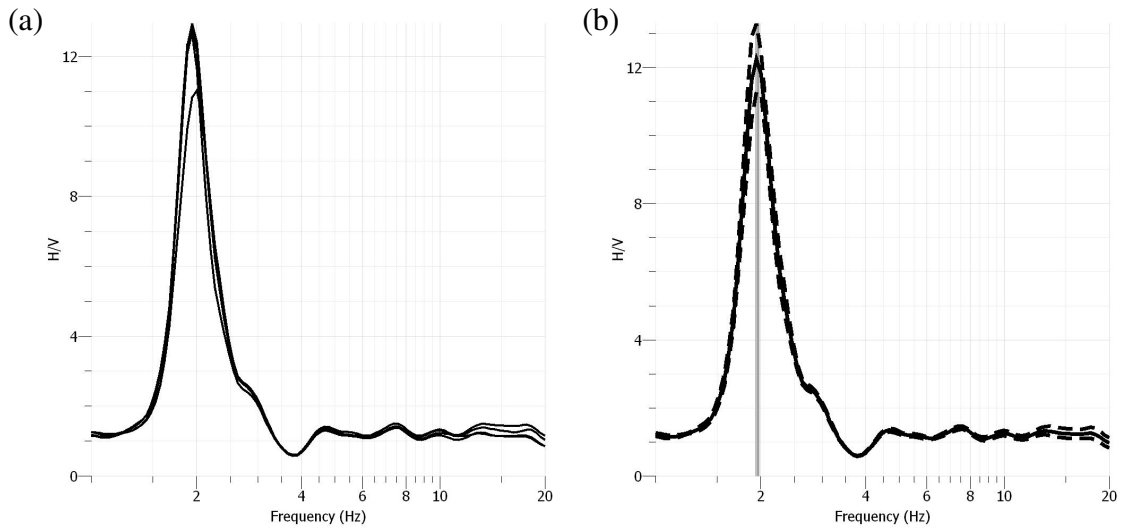

Figure 3.10a-b. Class D: HVSR Huddle Test Measurements from Knollwood Lane, in Avon, CT. (a) Each of the four single-station measurements exhibit a common sharp peak at frequency 1.9 Hz with amplitudes >12. This peak is identified as the fundamental frequency. This single peak observed on all four records confirms the 1-D earth assumption at the field site. (b) The average HVSR curve gathered from the four curves in (a) is displayed as the solid black line with respect to frequency and H/V amplitude. The two dashed lines represent the upper and lower standard deviation bounds. The vertical gray line indicates the observed fundamental frequency value, 1.9 Hz.

A D class (glacial outwash, sand and gravel) site was selected in Avon, CT at the intersection of Knollwood Lane and Reverknoll Lane where four seismometers were used in a huddle test around a monitoring well. The observed resonance frequency from the huddle test was 1.9 Hz (Figure 3.10a-b), which infers a deep depth to rock, which according to the well log, is confirmed at 61.4 m. Based on these values and Eq. 3.5, the average shear-wave velocity of the sediments is 467 m/s, a C class by NEHRP, not D.

The TFA and inversion results did not provide favorable results. The extracted ellipticity curve gave a peak at 4 Hz (Figure 3.10c), a 2 Hz increase over the HVSR curve. The models (colored lines) show a peak around 2 Hz, most likely due to the inclusion of the HVSR curve as a constraint. The associated velocity profiles in Figure 3.10d show two well-defined layer boundaries around 28 m and 70 m, indicated by the warm colored lines. Neither layers correlate

with the bedrock boundary and no explanation can be deduced from the well log. Based on the irregularity of the extracted ellipticity curve, this processing method should not be considered for assigning a hazard classification at this site.

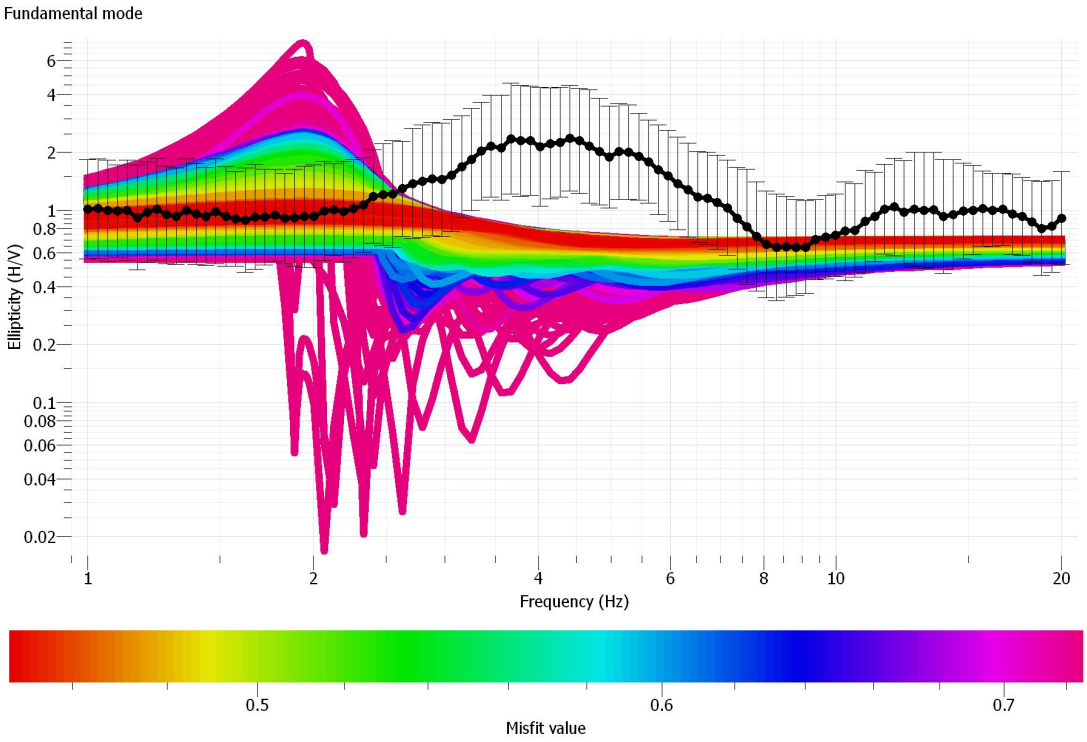

Figure 3.10c. Class D: Knollwood Lane Field Site Rayleigh Wave Ellipticity Models. The extracted TFA curve from the HVSR curve in Figure 3.10a is displayed as the dotted black line. The colored lines are the resulting inversion ellipticity models where the color infers the misfit model value. A best fit model would align with the peak and right flank of the black extracted curve, however, the ellipticity curve in this figure is shifted 2 Hz higher than every model. When the TFA is applied to an HVSR curve, the amplitude is decreased, but the overall frequency should not change. Due to this discrepancy between the HVSR curve and extracted ellipticity curve, the Vs profiles generated should not be considered.

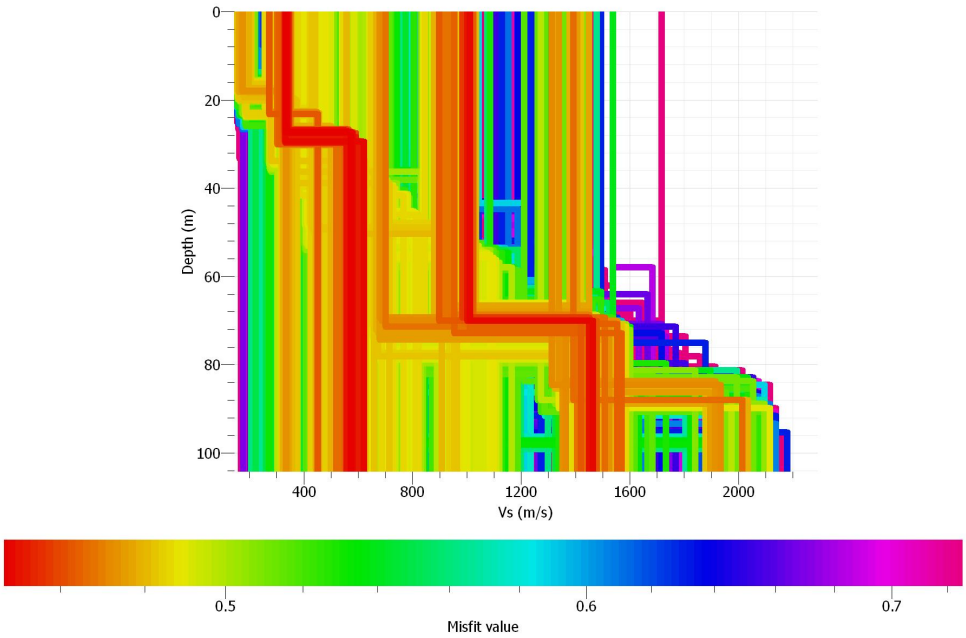

Figure 3.10d. Class D: Knollwood Lane Field Site Shear-wave Velocity Profiles from Inversion. Each colored line represents a different 2-layer model generated by the ellipticity models in Figure 3.10c. The color refers to the model's misfit value. Although a depth to rock is known at this site, there is low confidence in these velocity profiles because of the inconsistencies between the extracted ellipticity curve and the HVSR curve in Figure 3.10a.

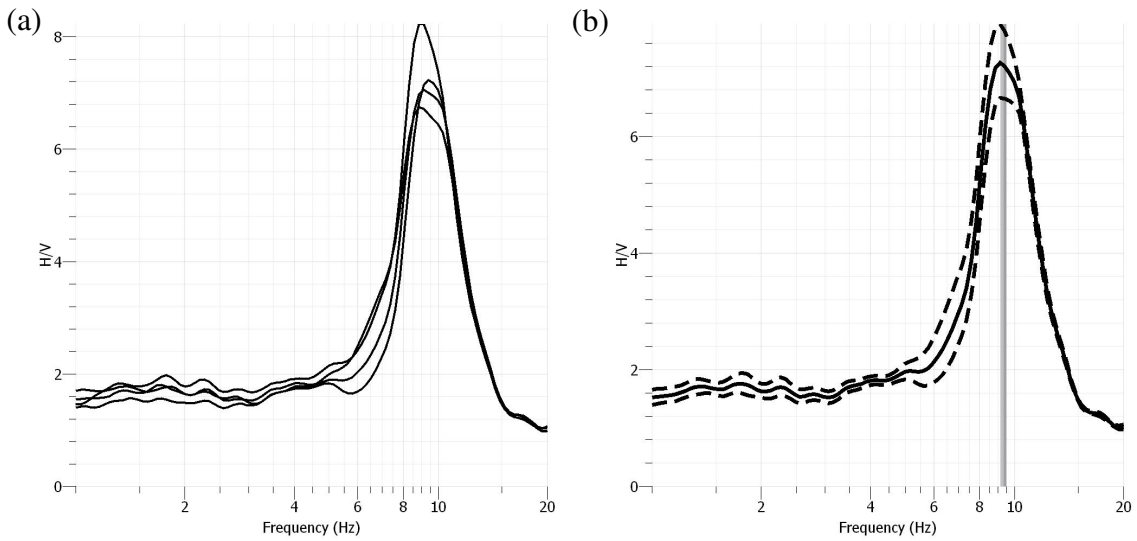

Figure 3.11a-b. Class E: HVSR Huddle Test Measurements from Elizabeth Park in West Hartford, CT. (a) Four single-station measurements are displayed by the black lines with respect to frequency and H/V amplitude. These clean peaks all exhibit a high amplitude and common peak frequency around 9.3 Hz. This frequency is observed as the fundamental frequency of the field site, which is recognized to meet the 1-D earth assumption since no other peaks excite. (b) The average HVSR curve, displayed in black, is determined from the four curves in (a). The two dashed black lines represent the upper and lower standard deviations. The vertical gray line indicates the fundamental mode frequency, 9.3 Hz.

An E class, the highest hazard level defined by glacial lake clays and fines, site was assigned to the area around a monitoring well at Elizabeth Park in West Hartford, CT. This monitoring well was not drilled to rock; however, another well log from the park recorded a rock depth of 17.7 m. That monitoring well was never found, but had a recorded location less than 50 m away from the borehole used for this survey. From the huddle test, a resonance frequency of 9.3 Hz was observed on the HVSR curve (Figure 3.11a-b). If the depth to rock was the same at both wells, the average Vs of the sediments would be ~658 m/s based on Eq. 3.5.

After the TFA and inversions, the extracted ellipticity curve shows a peak around 6 Hz (Figure 3.11c), rather than 9.3 Hz on the HVSR curve. Due to this irregularity, the Vs models created from this inversion technique and ellipticity should not be considered without additional information. However, the inversion (Figure 3.11d) shows two distinctive layer models with

interfaces around 12 m, 250 m/s and 33 m 1200 m/s. Based on Eq. 3.5, these models would have 5.2 Hz and 9.1 Hz resonance frequencies respectively. The first layer model (12 m, 250 m/s) can immediately be discarded; the second layer model (33 m, 1200 m/s) appears more plausible, but without a known depth to bedrock at this location and the ellipticity irregularity, this result cannot be considered until additional information and geophysical techniques are performed.

After the passive surveys results from these five sites, the site classes assigned using the field results should not be considered unless there is a known depth to rock. However, issues appear when the depth to rock is above 30 m because it can increase the Vs30 and alter the NEHRP classification. Additional geophysical techniques are recommended in order to assign a hazard classification with confidence. The next chapter discusses the use of the Multi-channel Analysis of Surface Waves active field technique in addition to HVSR for assigning a hazard classification.

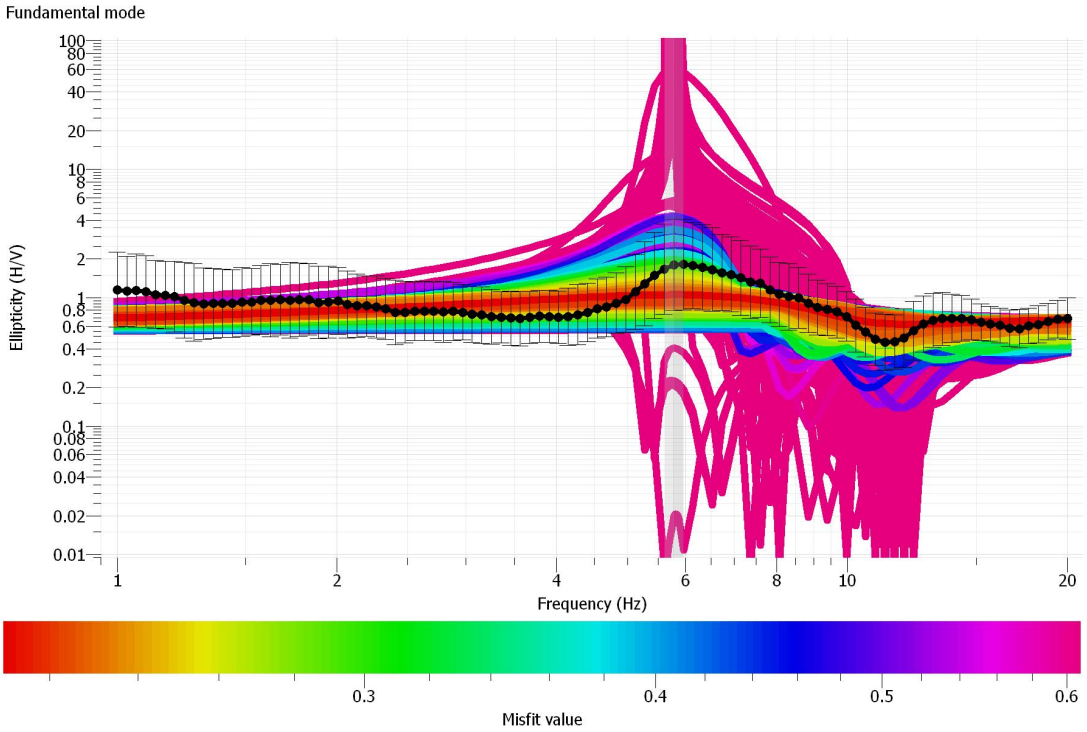

Figure 3.11c. Class E: Elizabeth Park Field Site Rayleigh Wave Ellipticity Models. The extracted TFA ellipticity curve from the HVSR curve in 4.11a is shown as the dotted black line and error bars. Each colored line represents the ellipticity models generated where color indicates the level of misfit. The faint, vertical purple box around 6 Hz indicates the standard deviation of the ellipticity peak frequency; this peak differs by 3 Hz from the HVSR curve which decreases the confidence of the models. Without additional information, the models generated should not be considered for assigned a hazard classification. A best fit inversion model would correspond to the peak and right flank of the extracted ellipticity peak.

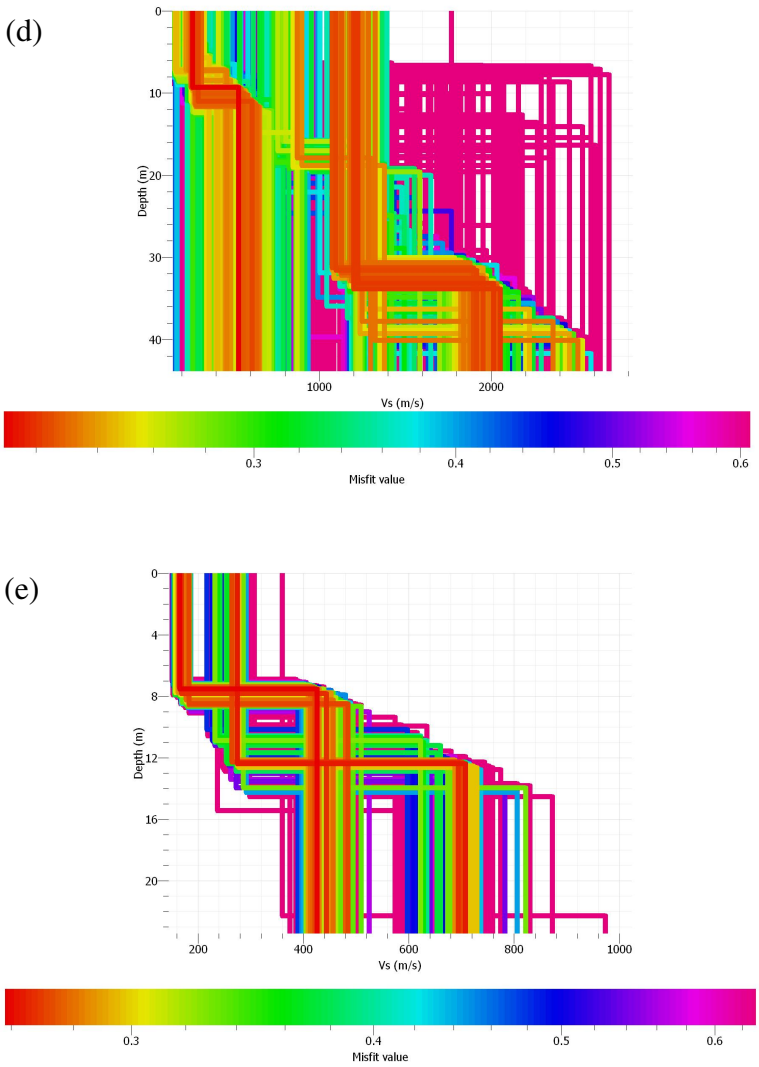

Figure 3.11d-e. Class E: Elizabeth Park Field Site Shear-wave Velocity Profiles from Inversion. Each colored line represents a different 2-layer model corresponding to the ellipticity models in Figure 3.11c; the line's color refers to the model's misfit value. (d) Two obvious layer interfaces dominate the velocity profile at 12 m and 33 m. The 12 m interface is not considered as the depth to rock because the observed Vs = 250 m/s. The 33 m depth is plausible as a depth to rock based on calculations; the corresponding fundamental frequency is 9.1 Hz. However, the borehole log does not record a bedrock interface, therefore additional information should be considered before making a confident seismic hazard classification.

4. ACTIVE MULTI-CHANNEL ANALYSIS OF SURFACE WAVES

In this chapter, results of the active Multi-channel Analysis of Surface Waves (MASW) field technique used at ten of the thirty field sites in Hartford County, Connecticut are discussed. Two sites per seismic hazard class were surveyed. The data acquisition, processing procedures and results from these active surveys in conjunction with passive data are discussed and compared to the original hazard class assessment.

4.1. BACKGROUND INFORMATION

In addition to conventional seismic reflection and refraction seismic methods, geophysicists also use surface wave dispersion techniques to characterize the subsurface (e.g. Haskell, 1953; Ewing *et al*., 1957; Oliver, 1962). This method utilizes surface wave dispersion as it travels across a free surface (Park *et al*., 1999). Surface wave energy exhibits dispersive characteristics as it propagates through the earth's uppermost layers. Based on the theory of wave propagation through a layered media (Eq. 4.1), dispersion is observed as the wave's phase velocity changes at different wavelengths or frequencies; a dispersion curve is the illustrated representation of this relationship. By quantifying how surface waves disperse through a vertical plane, the velocity structure can be estimated as it is a function of the shear modulus. The shear modulus is important to geophysicists and geotechnical engineers because it describes the rigidity of a given material (Park et al., 1997).

The active Multi-channel Analysis of Surface Waves (MASW) method, as developed by the Kansas Geological Survey has been used to estimate subsurface shear-wave velocity structure (Park et al., 1999). The procedure involves three main parts: data acquisition, dispersion curve

picking and dispersion curve inversion (Xia et al., 2004). In contrast to passive seismic surveys, active surveys use an impulsive energy source to excite the ground and induce surface wave propagation. This surface wave motion, typically Rayleigh Wave motion, is measured along an array of geophones that are coupled with the ground's surface. Wave propagation is observed as a dispersion curve, where dispersion is the relationship between frequency and its associated propagation velocity known as phase velocity (Park, 1999). The velocity profile is the result of dispersion curve inversion where layer interfaces are differentiated by changes in these velocities with depth.

The geometry of the MASW array depends on the anticipated results. Geometric variables to consider are geophone station spacing, source offset, sampling frequency and total length of the array. An improper field setup can lead to data acquisition problems such as spatial aliasing, higher modes dominating the fundamental mode and poor signal-to-noise ratios which may obstruct the results (Park et al., 2004). A more detailed description of data acquisition parameters are discussed in Section 4.2.

Dispersive characteristics are derived from the elastic properties of the earth material layers such as density, ρ, and associated elastic constants. The linear stress-strain relationship within these materials is described by these elastic constants. These variables are listed in Table 4.1. From the relationships between these elastic properties, the governing equation for elastic motion through a medium as described by (Pei, 2007):

$$\rho \frac{\partial^2 u_i}{\partial t^2} = \tau_{ji,j} + f_i \qquad \text{(Eq. 4.1)}$$

Where ρ is density of the medium, u_i the component displacement, τ the stress and *f* the body force.

	λ *or* μ	μ *or* σ	*E or* σ	*K or* μ
Lame's constant λ	λ	$\lambda = \frac{2\mu\sigma}{1-2\sigma}$	$\lambda = \frac{\mu E}{(1+\sigma)(1-2\sigma)}$	$\lambda = K - \frac{2}{3}\mu$
Shear Modulus μ	μ	μ	$\mu = \frac{E}{2(1+\sigma)}$	μ
Bulk Modulus K	$K = \frac{(3\lambda+2\mu)}{\lambda+\mu}$	$K = \frac{2\mu(1+\sigma)}{3(1-2\sigma)}$	$K = \frac{E}{3(1-2\sigma)}$	K
Young's Modulus E	$E = \frac{\mu(3\lambda+2\mu)}{\lambda+\sigma}$	$E = 2\mu(1+\sigma)$	E	$E = \frac{9K\mu}{3K+\mu}$
Poisson's Ratio σ	$\sigma = \frac{\lambda}{2(\lambda+\mu)}$	σ	σ	$\sigma = \frac{9K-2\mu}{2(3K+\mu)}$

Table 4.1. Relationship between Elastic Constants for Isotropic Media (Pei, 2007).

Surface waves are composed of Rayleigh waves and Love waves, which are differentiated by their particle motion. Rayleigh wave motion is described as "ground roll" due to its elliptic motion; this is the result of combined vertical and horizontal particle motions in three directions (*u, v, w*) in the vertically polarized (SV) plane:

$$\begin{cases} u = r_1(k,z,\omega)e^{i(kx-\omega t)} \\ v = 0 \\ w = ir_2(k,z,\omega)e^{i(kx-\omega t)} \end{cases} \quad \text{(Eq. 4.2)}$$

Love wave particle motion consists only of horizontal movement in three directions (*u, v, w*) in the horizontally polarized (SH) plane in the form of:

$$\begin{cases} u = 0 \\ v = l_1(k, z, \omega)e^{i(kx-\omega t)} \\ w = 0 \end{cases} \quad \text{(Eq. 4.3)}$$

However, Rayleigh waves are non-dispersive over a uniform half-space and in the absence of a vertical velocity gradient. When Rayleigh wave dispersion is observed, waves penetrate deeper depths with longer wavelengths, but shallower depths with shorter wavelengths. By analyzing Rayleigh waves, shear-wave velocity profiles can be constructed where the shear modulus (μ) is the relationship between shear-wave velocity (Vs) and density (ρ):

$$V_s = \sqrt{\frac{\mu}{\rho}} \qquad \text{and} \qquad \mu = V_s^2\rho \qquad \text{(Eq. 4.4)}$$

For the Vs profile, Poisson's ratio is assumed and the change in density with depth is negligible in comparison to change in shear modulus. From these parameters and the Vs profile, the compressional-wave (P-wave) velocity can also be estimated (Park et al., 1997); however, the p-wave velocity structure is not being considered at this time.

4.2. FIELD SURVEY SETUP

Prior to the field experiment, the depth to rock was identified given the information from the borehole log; the field geometry was also determined based on this known value. The total length of the array depends on the desired depth of penetration; for the purpose of this thesis, the desired depth of penetration is the depth to bedrock. For an optimum active survey, the sampling

depth (z_{max}) is typically considered to be half the wavelength of the profile (Miller, 1999; Park et al., 2002):

$$z_{max} = C_1/2f_1 \quad \text{(Eq. 4.5)}$$

Such that C_1 is the phase velocity of f_1, the lowest frequency that can be recorded. The sampling frequency of the geophone receivers will also determine the allowable depth of penetration to be observed; a lower sampling frequency (e.g. 4.5 Hz) is able to record to deeper depths than a higher sampling frequency receiver (e.g. 40 Hz). Source offset and geophone takeout is also dependent on total array length, however, it must be long enough to allow for the full development of the surface wave, but short enough to avoid strong body and surface wave higher modes dominating the fundamental mode (Park, 2004).

MASW observes horizontally propagating plane waves; once the surface wave has traveled a certain distance from its source, it is considered stable. Therefore it is important to remember that longer wavelengths or lower frequencies require a longer distance to stabilize (Park *et al*., 2002). However, the maximum geophone spread can be influenced by body waves and higher mode surface waves, which can then overwhelm the fundamental mode. Higher mode domination, or spatial aliasing, usually occurs at far source offsets due to differing damping ratios that cause the fundamental mode energy to decay more rapidly than higher modes or intrinsic property of the material's elastic modulus (Park, 2005). Geophone takeout will also influence the overall resolution of the dispersion curve; a longer total spread will increase the dispersion curve resolution. Another important parameter to consider is the active seismic source. Depending on the desired depth of penetration, a sledge hammer or weight drop source can be used. In order to obtain deeper depth information (i.e. >30 m), an accelerated weight drop

should be considered for data acquisition; for shallower depths, a sledgehammer >10 lb. should suffice. Optimum field parameters for an MASW survey are displayed in Table 4.1 concerning the relationship between sampling frequency, depth of penetration, offset and geophone takeout (Park *et al*., 2002):

Receiver (Hz)	Max. Depth (m)	Min. Offset (m)	Max. Offset (m)	Receiver Spacing (m)
4.5	50	10	100	1
10	30	10	100	1
40	15	10	100	1

Table 4.1. Optimum Field Parameters for MASW.

An active MASW survey was performed at Haddam Meadows State Park in East Haddam, Connecticut near borehole JL-1. The borehole log provided information about the underlying sediments and depth to bedrock (38 m) which was the survey's desired depth of penetration. Pairs of vertical and horizontal 4.5 Hz geophones were planted every 3 m in the ground along a 72 m fixed, linear array (Photo 4.1) and connected to two geodes to record on 48 channels (Photo 4.2a). The record length was 1 second where the sampling interval was 1 millisecond. A 10 lb. sledgehammer was used as the active source with both vertical and horizontal blows (Photo 4.2 b-c) to induce Rayleigh wave motion. The processing procedures and results from this survey are discussed in the next section.

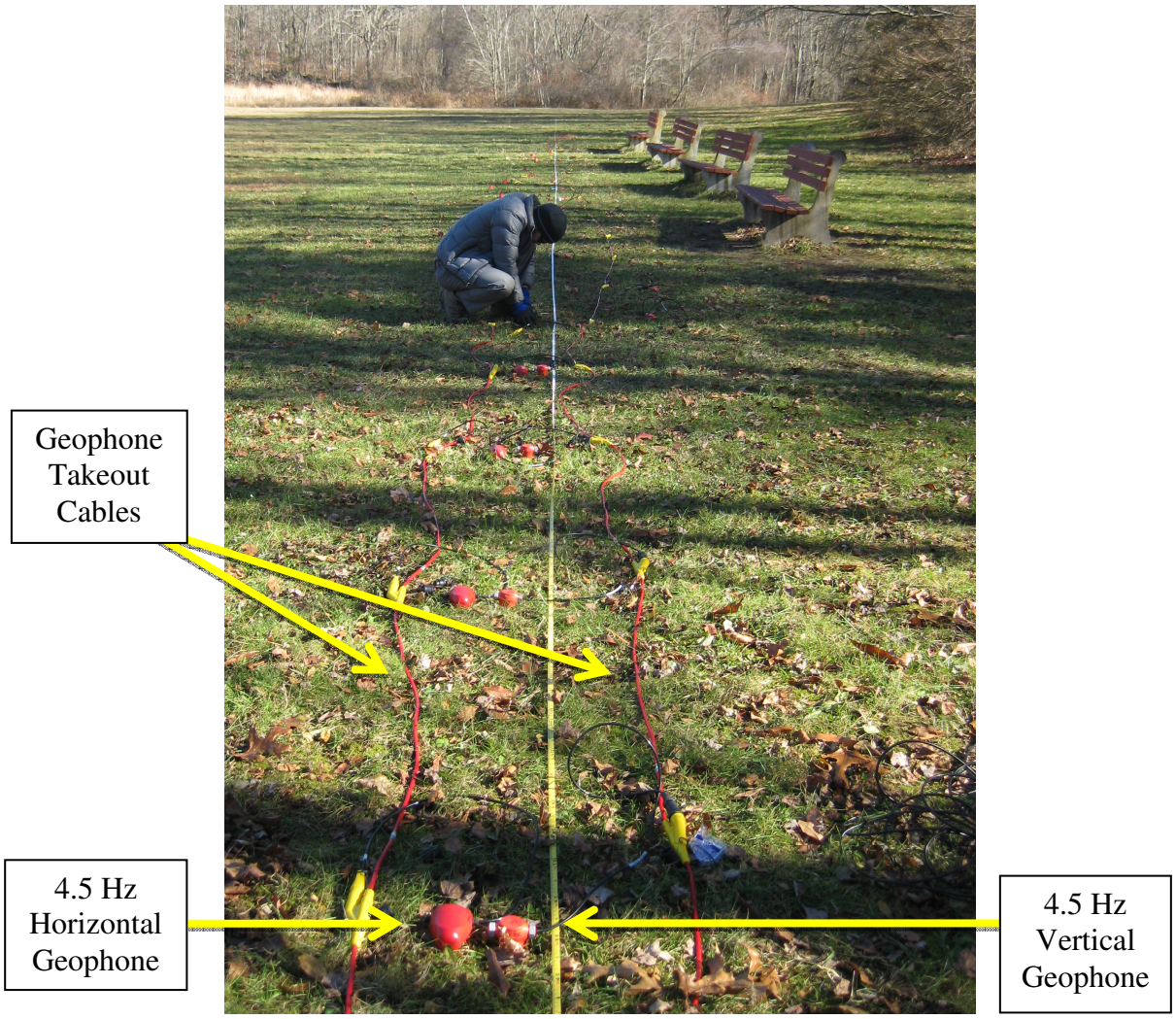

Photo 4.1. Example of MASW Field Setup. Two takeout cables were used to connect the 48 geophones in a linear array. One takeout cable connects twenty-four 4.5 Hz vertical geophones and one takeout cable connects twenty-four 4.5 Hz horizontal geophones. The geophones are placed side-by-side every 1.5 m for a 34.5 m total spread.

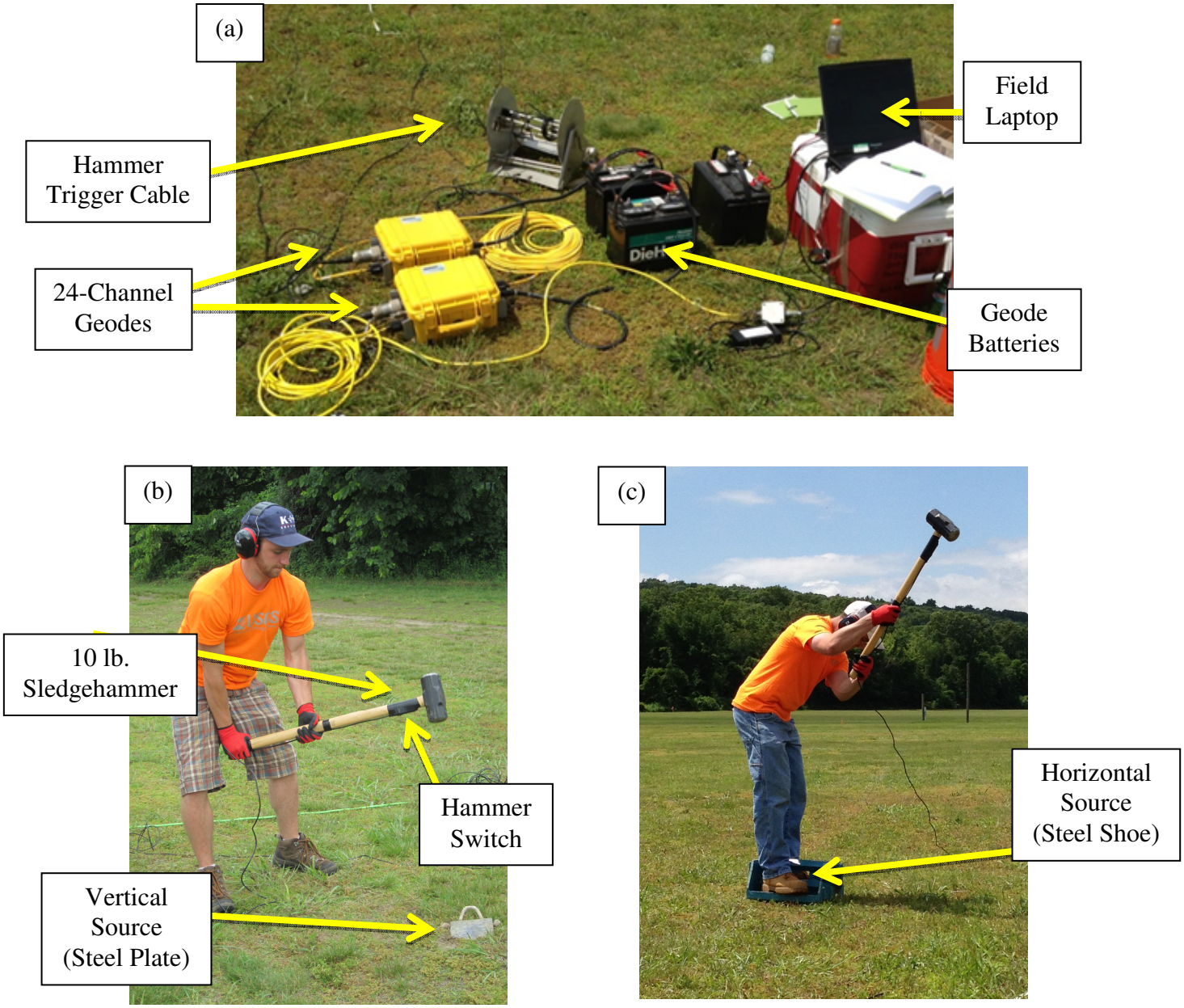

Photo 4.2. MASW Field Equipment. (a) Seismic equipment setup including two 24-channel Geodes to support two take out cables; one cable for 24 vertical geophones and one cable for 24 horizontal geophones seen in Photo 4.1. The hammer trigger cable connects the geode to the hammer to initiate signal recording. The field laptop controls the software for data acquisition and the deep cycle batteries power the entire system. (b) The 10 lb. sledgehammer has a trigger switch duct taped to the hammer arm below the head. A flat, steel plate is coupled to the ground for vertical hammer shots. (c) A blue, steel "shoe" with upright steel plates on two sides is coupled to the ground with metal spikes for horizontal hammer shots.

4.3. DATA PROCESSING

The following three subsections provide the mathematical background and explanation of the processing procedures for data collected at Haddam Meadows State Park, in East Haddam, CT using the Multi-channel Analysis of Surface Waves. All data was collected using the parameters described in Section 4.2 and then processed in *SurfSeis*. After data acquisition, dispersion curves were extracted from the vertical and horizontal geophone data and then inverted in order to obtain a shear-wave velocity profile. HVSR data was also collected at each site and used to constrain the MASW data results.

4.3.1. Data Acquisition

As previously stated, data were collected along an East-West linear array that ran perpendicular to the Connecticut River with borehole JL-1 located halfway through the line at geophone pair 12 (Photo 4.3). Two takeout cables, each with 24 channels, were laid out every 3 m to form the array; one cable connected vertical geophones and one cable connected horizontal geophones. A 10 lb. sledgehammer and flat steel plate were used as the active vertical source; three shots were performed 1 m off the array starting at geophone 1 and finishing at geophone 24. After this survey, the same 10 lb. blue shoe source (Photo 4.2c) was used to induce horizontal motion; the source was placed so that horizontal motion would be in the North-South direction, therefore perpendicular to the geophone array. Three shots were performed on the North and South side of the source at Geophone 1, Geophone 12 and Geophone 24; beginning, middle and end of the line respectively.

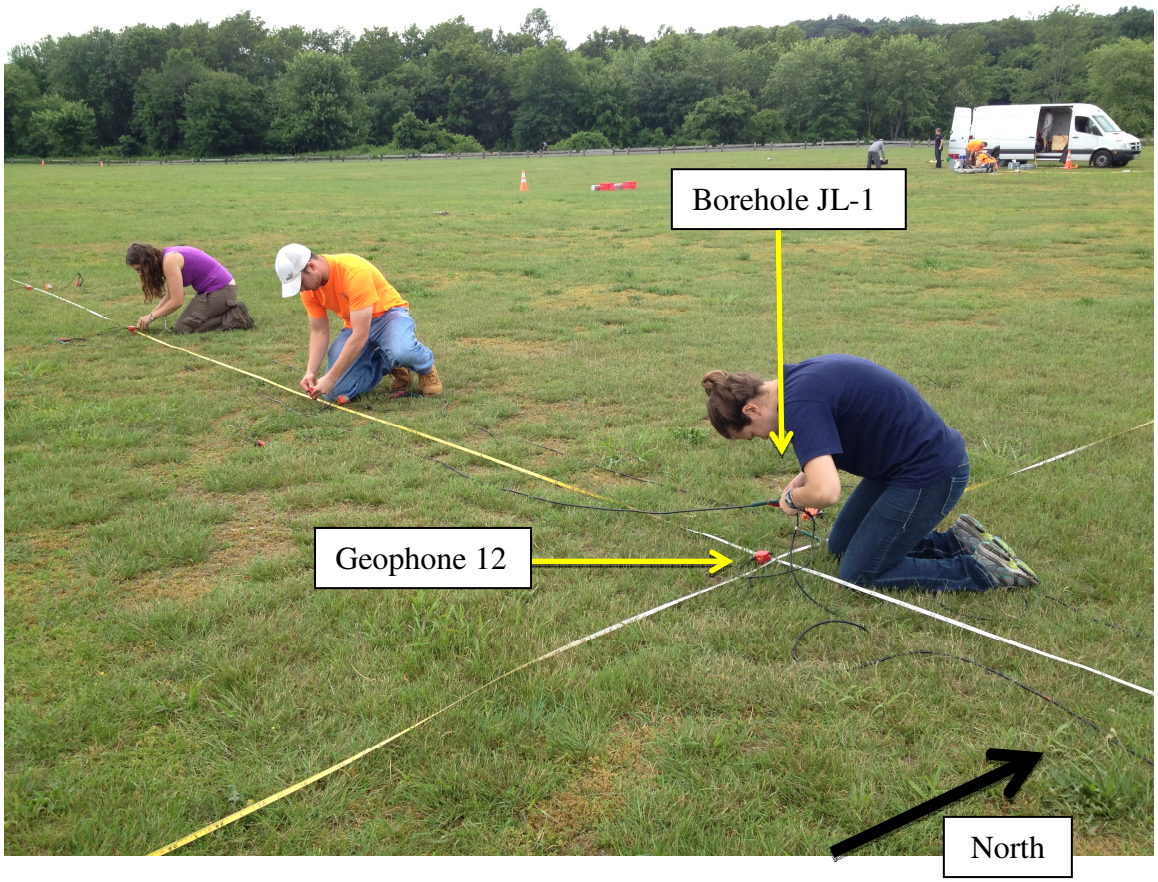

Photo 4.3. Haddam Meadows State Park MASW Field Setup. A linear array was distributed across Haddam Meadows State Park so that JL-1 was located mid-line at Geophone 12. Horizontal and vertical geophone pairs were planted in the ground every 3 m along a 72 m profile starting near the Connecticut River and moving West through the park. A 10 lb. sledgehammer was used to induce both vertical and horizontal surface wave motion throughout the array.

As each sledgehammer shot was done, a shot gather consisting of 48 channels or traces was created (Figure 4.1). This plot is represented as a trace vs. time; as the wave travels across the surface, amplification is seen on the shot record. On trace 24, amplification is obvious at time 0 ms; this implies the location of the source. The record extends for 1 second (or 1000 ms) per shot and three records are created per shot location before moving to the next position along the array. Multiple shots were performed at each geophone location to enlarge the dataset so that the chance of extracting an adequate dispersion curve was increased. A total of 72 vertical shots and 18 horizontal shots were performed along this profile.

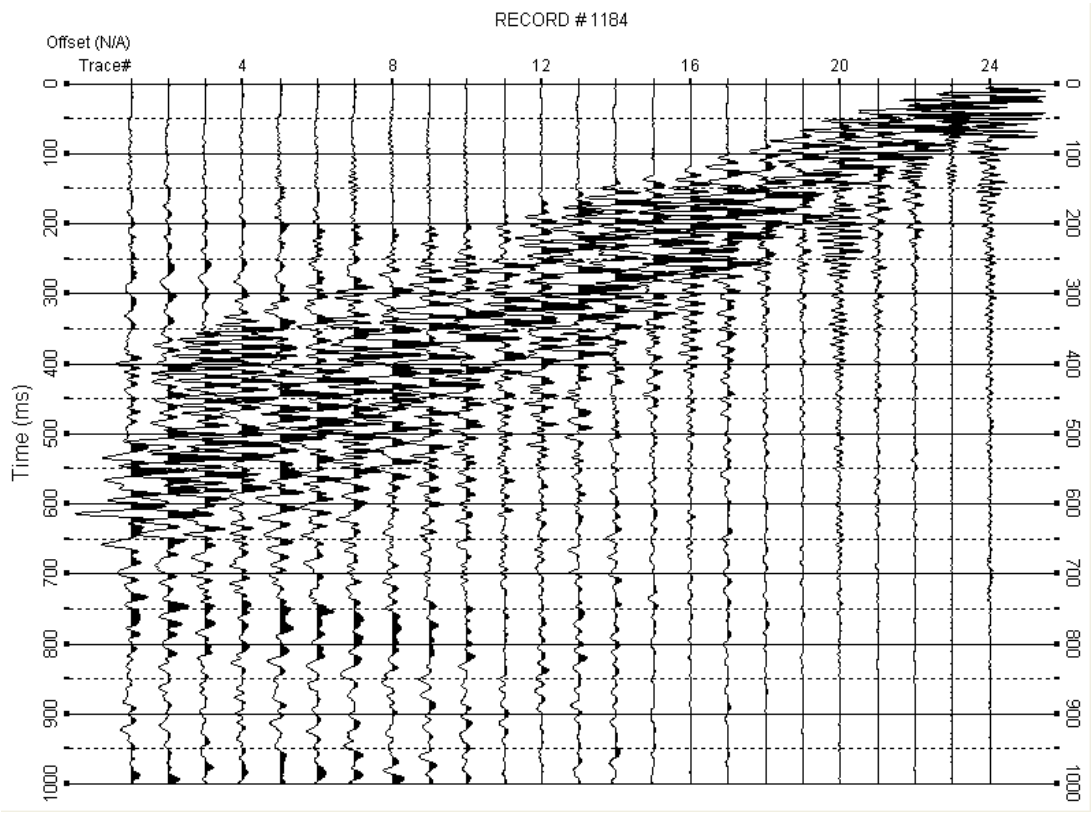

Figure 4.1. Raw Data from Vertical Sledgehammer Shot. This shot gather displays the 24 channels connected to the vertical geophones as trace vs. time (ms). Each trace is recorded for 1000 ms per shot. The location of the source is indicated where amplification is observed on the trace at time 0 ms.

4.3.2. Dispersion Curve Extraction

Each shot gather was processed in the KGS's *SurfSeis* surface wave processing software in order to extract a dispersion curve and create a 1-D shear-wave velocity profile. These dispersion curves, $I(w, c_w)$, were generated from shot gathers $u(x, t)$using the KGS wavefield transformation (Park et al., 1998). This algorithm applies a Fast Fourier Transform (FFT) to time domain data, $u(x, t)$ to create frequency domain data, $U(x, w)$. The frequency domain data $U(x, w)$ can be expressed as the multiplication of the phase P(x,w) and amplitude A(x.w) spectrum (Eq. 4.6):

$$U(x, w) = P(x, w)A(x, w) \quad \text{(Eq. 4.6)}$$

Such that each frequency is separated and arrival time information is preserved in the phase spectrum. The phase spectrum includes the dispersion information while the amplitude spectrum includes other information such as attenuation and spherical divergence. Since $U(x, w)$ can also be expressed as:

$$U(x, w) = \int u(x, t)e^{iwt}dt \quad \text{(Eq. 4.7)}$$

Which can be rewritten as:

$$U(x, w) = e^{-i\Phi x}A(x, w) \quad \text{(Eq. 4.8)}$$

Where $\Phi = w/c_w$ such that w is frequency (radians) and c_w is the phase velocity of w. By applying an integral transformation to Eq. 4.8, $V(w, \phi)$ is created:

$$V(w, \phi) = \int e^{i\phi x}\left[\frac{U(x, w)}{|U(x, w)|}\right]dx$$

$$= \int e^{-i(\Phi-\phi)x} \left[\frac{A(x,w)}{|A(x,w)|}\right] dx \qquad \text{(Eq. 4.9)}$$

This integral transformation applies a phase shift to the frequency wavefield for the assumed phase velocity in Equation 4.8. $U(x,w)$ is also normalized to compensate for $A(x,w)$ effects; attenuation and spherical divergence. Based on this, $V(w,\phi)$ will exhibit a maximum for each frequency w since $A(x,w)$ is a positive, real value. This maximum is expressed as:

$$\phi = \Phi = w/c_w \qquad \text{(Eq. 4.10)}$$

A phase velocity c_w can be determined at each ϕ that displays a peak. A dispersion curve (Figure 4.2) is the expression of these peaks such that $V(w,\phi)$is transformed into $I(w,c_w)$.

Once all the dispersion curves are generated, each must be picked so that the phase velocities and corresponding frequencies can be inverted in order to obtain the shear-wave velocity profile. In Figure 4.2, the dispersion curve was picked is displayed where the amplitude is greatest as represented by the hot colors. Each picked point is symbolized as a small white box where a solid black line connects these to form a curve. This is done for each dispersion curve observed throughout the array. The dashed black line above the curve is the signal-to-noise ratio associated with each picked point. The picked curve is used in the inversion analysis to construct shear-wave velocity profiles. The inversion theory is explained in the next section as well as the results from this dataset.

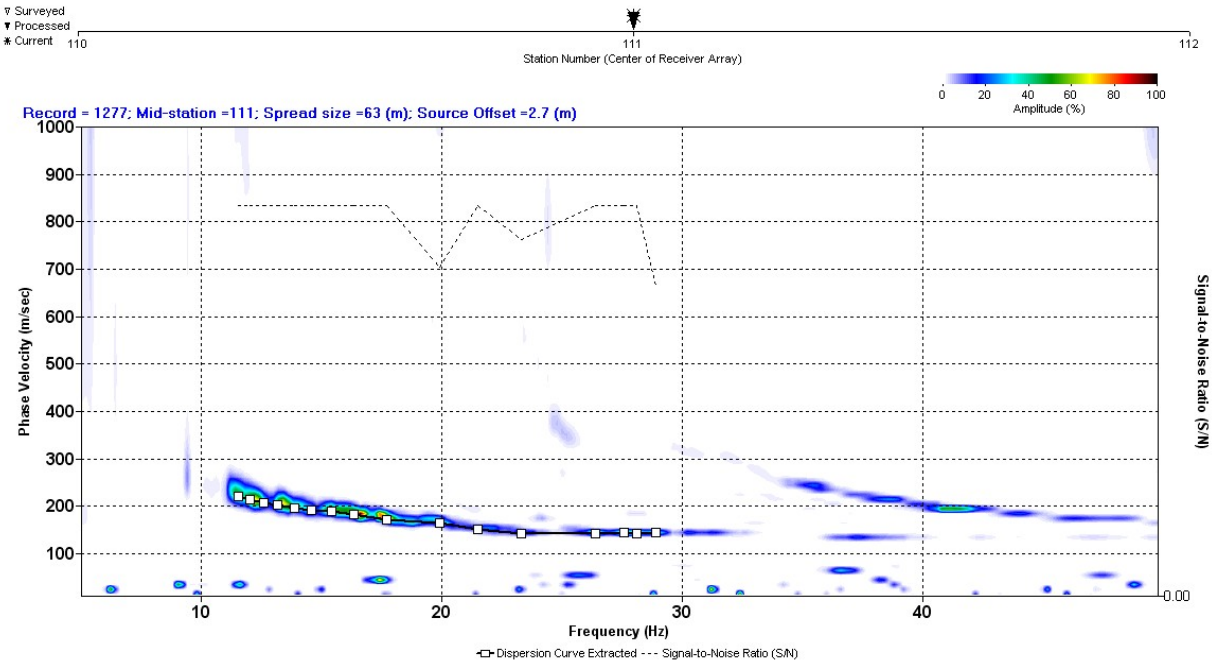

Figure 4.2. Individual Dispersion Curve from Haddam Meadows MASW Dataset. A dispersion curve is the relationship between Rayleigh wave phase velocity and frequency where amplitude is greatest. For this example at Haddam Meadows State Park, a 4.5 Hz vertical geophone and vertical hammer impact were used. This dispersion curve only extends from about 12-30 Hz with a corresponding phase velocity range 150-250 m/s. Typically, a dispersion curve exhibits a vertical asymptote in the low frequency range and a horizontal asymptote in the higher frequency range; only a horizontal asymptote is visible on this curve. The absence of this low frequency may be attributed to the sledgehammer source not transferring enough energy or the natural frequency of the geophones. In the previous chapter, the natural resonance frequency of the sediments was observed at 2.14 Hz, which is lower than the natural frequency of the geophones, which is 4.5 Hz. However, there is still a large gap in the dispersion curve which means that the model will be limited in terms of depth. Based on this, the missing low frequencies were attributed to the source. The dashed line at the top of the plot displays the signal-to-noise ratio of each picked point ranging from 0-1. The inversion results from this curve as seen in Figure 4.4.

4.3.3. Inversion

Once the dispersion curve is picked, it is used in an iterative inversion algorithm to construct the shear-wave velocity profile (Xia et al., 1999). This utilizes a weighted least-squares method such that the shear-wave velocities are updated with each iteration step, but Poisson's ratio, density and layer thickness do not. The convergence of the model is dependent on the shear-wave velocity. Based on Stokoe *et al.* (1994), the initial Vs profile assumes that a shear-wave velocity with depth z_f is 1.09 times the apparent phase velocity C_f at wavelength λ_f:

$$z_f = a\lambda_f \qquad \text{(Eq. 4.11)}$$

Where a is a coefficient that minimally changes with frequency as it is empirically deduced (Park *et al*., 2002).

Before inversion, a forward calculation is performed; this creates a layered earth model with parameters s-wave velocity ($\boldsymbol{v_s}$), p-wave velocity ($\boldsymbol{v_p}$), density ($\boldsymbol{\rho}$) and layer thickness ($\boldsymbol{h}$) (Figure 4.3). From the Knopoff method (Schwab and Knopoff, 1972) the Rayleigh wave phase velocities (C_{Rj}) are determined by equation 4.12, which is nonlinear and implicit:

$$F\left(f_j, C_{Rj}, \boldsymbol{v_s}, \boldsymbol{v_p}, \boldsymbol{\rho}, \boldsymbol{h}\right) = 0 \quad \text{where } (j=1, 2, \ldots, m) \qquad \text{(Eq. 4.12)}$$

f_j is frequency (Hz) of the Rayleigh wave phase velocity, $\boldsymbol{v_s}$is the shear-wave velocity vector in the *i*th layer (Eq. 4.13a), $\boldsymbol{v_p}$is the compressional-wave velocity vector in the *i*th layer (Eq. 4.13b), $\boldsymbol{\rho}$ is the density vector in the *i*th layer (Eq. 4.13c), and $\boldsymbol{h}$ is the layer thickness vector in the *i*th layer (Eq. 4.13d), *n* is the number of layers within the model and *m* is the number of data points.

$$v_s = (v_{s1}, v_{s2}, \dots, v_{sn})^T \quad \text{(Eq. 4.13)}$$

$$v_p = (v_{p1}, v_{p2}, \dots, v_{pn})^T$$

$$\rho = (\rho_1, \rho_2, \dots, \rho_n)^T$$

$$h = (h_1, h_2, \dots, h_{n-1})^T$$

From these four parameters at frequency f_j, the phase velocities can be found using a dispersion curve with *m* data points and *m* equations in Equation 4.12 form.

v_{s1}	v_{p1}	ρ_1	h_1
v_{s2}	v_{p2}	ρ_2	h_2
⋮			
v_{si}	v_{pi}	ρ_i	h_i
⋮			
v_{sn}	v_{pn}	ρ_n	infinite

Figure 4.3. Layered Earth Model for Forward Calculation. The model consists of four parameters: shear-wave velocity($\boldsymbol{v_s}$), compressional wave velocity($\boldsymbol{v_p}$), density ($\boldsymbol{\rho}$) and layer thickness ($\boldsymbol{h}$).

Inversion model convergence is affected by how accurately the partial derivatives or Jacobian matrices in Equation 4.12 are determined. If a high frequency range is used to determine the Jacobian matrix by Ridder's method, the inversion is stable; Ridder's method uses polynomial extrapolation (Press et al., 1992). The Jacobian matrix of a model's shear-wave velocity is affected by the four model parameters contained in F, which is expressed as:

$$\mathbf{J}_s = \left[\frac{\partial F/\partial v_{si}}{\partial F/\partial c_R}\middle| f = f_j\right] \quad \text{(Eq. 4.14)}$$

Such that F contains the model parameters in Equation 4.12. However, based on a previous analysis by Xia *et al*. (1999), it was concluded that s-wave velocity influences the Rayleigh wave phase velocity more than p-wave velocity, density and layer thickness which affect Rayleigh wave phase velocity significantly less. Therefore, shear-wave velocities control how Rayleigh wave phase velocities change with depth.

As described by Xia *et al*. (1999), these shear-wave velocities are obtained by linearizing Equation 4.12 with a Taylor expansion and an objective function with weighting matrix is defined. This utilizes Equation 4.15:

$$\mathbf{J}\Delta\mathbf{x} = \Delta\mathbf{b} \quad \text{(Eq. 4.15)}$$

Such that $\mathbf{J}$ is the Jacobian matrix m by n where $m>n$, vector $\mathbf{x}$ is composed of shear-wave velocities and $\Delta\mathbf{x}$ represents initial estimation modification. Vector $\mathbf{b}$ is composed of Rayleigh wave velocity measurements where $\Delta\mathbf{b} = \mathbf{b} - \boldsymbol{c_R}(\boldsymbol{x_0})$ is the difference between the measured Rayleigh wave phase velocities and the initial estimation of the model response; $\boldsymbol{c_R}(\boldsymbol{x_0})$is the model's response to the initial shear-wave velocity estimates $\mathbf{x}_0$. This equation is solved by optimization techniques since the dispersion curve is composed of more points than the number of layers within the earth model.

The objective function is defined by Equation 4.16 with weighting matrix $\mathbf{W}$:

$$\Phi = ||\mathbf{J}\Delta\mathbf{x} - \Delta\mathbf{b}||_2\mathbf{W}||\mathbf{J}\Delta\mathbf{x} - \Delta\mathbf{b}||_2 + \alpha||\Delta\mathbf{x}||_2^2 \quad \text{(Eq. 4.16)}$$

Where $\| \|_2$ is the vector's l_2-norm length and α is the damping factor. Once the computation is completed, the sum of the modifications is added to the initial model, thus creating the final model which can be significantly different from the initial model. Within the inversion, the weighting matrix **W** is constructed by the differences between Rayleigh wave phase velocities in relation to frequency. In addition, the damping factor α helps control the speed at which the model converges and its stability. When the damping factor is equal to zero, the model parameters are resolved, however, when the damping factor decreases, the variance of the model parameters increases (Xia *et al.,* 1999).

From the Jacobian matrix in Equation 4.14, shear-wave velocities at varying depths can be solved for using frequency dependent phase velocities. Each vector column of the matrix represents the sensitivity of different frequency bands within the dispersion data with respect to layer depth; the number of columns is equal to the number of layers where the first column is the first layer in the model and the last column is the half-space. From these columns, the shear-wave velocities are solved by:

$$v_{s1} = c_R(high)/\beta \qquad \text{(First layer)}$$

$$v_{sn} = c_R(low)/\beta \qquad \text{(Half-space)} \qquad \text{(Eq. 4.17)}$$

$$v_{si} = c_R(f_i)/\beta \qquad (i=2,3,\ldots,n\text{-}1)$$

Such that constant β ranges from 0.874-0.955 for the range of Poisson's ratio 0-0.5. When the dispersion curve displays asymptotes on either end of the curve, $c_R(high)$ of the high frequency range and $c_R(low)$ of the low frequency range are defined. However, these two values are defined as the highest and lowest phase velocities observed when no asymptotes exist on the dispersion curve. Once the algorithm is complete and the model has converged, the result is a

non-unique velocity profile that displays shear-wave velocity values at corresponding depths as seen in Figure 4.4 (Xia *et al*., 1999).

The velocity profile in Figure 4.4. is the inverted model of the dispersion curve in Figure 4.3. As described earlier, there was a lack of energy observed in the low frequency range of the dispersion curve, which implies that the depth to bedrock may not have been reached by the source. The velocity profile supports this supposition because the highest velocity observed was not greater than 365 m/s. Within the five layer model, the last layer interface was observed at 22 m; according to the well log the depth to bedrock is 38.1 m, therefore the MASW survey did not have enough energy to reach the bedrock interface. The average velocity of the five layers to 27.4m is 278 m/s. Assuming the last layer continues to 30 m, the Vs30 is 260 m/s, which is a D classification according to the NEHRP. HVSR data was also taken along the surface at 0, 36 and 69 m. The average HVSR peak among the three measurements was 2.10 Hz (Figure 4.5), which corresponds to the passive data taken at borehole JL-1 (Figure 3.2). The hazard classification gathered from the passive data was also Class D with a Vs30=257 m/s. Although the bedrock depth was not observed from the MASW survey, the calculated Vs30 from MASW (260 m/s) and the HVSR (257 m/s) are in agreement, thus this site should be assigned Class D.

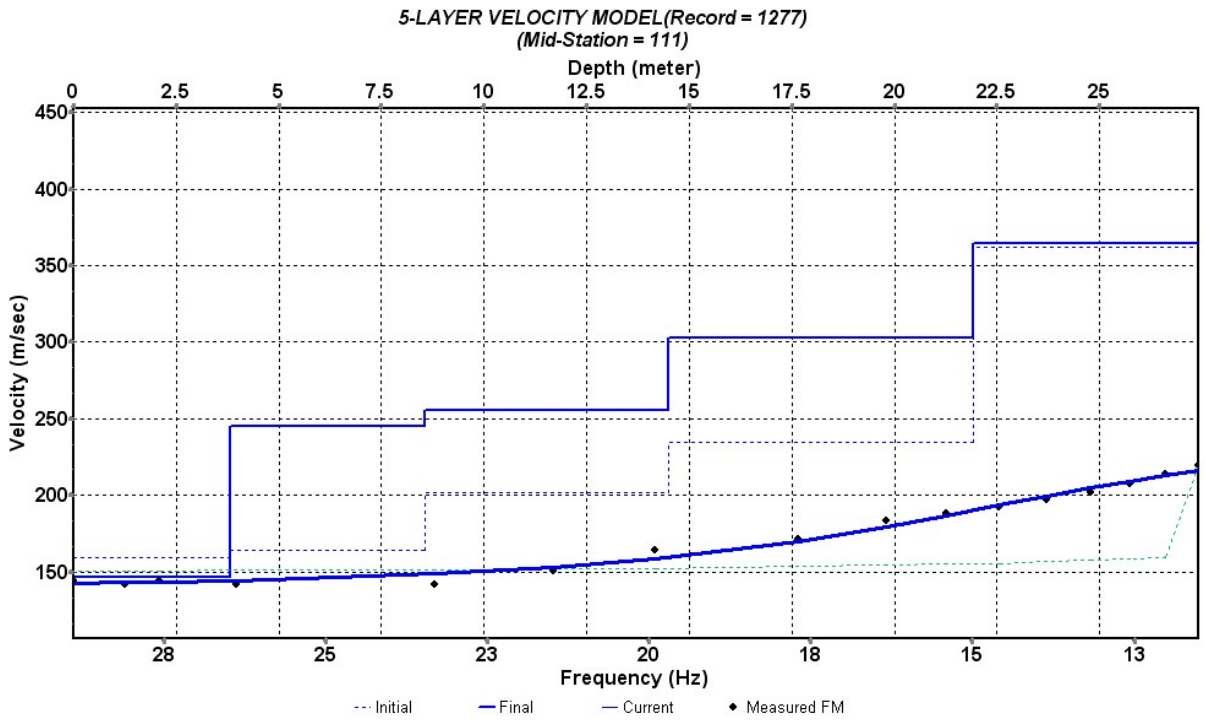

Figure 4.4. Shear-wave Velocity Profile from MASW at Haddam Meadows. After inverting the phase velocities picked on the dispersion curve, the result is a shear-wave velocity profile with depth. The profile displayed corresponds to the dispersion curve in Figure 4.2. The points at the bottom of the plot refer to the picked dispersion curve points with respect to frequency and velocity as seen on the bottom and left axes. The solid blue curve is the fitted final model generated after 10 iterations with a RMS=3. The light blue dotted line under the solid blue curve is the initial model. The initial velocity model is represented as the stepped, blue dotted line below the final velocity model, which is the stepped, solid blue line. From the velocity profile, the maximum depth of penetration was only 27.4 m and the highest shear-wave velocity observed was 365 m/s; the average shear-wave velocity of the 27.4 m is 260 m/s. However, the well log recorded a depth to rock as 38.1 m, which is deeper than any layer observed in the velocity profile. From the dispersion curve in Figure 4.3, there was a lack in energy in the low velocity range which contributes to the lack of deeper depths on this velocity profile.

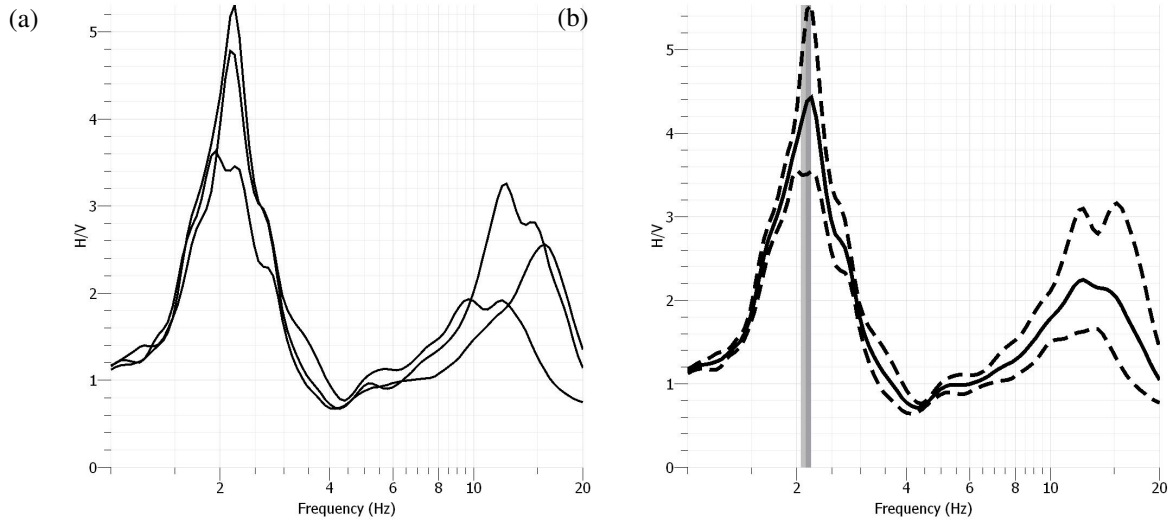

Figure 4.5. Average HVSR taken along MASW profile at Haddam Meadows. Three passive single-station measurements were taken along the same MASW profile at 0, 36 and 69 m; beginning, middle and end respectively. The measurement at 36 m was taken closest to borehole JL-1 for redundancy with data in Chapter 3, Figure 3.2. (a) Each black line refers to an individual record taken along the survey line. The first peak located around 2.1 Hz is the fundamental frequency. Although a second peak, known as a higher mode, is observed between 10-20 Hz, only the fundamental peak is being considered at this time for simplicity. (b) The average curve of all three measurements is displayed as the solid black line with corresponding standard deviations as the dashed curves above and below the average curve. The vertical gray rectange indicates the average HVSR frequency value, 2.1 Hz.

4.4. RESULTS

Marlborough, CT

At a 4-H Camp in Marlborough, an active MASW survey was performed near borehole MB32. The survey was a linear array that extended 34.5 m with twenty-four 4.5 Hz vertical and horizontal geophone pairs planted every 1.5 m. A 10-lb. sledgehammer source was used to make vertical impacts on a flat, steel plate. The record length for each shot was 1 second with a 0.5ms sampling interval. The source initial offset was 24 m from the first geophone pair, three shots were done at each shot location and the source location moved 3 m until it reached the last geophone pair. The well log for this site only descends 5 m (16.5 ft), but was not drilled to rock. Passive single-station measurements were also taken at geophone pair 1, 8, 16 and 24 or every 8.5m along the MASW profile. The HVSR results from the MASW profile are displayed in Figure 4.8 where the observed fundamental frequency ranged from 15.86 to 24.20 Hz; since the peak frequency changes throughout the line, this implies vertical variation exists of the underlying sediments. From the HVSR well huddle test results in Chapter 3, the fundamental frequency was observed at 20.1 Hz, which differs from the passive data collected along the MASW profile.

From the MASW survey, a dispersion curve from the vertical geophones is displayed in Figures 4.6. The vertical geophone data shows a weak amplitude dispersion curve starting at ~27 Hz and extending to ~43 Hz. The dispersion curve may start earlier, towards 22 Hz, however, the amplitude is low and the signal-to-noise ratio decreases greatly when picked in this frequency range. This dispersion curve was generated from a 3m offset shot location from the first geophone pair where the observed HVSR was 19.27 Hz (vertical dashed line). Low amplitude is observed around this resonance frequency; however, stronger dispersion amplitudes

are not evident and were not picked due to low confidence in the data. The dispersion curve was inverted and the resulting velocity profiles are shown in Figure 4.8.

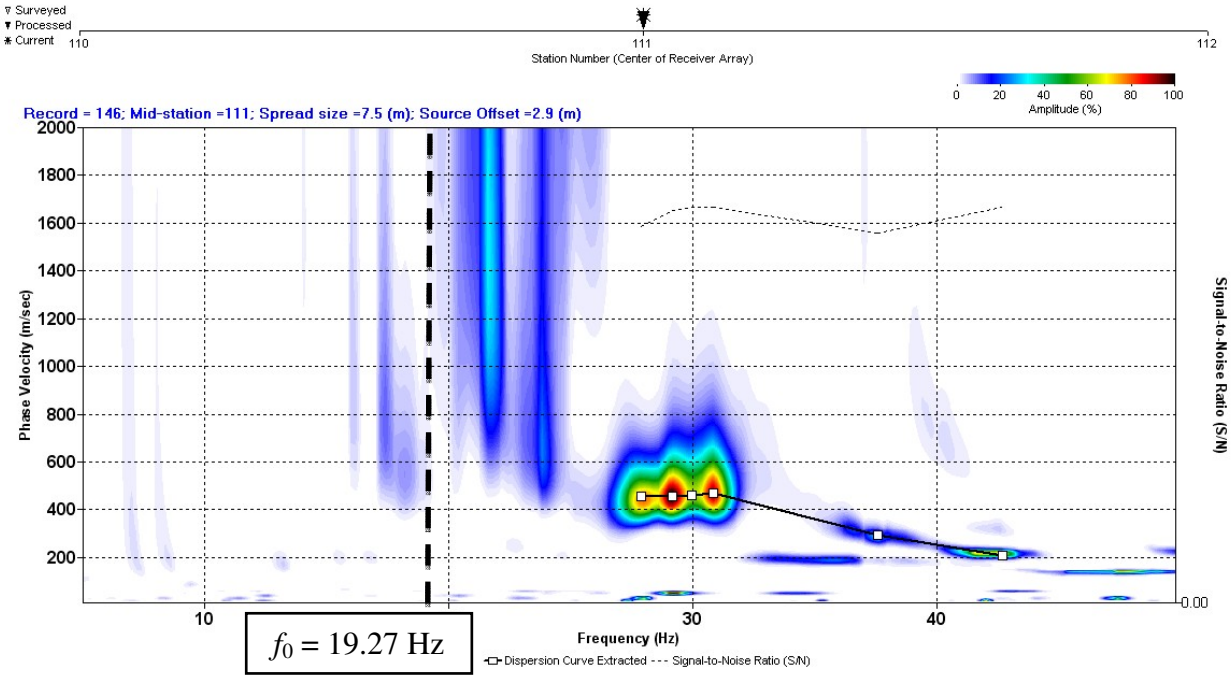

Figure 4.6. Class A: 4-H Camp Dispersion Curve from Vertical Geophone. The dispersion data extracted from the vertical geophone data shows a weak amplitude dispersion curve starting at around 27 Hz and extending to 43 Hz. The dispersion curve may start earlier, towards 22 Hz, but appears to have been influenced by higher modes causing this in consistency. The amplitude is also low and the signal-to-noise ratio decreased greatly when picked in this frequency range. This dispersion curve was generated from a 3m offset shot location from the first geophone pair where the observed HVSR was 19.27 Hz (vertical dashed line). Low amplitude was observed around this resonance frequency. Due to the lack of stronger dispersion amplitudes, the dispersion curve was not picked below 22 Hz.

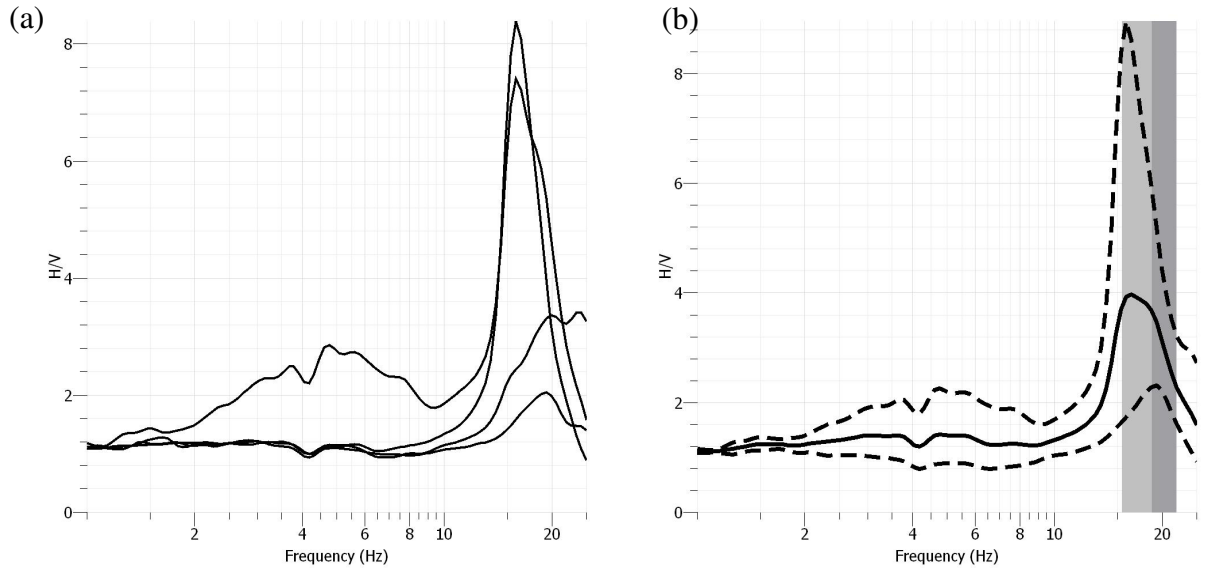

Figure 4.7. Class A: 4-H Camp HVSR Measurements Taken along MASW Profile. Passive single-station measurements were taken along the MASW profile at geophone pairs 1, 8, 16 and 24 or every 8.5m along the MASW profile. (a) Each of the four measurements is represented by the solid black lines. Commonality does not exist across all four curves as the observed fundamental frequency ranged from 15.86 to 24.20 Hz; since the peak frequency changes throughout the line, this implies vertical variation exists of the underlying sediments. (b) The average HVSR curve is represented as the solid black line with corresponding upper and lower standard deviations represented by the dashed curves. The vertical gray box shows the average fundamental frequency value of the curves.

From the vertical geophone dispersion curve, the velocity profile in Figure 4.8 was generated using a 5-layer model. Although the depth to bedrock is unknown, the deepest layer interface observed on this velocity profile is at 5.7 m with shear-wave velocity 716 m/s; this layer is slightly deeper than the onsite well depth, 5 m. If this 5.7 m deep layer is assumed to be the bedrock interface, the average velocity of the overlying sediments is 351.4 m/s, but the Vs30 is 582.7 m/s; seismic hazard Class C by the NEHRP. Because weak and inconsistent dispersion curves were extracted, the MASW survey method provided inadequate results at this site. Based on the surficial materials classification, the assumed shallow bedrock would account for the poor MASW results since the shear-wave velocity of the bedrock would overwhelm the overlying materials and therefore create unsuitable conditions for this field technique. Overall, a confident seismic hazard classification was unable to be assigned to this site based on the MASW results.

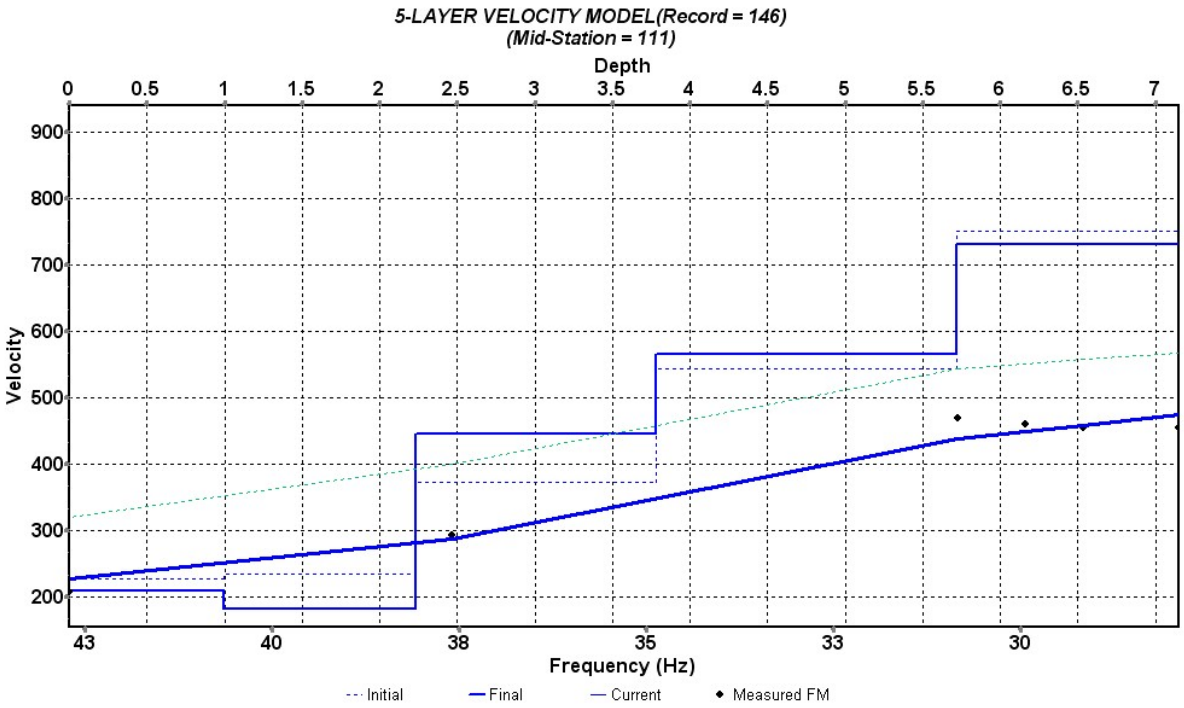

Figure 4.8. Class A: 4-H Camp Velocity Profile from Inversion. This velocity profile extracted from the dispersion curve observed on the vertical geophone dataset was generated using a 5-layer model. The deepest layer interface observed on this velocity profile is at 5.7 m with corresponding shear-wave velocity 716 m/s; this layer is slightly deeper than the onsite well depth, 5 m. Although the depth to actual bedrock is unknown, assuming this 5.7 m deep layer is the bedrock interface, the average velocity of the overlying sediments is 351.4 m/s with a Vs30 of 582.7 m/s. Based on this value, the NEHRP seismic hazard level is Class C.

Rocky Hill, CT

At Dinosaur State Park in Rocky Hill, CT, an MASW survey was conducted near a domestic well outside the house and old barn. The survey utilized twenty-four 4.5 Hz vertical and horizontal geophone pairs spaced 1.5 m apart along a linear array; the total length of the array was 34.5 m. A 10-lb. sledgehammer was used with a flat, steel plate to initiate vertical impacts and surface wave motion. Each shot record was 1 second with 0.5 ms sampling interval. Three shots were performed at each source location starting 3 m from the first geophone pair and moved outwards 3 m until the farthest offset of 24 m. As stated in Chapter 3, no well log was able to be recovered for the domestic well, but the HVSR huddle test results observed an average fundamental frequency at 3.78 Hz. Additional passive single-station measurements were taken along the MASW array at Geophone pair 1, 8, 16 and 24; however the record taken at Geophone pair 24 was not used due to technical error. The HVSR results from the MASW survey are recorded in Figure 4.13 with an average resonance frequency 4.1 Hz. All peaks recorded along the line show a common fundamental frequency therefore the 1-D earth assumption along this line is confirmed. These HVSR measurements along the MASW array coincide with the data taken around the well; the well was located within 10 ft of the array.

The dispersion curve extracted from the vertical geophones and an 18 m offset is displayed in Figure 4.11 with large amplitudes across all frequency bands. The black line with small white boxes is the picked dispersion curve used for inversion; however the curve was only picked starting ~22 Hz. Although high amplitudes extend into the lower frequencies, the energy is not consistent and appears to have been affected by higher modes as indicated by the blue colored gaps. With this interference, the dispersion curve was not picked below 22 Hz. For this site, the dispersion has high phase velocities starting at 900 m/s, which infers that the underlying

sediments have a very stiff structure. The surficial materials assigned to this site are sedimentary rock and till, which could account for the high phase velocities observed. The vertical geophone data were used for inversion and the results are shown in Figure 4.11.

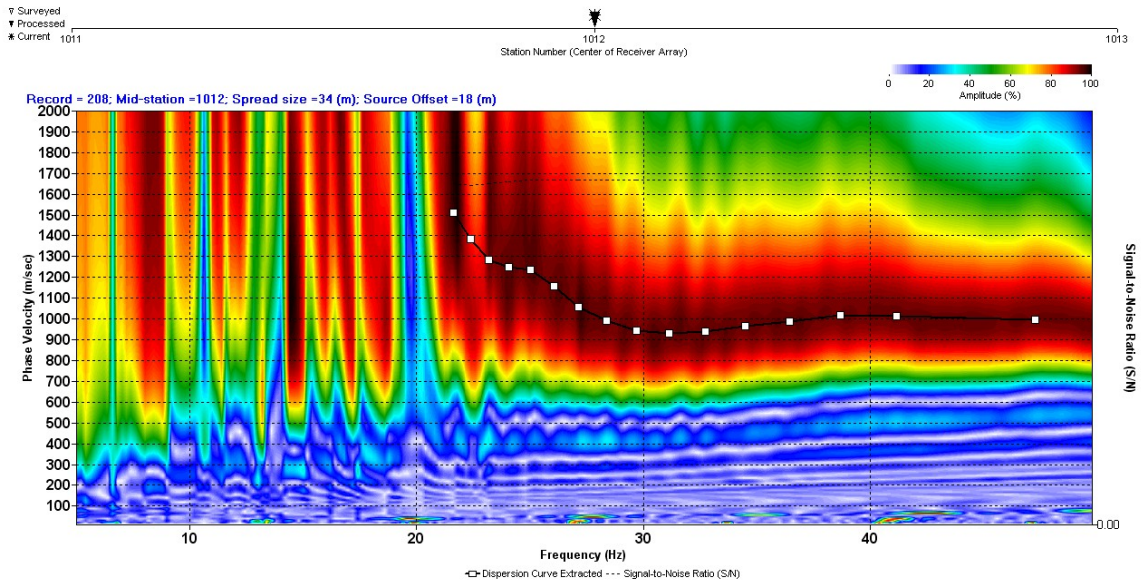

Figure 4.9. Class B: Dinosaur State Park Dispersion Curve from Vertical Geophones. The dispersion curve extracted from the vertical geophone dataset is displayed here with large amplitudes across all frequency bands. The black line with small white boxes is the picked dispersion curve that was later used for inversion. In this case, the curve was only picked starting ~22 Hz even though high amplitudes extend into the lower frequencies. This is because the energy is not consistent and appears to have been affected by higher modes illustrated by the blue colored gaps. The dispersion also exhibits high phase velocities starting at 900 m/s; this infers that the underlying sediments have a very stiff structure. The surficial materials assigned to this site are sedimentary rock and till, which could account for these high phase velocities.

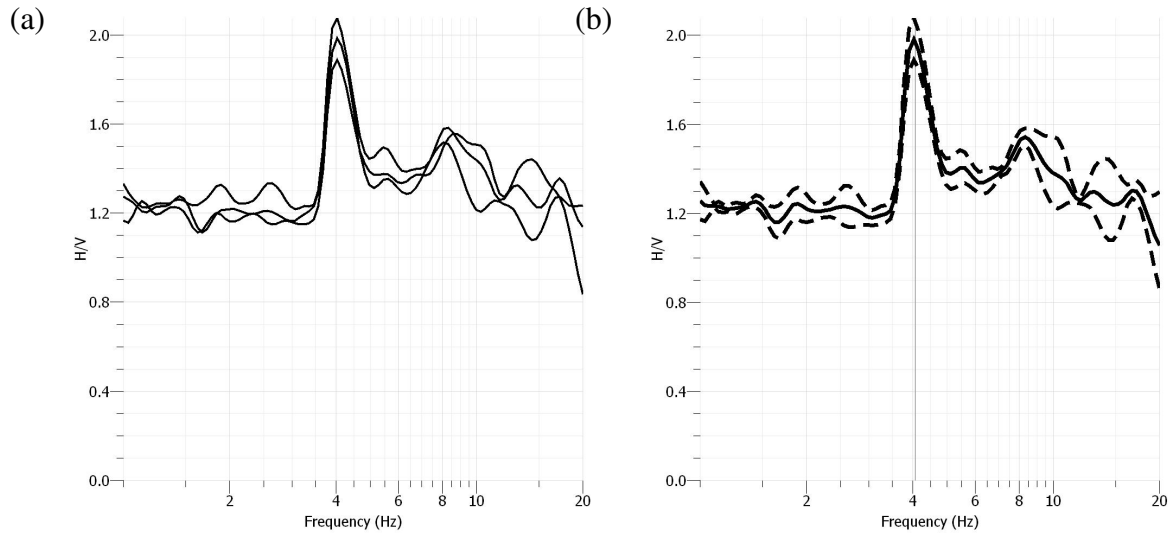

Figure 4.10. Class B: Dinosaur State Park HVSR Measurements Taken along MASW Profile. (a) Four passive single-station measurements were taken along the MASW array at Geophone pair 1, 8, 16 and 24; however the record taken at Geophone pair 24 was not used due to technical error. Each measurement is represented by a solid black curve. (b) The average resonance frequency was observed at 4.1 Hz as represented by the vertical gray rectangle. The average curve is the solid black line and the corresponding standard deviations are the upper and lower dashed curves. Since all four peaks recorded along the line show a common fundamental frequency, the 1-D earth assumption along this line is confirmed.

After the vertical geophone data was inverted, a 5-layer velocity profile was generated its deepest layer observed at 30.6 m with a shear-wave velocity of 2317 m/s. As described in the dispersion curve analysis, the shear-wave velocities do not decrease lower than 772 m/s which may be till as prescribed by the surficial materials. Assuming the bedrock layer from the velocity profile is at 16.2 m depth, the average velocity of the sediments is 952.6 m/s, but after the inclusion of bedrock the Vs30 is 1216.4 m/s; NEHRP site class B. Without a known depth to bedrock value, it is difficult to make a firm seismic hazard site classification, but based on the HVSR data and the vertical geophone data, this site has been assigned a B class after Vs30. After combining the HVSR results with the active MASW results, there is disagreement between the average shear-wave velocities calculated from the resonance frequencies and the velocity profiles. Using Equation 3.5, the depth to rock recorded in the velocity profile and the observed

resonance frequency along the MASW line, the average velocity of the sediments is 259.2 m/s, which is significantly less than the 952.6 m/s average velocity from the vertical geophone data. Due to the high velocity of the sediments and the lack of lower frequencies on the dispersion curve, the MASW survey is not adequate for seismic hazard classification at this site.

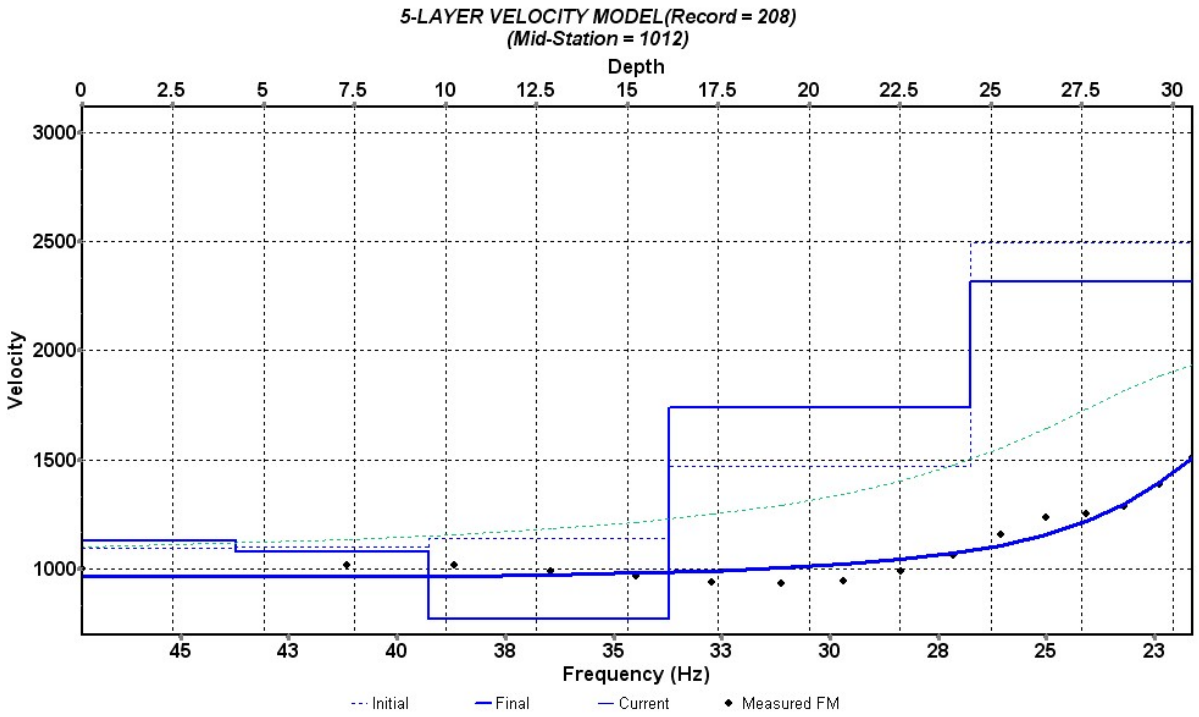

Figure 4.10. Class B: Dinosaur State Park Velocity Profile from Inversion. A 5-layer shear-wave velocity profile was generated from the picked dispersion curve in Figure 4.11. The deepest layer was observed at 30.6 m with a shear-wave velocity of 2317 m/s. As described in the dispersion curve analysis, the shear-wave velocities do not decrease lower than 772 m/s which may be till as prescribed by the surficial materials. Based on the indicated bedrock layer at 16.2 m depth on the velocity profile, the average velocity of the sediments is 952.6 m/s, however, after the inclusion of bedrock the Vs30 is increased to 1216.4 m/s. This site is a NEHRP site class B established by the Vs30 value.

Enfield, CT

An MASW survey was performed in Enfield, CT outside the perimeter of the Department of Corrections facility, near borehole EF 111. At this site, the depth to bedrock is 41 m. A linear array of twenty-four 4.5 Hz vertical and horizontal geophone pairs spaced 1.5 m with a 34.5 m total spread length was used. Since the depth to rock is greater than 30 m, a 40-kg accelerated weight drop (PEG-40) was used instead of the usual 10-lb. sledgehammer. The PEG-40 was attached to the hitch of the field vehicle; three shots were performed at each shot location starting at 1.5 m from the last geophone pair and moved 3 m until the farthest offset distance was 34.5 m, double the length of the geophone spread. Each shot record was 1 second with a 0.5 ms sampling interval. Passive single station measurements were taken at geophone pairs 1, 8, 16 and 24. The HVSR huddle test results from Chapter 3 were used to calibrate the data taken along the MASW profile. The huddle test HVSR observed a fundamental frequency at 4.4 Hz, which correlates with the results from the MASW profile, 4.4 Hz (Figure 4.14).

From the MASW survey, the dispersion curve from the vertical geophones is displayed in Figure 4.16 where the vertical and horizontal asymptotes are obvious. The data extends across the entire frequency band with no influence from higher modes. The fundamental frequency observed in the HVSR data coincides with the vertical asymptote. The black lines with small white boxes are the picked dispersion curves used for inversion.

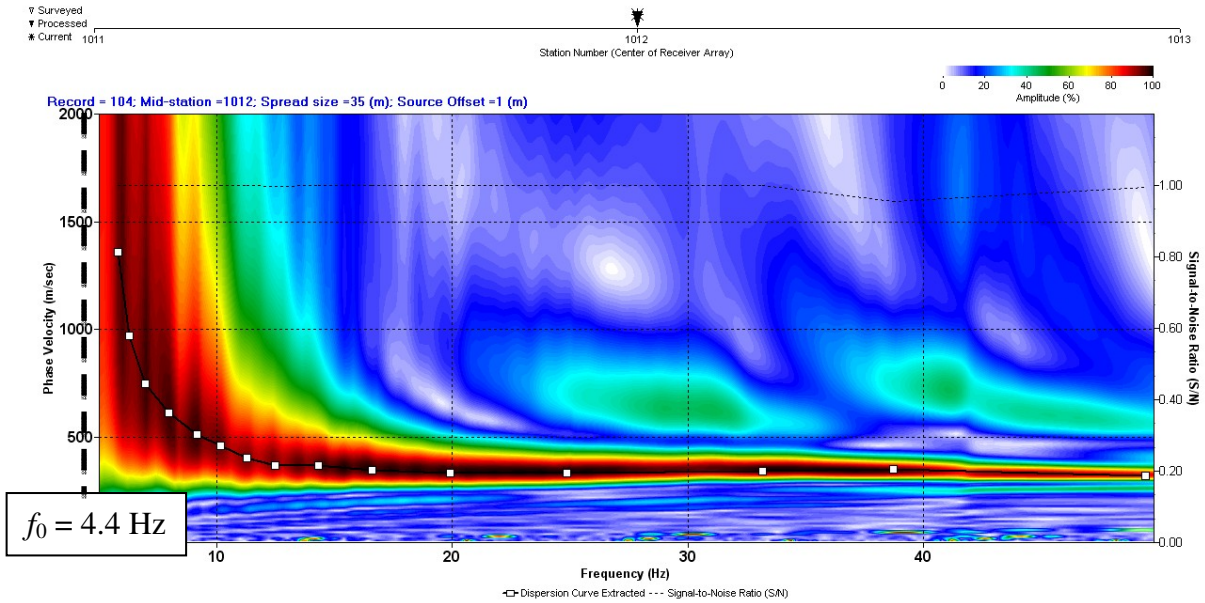

Figure 4.11. Class C: Department of Corrections Dispersion Curve from Vertical Geophones. The dispersion curve illustrated here was created using the vertical geophones. This shows clean vertical and horizontal asymptotes with high amplitudes extending across the entire frequency band with no influence from higher modes. The fundamental frequency displayed at 6.5 Hz is from the HVSR measurements taken alongside the MASW profile. This fundamental frequency coincides with the vertical asymptote at the beginning of the dispersion curve. The black lines with small white boxes are the picked dispersion curves used for inversion.

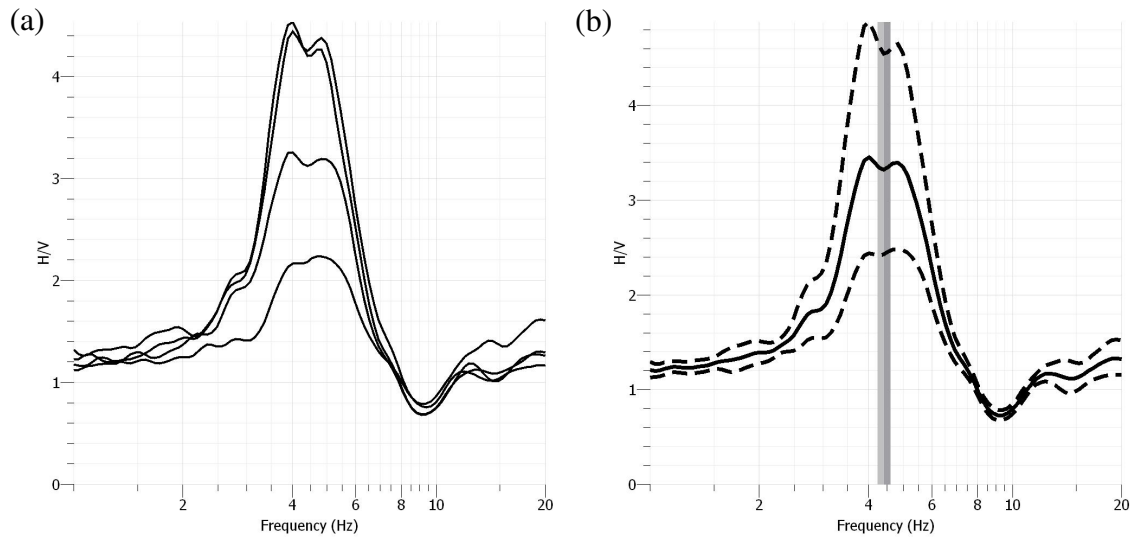

Figure 4.12. Class C: Department of Corrections Facility HVSR Measurements Taken along MASW Profile. (a) Four passive single station measurements were taken along the MASW profile at geophone pairs 1, 8, 16 and 24. Each measurement is represented by a solid black line. The peak frequency exhibits a double peak, which can be attributed to the structure of the subsurface; however, the fundamental frequency values remain constant throughout the array. (b) The average resonance frequency is 4.4 Hz, as displayed by the vertical gray box. The average HVSR curve is represented by the solid black line and the upper and lower dashed curves are the standard deviations.

A 5-layer model was used to generate the velocity profile in Figure 4.13 where the depth to bedrock was recorded at ~42m and a shear-wave velocity 1600 m/s; this corresponds to the well log depth to bedrock, 41 m. The calculated average shear-wave velocity of the sediments is 584 m/s, but the depth to rock is deeper than the necessary 30 m for the NEHRP classification. The Vs30 for this site is only 490 m/s, a C class by the NEHRP, which matches the initial surficial materials site classification. However, HVSR data indicate a resonance frequency at 4.4 Hz, the results do not match. After further investigation, it was deduced that the 4.4 Hz resonance frequency was actually from the overlying till layer, rather than the bedrock layer below it. Since till has a very high velocity, it did not achieve a 2:1 velocity contrast between the till and rock, so the rock interface was masked. Due to this limitation of the HSVR method, the

active MASW was necessary to make a full seismic hazard assessment at this site. From both the active and passive data collected at this field site, it was assigned a C class based on Vs30.

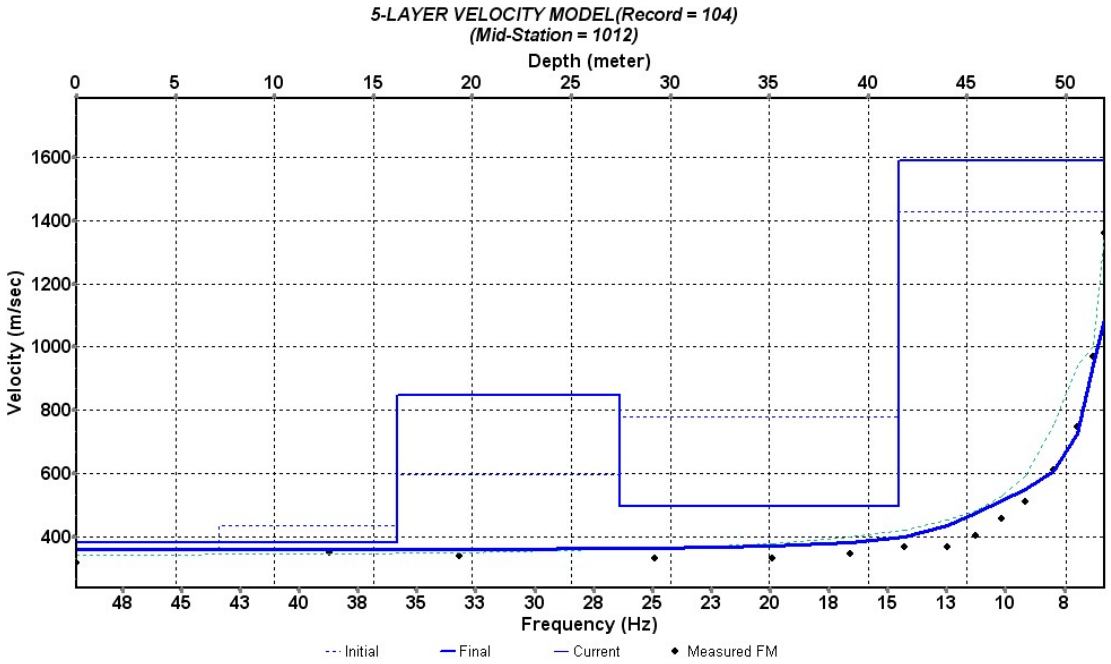

Figure 4.13. Class C: Department of Corrections Velocity Profile from Inversion. A 5-layer model was used to generate a shear-wave velocity profiles from the picked dispersion curve in Figure 4.16. On the profile, the depth to bedrock was recorded at 42m with a corresponding shear-wave velocity 1600 m/s; these values correspond to the well log depth to bedrock, 41 m. The calculated average shear-wave velocity of the sediments is 584 m/s, but the Vs30 for this site is only 490 m/s, a C class by the NEHRP. This matches the initial surficial materials site classification.

Avon, CT

Near the corner of Knollwood Lane and Reverknoll Lane in Avon, CT, an active MASW survey was performed along Knollwood Lane and a town owned monitoring well; the depth to rock is 61.4 m. The linear array had a 34.5 m total spread, with twenty-four 4.5 Hz vertical and horizontal geophone pairs every 1.5 m. A 10-lb. sledgehammer with a flat, steel plate was used to make vertical impacts as the active source starting 24 m from the first geophone pair and advancing every 3 m until it was 6 m into the survey line. The same procedure was done on the opposite side of the survey line. Each shot record was 1 second with a 0.5 ms sampling interval. HVSR measurements were also taken along the profile at geophone pairs 1, 8, 16 and 24; the results are displayed in Figure 4.23 where the average resonance frequency was observed at 1.95 Hz. This passive data corresponds to the HVSR huddle test results in Chapter 3 (Figure 3.10). Due to the similarities in the fundamental frequencies, the 1-D earth assumption is met for this site.

The dispersion curve extracted from vertical geophones data is shown in Figure 4.14. A low frequency vertical asymptote was not observed, and the dispersion curve remains flat from 10-46 Hz. This lack of high dispersion amplitude in the lower frequency range may be attributed to an insufficient amount of energy exerted by the sledgehammer source. The picked dispersion curves as represented by the black line with small white boxes were used to obtain velocity profiles in inversion.

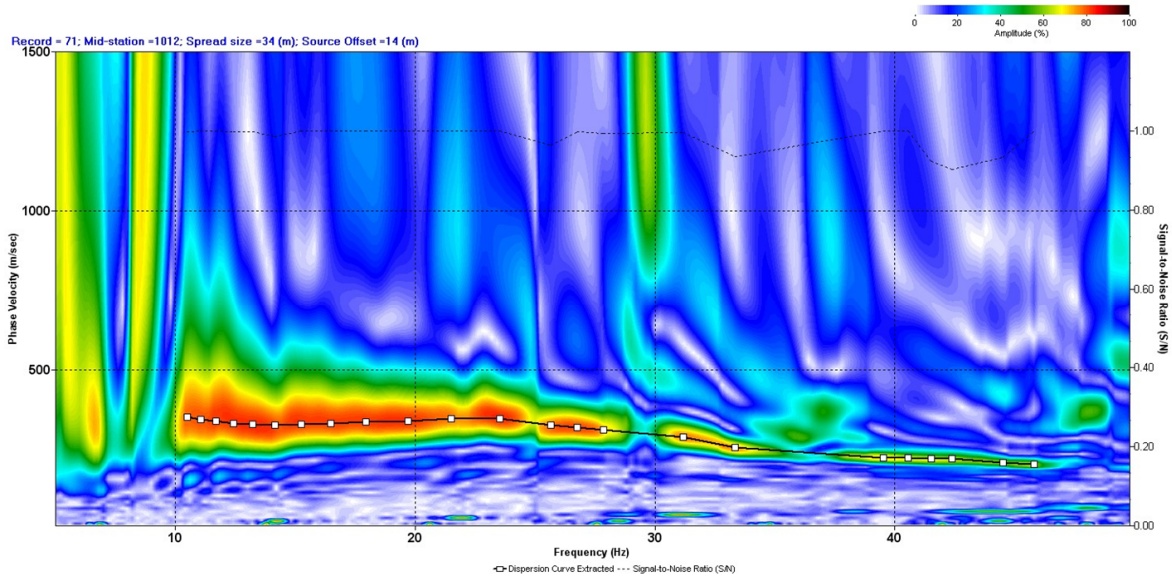

Figure 4.14. Class D: Knollwood Lane Dispersion Curve. The dispersion curve extracted from the vertical geophones dataset is displayed here. The dispersion curve remains flat from 10-46 Hz as a low frequency vertical asymptote was not observed. This lack of high dispersion amplitude in the lower frequency range may be attributed to an insufficient amount of energy exerted by the sledgehammer source during data acquisition or interfering higher modes. Had these low frequency amplitudes been observed, the dispersion may have exhibited a vertical asymptote near the observed HVSR resonance frequency at 1.95 Hz. This peak is not displayed on the figure because its value is significantly lower than the limits of the dispersion data. The picked dispersion curves as represented by the black line with small white boxes were used to obtain velocity profiles in inversion.

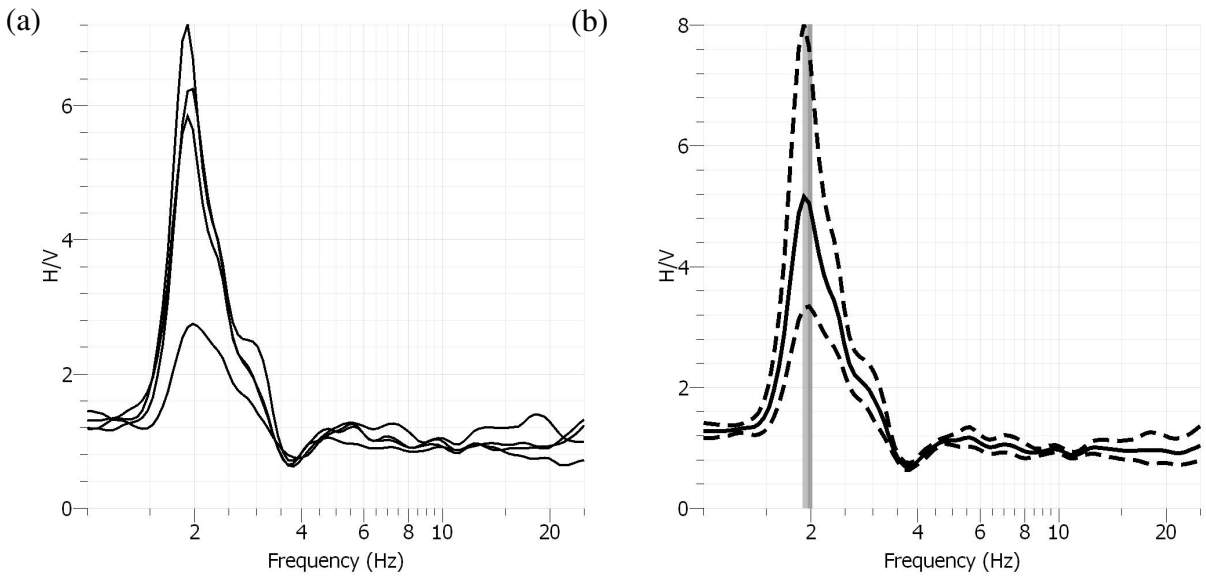

Figure 4.17. Class D: Knollwood Lane HVSR Measurements Taken along MASW Profile. (a) Four HVSR measurements were taken along the MASW profile at geophone pairs 1, 8, 16 and 24 where each measurement is represented by a black curve. Due to the similarities in the fundamental frequencies, the 1-D earth assumption is met for this site. (b) The average resonance frequency was observed at 1.95 Hz as indicated by the vertical gray rectangle. The average HVSR curve is displayed as the solid black line with corresponding upper and lower standard deviations dashed curves.

In Figure 4.18, the velocity profile from the vertical geophone is displayed as a 5-layer model with a maximum depth of 14.6 m. As previously stated, the sledgehammer did not provide a sufficient amount of energy to penetrate to the bedrock layer, which is evident in this velocity profile. Based on this profile, the average velocity of the sediments is 310.7 m/s, which is less than the average velocity calculated by the HVSR data, 467 m/s. An important feature to notice is the low velocity layer that exists below 8 m. These low velocity layers are crucial to seismic hazard site classification because they can be masked by overlying, high velocity layers. Since the MASW survey did not penetrate deeper, the results are unable to calculate a Vs30; nonetheless, the HVSR results still provide a confident C class result.

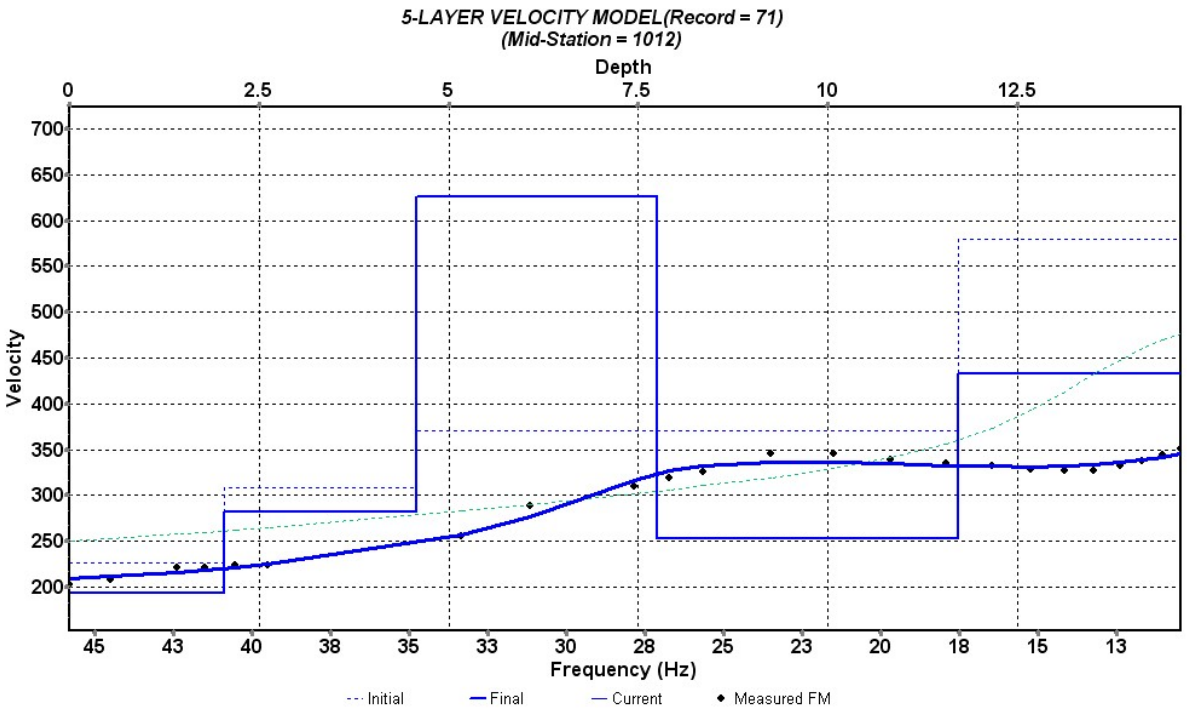

Figure 4.18. Class D: Knollwood Lane Velocity Profile from Inversion. The shear-wave velocity profile from the vertical geophone dataset is displayed as a 5-layer model with half space observed at 14.6 m. This maximum depth is not the depth to bedrock, which according to the well log is 61.4 m. Based on this profile, the average velocity of the overlying sediments is 310.7 m/s, which is less than the average 467 m/s velocity calculated by the HVSR data. However, the HVSR data accounts for sediments directly over the bedrock interface, whereas this profile is too shallow which accounts for the lower average velocity value.

West Hartford, CT

At Elizabeth Park around the park pond in West Hartford, CT a 34.5 m MASW survey was performed between the pond and chain fence, parallel to Asylum Ave. The linear array utilized twenty-four 4.5 Hz vertical and horizontal geophone pairs planted 1.5 m to create the array. As stated in Chapter 3, the onsite monitoring well was not drilled to rock, however a nearby monitoring with a 17.7 m depth to rock remains unidentified at the site. The depth of the identified monitoring well was 5.3 m, but it was not drilled to rock. For this survey, the near offset was 9 m and the far offset was 27 m on both ends of the survey. HVSR measurements were taken along the MASW line at geophone pair 1, 12 and 24 (Figure 4.28). The huddle test taken around the known monitoring well had an average observed resonance frequency of 9.3 Hz. This differs slightly from the measurements taken along the MASW line which increased from 6.48 to 9.89 Hz as the station locations approached the nearest distance to the well. This increase in resonance frequency implies a vertical variation across the array.

The dispersion curve in Figure 4.19 was extracted from the vertical geophone data. Dispersion amplitudes are greatest from 9-25 Hz with some influence by higher modes in the lower frequency range which interrupt the potential vertical asymptote. However, without the higher modes, the starting position of the dispersion curve would be supported by the observed HVSR resonance frequencies, 6.5 Hz. The extracted curve, as indicated by the black line with small white boxes, was used for inversion.

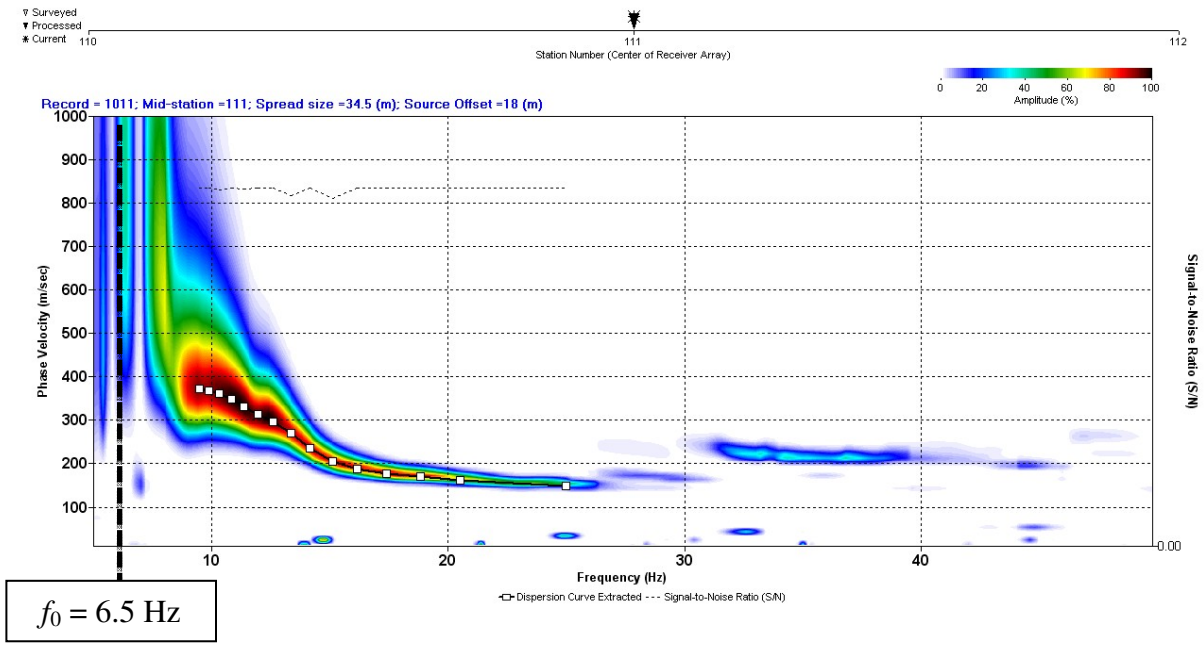

Figure 4.19. Class E: Elizabeth Park Dispersion Curve. This dispersion curve was created using a vertical impact observed across the vertical geophone dataset. The dispersion amplitudes are greatest from 9-25 Hz with some influence by higher modes in the lower frequency range. These higher modes interrupt the potential vertical asymptote; otherwise the starting frequency of the dispersion curve would be supported by the observed HVSR resonance frequencies at 6.5 Hz. The picked dispersion curve is illustrated as the black line with small white boxes. The values used to construct the curve were picked based on where the amplitude between frequency and phase velocity was greatest.

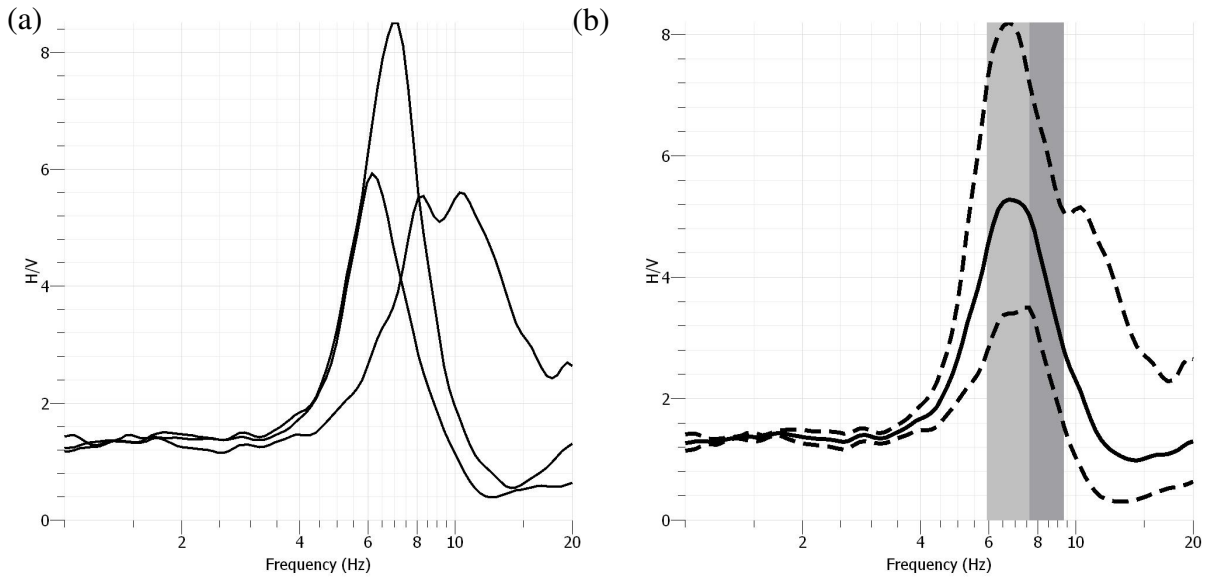

Figure 4.20 Class E: Elizabeth Park HVSR Measurements Taken along MASW Profile.
(a) Three HVSR measurements were taken along the MASW line at geophone pairs 1, 12 and 24. Each station measurement is represented by a solid black line. Here the fundamental frequency is not consistent throughout the line as it increased from 6.48 to 9.89 Hz. This increase in resonance frequency implies a vertical variation across the array. (b) The average HVSR curve from all four stations is represented as the solid black line with corresponding upper and lower standard deviation dashed curves. The average of all three stations is 7.8 Hz as indicated by the vertical gray box, which also has an upper and lower frequency standard deviation.

After inversion, two 5-layer velocity profiles were generated; one from the vertical data (Figure 4.21). The bedrock interface was not observed, but the profile did achieve a half space depth at 17 m. The velocity profile in Figure 4.29 had an average sediment velocity of 272.4 m/s for the 17.2 m of sediment. The passive data from Chapter 3 was used to calibrate the HVSR data taken along the MASW profile. Since the average velocity at the monitoring well was 658 m/s, the corresponding depths at geophone pairs 1, 12 and 24 are 25.4 m, 23.4 m, and 16.6 m respectively. Based on the MASW data alone, the bedrock interfaces are still shallower than the necessary 30 m requirement for the NEHRP classification. Therefore, the average velocities of the sediments would increase dramatically with the inclusion of bedrock velocities in the Vs30 calculation. This site was originally classified as an E class by the surficial materials, then a C

class after the HVSR data. With the addition of the MASW data, which have average sediment velocities of 272 m/s, the site classification is already lowered to a D class. If the deeper bedrock interface was observed by the MASW survey, the average velocity would decrease again. For the purpose of this project, this field site was assigned a C class.

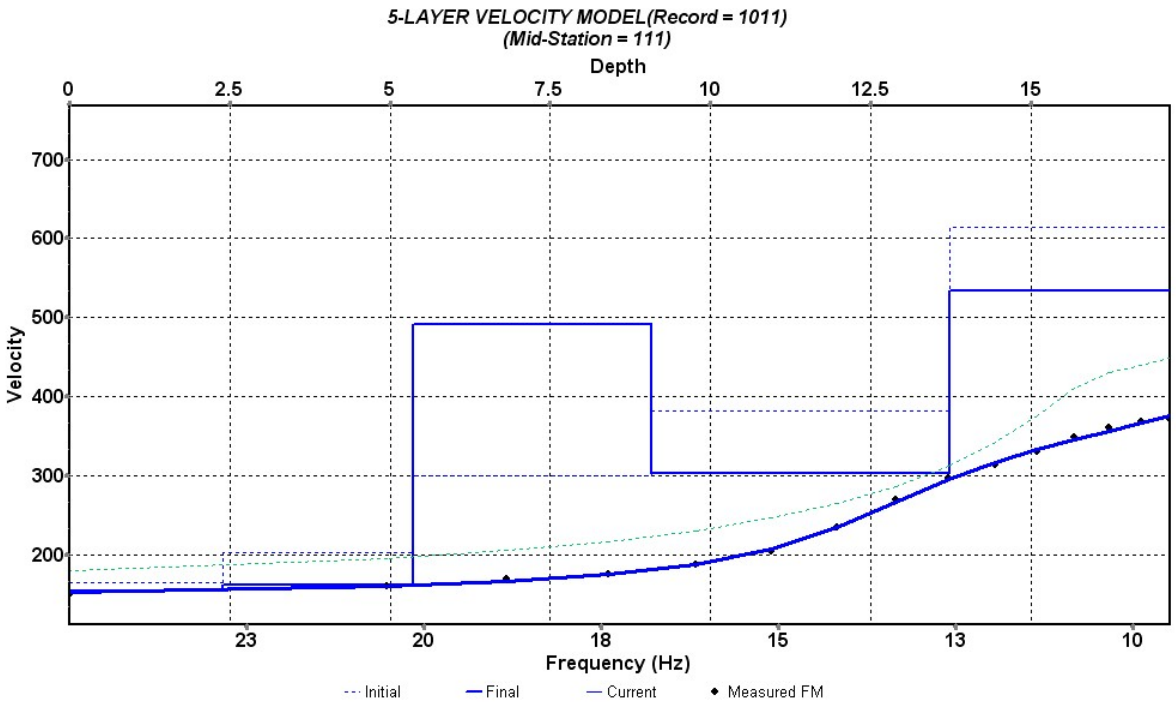

Figure 4.21. Class E: Elizabeth Park Velocity Profile from Inversion. After the dispersion curve in Figure 4.19 was inverted, a 5-layer shear-wave velocity profile was generated. Although the actual bedrock depth is unknown at this location, the bedrock interface was not observed as the resulting layer velocities are too low for characteristic rock layers. The maximum depth recorded on this profile was 17.2 m with an average sediment velocity of 272.4 m/s. Based on the MASW data alone, the bedrock interface is shallower than the 30 m requirement for the NEHRP. Therefore, the average velocities of the sediments will increase dramatically with the inclusion of bedrock velocities in the Vs30 calculation.

5. VERTICAL SEISMIC PROFILING

5.1. BACKGROUND INFORMATION

In contrast to the two non-invasive methods previously discussed, Vertical Seismic Profiling (VSP) is an invasive active seismic method that utilizes a geophone inside a borehole at multiple depths to estimate sediment velocities, geologic structure and interpret common midpoint reflection data (Balch *et al*., 1982; Walters *et al*., 2009). The borehole technique dates back to the 1930s by the USSR for exploration purposes such as detecting and mapping salt domes. The technique was later adopted in the 1970s by the United States after Russian papers were translated into the English language.

In seismic reflection, induced energy is reflected or bounced off a medium interface where the elastic properties of two layers abruptly change. The laws of reflection can be derived from Huygens' principle, which describes the relationship between time interval Δt, distance $V_1 \Delta t$ and the angles energy travels to and from a boundary interface (Sheriff 1995). For a reflected wave, the angle of incidence θ_1 is equal to the angle of reflection θ_1' (Figure 5.1). Since the distance between the geophone and source is known, the time is takes for the wave to travel to an interface and reflect back is measured; from these, the interval velocity is determined. This is based on the assumption that rays travel vertically such that *dz/dt* is the apparent velocity where *dz* is the change in geophone depth and *dt* is the change in arrival time (Pujol 1985). This interval velocity is calculated for each geophone depth.

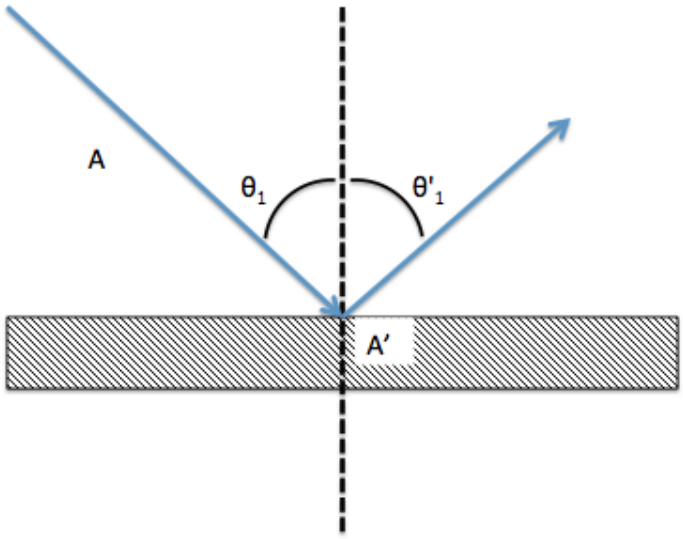

Figure 5.1. Reflection of a Plane Wave. Ray A propagates towards an interface at angle of incidence . Ray A' is reflected from the boundary at angle of reflection which is equal to the angle of incidence. Each angle is measured from the vertical indicated by the dashed line.

For offset VSP, the source is not located directly over the wellhead, but at a determined distance known as the source offset. This offset is used to reduce the potential generation of tube waves, which are disturbances occurring, most commonly identified as compressional waves traveling through fluid in the borehole (Pujol, 1985; Balch *et al*., 1982). Tube waves can disturb the wave record by increasing the overall amplitudes; this risk increases as borehole depth increases. By the use of an offset, any wave disturbances induced by the source or a shallow refraction are less likely to affect the wave patterns. The generation of tube waves is important to consider during analysis because they determined the overall resolution.

The geophone is held in place within the borehole either by a mechanical arm or by an electrohydraulic bladder (Balch *et al*., 1982). The mechanical arm is controlled from the surface and uses an adjustable arm to press and lock the geophone against the wall of the borehole. The electrohydraulic bladder is also controlled from the surface, but uses water to inflate the bladder

to lock the geophone at the desired depth within the borehole. Noise can also be generated by the cable if the geophone were to slip from its locked position. To reduce these effects, excess cable is put down the well to create slack and suppress any noise that would propagate through the taut cable.

The VSP method provides reliable information about the immediate subsurface in which the borehole is located. In the previous two chapters, non-invasive seismic techniques were utilized throughout Hartford County such that although well log information was available at a majority of the sites, not all areas to be investigated have this advantage. Therefore, the VSP method is not applicable to all field sites. The option to drill a borehole at that locale still exists, however, it is not desired due to the high costs. The data provided in this chapter are to check the work and results gathered from the passive HVSR and active MASW field methods. Another disadvantage of the VSP method is that many wells throughout Connecticut are not drilled to bedrock and that more often than not; the water table of the area is very high. If a borehole being surveyed contains water, such as a monitoring well, shear-wave velocities (β) cannot be determined at those depths. Shear-waves cannot propagate through fluids.

$$\beta = (\frac{\mu}{\rho})^{1/2} \qquad \text{(Eq. 5.1)}$$

In a fluid, the shear modulus μ is equal to zero; therefore, the shear-wave velocity β is also equal to zero. However, if the downhole tool is securely clamped to the well casing, shear-wave velocities may still be obtained from the VSP survey. The following sections discuss VSP data acquisition, processing and results from Haddam Meadows State Park. The final section discusses VSP results from three field sites in Hartford County.

5.2. FIELD SURYEY SETUP

At Haddam Meadows State Park in East Haddam, CT, the three-component VSP downhole tool was used in borehole JL-1 in order to determine interval velocities and Vs30 (Photo 5.1a). The depth to rock observed by JL-1 was 38.1 m (124 ft) and the depth to the water table was 2.3 m (7.5 ft). In addition to the three-component geophone inside the downhole tool, which consumes three channels on the seismograph, an additional 4.5 Hz vertical geophone was planted near the well surface to check for surface noise that may interfere with the survey. A 10-lb. sledgehammer was used to induce both vertical and horizontal motion, same as used for MASW. The long offset for the vertical source was determined by Equation 5.2:

$$x_s \geq \frac{z_{max}}{tan\,(60)} \qquad \text{(Eq. 5.2)}$$

Where x_s is the source offset and z_{max} is the maximum depth of penetration. For JL-1, the long offset was 70 ft (21 m); Photo 5.3 shows the field setup on the ground surface. A near offset was also used for both the vertical and shear source (Photo 3b-c); this was set to 10 ft (3 m). The first VSP measurement was taken 5 ft below the borehole surface (Photo 5.2). Depth measurements were taken in feet rather than meters because the geophone cable provided was calibrated using the US Standard. With each depth, three shots were performed on the vertical source at the long and near offset. For the horizontal source, shots were performed such that the source was parallel to the direction of the well and then additional shots were performed such that the source was perpendicular to the direction of the shear source. A total of eighteen shots were acquired for each depth increment. The change in geophone depth increased by 2.5 ft with each depth measurement; the depth is measured from the middle of the downhole tool. A sketch of this field setup is illustrated in Figure 5.2.

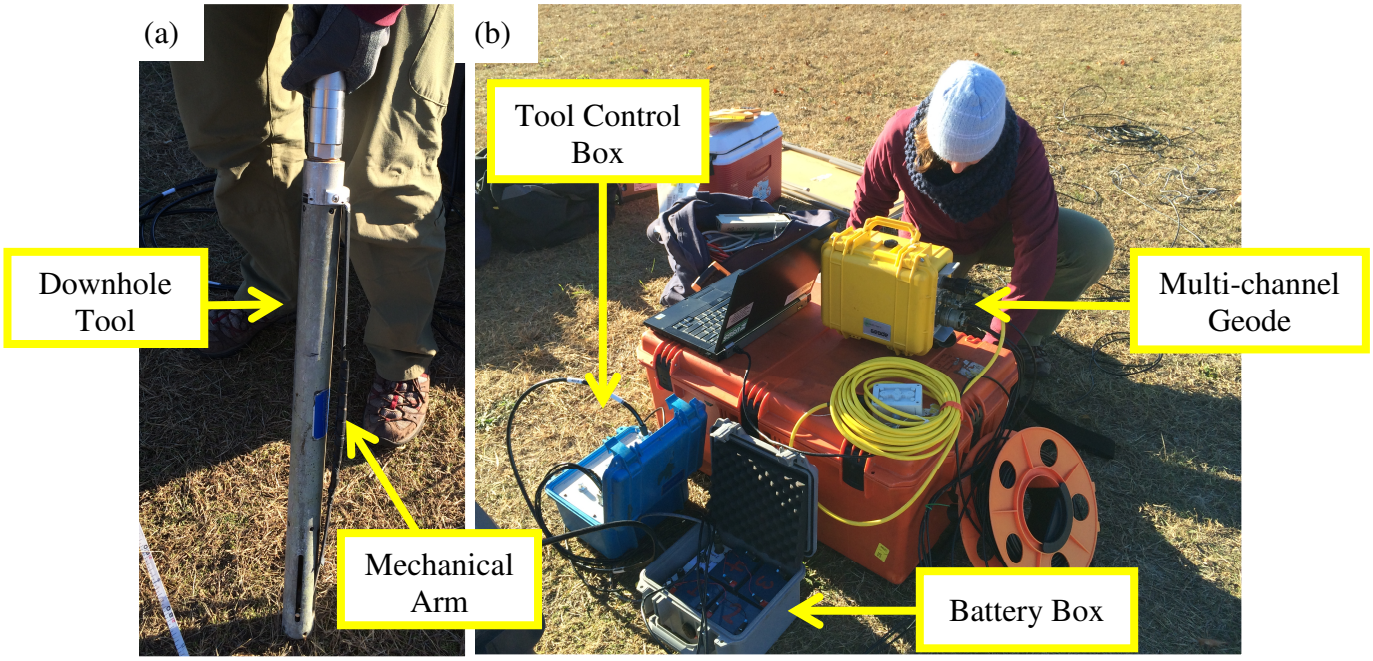

Photo 5.1. VSP Field Equipment. (a) The downhole VSP tool is a long cylinder containing three geophone components vertically stacked inside the tool column. The mechanical arm is controlled from a control box at the surface as seen in the second image. (b) The blue control box, battery, yellow geode and field computer are located at the surface near the wellhead. The geophone cable connects the three components inside the tool to the yellow multi-channel geode; only four channels are used for the survey including the vertical, two horizontal components within the tool and another vertical geophone located at the well surface for observing noise.

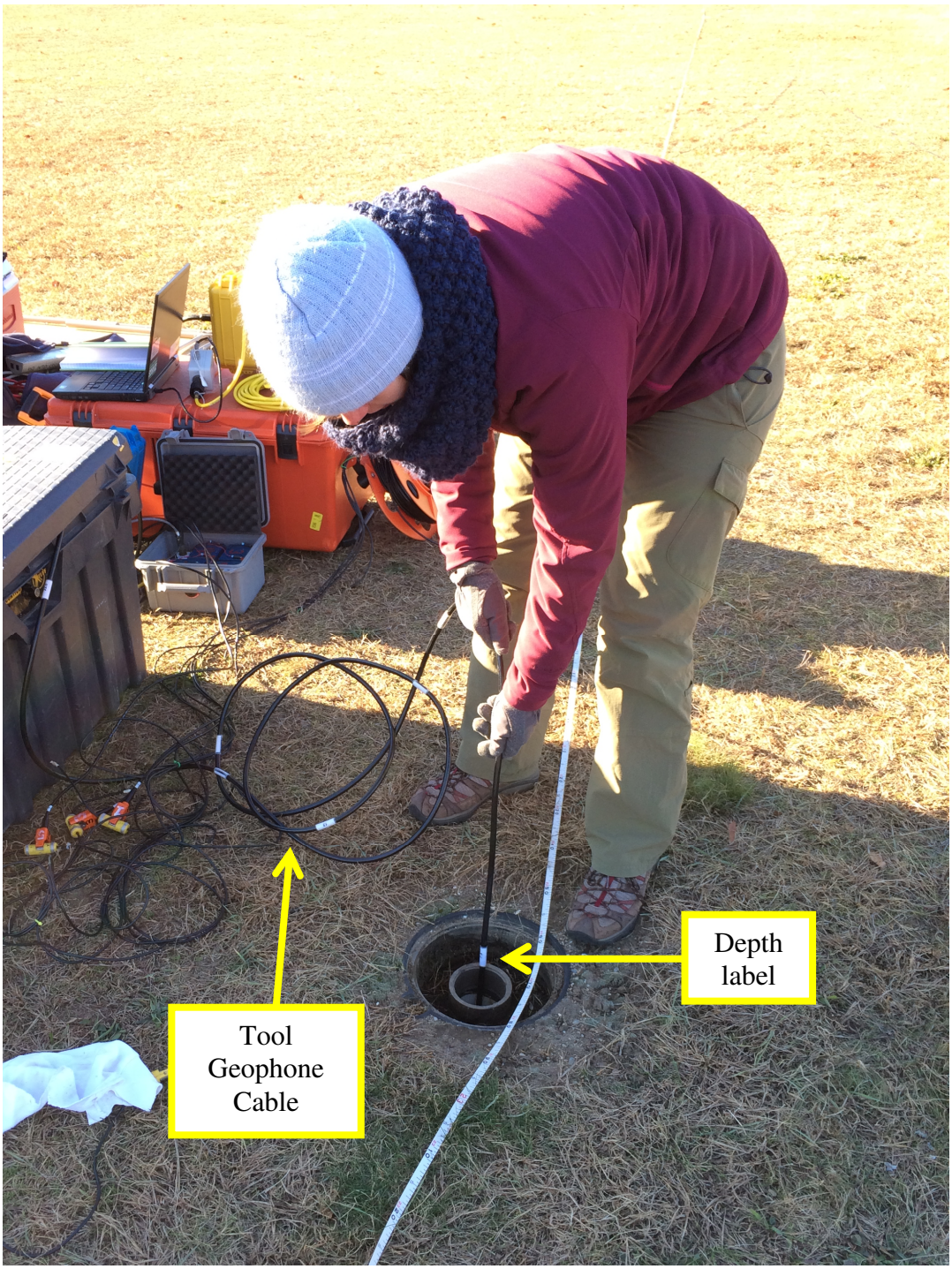

Photo 5.2. Downhole Tool during VSP Survey. The tool, as seen in Photo 5.1a, is inserted into the borehole. The depth measurements are taken from the wellhead such that the white label rests on top of the well casing.

Photo 5.3. VSP Field Survey. At Haddam Meadows State Park, the vertical far offset is located 70 ft from the wellhead. The vertical and horizontal near offset is 10 ft from the wellhead. The control equipment resides near the well head. The Connecticut River is right of the field site, East of the survey line.

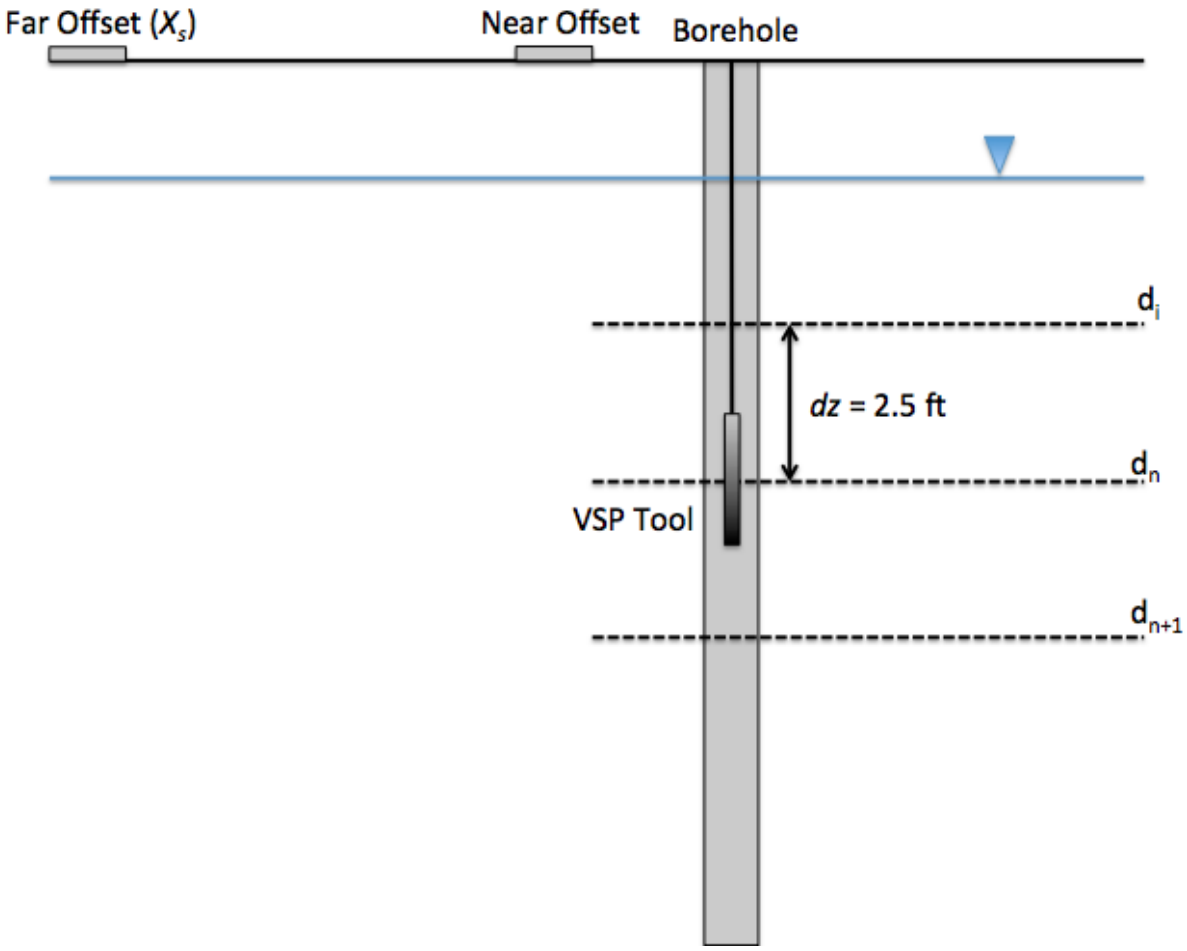

Figure 5.2. Sketch of VSP Method in the Field. For each downhole measurement, the depth *dz* increases by 2.5 ft, the minimum unit of measurement designated on the cable. The total depth is measured from the middle of the downhole tool to the top of the borehole.

5.3. DATA PROCESSING

Based on the assumption that waves propagate through a laterally layered medium, the p-wave (v_p) and s-wave velocities (v_s) can be determined from VSP data using Esmersoy's (1990) time-depth equation.

$$v_p = \frac{\cos\psi_p}{q_p}$$

$$v_s = \frac{\cos\psi_s}{q_s} \qquad \text{(Eq. 5.3)}$$

Where ψ_p and $\psi_s$are the p-wave and s-wave angles of incidence as measured from the vertical, q is the relationship between arrival time and depth such that $q = dt/dz$. By the substitution of q in Equation 5.3, the velocity becomes:

$$v_p = \frac{\mathrm{dz}(\cos\psi_p)}{dt}$$

$$v_s = \frac{\mathrm{dz}(\cos\psi_s)}{dt} \qquad \text{(Eq. 5.4)}$$

Where $\mathrm{dz}(\cos\psi)$ is equal to the change in pathlength *dl*. Therefore, velocity is the change in pathlength *dl* divided by the corresponding arrival time *dt*.

At Haddam Meadows State Park, average and interval p-wave and s-wave velocities were determined using VSP data. After the data were collected, the files were divided into six groups: far-offset shots, near-offset shots, shear 1, shear 2, shear 3, and shear 4. The vertical component data acquired from the near-offset shots were used to determine p-wave velocities. The longitudinal and transverse horizontal component data from the shear 1-4 shots were used to determine s-wave velocities; this includes two shots parallel to the direction of the well and two shots perpendicular to the direction of the well. Four directionally different shear shots were

performed to increase the probability that adequate first arrivals would be observed on at least one record (Crice 2011).

Data were processed in KGS-developed software, *SeisUtilities*. After the data files are separated into the six groups, data processing consists of three sets: assign array geometry, pick arrival times, and calculate velocities. Geometry parameters include depth interval, lateral source offset, receiver and source station, receiver station increment and spread movement. Then the arrival times of the wavelet are picked on each record, each time is observed as the first sharp change of the wavelet along the record. In Figure 5.3, the p-wave picked arrival times are indicated by the small boxes at the beginning of each record; the red line more obviously illustrates these times. As the downhole tool descended the borehole, the first arrival became more apparent or sharper on each signal record. The arrival times were then picked on the shear records. S-wave arrival time picking was more difficult than p-wave arrival times. In general, s-waves are observed as the secondary wave on a record and can be influenced by the earlier p-waves which can result in mode conversion. Figure 5.4 displays the picked s-wave arrival times from the perpendicular shear source where the wavelet shape differs from the cleaner p-wave picks in Figure 5.3. The s-wave arrivals display a shallow slope that increases more gradually with depth than the p-wave arrivals.

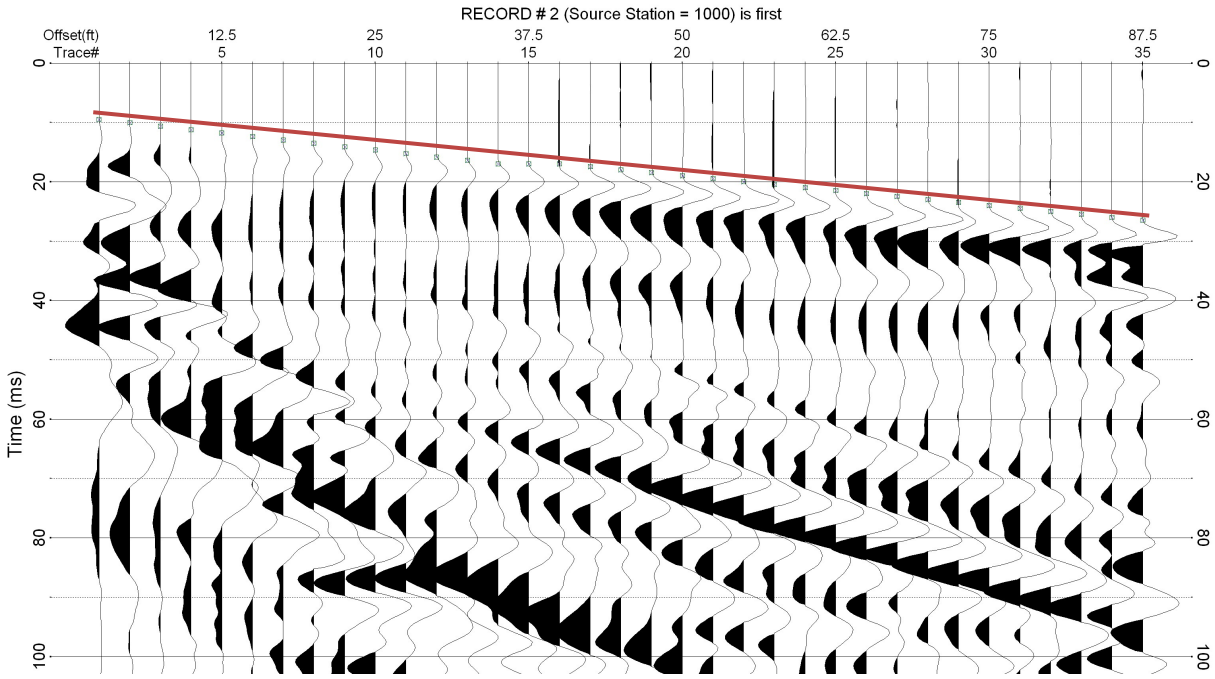

Figure 5.3. P-wave First Arrivals from 10 ft Near-offset Source. The picked arrival times are indicated by the small boxes on each record from 10-26 ms. The red line illustrates the slope of these fast arrival times.

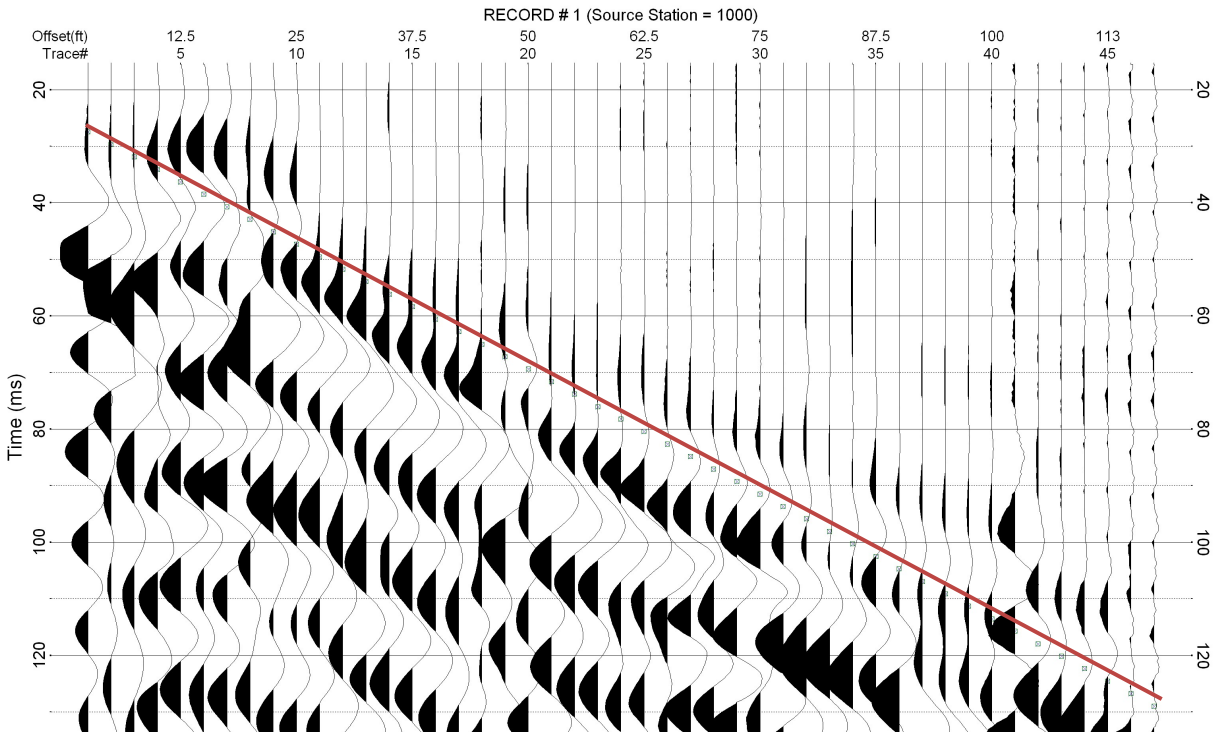

Figure 5.4. S-wave First Arrivals from 10 ft Perpendicular Shear Source. The picked arrival times are indicated by the small boxes on each record from 25-130 ms. The red line illustrates the slop of these slower arrival times.

Each longitudinal and transverse record from the four shear sources were analyzed for first arrivals. Some records were more easily picked than others, but some were not used for velocity calculation due to picking uncertainties and inability to determine adequate s-wave first arrivals. After the records were picked, the arrival times were used to determine interval and average v_p, v_s, and the ratio between v_p and v_s. Table 5.1 displays these values as well as the corresponding depths and path lengths. It is important to note that the entire depth of the well was not surveyed due to sediment buildup at the bottom of the well; however, more than 30 m of data was retrieved. From depth 5-20 ft, the interval p-wave velocities are significantly higher than the other depths, but great confidence remains with the picked p-wave arrivals. However, the p-wave values were not used for site classification. The average p-wave and s-wave sediment velocity was 8413.7 ft/second (2564.5 m/s) and 1058.74 ft/second (322.7 m/s) respectively. As a result, the Vs100 and Vs30 of this site was 1050 ft/second and 320 m /s respectively, which are a NEHRP, site class D. From the VSP, MASW, and HVSR data at this site, all three methods agree that Haddam Meadows is site class D.

Table 5.1 Velocity values from JL-1 VSP Survey

Depth (ft)	PathLength	Average Vp	Interval Vp	Average Vs	Interval Vs	Vp/Vs
2.5	10.31	624.71	624.71	374.83	395.55	1.58
5	11.18	675.06	14073.80	376.37	597.94	23.54
7.5	12.50	751.88	20946.99	391.69	744.40	28.14
10	14.14	847.49	26486.06	414.49	845.34	31.33
12.5	16.01	955.69	29613.89	440.67	915.66	32.34
15	18.03	1072.31	32579.77	467.86	964.15	33.79
17.5	20.16	1194.41	33776.00	494.75	999.56	33.79
20	22.36	1315.33	17640.28	520.68	1024.68	17.22
22.5	24.62	1412.31	5210.75	545.32	1044.28	4.99
25	26.93	1506.85	5295.82	568.56	1058.42	5.00
27.5	29.26	1598.65	5369.94	590.37	1070.28	5.02
30	31.62	1687.54	5427.65	610.82	1078.79	5.03
32.5	34.00	1773.52	5485.94	629.95	1086.52	5.05
35	36.40	1856.41	5510.05	647.88	1091.93	5.05
37.5	38.81	1936.36	5539.97	664.66	1097.29	5.05
40	41.23	2013.43	5564.64	680.41	1100.85	5.05
42.5	43.66	2087.73	5585.21	695.19	1104.76	5.06
45	46.10	2159.45	5615.44	709.09	1107.16	5.07
47.5	48.54	2228.50	5617.24	722.16	1110.14	5.06
50	50.99	2295.10	5629.83	734.49	1111.78	5.06
52.5	53.44	2359.35	5640.69	746.11	1114.14	5.06
55	55.90	2421.45	5663.14	757.11	1115.26	5.08
57.5	58.36	2481.32	5658.36	767.50	1116.69	5.07
60	60.83	2539.14	5665.60	777.35	1118.46	5.07
62.5	63.29	2595.01	5672.00	786.70	1119.07	5.07
65	65.76	2649.03	5677.67	795.58	1120.57	5.07
67.5	68.24	2701.37	5695.83	804.02	1120.96	5.08
70	70.71	2751.92	5687.26	812.06	1122.27	5.07
72.5	73.19	2800.86	5691.33	819.72	1122.48	5.07
75	75.66	2848.25	5695.00	827.03	1123.65	5.07
77.5	78.14	2894.17	5698.32	834.01	1123.73	5.07
80	80.62	2935.36	5322.06	840.68	1124.78	4.73
82.5	83.10	2975.11	5313.22	847.07	1124.77	4.72
85	85.59	3013.71	5326.96	853.17	1125.73	4.73
87.5	88.07	3050.98	5317.69	859.04	1125.64	4.72
90	90.55	3087.10	5319.65	864.66	1126.53	4.72
92.5	93.04	3122.22	5332.87	870.06	1126.37	4.73
95	95.52	3156.18	5323.12	875.24	1127.20	4.72
97.5	98.01	3189.13	5324.65	880.23	1126.99	4.72
100	100.50	3221.11	5326.08	885.03	1127.78	4.72

102.5	102.99	3252.28	5338.83	889.66	1127.53	4.74
105	105.48	3282.45	5328.62	894.11	1128.29	4.72
107.5	107.96	3311.88	5341.20	898.41	1128.00	4.74
110	110.45	3340.40	5330.83	902.55	1128.72	4.72
112.5	112.94	3368.13	5331.82	906.55	1128.41	4.73
			8413.71	ft/s	1058.74	ft/s
		Velocity of Sediments	2564.50	m/s	322.70	m/s
				Vs100	1050.06	ft/s
				Vs30	**320.06**	**m/s**

5.4. RESULTS

The VSP data acquisition procedure and data processing previously described were used at three sites in Hartford County: the 4-H Camp in Marlborough, Elizabeth Park in West Hartford and at the U.S. Geological Survey, Water Science Center in East Hartford.

Marlborough, CT

At the 4-H Camp, a 15 ft depth was surveyed from 7.5-15 ft every 2.5 ft with a 5 ft near offset; water was observed at 13 ft. Borehole MB32's casing starts 1.5 ft above ground which is why the survey started at 7.5 ft, which is actually 6 ft into the subsurface. Picked arrival times for p-wave and s-wave are shown in Figure 5.5 and 5.6 and the corresponding velocities are in Table 5.2. Based on the surface phone wave record, there was an inconsistent arrival time for each depth increment which was caused by an issue with the time break. For depths 12.5 ft and 15 ft, the records were adjusted by 1 ms and 1.5 ms respectively. In addition, the dataset was limited by the shallow borehole depth which almost made first arrival picking difficult since a data trend between time and depth was less obvious. Although adjustments were made to the data, based

on the interval velocities listed in Table 5.2, a confident site classification was unable to be assigned. Therefore, the VSP survey provided inconclusive results for this site.

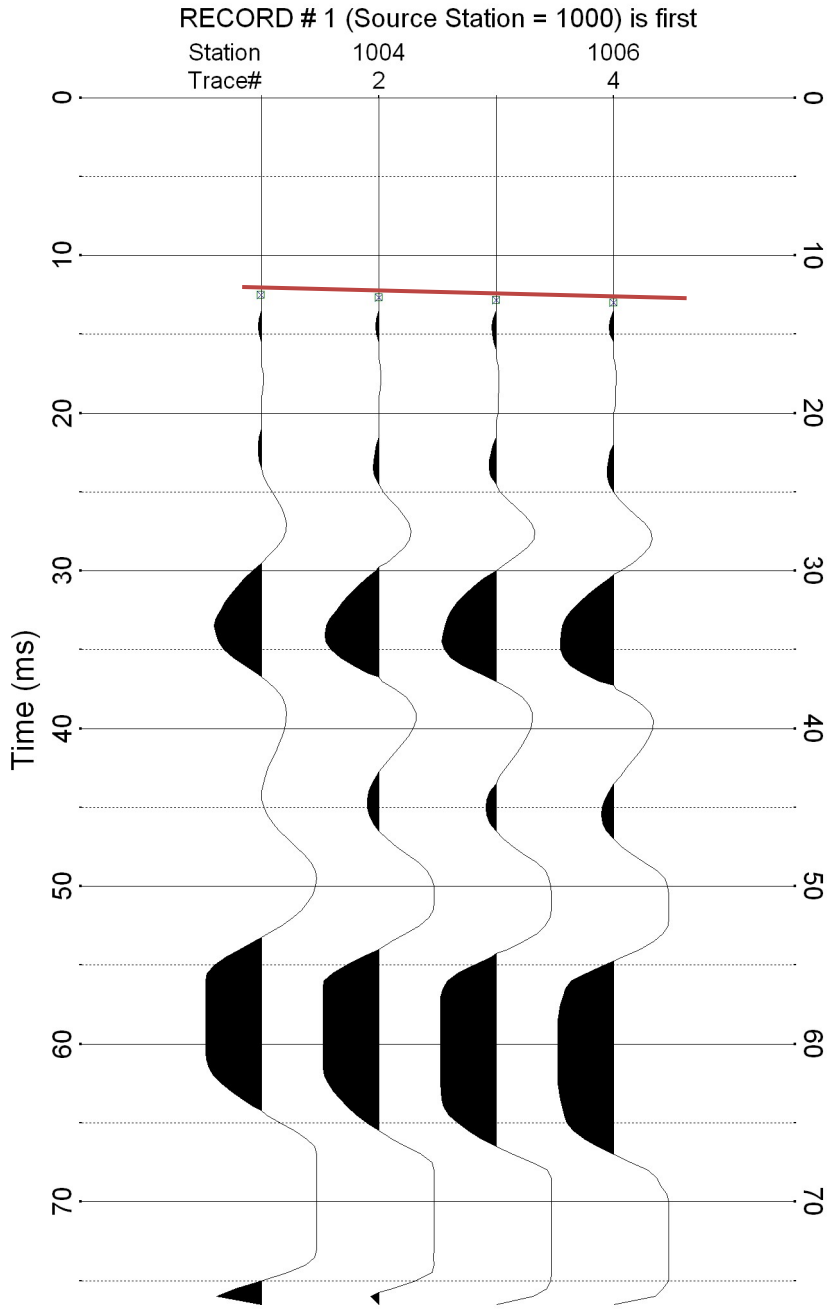

Figure 5.5. P-wave First Arrivals for 4-H Camp in Marlborough, CT. The picked arrivals from 13-14 ms are displayed by the small boxes on each record and the red line shows the apparent slope of those points.

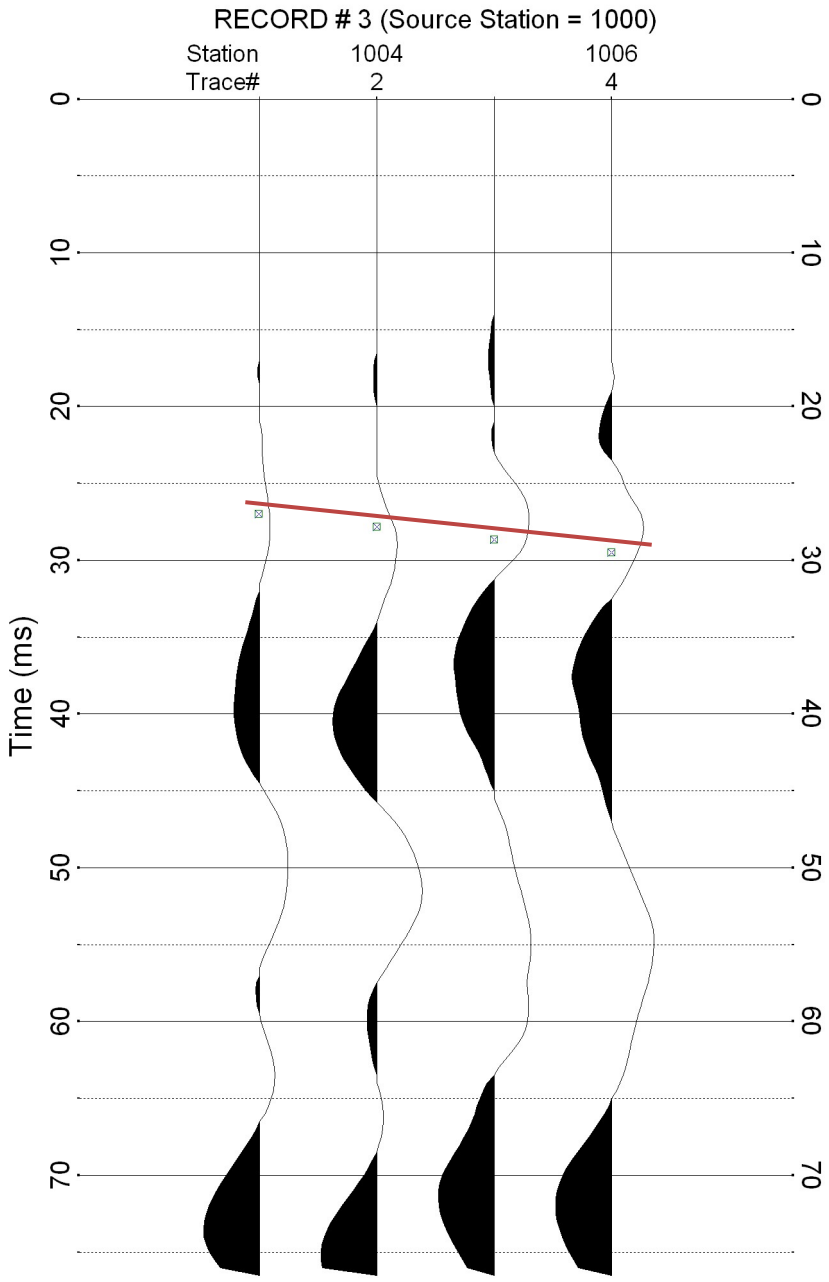

Figure 5.6. S-Wave First Arrivals from 4-H Camp in Marlborough, CT. The picked arrivals from 26-29.5 ms are displayed by small boxes on each record and the red line illustrates the apparent slope of these points. These records are from shots performed perpendicular to the direction of the well.

Table 5.2 Determine Vp and Vs values from VSP Survey at 4-H Camp.

Depth (ft)	PathLength	Average Vp	Interval Vp	Average Vs	Interval Vs	Vp/Vs
7.5	7.81	624.82	624.82	289.27	289.27	2.16
10	9.86	778.58	12357.18	354.31	2462.54	5.02
12.5	12.08	941.56	13302.42	421.51	2666.87	4.99
15	14.40	1107.40	13851.10	488.01	2773.54	4.99
			10033.88	ft/s	2048.05	ft/s
		Average Velocity of Sediments	836.16	m/s	170.67	m/s

West Hartford, CT

At Elizabeth Park, a 17.5 ft depth was surveyed every 2.5 ft with a 5 ft near offset; water was observed at 3.3 ft. The VSP survey at Elizabeth Park also acquired a small dataset, which made picking the first arrivals more difficult for all components. The p-wave picks are displayed in Figure 5.7, however the apparent interval velocities are too high (Table 5.3). Although the picks are reasonable based on the observed wavelet characteristics on each trace, these p-wave velocity values cannot be used for further analysis. These high interval velocities may have been caused by the waves refracting off the well grout. However, more reliable s-wave first arrival picks were made (Figure 5.8) as indicated by the boxes on each record. Based on the determined Vs interval velocities, the values are reasonable for the soft, unconsolidated sediments of this site except for depth 2.5 ft, which is too low. After removing this value, the average value of the remaining sediments increases to 817.7 ft/s (248.1 m/s). Although the well does not penetrate 30 m, when combined with the MASW and HVSR data also collected at this site, the average sediment velocity correlates to the average sediment velocity determined. From the MASW survey, the average sediment velocity was 272.4 m for 17.2 m. Based on these three techniques, Elizabeth Park was assigned a seismic hazard class C based on Vs30.

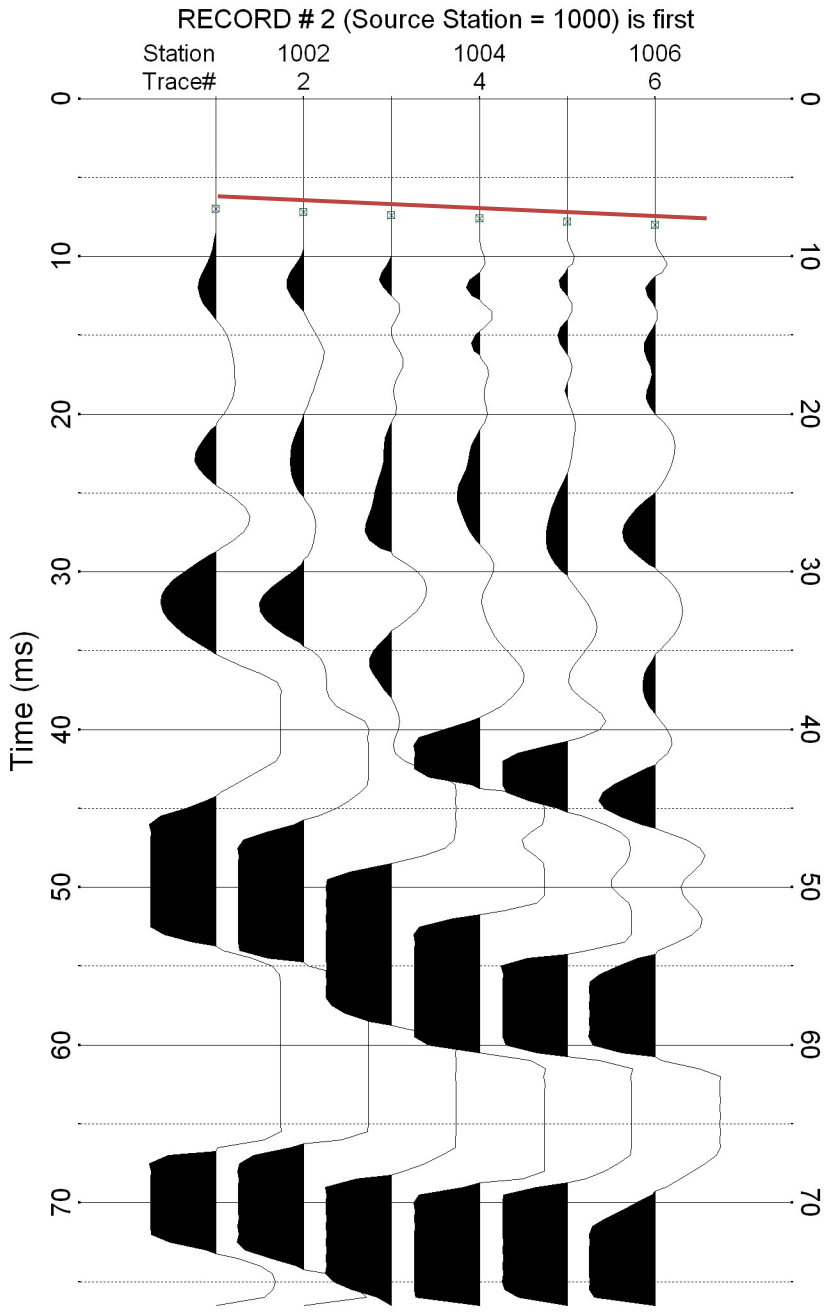

Figure 5.7. P-wave First Arrivals for Elizabeth Park. The boxes indicate the picked first arrivals on each record from 7-9 ms and the red line shows the apparent slope of these points.

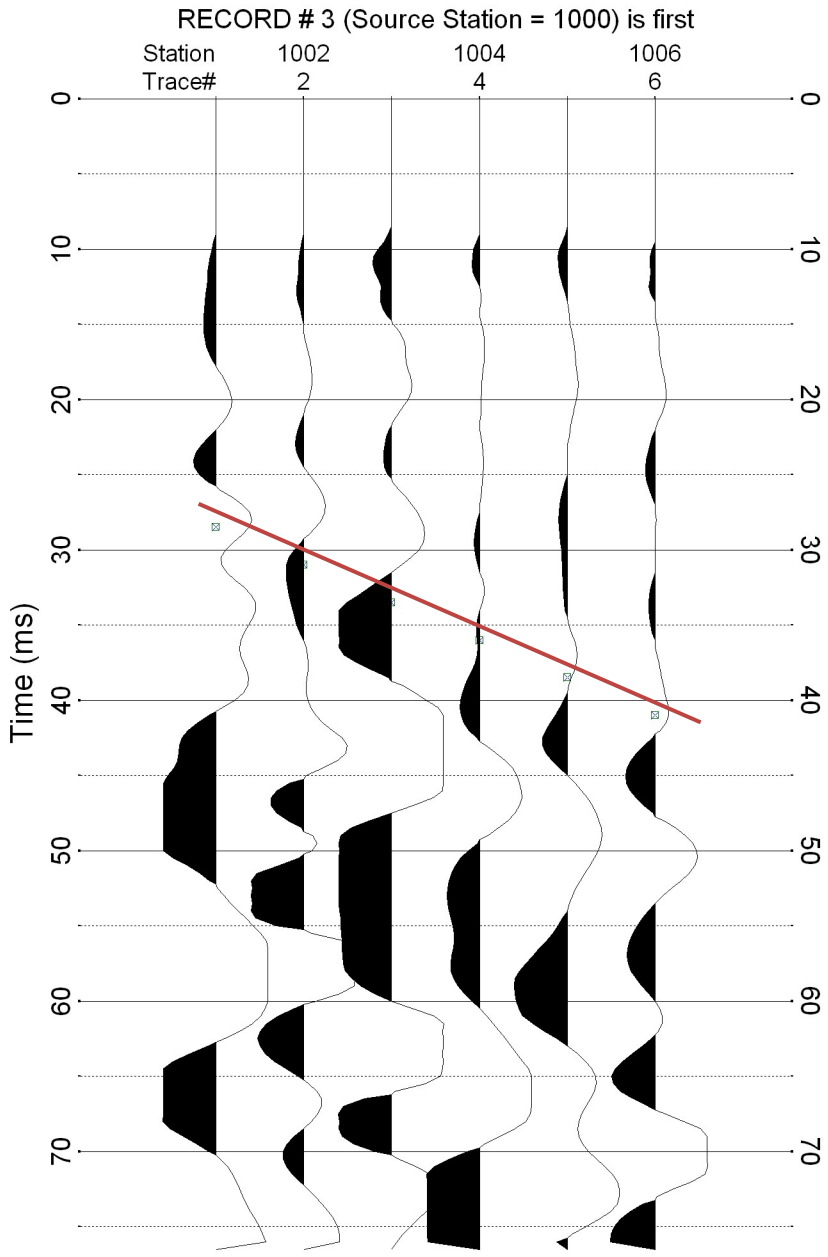

Figure 5.8. S-wave Picked First Arrivals for Elizabeth Park. The picked arrival times are indicated by the small boxes on each trace from 28-42 ms. The red line illustrates the slope of these points. These records are from shots performed perpendicular to the direction of the well.

Table 5.3. Determined Velocity Values for VSP Survey at Elizabeth Park.

Depth (ft)	PathLength	Average Vp	Interval Vp	Average Vs	Interval Vs	Vp/Vs
2.5	5.59	798.60	798.60	196.15	196.15	4.07
5	7.07	982.23	7441.70	228.10	592.36	12.56
7.5	9.01	1218.09	9665.72	269.07	777.12	12.44
10	11.18	1471.29	10886.74	310.57	866.58	12.56
12.5	13.46	1726.01	11356.08	349.69	913.03	12.44
15	15.81	1976.42	11742.38	385.64	939.39	12.50
			8648.54	ft/s	714.11	ft/s
		Average Velocity of Sediments	2636.07	m/s	217.66	m/s

East Hartford, CT

At the USGS office in East Hartford borehole EH178 with 87.5 ft depth was surveyed every 2.5 ft with a 10 ft near offset; water was observed 6 ft below the subsurface and the depth to bedrock was 96 ft. The survey did not extend the full length of the borehole due to sediment buildup at the bottom. The vertical and horizontal sources were placed on pavement rather than directly on the ground surface. Clean p-wave first arrivals were observed on each record and were picked from 10-18 ms (Figure 5.9). The s-wave first arrivals were picked from 29-164 ms using shots parallel to the borehole (Figure 5.10). For both the p-wave and s-wave records, the first arrivals were more easily selected than the two sites previously discussed in this section. The determined velocities are listed in Table 5.4 where the average sediment Vp and Vs velocities (87.5 ft) were 4242 ft/s (1292.96 m/s) and 585.78 ft/s (178.54 m/s). Based on this average shear-wave velocity, the sediments are considered site class E.

HVSR measurements were also taken in the form of a huddle test around the borehole (Figure 5.11). A dominant resonance frequency was observed at 1.91 Hz, which corresponds to the 96 m depth to rock recorded on the well log. From this resonance frequency and the depth to rock, the average shear-wave velocity of the sediments was determined to be 222 m/s, which would be considered site class D. After Rayleigh-wave ellipticity inversion, a 2-layer model was generated with depth to rock observed between 26-28 m with average shear-wave velocities from 170-180 m/s, which agree with the results retrieved from the VSP survey (Figure 5.12). Based on these two surveying techniques, the USGS office site was assigned site class E.

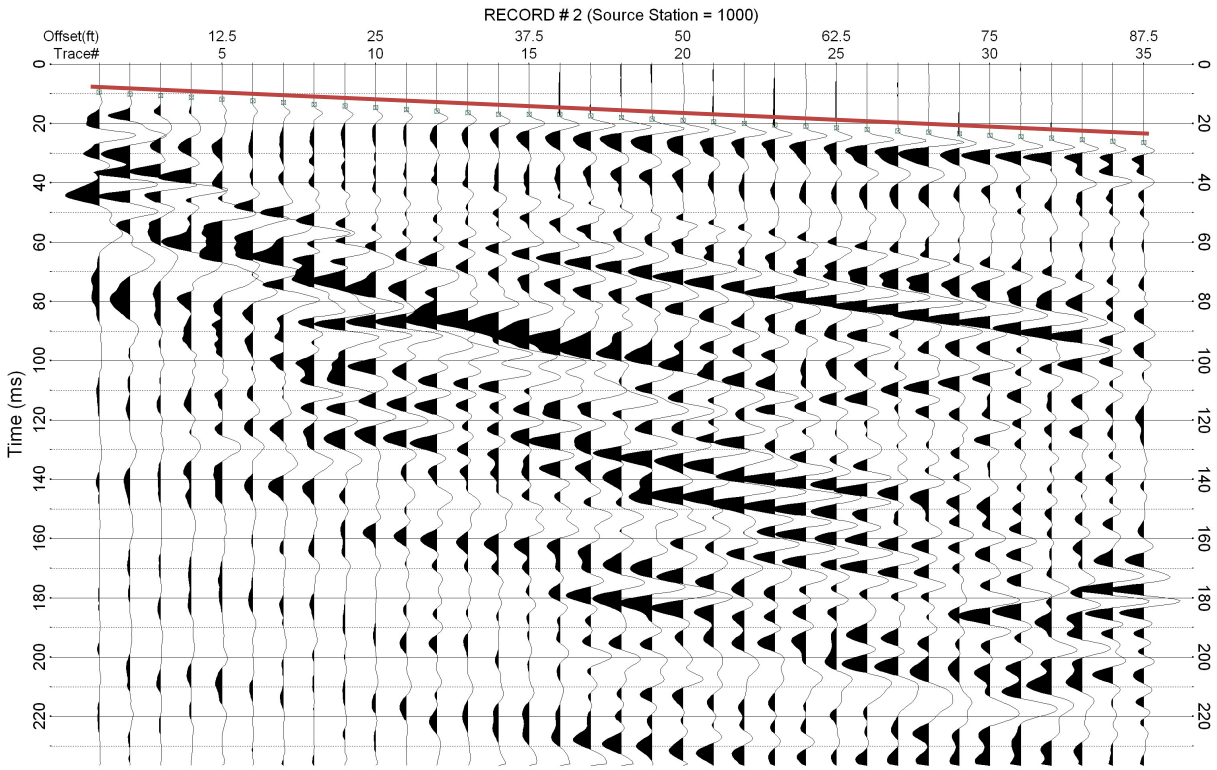

Figure 5.9. P-wave First Arrivals from USGS Office in East Hartford. The picked arrival times are indicated by the small boxes on each record from 10-18 ms. The red line illustrates the slope of these picked times.

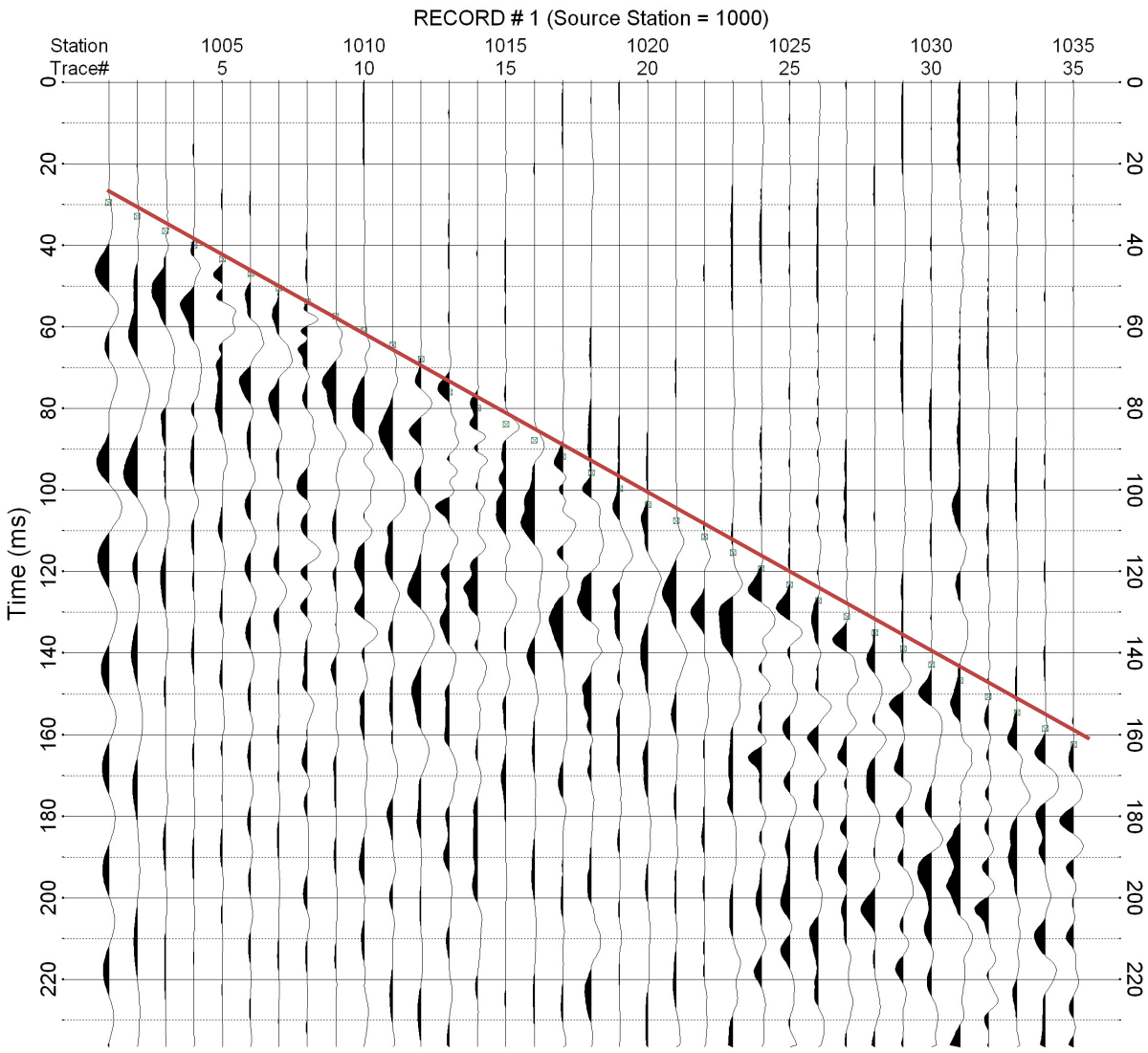

Figure 5.10. S-Wave First Arrivals from USGS Office in East Hartford. The picked arrival times are indicated by the small boxes on each record from 29-164 ms and the red line illustrates the slope of these points.

Table 5.4 Determined Velocities from VSP Survey at USGS Office.

Depth (ft)	PathLength	Average Vp	Interval Vp	Average Vs	Interval Vs	Vp/Vs
2.5	10.31	1085.03	1085.03	349.42	349.42	3.11
5	11.18	1109.60	1514.89	338.80	249.31	6.08
7.5	12.50	1173.38	2287.11	342.47	377.05	6.07
10	14.14	1259.32	2845.99	353.55	469.18	6.07
12.5	16.01	1355.79	3233.41	368.00	533.05	6.07
15	18.03	1455.73	3500.77	383.57	577.13	6.07
17.5	20.16	1555.10	3687.85	399.12	607.97	6.07
20	22.36	1651.70	3821.55	414.09	630.01	6.07
22.5	24.62	1744.40	3919.35	428.21	646.13	6.07
25	26.93	1832.69	3992.51	441.41	658.19	6.07
27.5	29.26	1916.42	4048.40	453.67	667.41	6.07
30	31.62	1995.63	4091.90	465.04	674.58	6.07
32.5	34.00	2070.49	4126.34	446.73	293.32	14.07
35	36.40	2141.21	4154.03	454.76	610.36	6.81
37.5	38.81	2282.97	0.00	462.19	613.83	0.00
40	41.23	2425.36	0.00	469.08	616.40	0.00
42.5	43.66	2494.89	4859.13	475.49	618.84	7.85
45	46.10	2560.98	4874.20	481.44	620.60	7.85
47.5	48.54	2623.85	4886.99	486.99	622.39	7.85
50	50.99	2683.69	4897.95	492.17	623.78	7.85
52.5	53.44	2740.71	4907.40	497.02	624.83	7.85
55	55.90	2795.09	4915.61	501.56	626.03	7.85
57.5	58.36	2846.98	4922.78	505.82	626.79	7.85
60	60.83	2896.55	4929.08	509.84	627.75	7.85
62.5	63.29	2943.95	4934.64	513.61	628.30	7.85
65	65.76	2989.31	4939.58	517.18	629.09	7.85
67.5	68.24	3032.74	4943.98	520.54	629.49	7.85
70	70.71	3074.38	4947.92	523.73	630.15	7.85
72.5	73.19	3114.32	4951.46	526.74	630.44	7.85
75	75.66	3152.66	4954.65	529.61	631.00	7.85
77.5	78.14	3189.49	4957.54	532.33	631.21	7.85
80	80.62	3224.90	4960.16	534.92	631.71	7.85
82.5	83.10	3258.97	4962.55	537.38	631.85	7.85
85	85.59	3291.78	4964.73	539.73	632.29	7.85
87.5	88.07	3323.38	4966.72	541.97	632.38	7.85
			4242.00	ft/s	585.78	ft/s
		Average Velocity of Sediments	1292.96	m/s	178.54	m/s

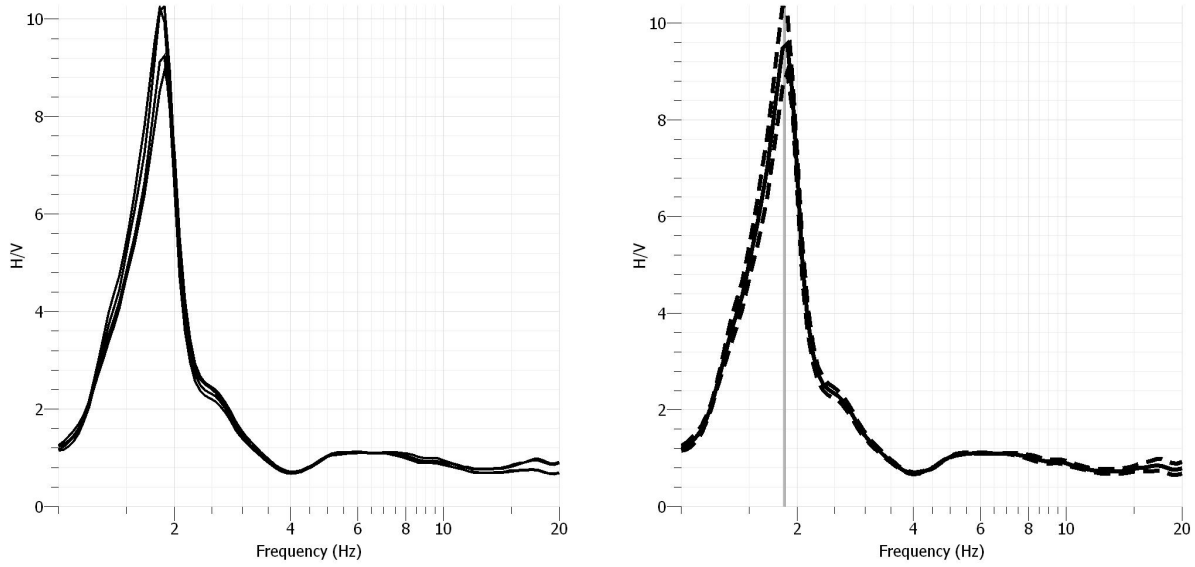

Figure 5.11. HVSR Result from EH178 Borehole at USGS Office in East Hartford. (a) All four HVSR curves from the seismometers used for the huddle test display a clean, sharp peak at 1.91 Hz, identified as the fundamental mode. (b) The average of the four curves is displayed by the solid line with corresponding standard deviations as the dashed lines. The vertical gray box indicates the average resonance frequency.

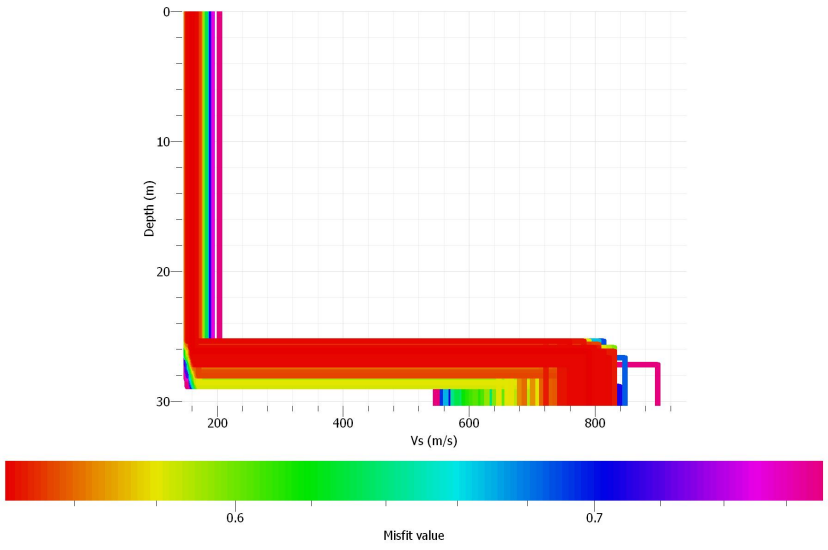

Figure 5.12. Velocity Profile from Rayleigh Wave Ellipticity of EH178 Borehole. A 2-layer model as sediment over half space was generated from the HVSR data in Figure 5.11. Each colored line refers to each model generated from the inversion. The layer interface was observed around 27 m with an average shear-wave velocities from 170-180 m/s.

6. SUMMARY AND RECOMMENDATIONS

Over the course of three years, several geophysical techniques were used to determine shear-wave velocity profiles from twenty-nine sites throughout Hartford County, Connecticut. These field techniques included passive single-station Horizontal-to-Vertical Spectral Ratio (HVSR), active Multi-channel Analysis of Surface Waves (MASW) and active Vertical Seismic Profiling (VSP). Before data was acquired, a seismic hazard class was assigned to each site based on previous work the Connecticut Department of Energy and Environmental Protection (Becker *et al*., 2013). One of five hazard classes was assigned based on the site's surficial materials as described in Table 1.2 and illustrated in Figure 1.2. In order to investigate the assigned hazard classes, geophysical data were collected to calculate a "Vs30" for each site. Vs30 is an internationally recognized approach used to not only assign a Seismic Hazard classification, but also by engineers during pre-construction site analyses. Vs30 measurements guide engineers on the type of structural design necessary to meet building code required for construction.

Three geophysical techniques were investigated and their results compared in order to determine the optimal method for obtaining shear-wave velocity profiles throughout Hartford County. HVSR was used at thirty field sites to observe the ground's natural resonance frequency. From the onsite well, the average shear-wave velocity of the sediments was calculated using Equation 3.5. However, for many sites, the bedrock depth was observed shallower than thirty meters; therefore at some sites the HVSR data did not provide sufficient data for calculating Vs30 because it lacked bedrock depth calculation. In order to determine the missing bedrock velocities, the Rayleigh wave ellipticity method was then used to create 2-layer velocity models. This algorithm made a correction to the HVSR curve to remove the effects of

unwanted body and love waves from the resonance curve and the resulting curve was then inverted to create a velocity profile. Bedrock depth, as provided by the onsite borehole, was used as an inversion constraint. For some sites, specifically C surficial classes, the 2:1 velocity contrast was not met due to the high velocity till that masked the bedrock interface. From the ellipticity inversion, bedrock velocities were extracted and used to calculate Vs30 (Equation 2.1). At one surficial A site, a resonance frequency was not observed, which is due to the shallow bedrock depth; this correlates with the characteristics of the surficial hazard classification. At two other surficial A sites, the ellipticity inversion failed to create a velocity profile because the resulting ellipticity curve was flat. Then at 4 other sites, the ellipticity inversion did not generate reliable velocity results. Overall, the passive single-station data was able to recover a resonance frequency at B-E site classes, which was used to determine an average shear-wave velocity for each site. Then the ellipticity inversion provided bedrock velocity values which were then used for Vs30 calculation. Based on this value, a NEHRP seismic hazard class was assigned to that field site which in general was at least one hazard class lower than the surficially mapped class.

At twelve of these thirty field sites, active MASW surveys were performed in order to extract dispersion curves and shear-wave velocity profiles. For these sites, the HVSR data taken at the borehole was used as a constraint for the MASW results. The HVSR data determined an average shear-wave velocity of the sediments and this value was compared to resulting velocity profiles extracted from the MASW data. Additional HVSR data was taken along the MASW line and the average velocity of the sediments from the borehole HVSR was used to determine how bedrock depth changes, if at all, along the MASW profile. For each site, one dispersion curve was used to represent the array that exemplified optimal dispersion with a velocity profile that had a low misfit model and reasonable results. After comparing the velocity profiles from

the active MASW data to the passive ellipticity velocity profiles, six agreed on the assigned surficial site classification, but six sites had geophysical results that did not match the surficial site class.

At one site, Philip R Smith School in South Windsor, the MASW survey results identified a bedrock interface deeper than that recorded in the site's borehole log. This site exhibits surficial class C materials, thick till, and the observed resonance frequency changed dramatically across the MASW profile from 19.31-26.82 Hz (Geophone 1-24). From this change, one can infer that the bedrock depth becomes shallower from Geophone 1-24, which was estimated to change from 3.57-2.57 m with respect to the 4.8 m at the well. The onsite well was located about 30 ft southwest of Geophone 1. Passive HVSR and MASW surveys are known to have difficulty obtaining adequate results in areas of shallow bedrock which may account for the velocity differences. However, this site will remain a C class until a better analysis can be made.

At two MASW sites the depth to bedrock was unknown; Dinosaur State Park in Rocky Hill and Nevers Park in South Windsor. Although the passive and active results at Nevers Park gave the same site classification, the determined depth to rock values differed greatly; originally a surficial D class, this site was assigned a C class based on the field results. At Dinosaur State Park, the depth to bedrock values from the passive and active surveys were similar (15m, 16.2 m respectively) but the average sediment velocity differed by 700 m/s (240 m/s, 953m/s respectively). Based on the passive results, this site would be a D class, but the active results give a B class which is the same as the surficial materials class. When the active results are used in Equation 3.5, the calculated resonance frequency (14 Hz) does not correspond to the observed resonance frequency (4 Hz), whereas the passive results do. Uncertainty remains for this site without additional depth information, but Dinosaur State Park was assigned a B class.

VSP was used at three of the thirty field sites in Hartford County. This included the surficial A class, 4-H Camp in Marlborough, and two surficial E classes, Elizabeth Park in West Hartford and the USGS office in East Hartford. Overall, the VSP method was least effective at the 4-H Camp due to the limited well depth, which was only 15 ft; no result was gained from this downhole method at this site. At Elizabeth Park, the VSP method was effective for gathering shear wave velocities, but not p-wave velocities. The first arrivals on the p-wave shot gathers were observed at very high velocities which were closer to the velocity of steel than that of the geologic formation. Although the downhole tool was used in PVC casing, the casing had an exterior metal casing that may have interfered with the survey. However, reliable shear wave velocities were observed at Elizabeth Park, which were incorporated into the overall analysis. The drilled borehole depth limited this survey such that the deepest depth observed by the tool was only 17.5 ft (5.3 m). Therefore, an overall average sediment velocity was not observed at Elizabeth Park.

In contrast to the two VSP sites previously discussed, the VSP survey at the USGS office in East Hartford proved effective for extracting interval and average p-wave and s-wave velocities. The deepest depth achieved at this site was 87.5 ft (26.7 m) where the depth to bedrock was recorded at 29 m. Although there was no MASW survey to supplement the VSP and HVSR results due to limited open space, the VSP and HVSR results corresponded well with each other. The average sediment velocities determined from the HVSR and VSP surveys differed by 40 m/s centered on the D-E NEHRP velocity boundary; this site was assigned E, which matches the surficial classification.

The relative location and corresponding surficial site class of the thirty sites are mapped in Figure 6.1. After the geophysical analysis and Vs30 calculation, the new site classifications for

each site are mapped in Figure 6.2 and explained in Table 6.3. Table 6.1 gives a basic summary of the results comparing the surficial-based site class and the geophysically-derived site class. Table 6.2 addresses how bedrock depth was observed less than 30 m at a majority of the field sites, which affected the Vs30 determined for each site since the bedrock velocity had to be included in the calculation. For sites where bedrock invades the upper 30 m, it has been argued that by some that the seismic hazard classification should be reduced to the upper 15 m, however for some sites, bedrock is shallower than 15 m. Other methods for evaluating seismic hazard are being explored by other groups such as moment-magnitude-based catalogs and seismicity maps.

For additional reference, Figure 6.3 shows a regression curve for Hartford County constructed by the resonance frequencies observed from the passive single-station surveys and the borehole recorded depth to bedrock; the points are color coordinated based on the geophysically-derived site classifications. Some sites were removed from this curve due to poor HVSR results, such that no resonance was observed or no depth to bedrock was recorded in the borehole information. From the curve, the regression equation for this area was:

$$y = 48.23x^{-0.672} \qquad \text{(Eq. 6.1)}$$

Where x is resonance frequency and y is thickness in meters. From this equation, a sediment thickness can be estimated based on an observed resonance frequency and vice versa.

For the purpose of this project, the use of multiple seismic methods improved the final hazard classification assignment. It is recommended that at least two methods are used at each field site in order to determine a reliable velocity profile of the subsurface. It is almost important that an adequate bedrock velocity is observed at sites where depths are less than 30 m. Before field investigation, it is also recommended that the actual depth to bedrock is known. For active surveys, a stronger seismic source should be considered for sites where the desired depth is

greater than 20 m or for areas where a stiffer geologic structure exists. For additional VSP surveys, boreholes that exceed the bedrock depth and penetrate deeper than 20 ft would be optimal based on the results of this project. Finally, the use of passive Rayleigh wave ellipticity inversion should be investigated further so that the results can be evaluated with higher confidence.

Table 6.1 Site Class Change between Surficial Class and Field Results

# Sites	Hazard Change
9	Stayed the same
12	Decreased by 1 hazard class
4	Decreased by 2 hazard classes
4	Increased by 1 hazard class
1	Increased by 2 hazard classes

Table 6.2 Bedrock Depth at Each Site

# Sites	Bedrock Depth
5	more than 30 m
24	Less than 30 m
18	Less than 15 m

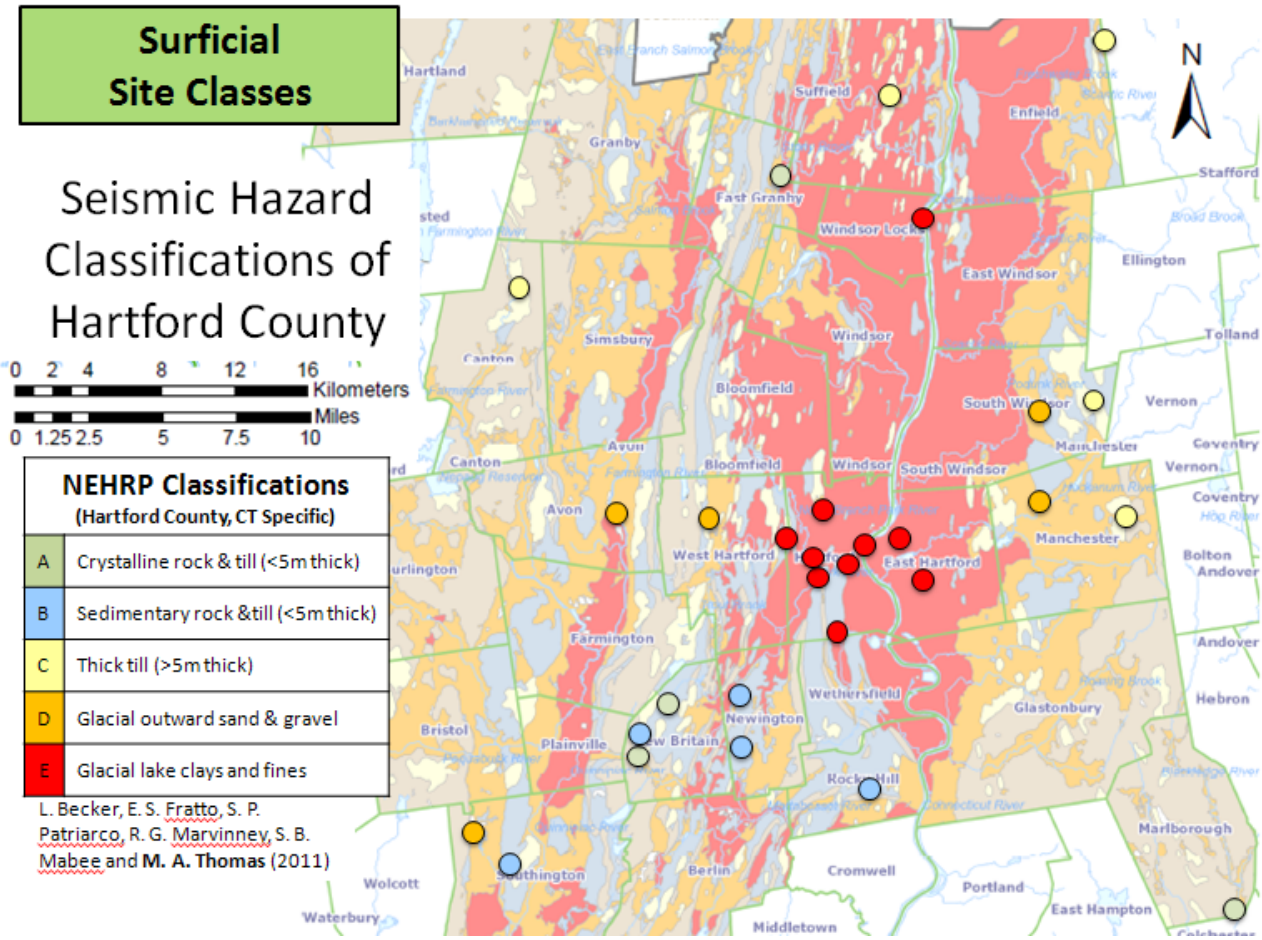

Figure 6.1. Distribution of Sites Investigated using Geophysical Techniques. The base map is the Becker et al. (2013) Seismic Hazard map of Hartford County and each point represents the location of each field site used in this study. The color of each point illustrates the surficial site class assigned to that site class.

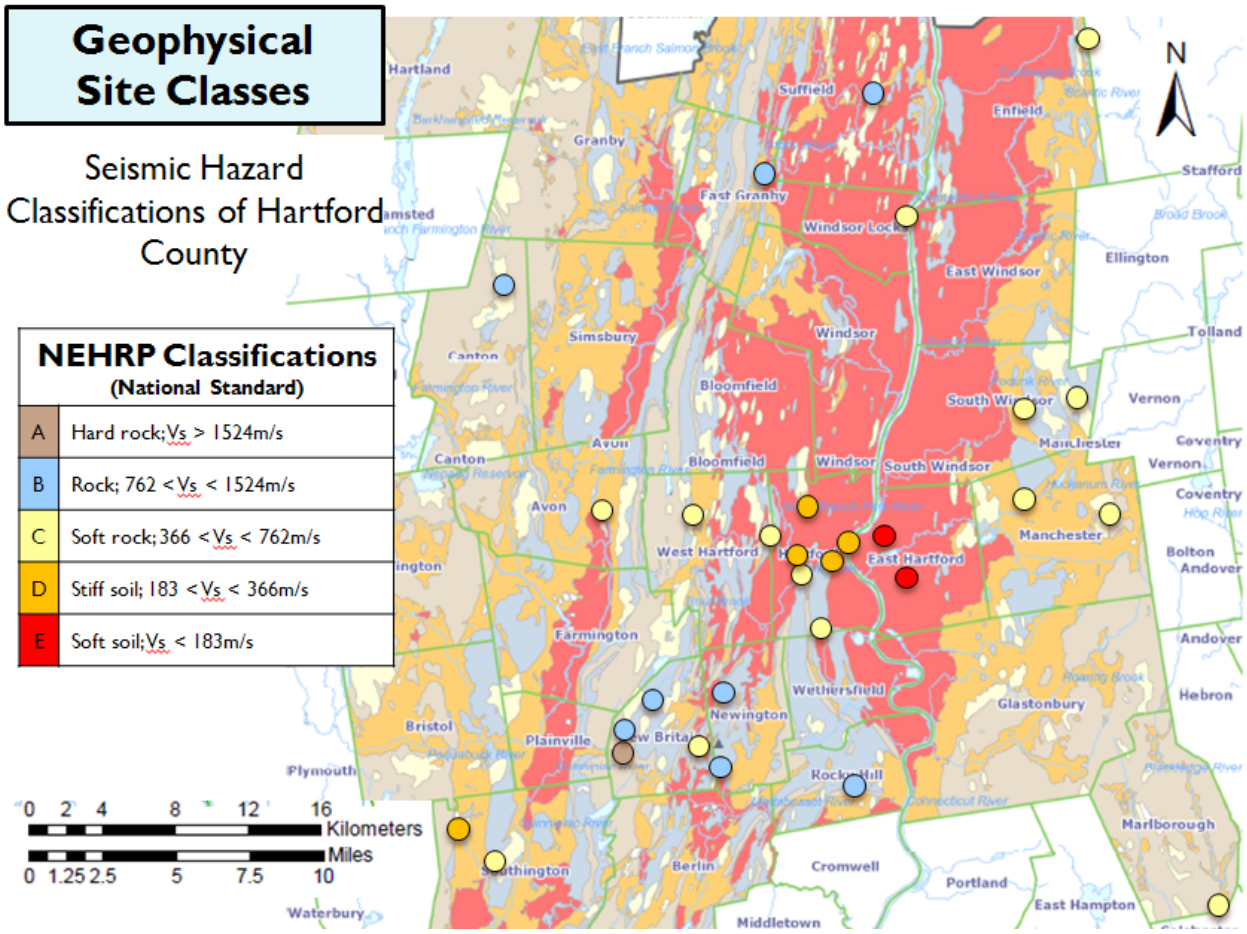

Figure 6.2. Reevaluated Site Classes based on Field Results. Similar to Figure 6.3, the base map is the Becker et al. (2013) Seismic Hazard map created specifically for Hartford County and each point represents the location of each field site used in this study. However, the color of each point represents the geophysically-derived (Vs30) site classification after the passive and active surveys were performed and analyzed. In general, a third of the sites classifications did not change in comparison to the initial surficial class and the other sites decreased by one hazard level.

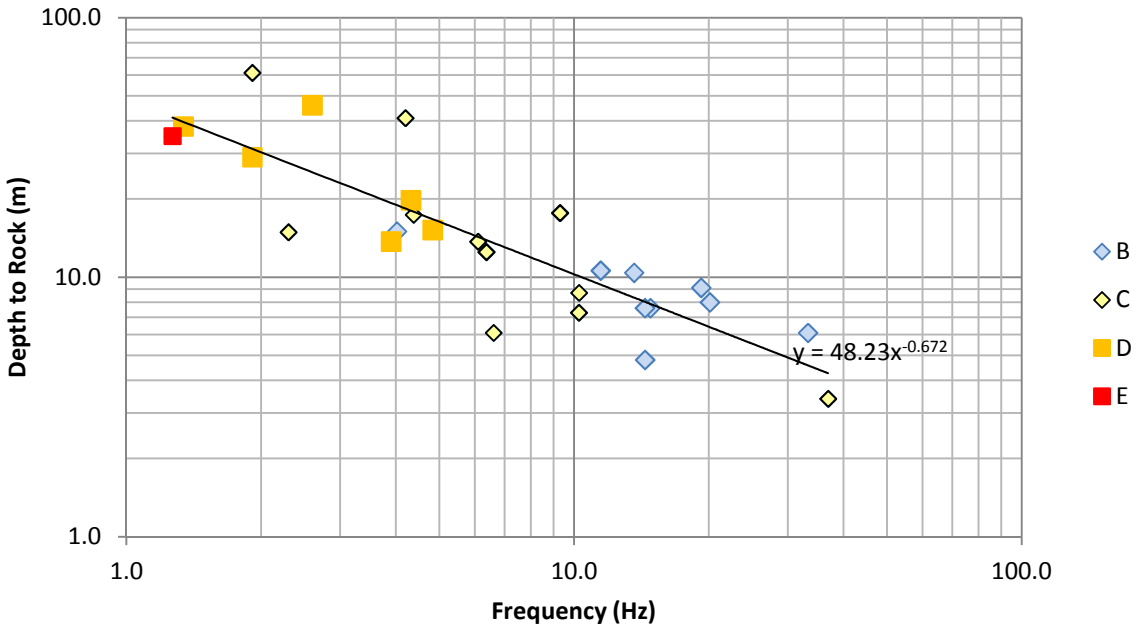

Figure 6.3. Regression Curve Based on HVSR and Well Information for Hartford County, Connecticut. Each point corresponds to a resonance frequency and borehole recorded depth to bedrock from field sites throughout Hartford County. All thirty sites are not plotted due to lack of observed resonance or no recorded borehole bedrock depth. The color of each points refers to the geophysically-derived site classification. In general, there is little to no relationship between site classification, bedrock depth and resonance frequency represented by site class C which extends across the entire plot. However, D classifications show resonance frequencies less than 5.0 Hz and generally B classifications were greater than 10.0 Hz. The equation is determined based on the black power trend line, known as a regression equation. If a depth to rock or sediment thickness value is known for a given site, the resonance frequency can be estimated using this equation.

Table 6.3 Surficial-based and Geophysically-derived Site Classifications

Surficial Class	Town	HVSR	MASW	VSP	FINAL
A	East Granby	B	B		B
A	Marlborough	B			B
A	New Britain	A			A
A	New Britain	n/a	C	**n/a**	C
B	New Britain	B			B
B	New Britain	B			B
B	New Britain	C	C		C
B	Newington	B			B
B	Rocky Hill	C			C
B	Southington	D	B		B
C	Canton	B			B
C	Enfield	B			B
C	Manchester	C			C
C	South Windsor	C	C		C
C	Suffield	C	B		B
D	Avon	C	C		C
D	Manchester	C			C
D	South Windsor	C			C
D	Southington	D			D
D	West Hartford	C	C		C
E	East Hartford	D			D
E	East Hartford	D		E	E
E	Hartford	C	D		D
E	Hartford	C	C	C	C
E	Hartford	C			C
E	Hartford	C	D		D
E	Hartford	C	D		D
E	Hartford	C			C
E	West Hartford	C			C
E	Windsor Locks	E			E

REFERENCES

Aboye S., Andrus, R.D., Ravichandran, N., Bhuiyan, A., and Harman, N. (2011). Site factors for estimating peaka ground acceleration in Charleston, South Carolina, Based on Vs30. Paper presented at the 4th IASPEI/IAEE International Symposium, Santa Barbara, CA, USA.

Alter, L. (1995, May 1). *Geology of Connecticut* [Lecture notes]. Retrieved from http://www.yale.edu/ynhti/curriculum/unit

Balch, A. H., Lee, M., Miller, J., and Ryder, R. T. (1982). The use of vertical seismic profiles in seismic investigations of the earth. *Geophysics*, *47*(6), 906-918.

Becker, L. R., Patriarco, S. P., Marvinney, R. G., Thomas, M. A., Mabee S. B., and Fratto, E. S., (2013), Improving Seismic Hazard Assessment in New England through the use of Surficial Geologic Maps and Expert Analysis, *Geological Society Of America Special Papers, Recent Advances In North American Paleoseismology and Neotectonics East Of The Rockies*, Vol. 493, 221-242.

Bonnefoy-Claudet, S., Cornou, C., Bard, P.-Y., Cotton, F., Moczo, P., Kristek J., and Fah, D. (2006). H/V ratio: a tool for site effects evaluation. Results from 1-D noise simulations. *Geophysics Journal International, 167*, 827-837.

Council, B. S. S. (2000). The 2000 NEHRP recommended provisions for new buildings and other structures: Part I (Provisions) and Part II (Commentary). *FEMA, 368*, 369.

Coleman, M. E. (2005). *The Geologic History of Connecticut's Bedrock*. Connecticut Department of Environmental Protection. State Geological and Natural History Survey. 30 p.

Connecticut Geological and Natural History Survey. (Rev. 2013). *Generalized Bedrock Geologic Map of Connecticut*. Connecticut Geological and Natural History Survey, Department of Energy and Environmental Protection. Available at

www.ct.gov/deep/lib/deep/geology/ct_generalized_bedrock_final.pdf

Connecticut Seismic Hazard Map. *Connecticut*. Retrieved from http://earthquake.usgs.gov/earthquakes/states/connecticut/hazards.php

Costa, P. T. (2005). Guidelines for the Implementation of the H/V Spectral Ratio Technique on Ambient Vibrations. 1-62.

Crice, D. (2011). Near-surface, downhole shear-wave surveys: A primer. *The Leading Edge*, 30(2), 164-171.

Delgado, J., Casado, C. L., Estévez, A., Giner, J., Cuenca, A., and Molina, S. (2000a). Mapping soft soils in the Segura river valley (SE Spain): a case study of microtremors as an exploration tool. *Journal of Applied Geophysics*, *45*(1), 19-32.

Delgado, J., Casado, C. L., Giner, J., Estévez, A., Cuenca, A., and Molina, S. (2000b). Microtremors as a Geophysical Exploration Tool: Applications and Limitations. *Pure and Applied Geophysics*, *157*(9), 1445-1462.

Earthquake Hazards Reduction Act of 1977, Public Law 95-124, 42 U.S.C. §§7701-7708 (2004).

Ebel, J. E., Vudler, V., and Celata, M. (1982). The 1981 microearthquake swarm near Moodus, Connecticut. *Geophysical Research Letters*, *9*(4), 397–400. doi:10.1029/GL009i004p00397

Esmersoy, C. (1990). Inversion of P and SV waves from multicomponent offset vertical seismic profiles. *Geophysics*, *55*(1), 39-50.

Ewing, M., Jardetzky, W. S., and Press, F. (1957). *Elastic Waves in Layered Media*. New York: McGraw-Hill.

Fah, D., Wathelet, M., Kristekova, M., Havenith, H., Endrun, B., and Stamm, G., (2008). Using Ellipticity Information for Site Characterization. *Network of Research Infrastructure for European Seismology*, 1-54.

Fah, D., Kind, F., and Giardini, D. (2003). Inversion of local S-wave velocity structures from average H/V ratios, and their use for the estimation of site-effects. *Journal of Seismology*, *7*(4), 449-467.

Fah, D., Kind, F., and Giardini, D. (2001). A theoretical investigation of average H/V ratios. *Geophysics Journal International*, *145*, 535-549.

Grotzinger, J. P., Jordan, T. H., Press, F., and Siever, R. (2007). *Understanding Earth* (5th ed.). New York: W.H. Freeman.

Haghshenas, E., Bard, P.-Y., and Theodulidis, N. (2008). Empirival evaluation of microtremor H/V spectral ratio. *Bulletin of Earthquake Engineering, 6,* 75-108.

Hardage, B.A., 1985, Vertical Seismic Profiling: *The Leading Edge*, 4, 59-60.

Haskell, N. A. (1953). The Dispersion of Surface Waves on Multilayered Media. *Bulletin of the Seismological Society of America*, *43*(1), 86-103.

Hobiger, M., Cornou, C., Ohrnberger, M., Theodoulidis, N., Wathelet, M., Giulio, G. D., (2012). Ground structure imaging by inversions of Rayleigh wave ellipticity: sensitivity analysis and application to European strong-motion sites. *Geophysical Journal International*, *192*, 207-229.

Lane, J.W., White., E.A., Steele, G.V., and Cannia, J.C. (2008). Estimation of Bedrock Depth Using the Horizontal-to-Vertical (H/V) Ambient-Noise Seismic Method. Paper presented at the meeting of Symposium on the Application of Geophysics to Engineering and Environmental Problems, Philadelphia, Pennsylvania, USA.

M5.6 Northern California, Feb. 13 2012. *Earthquake Hazards Program*. Retrieved from http://earthquake.usgs.gov/earthquakes/dyfi/events/nc/71734741/us/

M5.8 Virginia, Aug. 23, 2011. *Earthquake Hazard Program*. Retrieved from http://earthquake.usgs.gov/earthquakes/dyfi/events/se/082311a/us/index.html

McHone, J. G. (2004). *Connecticut in the Mesozoic World*. Connecticut Department of Environmental Protection, Connecticut Geological & Natural History Survey. 40 p. CD-ROM.

Miller, R. D., Xia, J., Park, C. B., and Ivanov, J. M. (1999). Multichannel analysis of surface waves to map bedrock. *The Leading Edge*, *18*(12), 1392.

Nakamura, Y. (2008, October). *On the H/V Spectrum*. Paper presented at the meeting of the 14th World Conference on Earthquake Engineering, Beijing, China.

Nakamura, Y. (2000, February). *Clear Identification of Fundamental Idea of Nakamura's Technique and its Applications.* Paper presented at the meeting of the 12th World Conference on Earthquake Engineering, Auckland, New Zealand.

Nakamura, Y. (1989). A Method for Dynamic Characteristics Estimate of Subsurface using Microtremor on the Ground Surface. *Quarterly Report of Railway Technical Research Institute (RTRI)*, Vol. 30, No. 1.

Ohrnberger, M., Schissele, E., Cornou, C., Bonnefoy-Claudet, S., Wathelet, M., Savvaidis, A., Scherbaum, F., and Jongmans, D. (2004, August). *Frequency Wavenumber and Spatial Autocorrelation Methods for Dispersion Curve Determination from Ambient Vibration Recordings.* Paper presented at the meeting of the 13th World Conference on Earthquake Engineering, Vancouver, Canada.

Oliver, J. (1962). A Summary of Observed Seismic Surface Wave Dispersion. *Bulletin of the Seismological Society of America*, *52*(1), 81-86.

Park, C., Miller, R., Ryden, N., Xia, J., and Ivanov, J. (2005). Combined Use of Active and Passive Surface Waves. *Journal of Environmental & Engineering Geophysics*, *10*(3), 323-334.

Park, C. B., Miller, R. D., and Miura, H. (2002). Optimum Field Parameters of an MASW Survey. Open-file Report 2002. The University of Kansas. Lawrence, KS: Kansas Geological Survey.

Park, C. B., Miller, R. D., and Xia, J. (1999). Multichannel analysis of surface waves. *Geophysics*, *64*(3), 800.

Park, C.B., Miller, R.D., and Xia, J. (1998). Imaging Dispersion Curves of Surface Waves on Multi-channel Record: Technical Program with biographies, SEG, 68th Annual Meeting, New Orleans, Louisana, 1377-1380.

Pei, D., (2007). Modeling and Inversion of Dispersion Curves of Surface Waves in Shallow Site Investigation (Doctoral Dissertation) University of Nevada, Reno, USA.

Petersen, Mark D., Frankel, Arthur D., Harmsen, Stephen C., Mueller, Charles S., Haller, Kathleen M., Wheeler, Russell L., Wesson, Robert L., Zeng, Yuehua, Boyd, Oliver S., Perkins, David M., Luco, Nicolas, Field, Edward H., Wills, Chris J., and Rukstales, Kenneth S., 2008, Documentation for the 2008 Update of the United States National Seismic Hazard Maps: U.S. Geological Survey Open-File Report 2008–1128, 61 p.

Picozzi, M., Parolai, S., and Albarello, D. (2005). Statistical Analysis of Noise Horizontal-to-Vertical Spectral Ratios (HVSR). *Bulletin of the Seismological Society of America, 95*(5)*,* 1779-1786.

Press, W.H., Teukosky, S.A., Vetterling, W.T., and Flannery, B.P. (1992). Numerical Recipes in C: Cambridge University Press.

Pujol, J., Burridge, R., and Smithson, S.B. (1985). Velocity Determination from Offset Vertical Seismic Profiling Data. *Journal of Geophysical Research*, *90(B2),* 1871-1880.

Reynolds, J. M. (1997). *An Introduction to Applied and Environmental Geophysics.* West Sussex: John Wiley & Sons Ltd.

Rodgers, J. (1985). *Bedrock Geological Map of Connecticut* [map]. Scale 1:125,000. Connecticut Natural Resources Atlas Series. Hartford, CT: Connecticut Geological and Natural History Survey, Department of Environmental Protection. 2 sheets. Available at: http://cteco.uconn.edu/map_catalog/maps/state/Bedrock_Geologic_Map_of_Connecticut.pdf

Ryder, R. B., and Weiss, L. A. (1971). Hydrogeologic Data for the Upper Connecticut River Basin, Connecticut. *Connecticut Water Resources Bulletin No. 25.*

Socco, L. V. and Boiero, D. (2008). Improved Monte Carlo inversion of surface wave data. *Geophysical Prospecting*, *56, 357-371*.

Stewart, R. R. and Disiena, J. P. (1989). The values of VSP in interpretation: *The Leading Edge*, 8, 16-23.

Stone, J. R., Schafter, J. P., London, E. H., Di-Giacomo-Cohen, M. L., Lewis, R. S., and Thompson, W. B. (2005). *Quaternary Geologic Map of Connecticut and Long Island Sound Basin* [map]. Scientific Investigations Map 2784; prepared in cooperation with the State of Connecticut Department of Environmental Protection, Geological and Natural History Survey. Denver, CO: U.S. Department of the Interior, U.S. Geological Survey. 2 sheets, 72 pp. pamphlet. Available at: http://pubs.usgs.gov/sim/2005/2784/index.html

Stone, J. R., Schafter, J. P., London, E. H., Lewis, R. S., and Thompson, W. B. (1992). *Surficial Materials Map of Connecticut* [map]. Scale 1:125,000. USGS Unnumbered series. Reston, VA: U.S. Geological Survey. 2 sheets. Available at: http://cteco.uconn.edu/map_catalog/maps/state/Surficial_Materials_Map_of_Connecticut.pdf

Tokimatsu, K. (1997). Geotechnical Site Characterization Using Surface Waves. *Earthquake Geotechnical Engineering,* 1333-1368.

Wathelet, M. (2005). *Array recordings of ambient vibrations: surface-wave inversion*. (Doctoral dissertation). Université de Liège, Liège, Belgium.

Wathelet, M., Jongmans, D., Ohrnberger, M., and Bonnefoy-Claudet, S. (2007). Array Performances for Ambient Vibrations on a Shallow Structure and Consequences over Vs Inversion. *Journal of Seismology, 12*(1) 1-19.

Xia, J., Miller, R. D., and Park, C. B. (1999). Estimation of Near-surface Shear-wave Velocity by Inversion of Rayleigh Waves. *Geophysics*, *64*(3), 691-700.

APPENDIX

This section includes information about each site that was not given in Chapters 3-5. This includes HVSR curves, Rayleigh wave ellipticity curves and inversion profiles, as well as MASW dispersion curves and velocity profiles from inversion.

79 North Main Street, East Granby, CT

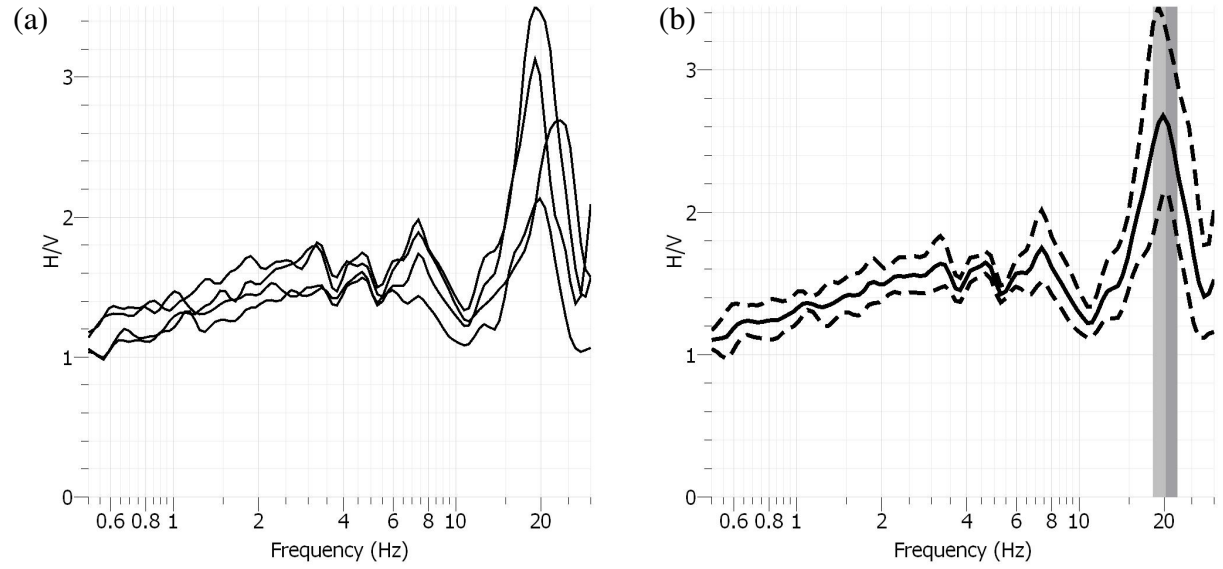

Figure A1. Class A: HVSR measurements from 79 North Main St. Four HVSR measurements were taken near a borehole and the resulting HVSR curves and resonance frequencies are displayed in (a). One measurement was conducted at the borehole and the three remaining measurements were taken 25 m North, South and West of the borehole. The average resonance frequency at this site was 20.1 Hz as indicated by the vertical gray rectangle in (b) with standard deviation. Based on well information, the depth to bedrock was 8 m; therefore the average velocity of the sediments was 643 m/s.

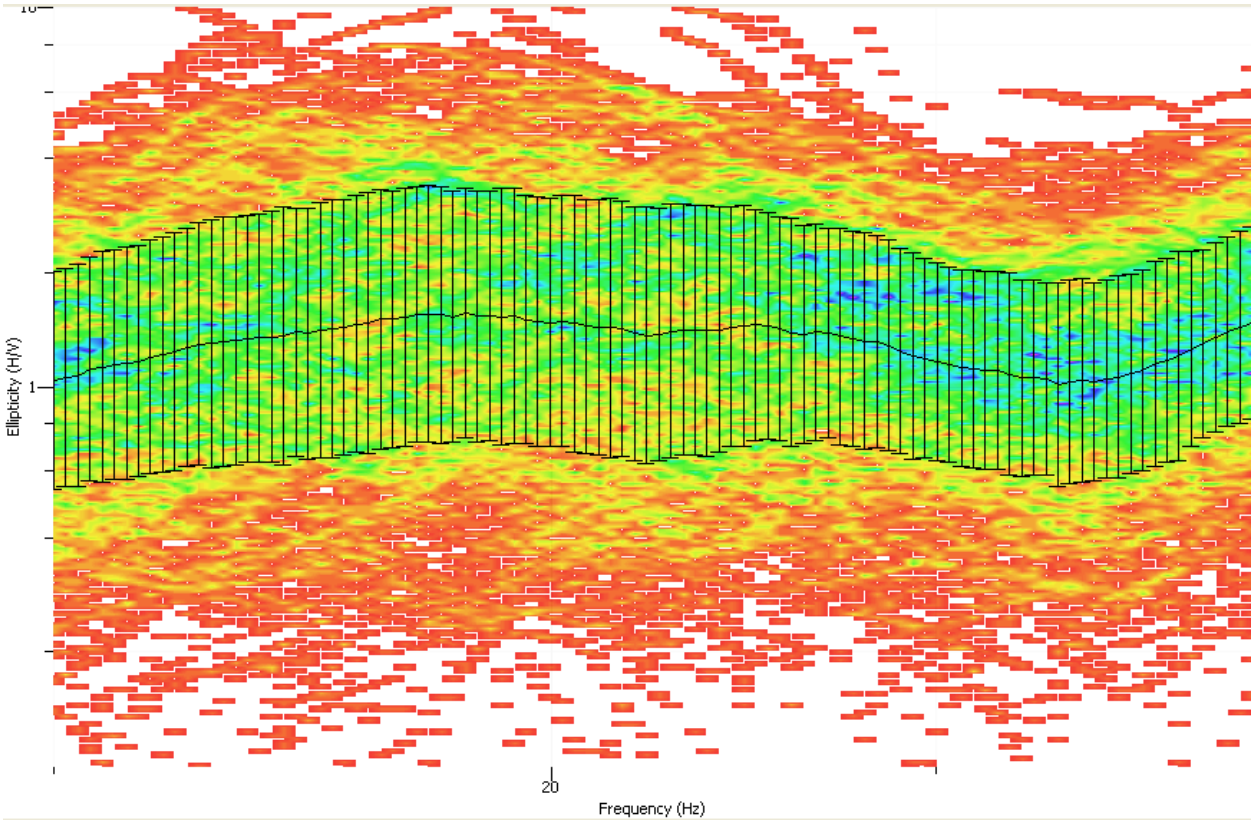

Figure A2. Class A: 79 N Main St. Rayleigh Wave Ellipticity Curve. No Rayleigh wave ellipticity was observed at this site as illustrated by the flat ellipticity curve at 1. The solid black line represents the field data taken at the borehole after the TFA was applied; each point along the curve has an associated error bar determined by the processing windows. The background colors refer to the level of energy concentration, which helps pick the ellipticity curve; higher energy is indicated by the cool blue and green colors, lower energy is indicated by the warmer red color.

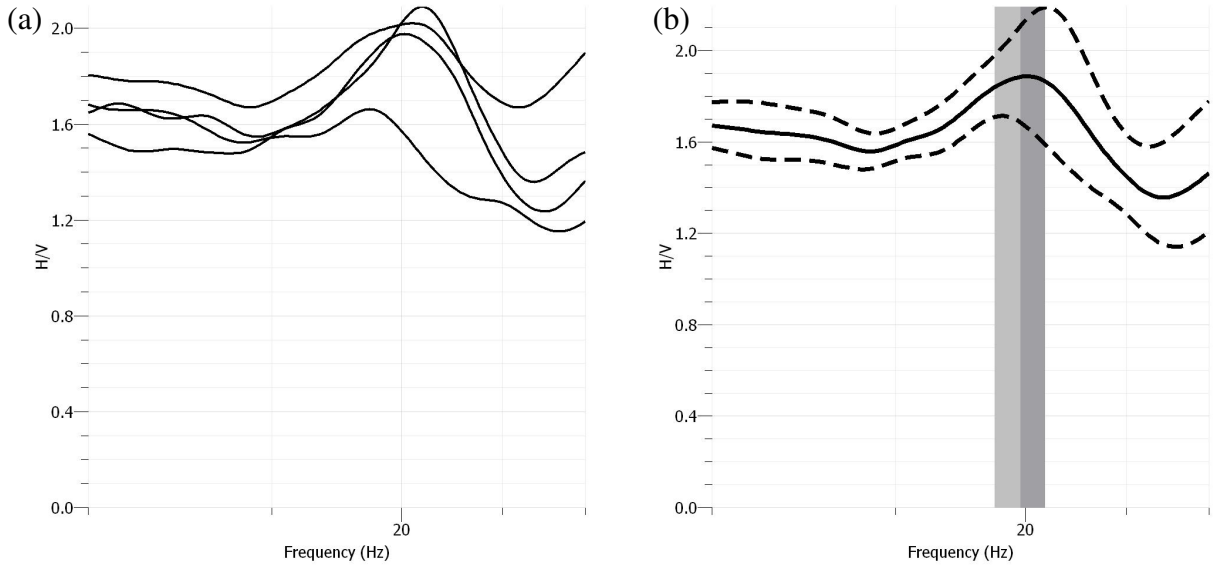

Figure A3. Class A: Average HVSR taken along MASW Profile at 79 North Main St. Four HVSR measurements taken along an MASW profile at geophone location 1, 8, 16, and 24. Each individual measurement is displayed in (a) and the average resonance frequency, 19.7 Hz, and standard deviation are displayed in (b). The resonance frequency at geophone location 1, 8, 16, and 24 was 18.15, 20.25, 20.53, and 20.26 Hz respectively.

Layer Depth (m)	Vs (m/s)
0.85	553.26
1.92	704.23
3.25	706.33
4.91	660.32
6.99	408.15
9.58	568.52
12.83	1059.75
16.89	1343.87
21.96	1496.25
Half Space	2123.60
Vs sediments	750.1
Vs30	987.9
Surficial Class	A
Vs30 Site Class	B

Table A1. Class A. Active MASW Results from 79 North Main St. A 10-layer model was generated from the dispersion curve in Figure A4. A summary of the depth and shear-wave velocity information is listed here. This site was initially assigned hazard class A by the surficial materials data, but assigned hazard class B using the geophysical field data and Vs30. The gray colored boxes indicate the assumed bedrock interface based on the inversion.

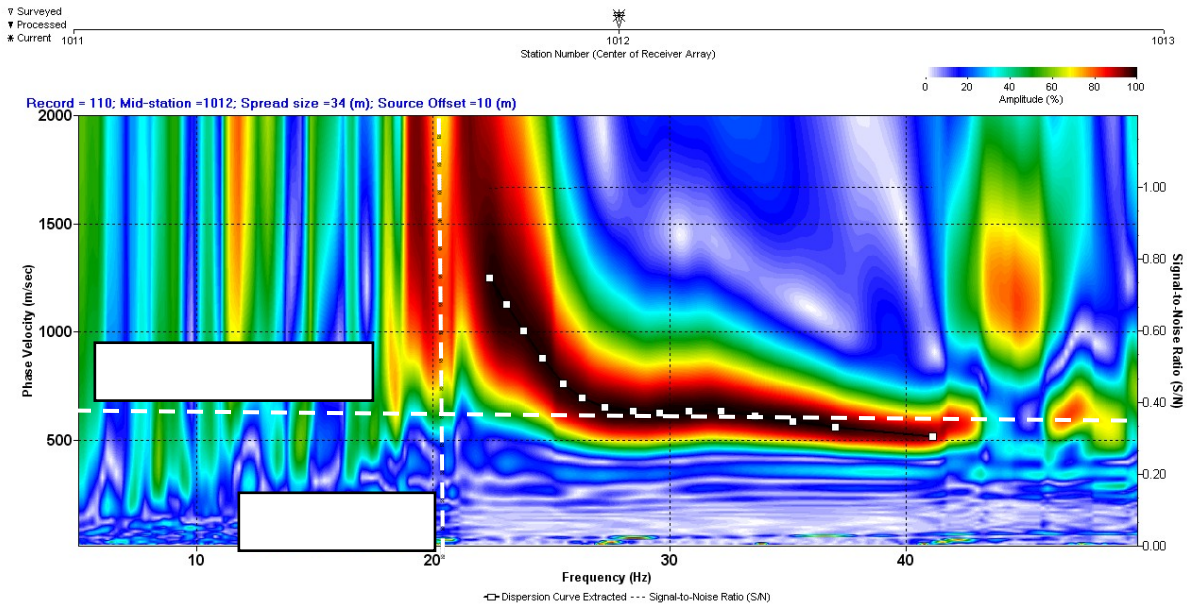

Figure A4. Class A: 79 North Main St. Dispersion Curve. The picked dispersion curve is represented by the white boxes connected by a black line with respect to frequency and phase velocity. The vertical white, dashed line indicates the 20.1 Hz average resonance frequency observed at the field site, which is relative to the dispersion curve's observed higher frequencies; these high frequencies are indicative of the bedrock interface. The white horizontal dashed line indicates the average shear-wave velocity of the sediments based on the resonance frequency. This line coincides with the dispersion curve's observed higher frequencies, which are relative to the underlying sediments.

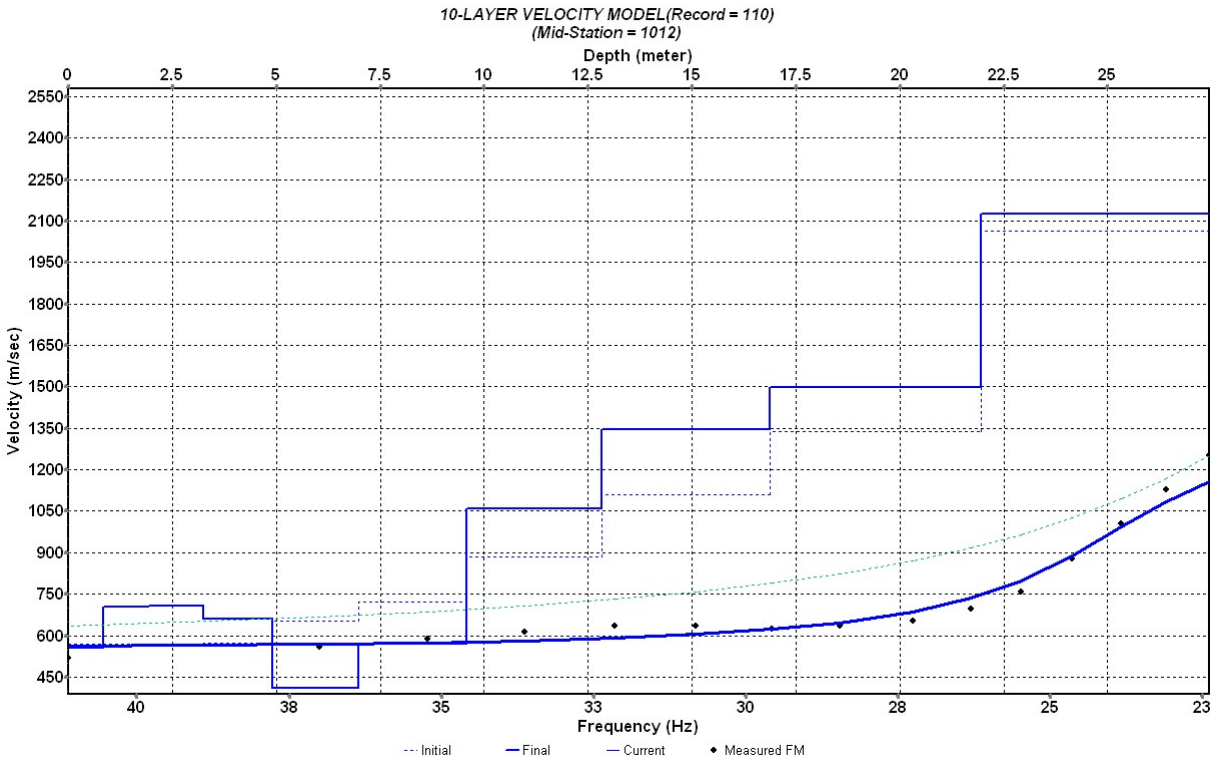

Figure A5. Class A: 79 North Main St. Velocity Profile from Inversion. A 10-layer model was generated using the dispersion curve in Figure A4. The black dotted curve is the extracted dispersion curve and the blue solid curve is the model's theoretical curve. Based on this profile, the bedrock surface was observed at 12.8 m, the average sediment velocity was 750 m/s and the Vs30 was 987.9 m/s, Class B.

436 Slater Road, New Britain, CT

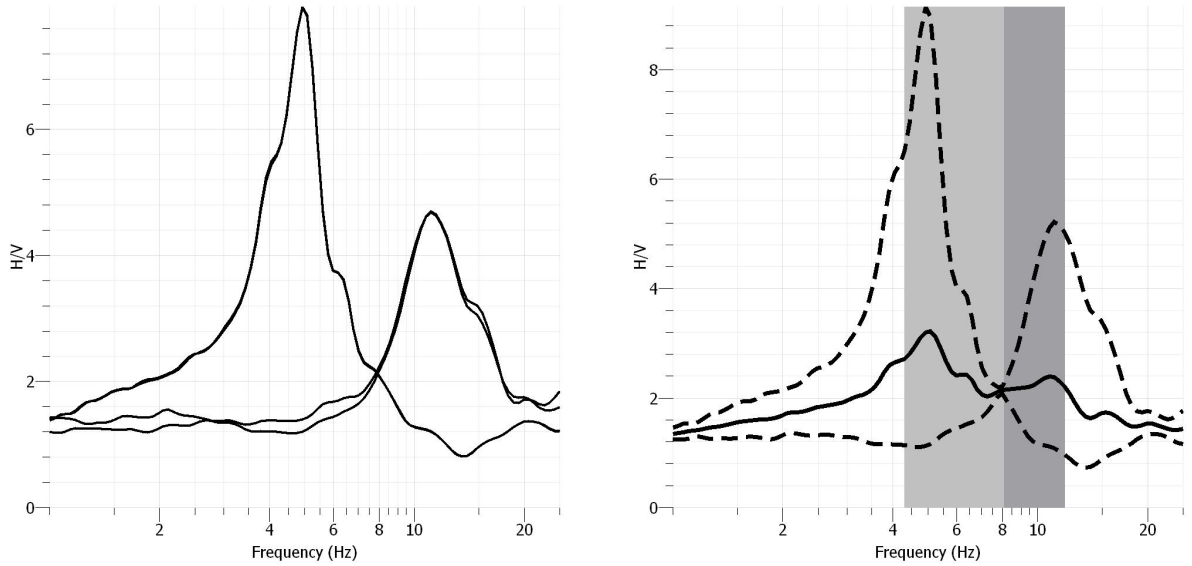

Figure A6. HVSR Huddle Test from 436 Slater Road, CT. Four HVSR measurements were taken around a borehole in a huddle test and the resulting HVSR curves and resonance frequencies are displayed in (a). Two different resonance frequencies were observed during this huddle test, 4.9 Hz and 11.1 Hz. Due to this uncertainty, no site class was assigned to this site based on the geophysical data. Therefore the field site remained class A with a 3.7 m depth to rock according to the well information. The standard deviation are indicated by the vertical gray rectangle in (b).

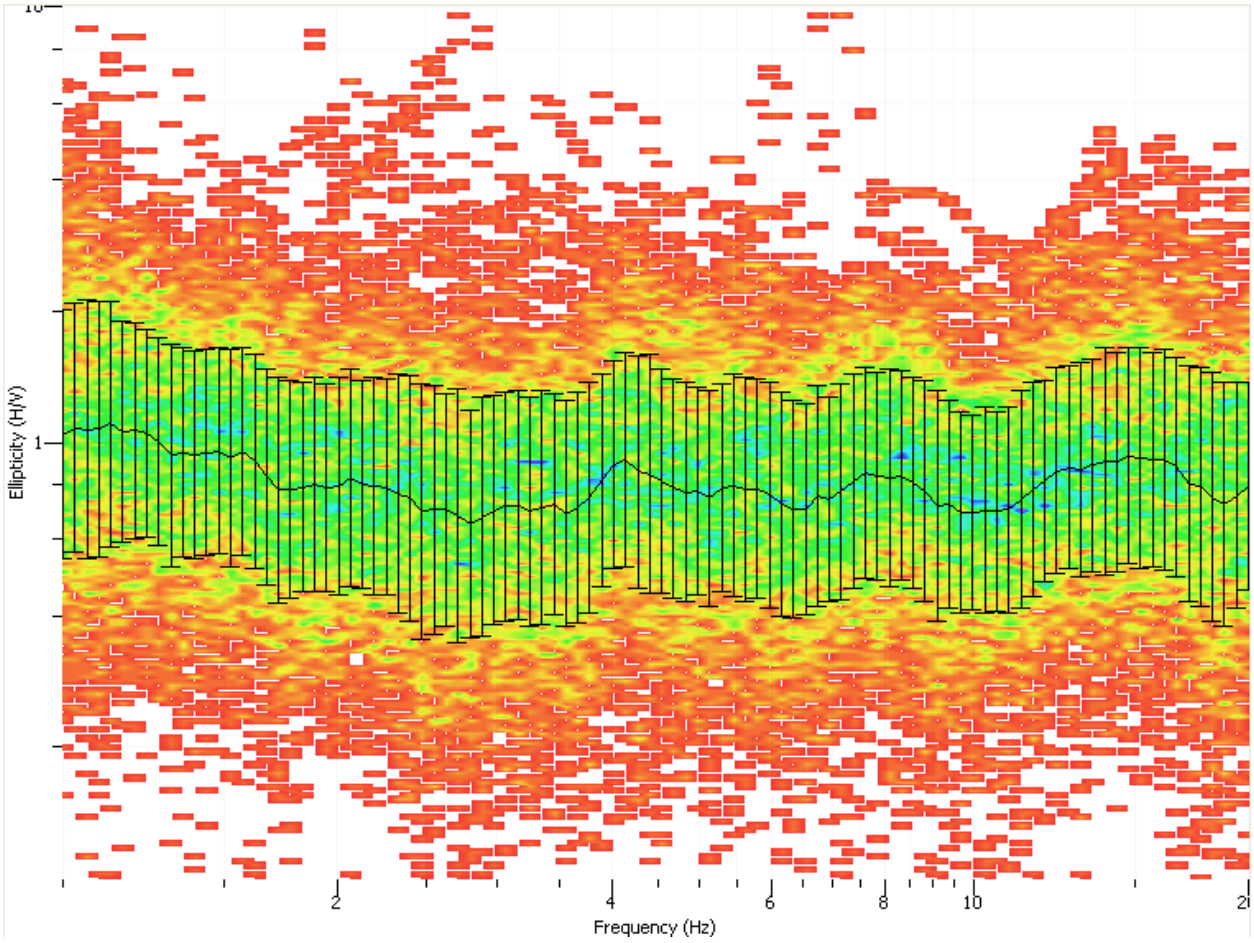

Figure A7. Rayleigh wave ellipticity curve for 436 Slater Road, New Britain, CT. No Rayleigh wave ellipticity was observed at this site as illustrated by the flat ellipticity curve at 1.

900 West Main Street, New Britain, CT

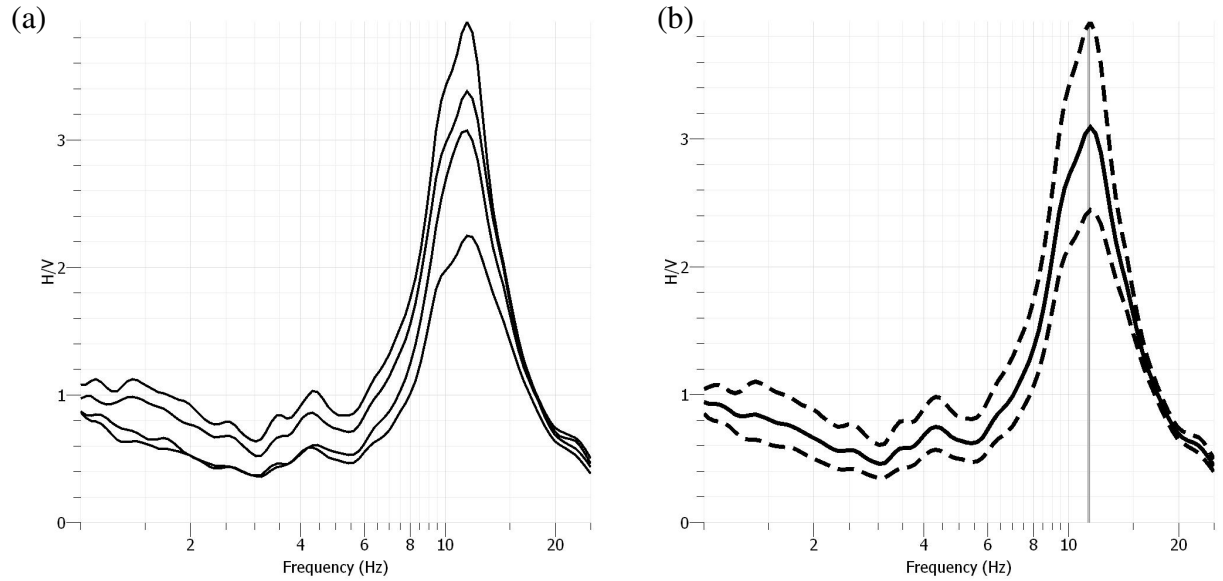

Figure A8. Class A: HVSR Huddle Test from 900 West Street, New Britain, CT. Four HVSR measurements were taken around the borehole in a huddle test and the resulting HVSR curves and resonance frequencies are displayed in (a). The average resonance frequency at this site was 11.5 Hz as indicated by the vertical gray rectangle in (b) with standard deviation. Based on the well information, the depth to bedrock was 10.6 m; therefore the average shear-wave velocity of the sediments was 490 m/s.

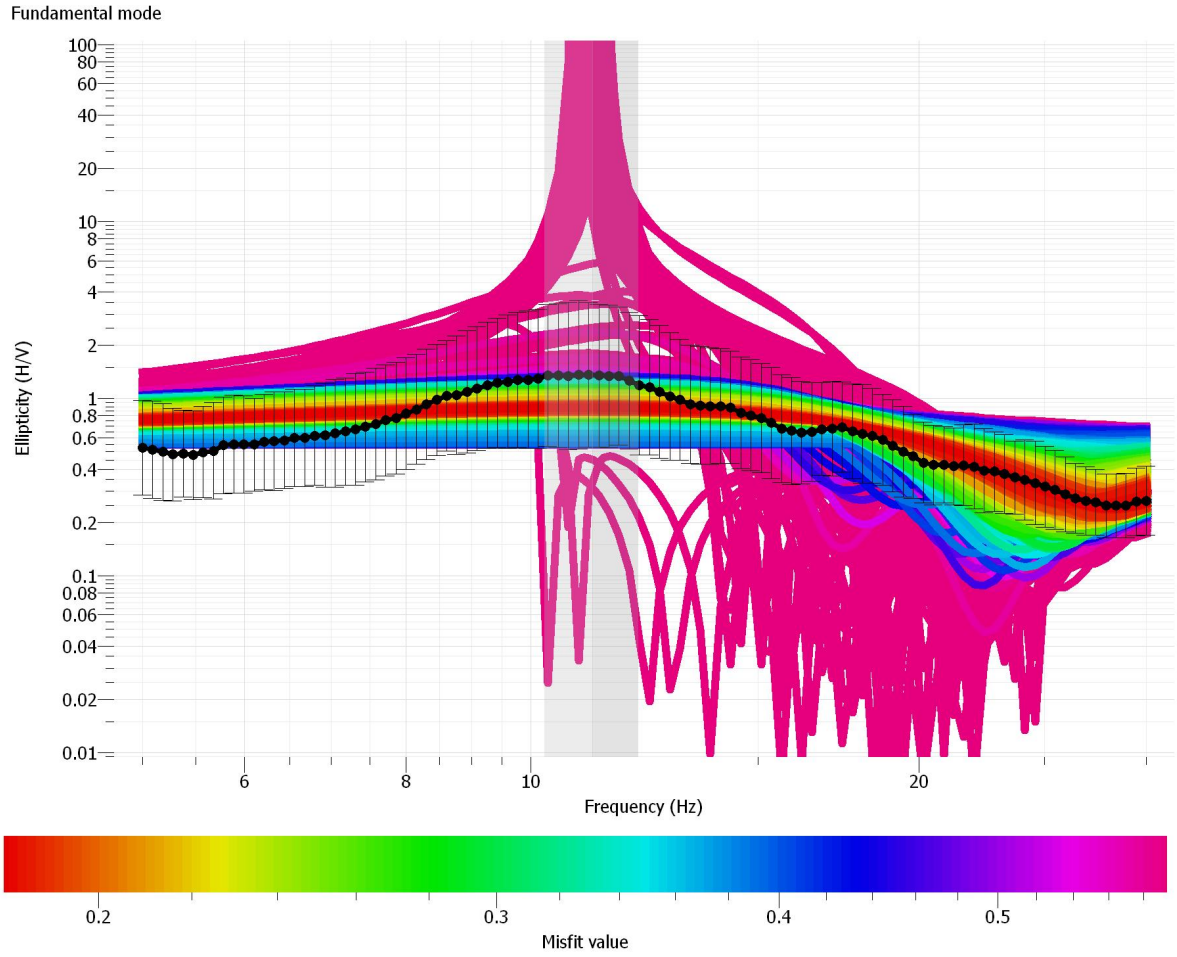

Figure A9. Class A: 900 West Main St. Rayleigh Wave Ellipticity. The black dotted curve represents the observed ellipticty curve after the TFA with associated error bars. The observed ellipticity curve has a flat peak, but slight trough between 30-40 Hz. Each colored curve behind the data represents a different model generated by the inversion where red curves have the lowest misfit and the pink have the highest misfit. The vertical purple rectangle indicates the peak frequency value and standard deviation. The models that best fit the data between 12-20 Hz were used for generating velocity profiles.

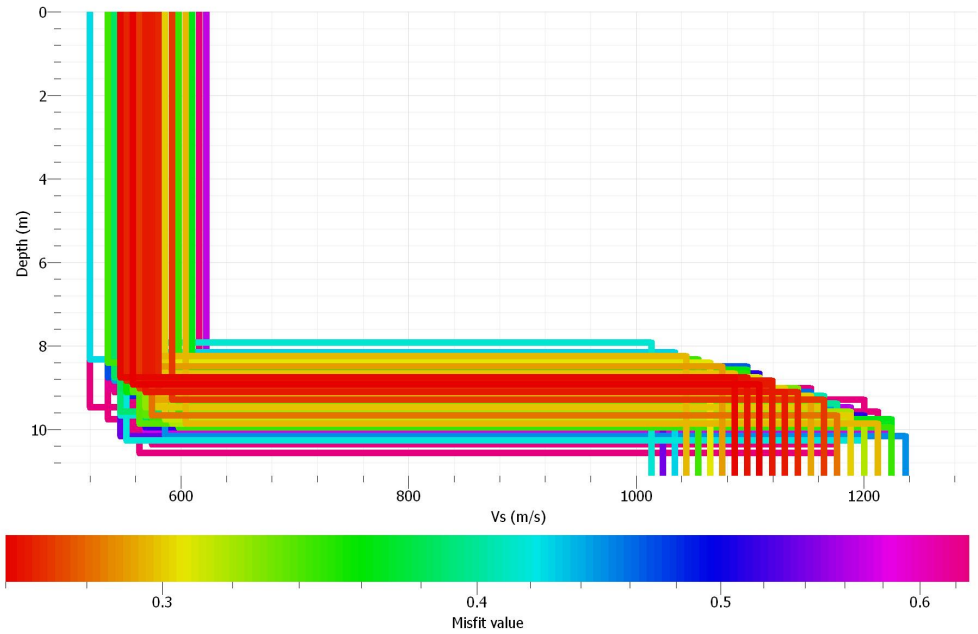

Figure A10. Class A: 900 West Main St. Velocity Profile from Rayleigh Wave Ellipticity Inversion. From the s-wave profile, there is obvious agreement for a layer interface at ~9 m. The goal of this model was to determine an average s-wave velocity of the sediment layer over rock, which is ~560 m/s. Each line is a different model from the inversion and the color refers to the misfit value of that model.

George Chesley Park, New Britain, CT

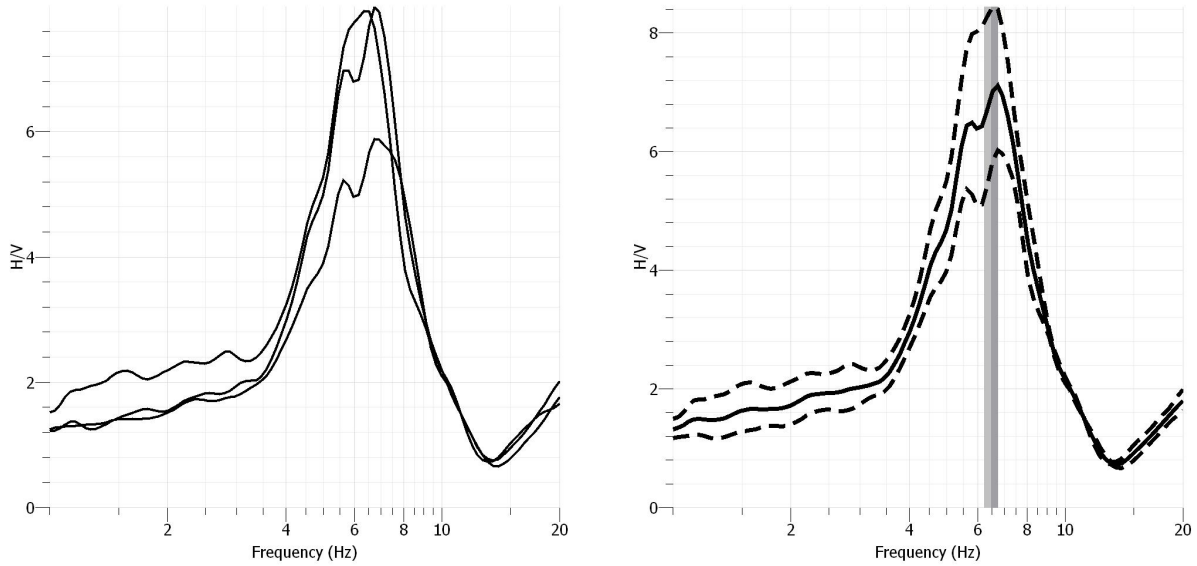

Figure A11. Class B: Average HVSR taken along MASW profile at George Chesley Park. Three HVSR measurements taken along an MASW profile at Geophone location 1, 12, and 24, which were separated by 17.25 m. Each individual measurement is displayed in (a) and the average resonance frequency and standard deviation are displayed in (b). The average HVSR curve from (a) is displayed as the solid black line with respect to frequency and H/V amplitude. The two dotted lines represent the upper and lower bounds of the standard deviation. The vertical gray line shows the location of the average fundamental frequency at 6.46 Hz.

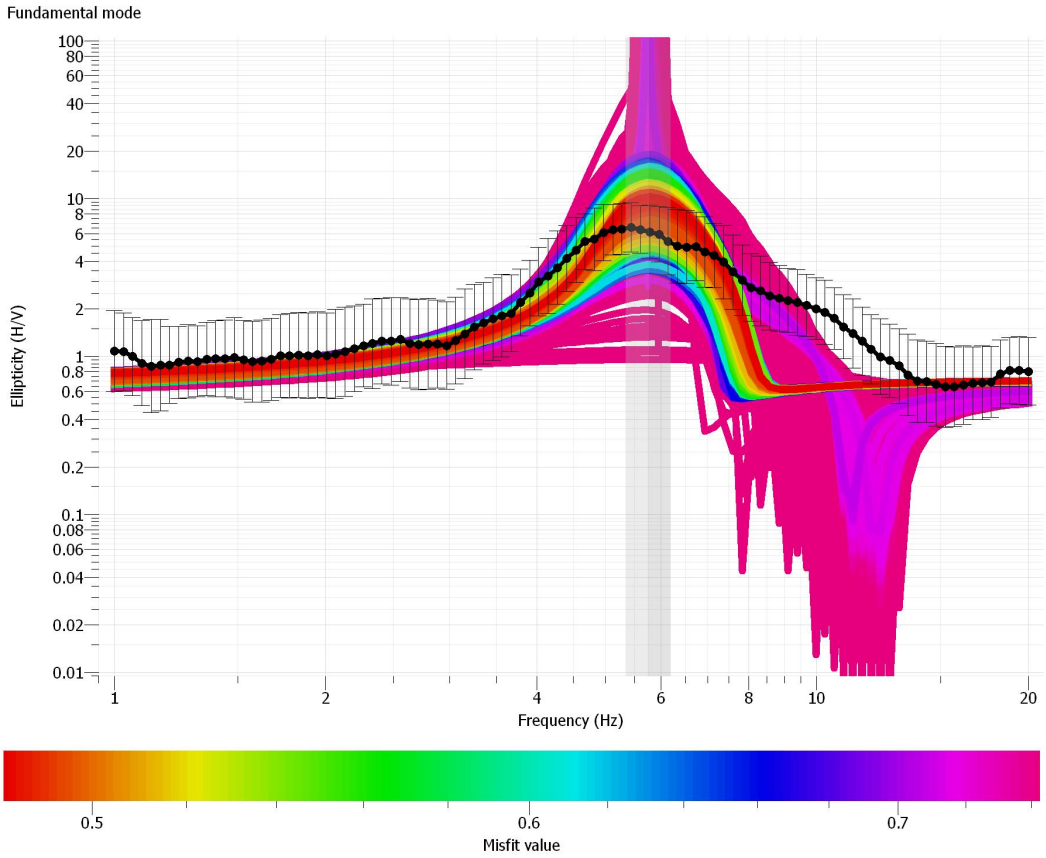

Figure A12. Class B: George Chesley Park Rayleigh Wave Ellipticity. The black dotted curve represents the observed ellipticty curve after the TFA with associated error bars. The observed ellipticity curve has a peak at 5.8 Hz as indicated y the vertical purple rectangle and a trough at 8 Hz. Each colored curve behind the data represents a different model generated by the inversion where red curves have the lowest misfit and the pink have the highest misfit. The vertical purple rectangle indicates the peak frequency value and standard deviation. The models that best fit the data between 5.8-8 Hz were used for generating velocity profiles.

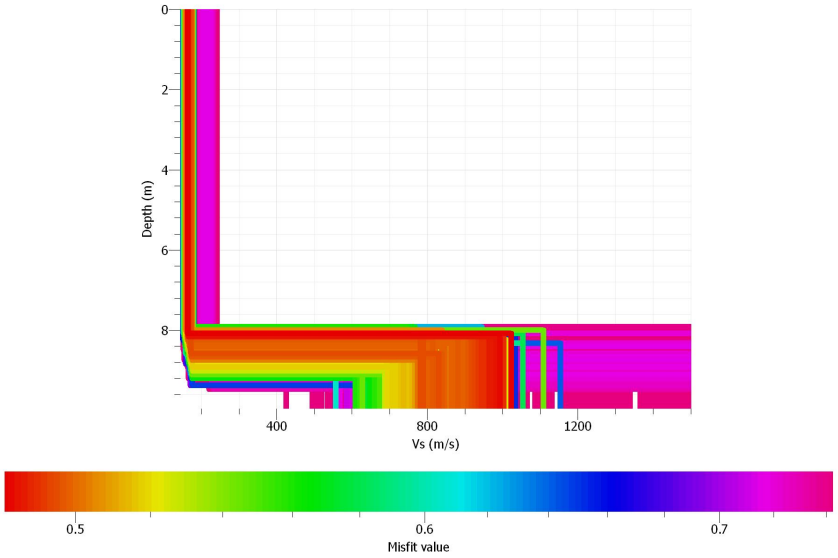

Figure A13. Class B: George Chesley Park Velocity Profile from Rayleigh Wave Ellipticity Inversion. Each 2-layer Vs model is represented by each colored line where the color refers to the misfit value. The red models have the lowest misfit and the pink models have the highest misfit. The lowest misfit models cluster around an interface at ~8m with an average sediment Vs of 171 m/s.

Layer Depth (m)	Vs (m/s)
1.175	331.3
2.644	327.1
4.48	344.5
6.775	244.4
9.643	390.4
13.228	545.7
17.71	638.7
23.312	751.6
30.315	927.3
Half Space	1537.9
Vs sediments	455.8
Vs30	516.5
Surficial Class	B
Vs30 Site Class	C

Table A2. Class B: Active MASW Results from George Chesley Park, New Britain. A 10-layer model was generated from the dispersion curve in A14. A summary of the depth and shear-wave velocity information is listed here. This site was initially assigned hazard class B by the surficial materials data but reassigned hazard class C based on the geophysical field data and Vs30. The gray colored boxes indicate the assumed bedrock interface based on the inversion.

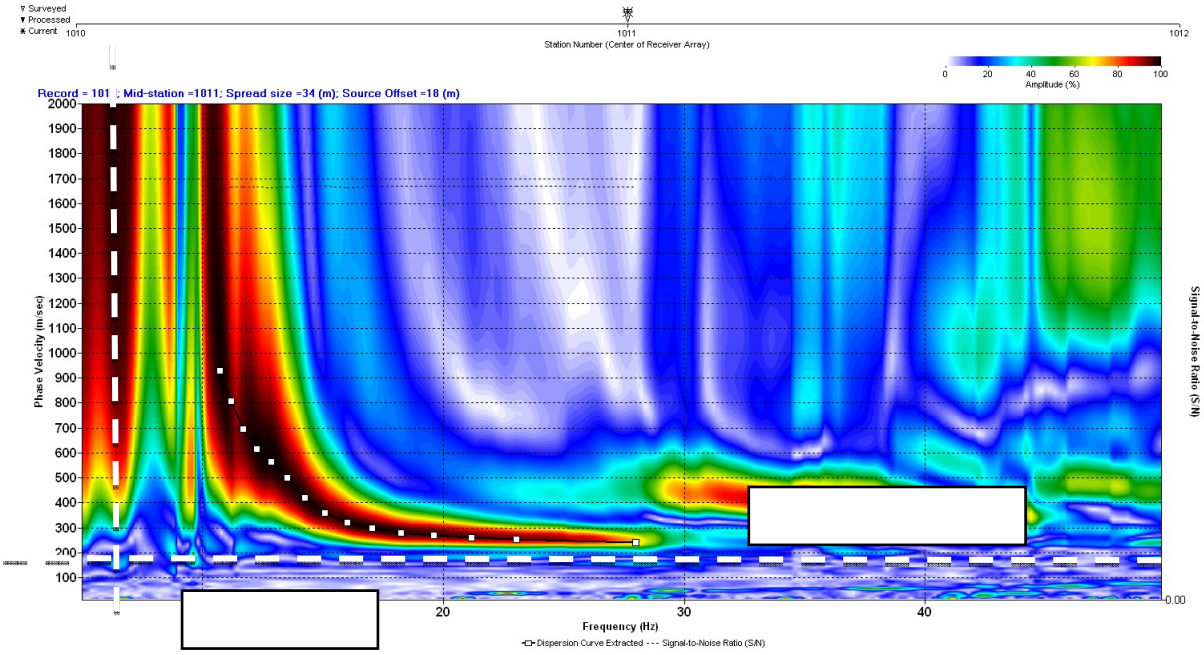

Figure A14. Class B: George Chesley Park Dispersion Curve. The picked dispersion curve is represented by the white boxes connected by a black line with respect to frequency and phase velocity. The vertical white, dashed line indicates the average resonance frequency observed at the field site, which is relative to the dispersion curve's observed higher frequencies; these high frequencies are indicative of the bedrock interface. The white horizontal dashed line indicates the average shear-wave velocity of the sediments based on the resonance frequency. This line coincides with the dispersion curve's observed higher frequencies, which are relative to the underlying sediments. Based on the plotted HVSR results, the dispersion curve is an underestimation of the velocity profile.

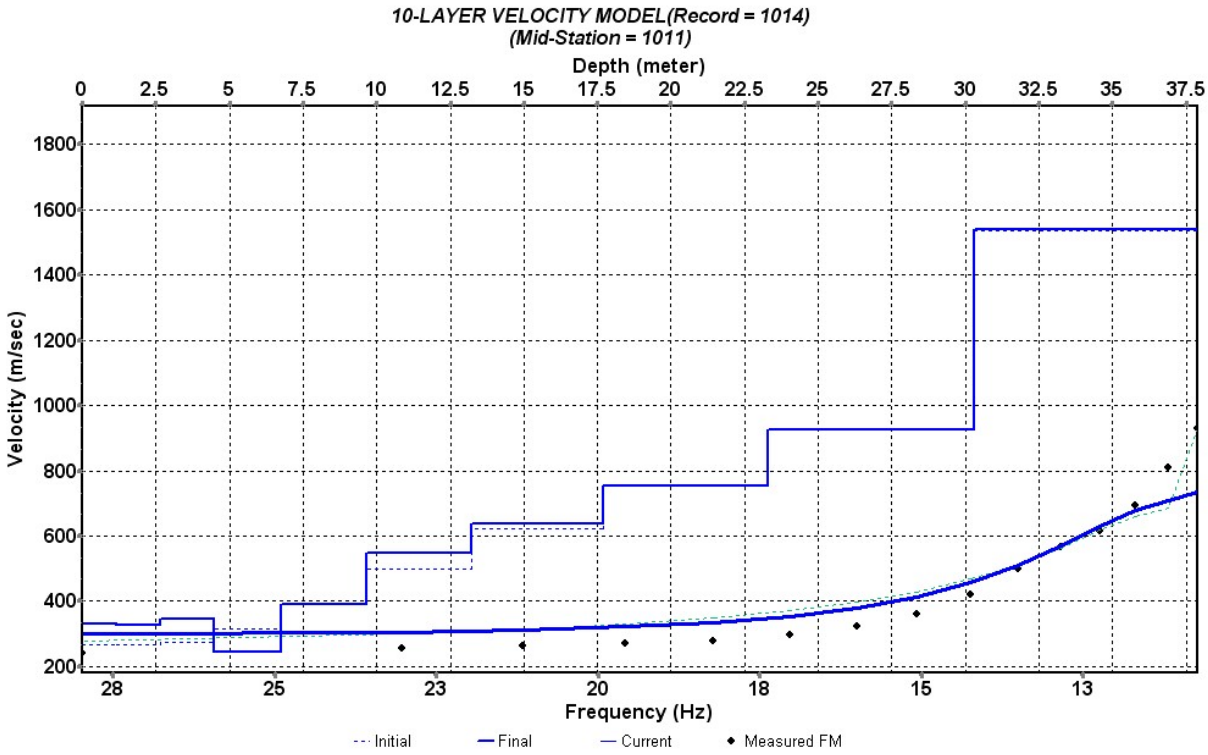

Figure A15. Class B: George Chesley Park Velocity Profile from Inversion. A 10-layer model was generated using the dispersion curve in Figure A14. The black dotted curve is the extracted dispersion curve and the blue solid curve is the model's theoretical curve. Based on this profile, the bedrock surface was observed at 18.4 m, the average sediment velocity was 495 m/s and the Vs30 was 598 m/s. The blue curve poorly fits the field data, which is indicative of the dispersion curve in Figure A15.

Corner of Booth St and Myrtle St, New Britain, CT

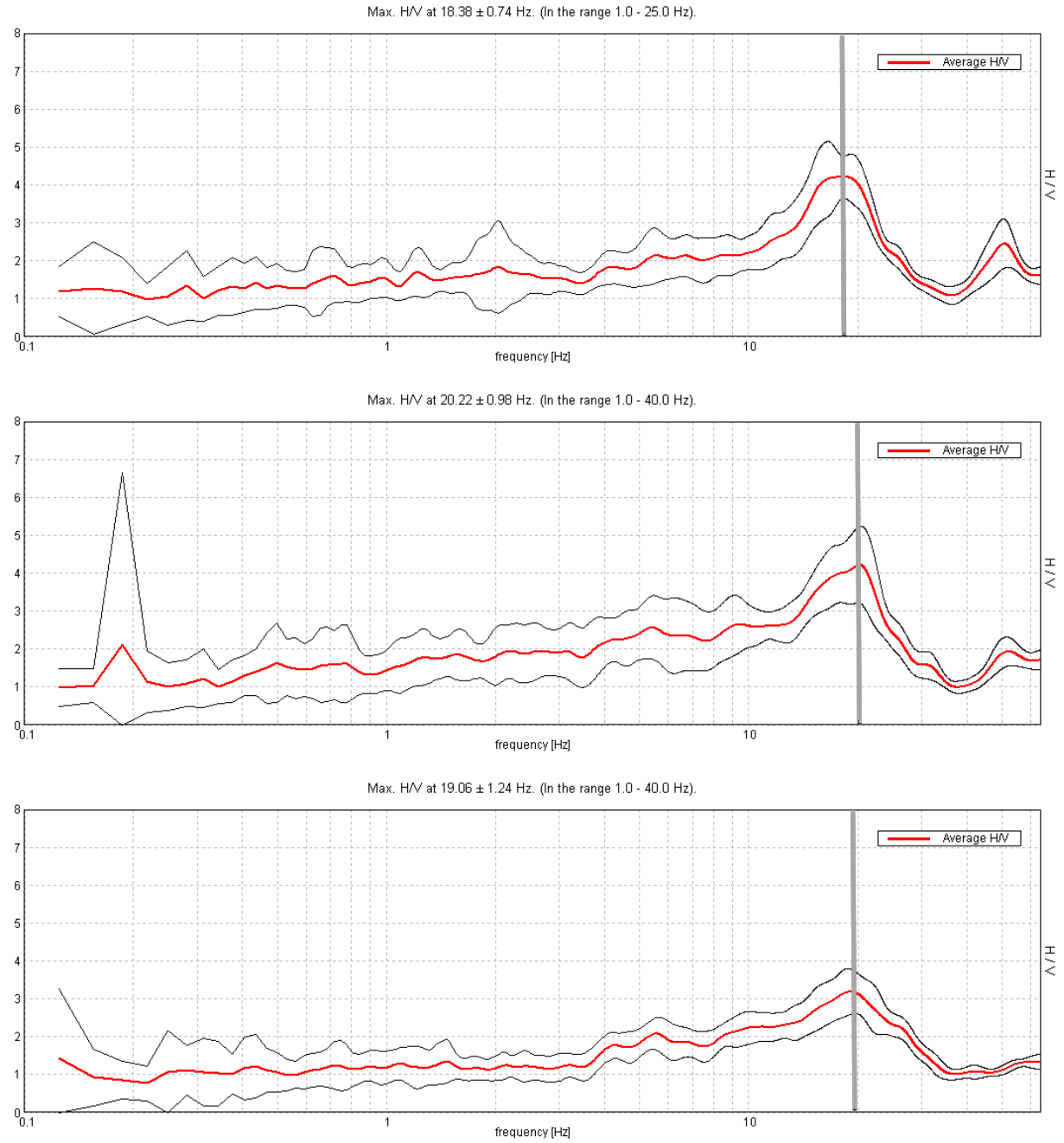

Figure A16. HVSR measurements from Booth St. Three HVSR measurements were taken near the borehole and the resulting HVSR curves and resonance frequencies are displayed. Each HVSR curve is plotted above with resonance frequencies observed at 18.38 Hz, 20.22 Hz, and 19.06 Hz; the average resonance frequency was 19.2 Hz. Based on well information, the depth to bedrock was 9.1 m; therefore the average velocity of the sediments was 700 m/s.

456 West Street, Southington, CT

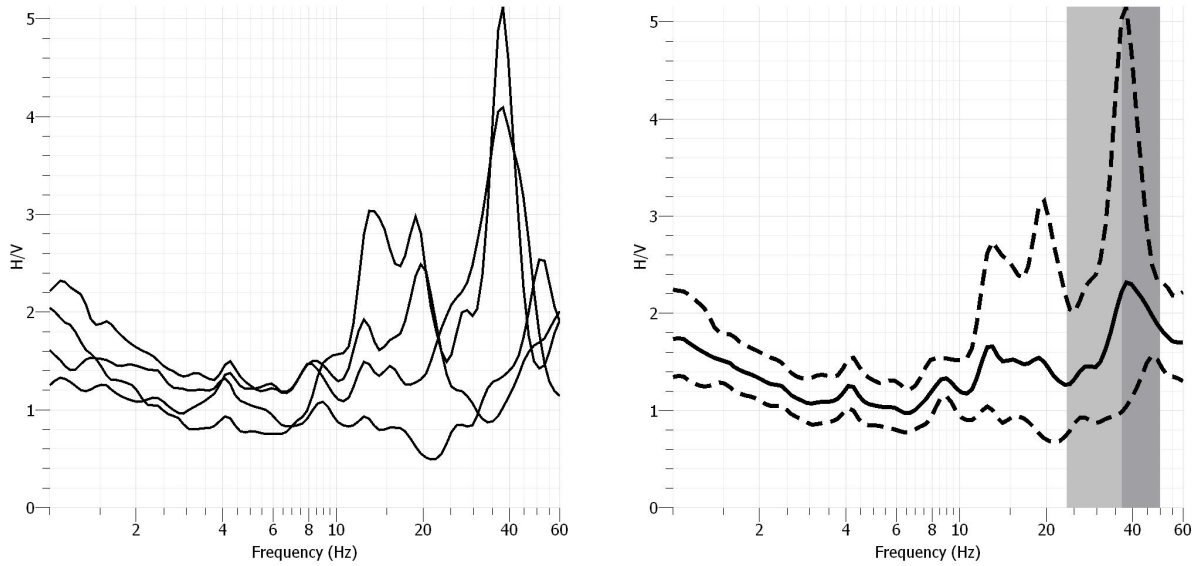

Figure A17. Class B: HVSR from 456 West Street, Southington, CT. Four HVSR measurements were taken near a borehole at a gas station and the resulting HVSR curves and resonance frequencies are displayed in (a). One measurement was conducted at the borehole and the three remaining measurements were taken 25 m North, South and West of the borehole. The average resonance frequency at this site was 36.9 Hz as indicated by the vertical gray rectangle in (b) with standard deviation. Based on well information, the depth to bedrock was 3.4 m; therefore the average velocity of the sediments was 502 m/s. Due to varying observed resonance frequencies at the site, the 1-D earth assumption was not met and the results are unreliable. This site remained a B class.

550 Cedar Street, Newington, CT

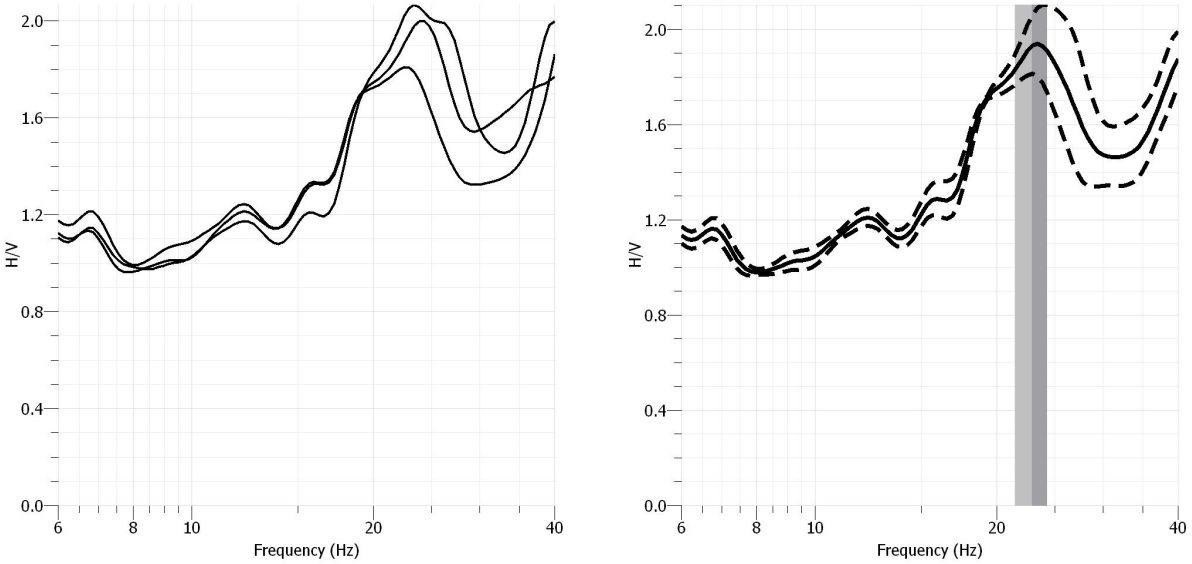

Figure A18. Class B: HVSR Huddle Test from 550 Cedar Street. Three HVSR measurements were taken around the borehole in a huddle test and the resulting HVSR curves and resonance frequencies are displayed in (a). The average resonance frequency at this site was 23.13 Hz as indicated by the vertical gray rectangle in (b) with standard deviation. Based on well information, the depth to bedrock was 6.1 m; therefore the average velocity of the sediments was 564 m/s.

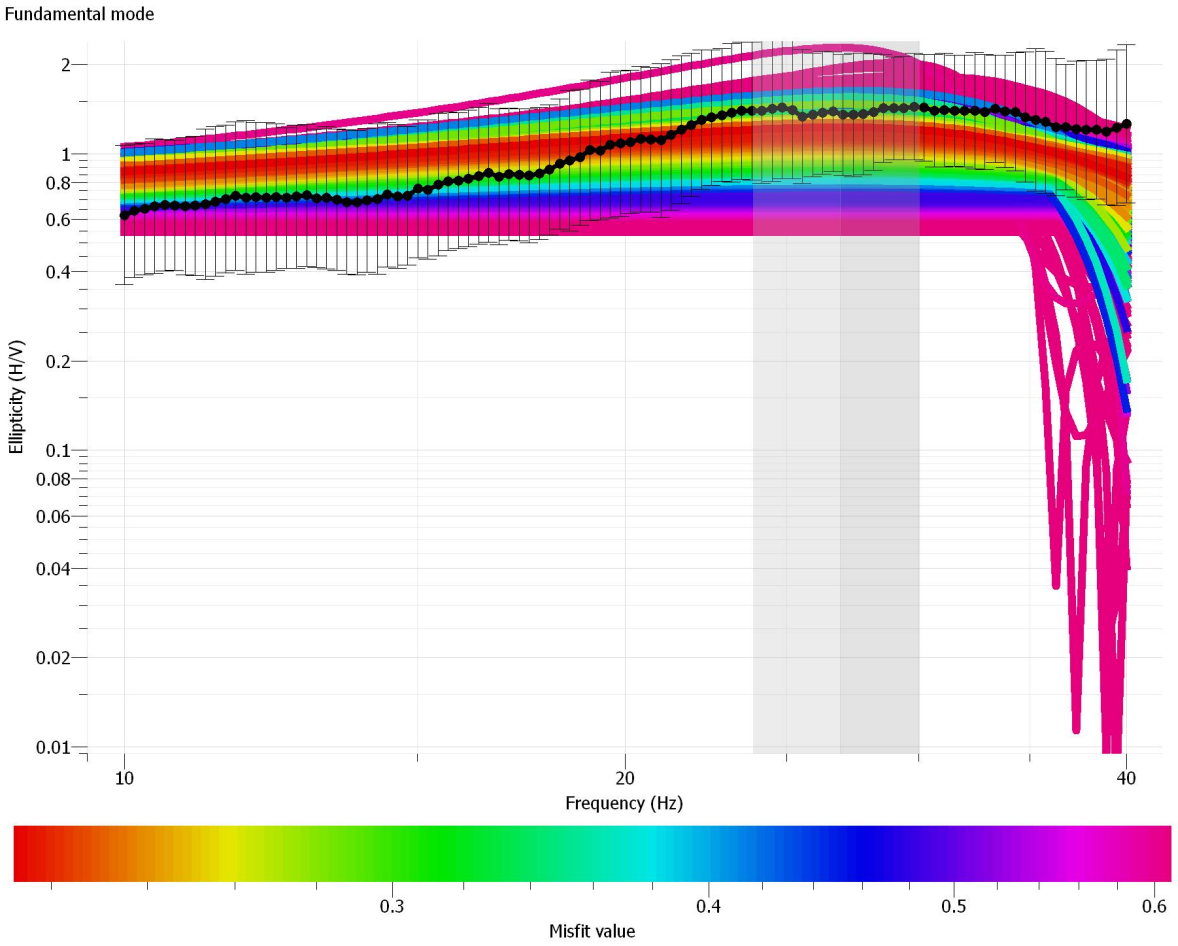

Figure A19. Class B: 550 Cedar Street Rayleigh Wave Ellipticity. No Rayleigh wave ellipticity was observed at this site as illustrated by the flat ellipticity curve around 1.

665 New Britain Ave, Newington, CT

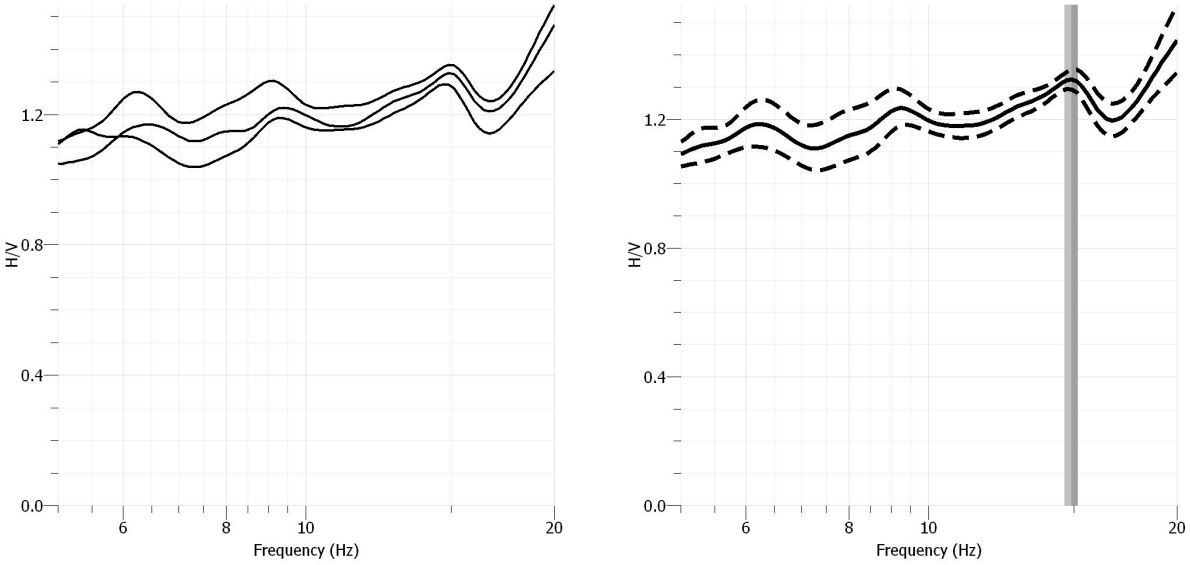

Figure A20. Class B: HVSR Huddle Test from 665 New Britain Ave. Three HVSR measurements were taken near a borehole and the resulting HVSR curves and resonance frequencies are displayed in (a). The average resonance frequency at this site was 14.8 Hz as indicated by the vertical gray rectangle in (b) with associated standard deviation. Based on well information, the depth to bedrock was 7.6 m; therefore the average velocity of the sediments was 450 m/s.

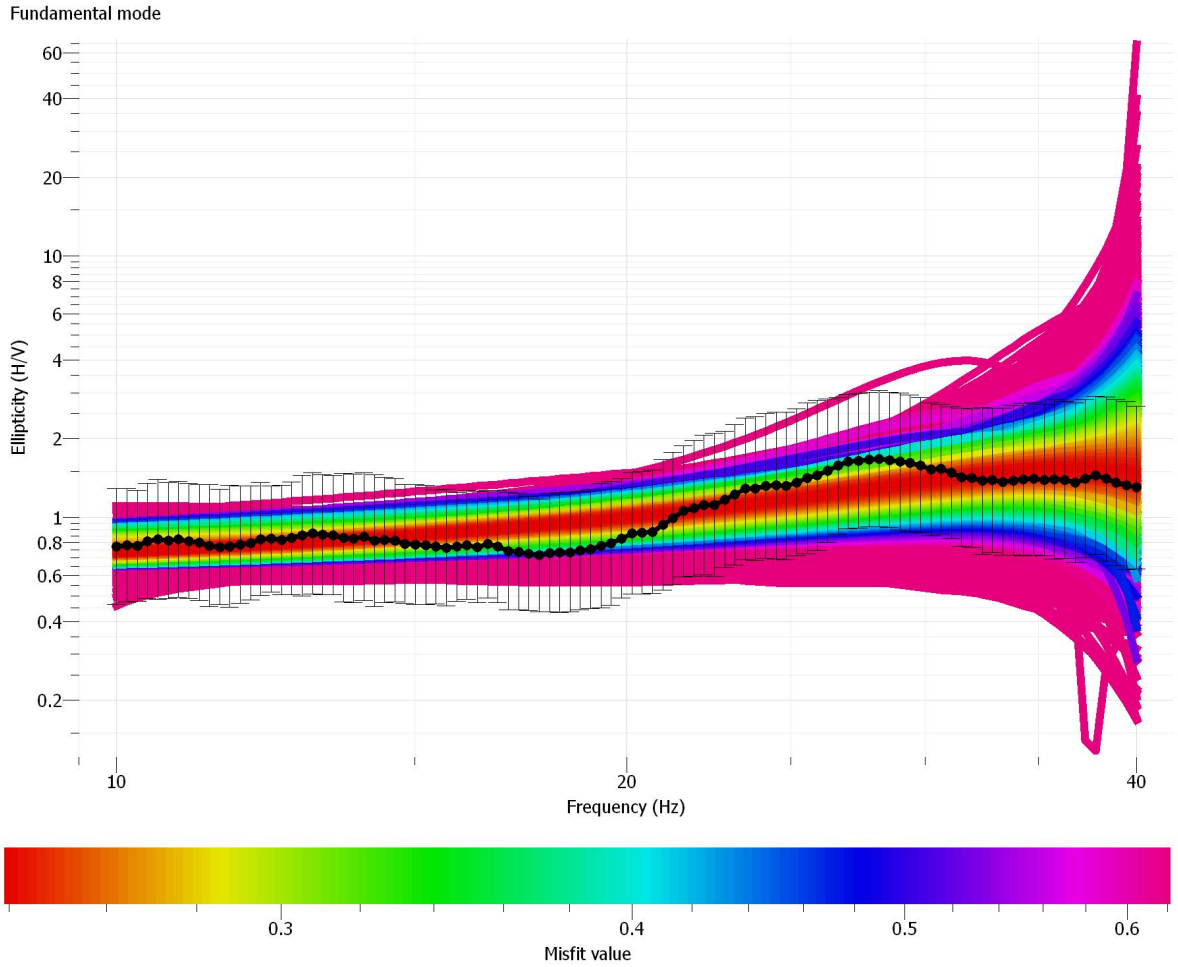

Figure A21. Class B: 665 New Britain Ave. Rayleigh Wave Ellipticity. No Rayleigh wave ellipticity was observed at this site as illustrated by the flat ellipticity curve at 1.

Philip R. Smith School, South Windsor, CT

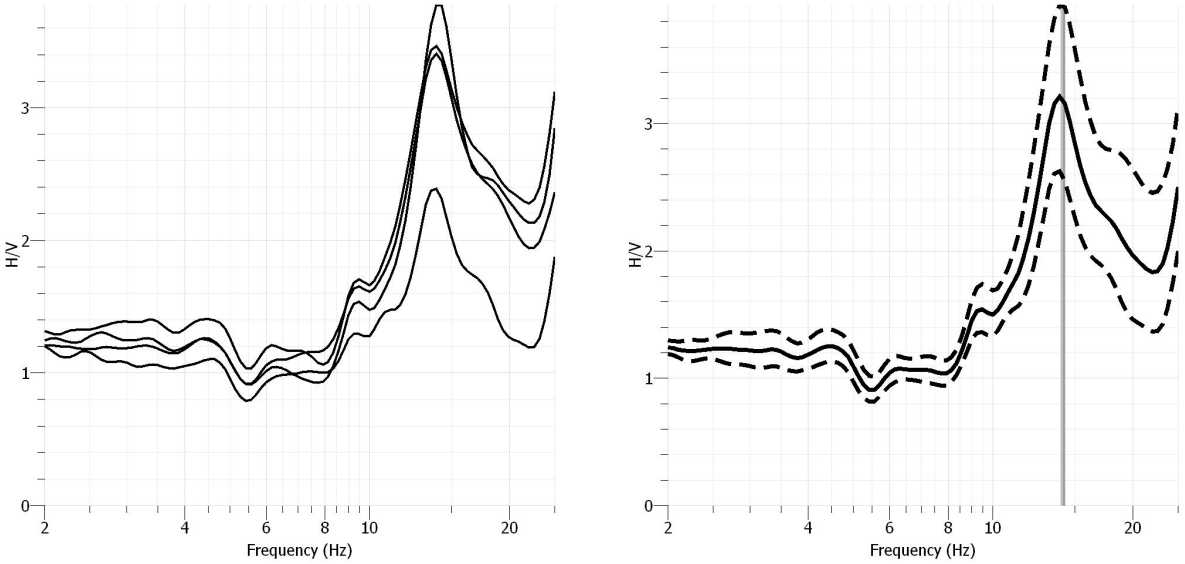

Figure A22. Class C: HVSR Huddle Test from Philip R. Smith School. Four HVSR measurements were taken around the borehole in a huddle test and the resulting HVSR curves and resonance frequencies are displayed in (a). The average resonance frequency at this site was 14.4 Hz as indicated by the vertical gray rectangle in (b) with standard deviation. Based on well information, the depth to bedrock was 4.8 m; therefore the average velocity of the sediments was 276 m/s.

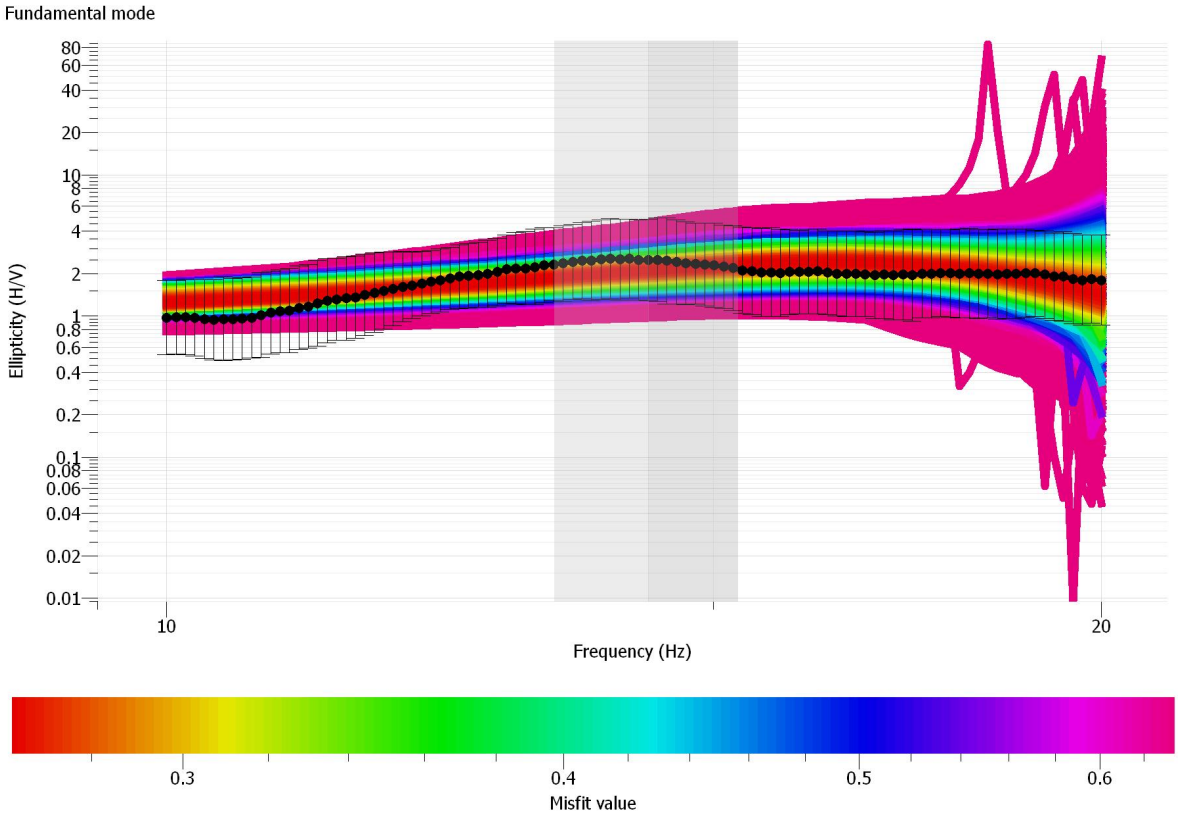

Figure A23. Class C: Philip R. Smith School Rayleigh Wave Ellipticity. No Rayleigh wave ellipticity was observed at this site as illustrated by the flat ellipticity curve around 1.

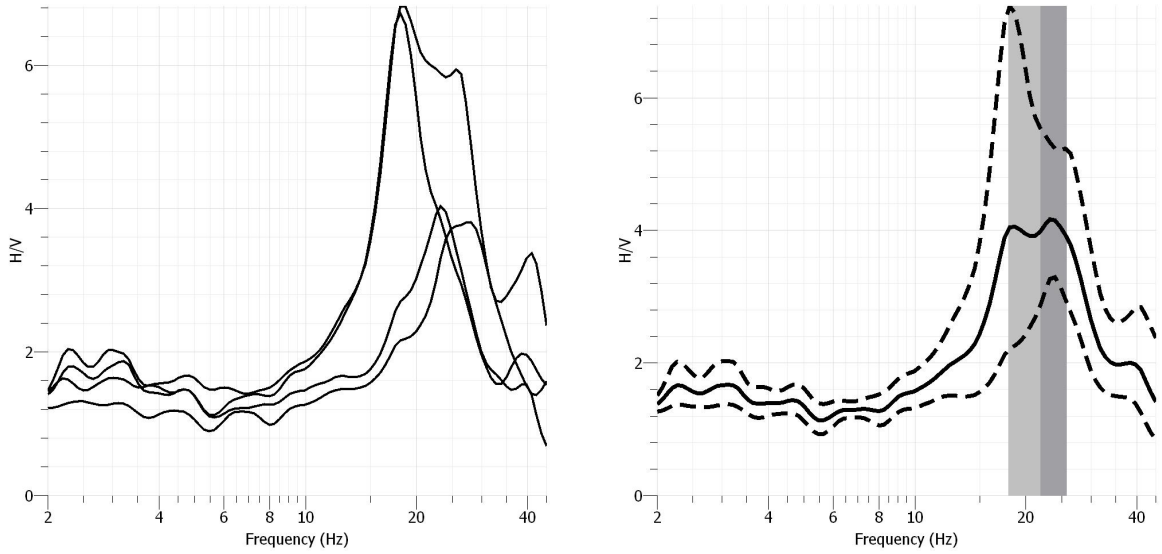

Figure A24. Class C: HVSR taken along MASW at Philip R. Smith School. Four HVSR measurements taken along an MASW profile at Geophone location 1, 8, 16, and 24. Each individual measurement is displayed in (a) and the average resonance frequency and standard deviation are displayed in (b). The average HVSR curve from (a) is displayed as the solid black line with respect to frequency and H/V amplitude. The two dotted lines represent the upper and lower bounds of the standard deviation. The vertical gray line shows the standard deviation of the observed resonance frequencies which range from 18.08-28.08 Hz from Geophone 1-24.

Layer Depth (m)	Vs (m/s)
0.44	707.85
0.99	739.81
1.67	759.85
2.53	742.58
3.60	667.24
4.94	520.91
6.61	476.50
8.70	807.84
11.31	1113.47
Half Space	1576.40
Vs sediments	826.4
Vs30	1075.8
Surficial Class	C
Vs30 Site Class	B

Table A3. Class C: Active MASW Results from Philip R. Smith School. A 10-layer model was generated from the dispersion curves in A27. A summary of the depth and shear-wave velocity information is listed here. This site was initially assigned hazard class C by the surficial materials data and then assigned hazard class B by the geophysical field data and Vs30. The gray colored boxes indicate the assumed bedrock interface based on the inversion.

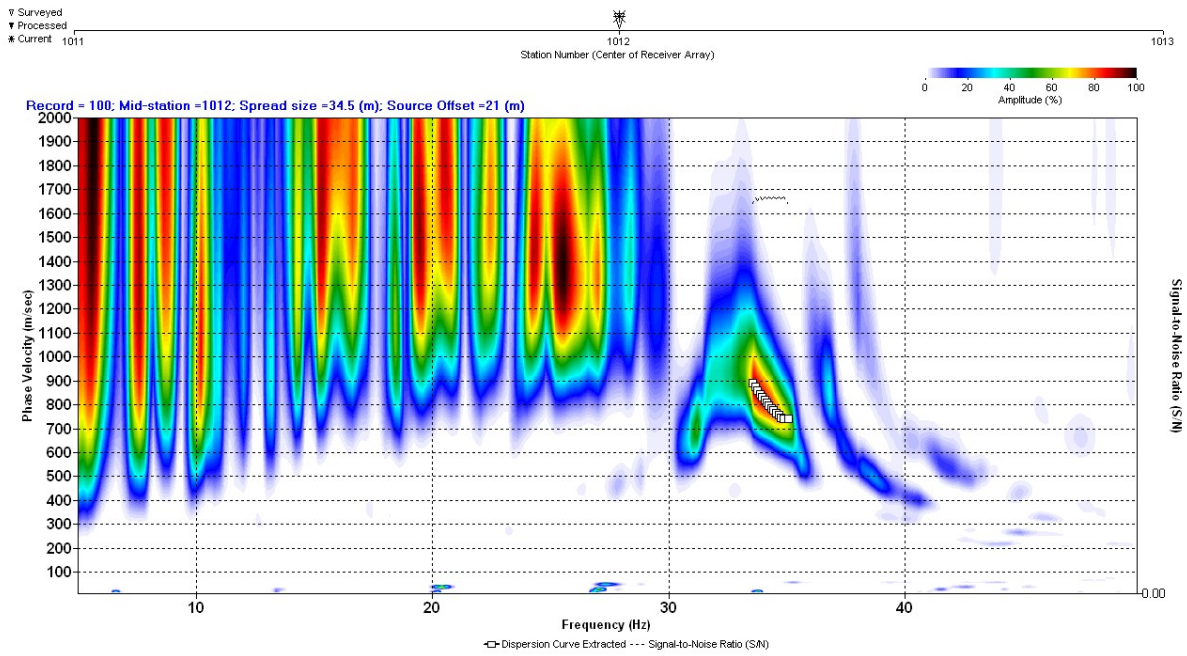

Figure A25. Class C: Philip R. Smith School Dispersion Curve. The picked dispersion curve is represented by the white boxes connected by a black line with respect to frequency and phase velocity. The vertical white, dashed line indicates the average resonance frequency observed at the field site, which is relative to the dispersion curve's observed higher frequencies; these high frequencies are indicative of the bedrock interface. The white horizontal dashed line indicates the average shear-wave velocity of the sediments based on the resonance frequency. This line coincides with the dispersion curve's observed higher frequencies, which are relative to the underlying sediments.

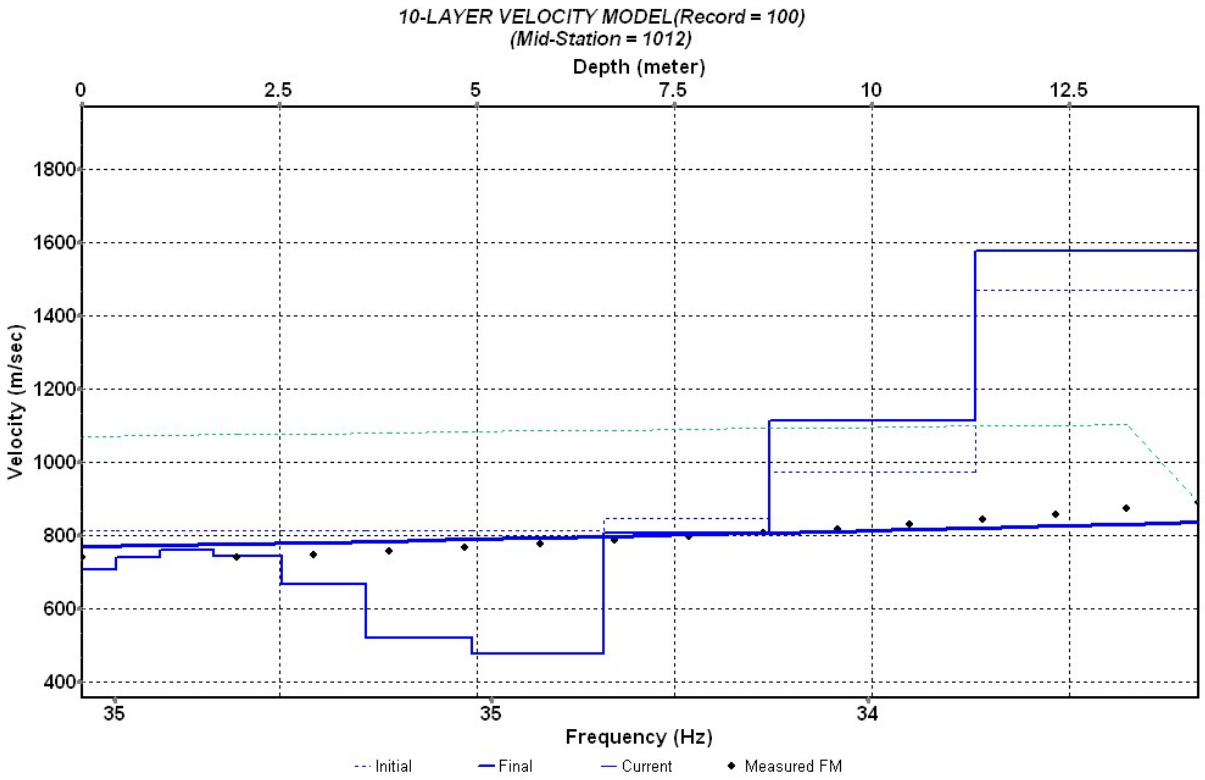

Figure A26. **Class C: Philip R. Smith School Velocity Profile from Inversion.** A 10-layer model was generated using the dispersion curve in Figure A15. The black dotted curve is the extracted dispersion curve and the blue solid curve is the model's theoretical curve. Based on this profile, the bedrock surface was observed at 18.4 m, the average sediment velocity was 826 m/s and the Vs30 was 1076 m/s, Class B.

3 Case Street, Avon, CT

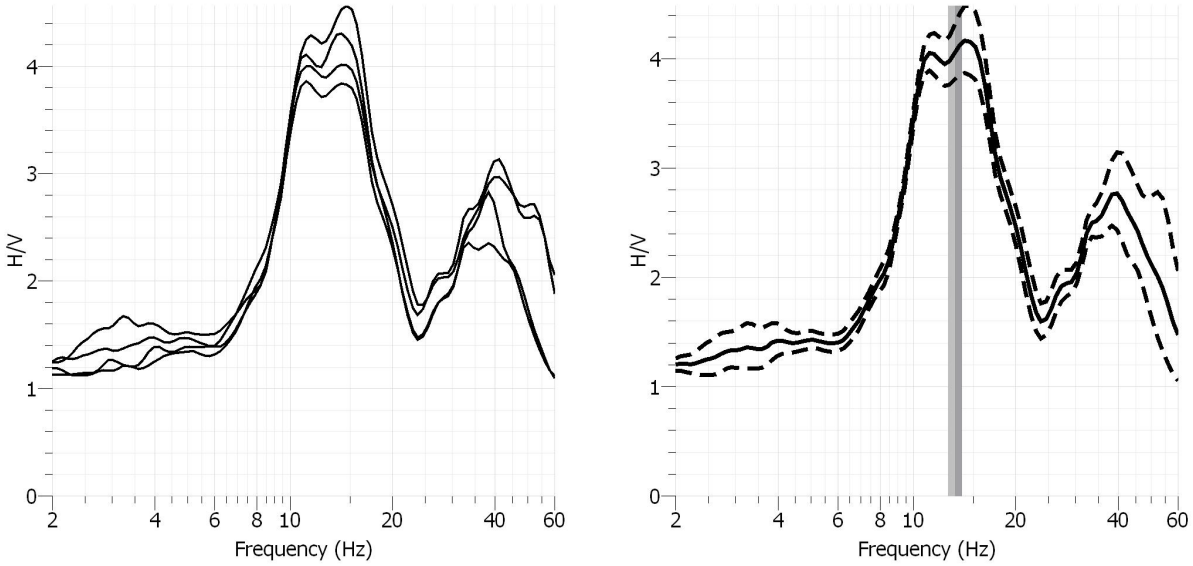

Figure A27. Class C: HVSR Huddle Test from 3 Case St. Four HVSR measurements were taken around the borehole at a church in a huddle test and the resulting HVSR curves and resonance frequencies are displayed in (a). The average resonance frequency at this site was 13.6 Hz as indicated by the vertical gray rectangle in (b) with standard deviation. Based on well information, the depth to bedrock was 10.4 m; therefore the average velocity of the sediments was 566 m/s.

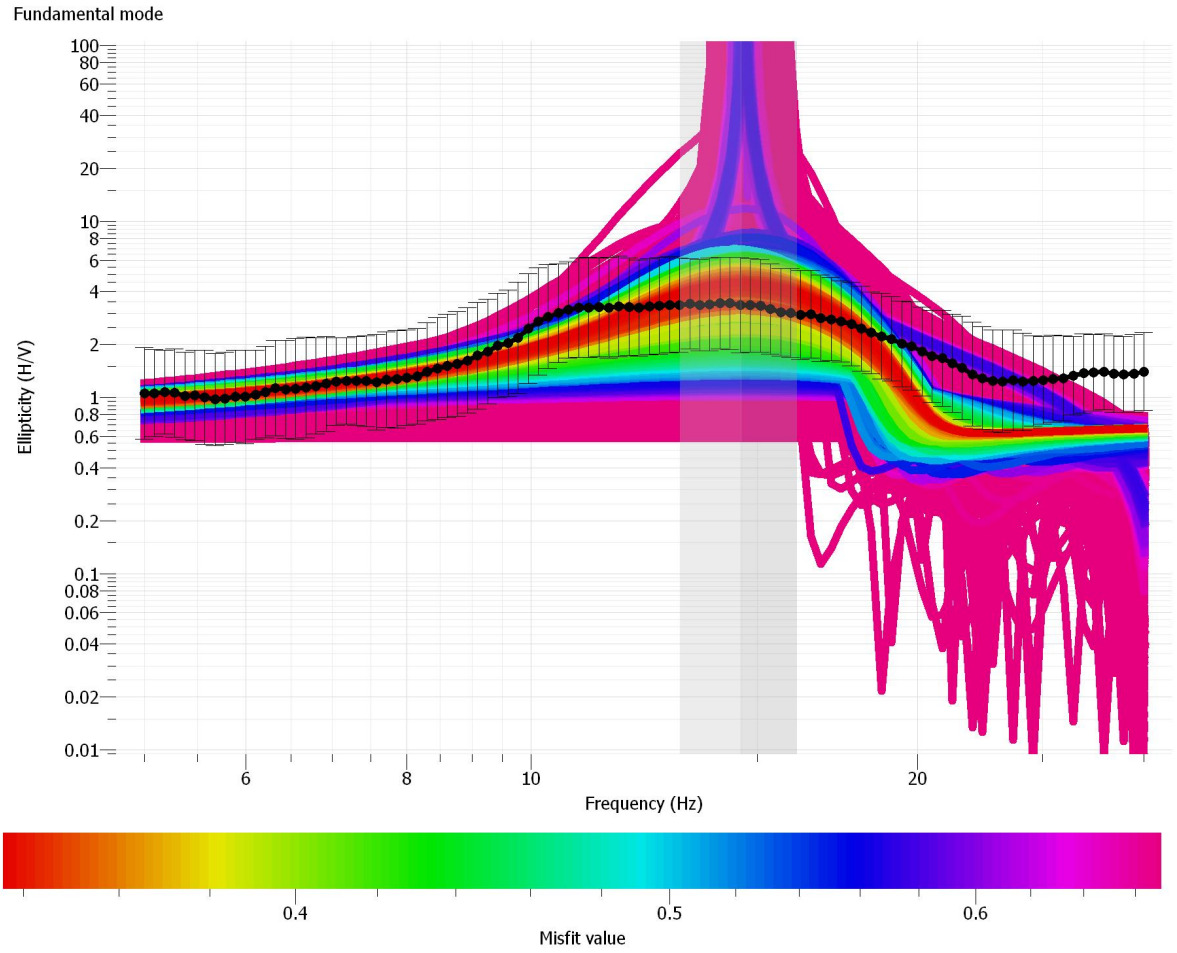

Figure A28. Class C: 3 Case St. Rayleigh Wave Ellipticity. The black dotted curve represents the observed ellipticty curve after the TFA with associated error bars. The observed ellipticity curve has a peak at 14 Hz as indicated by the vertical purple rectangle and a trough at 25 Hz. Each colored curve behind the data represents a different model generated by the inversion where red curves have the lowest misfit and the pink have the highest misfit. The vertical purple rectangle indicates the peak frequency value and standard deviation.

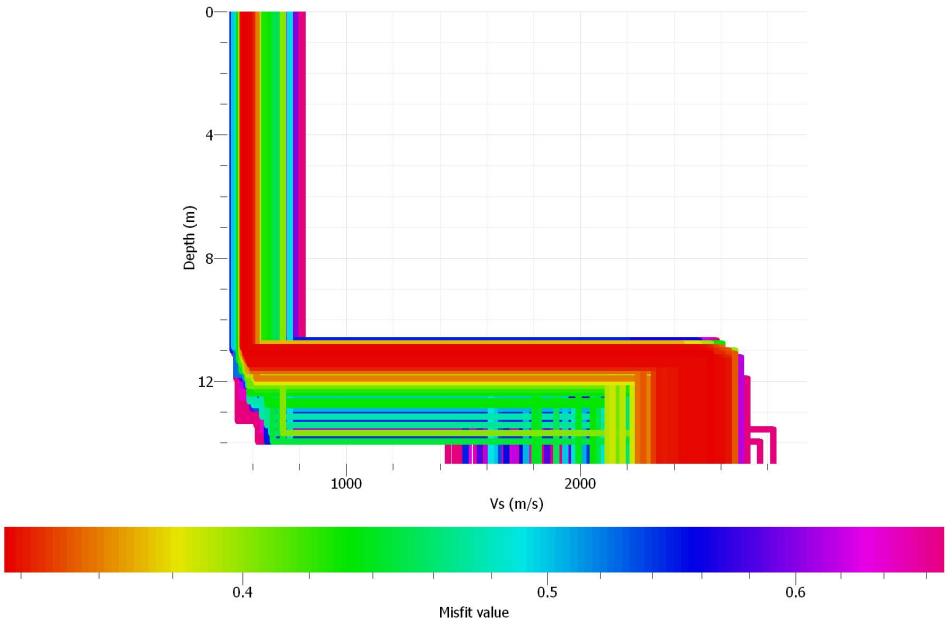

Figure A29. Class C: 3 Case St. Velocity Profile from Rayleigh Wave Ellipticity Inversion. Each 2-layer Vs model is represented by each colored line where the color refers to the misfit value. The red models have the lowest misfit and the pink models have the highest misfit. The lowest misfit models cluster around an interface at ~11.15 m with an average sediment Vs of 594 m/s.

40 Marbern Drive, Suffield, CT

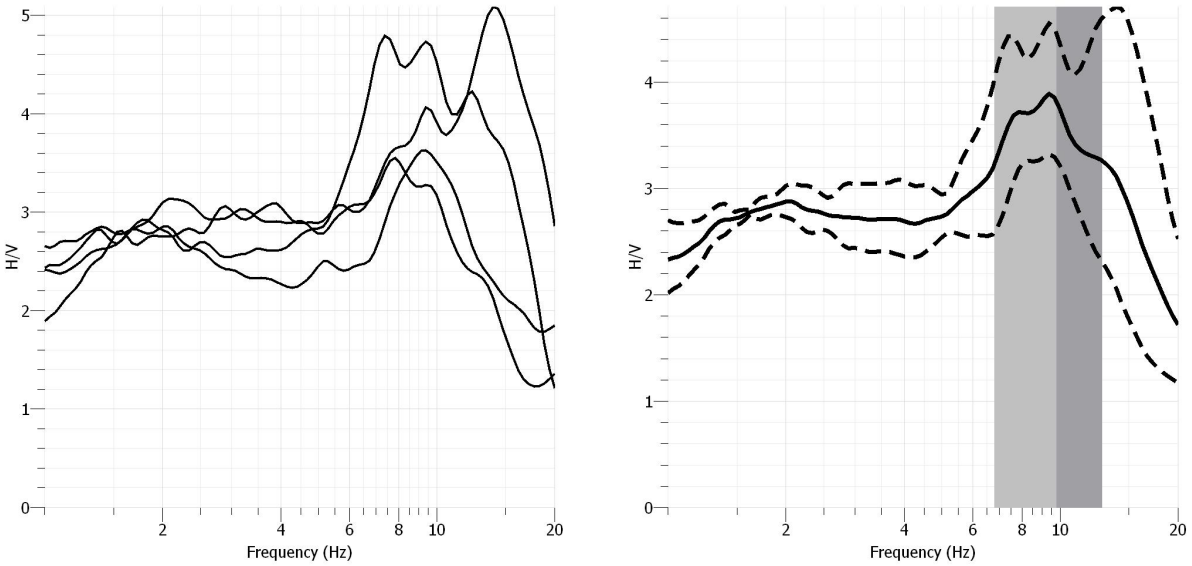

Figure A30. Class C: HVSR Huddle Test from 40 Marbern Drive. Four HVSR measurements were taken near the borehole and the resulting HVSR curves and resonance frequencies are displayed in (a). One measurement was conducted at the borehole and the three remaining measurements were taken 25 m North, South and West of the borehole. The average resonance frequency at this site was 9.84 Hz as indicated by the vertical gray rectangle in (b) with standard deviation. Based on well information, the depth to bedrock was 7.6 m; therefore the average velocity of the sediments was 299 m/s.

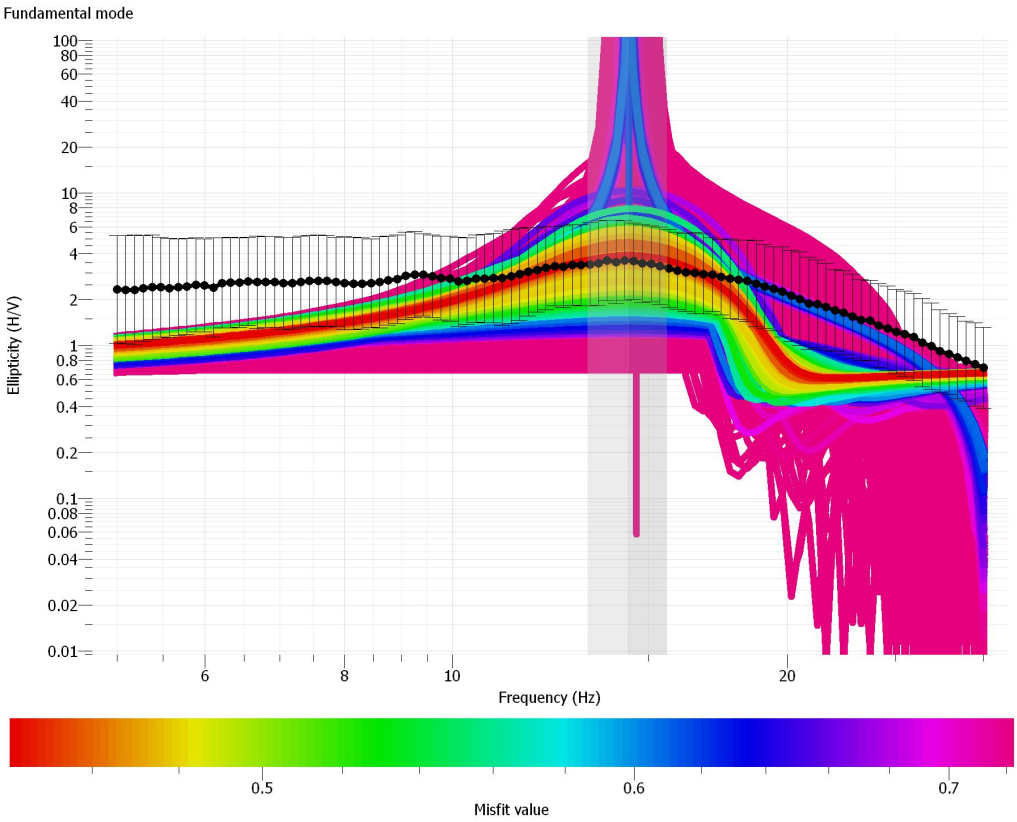

Figure A31. Class C: 40 Marbern Drive Rayleigh Wave Ellipticity. The black dotted curve represents the observed ellipticty curve after the TFA with associated error bars. The observed ellipticity curve has a peak at 14 Hz as indicated by the vertical purple rectangle. Each colored curve behind the data represents a different model generated by the inversion where red curves have the lowest misfit and the pink have the highest misfit. The vertical purple rectangle indicates the peak frequency value and standard deviation.

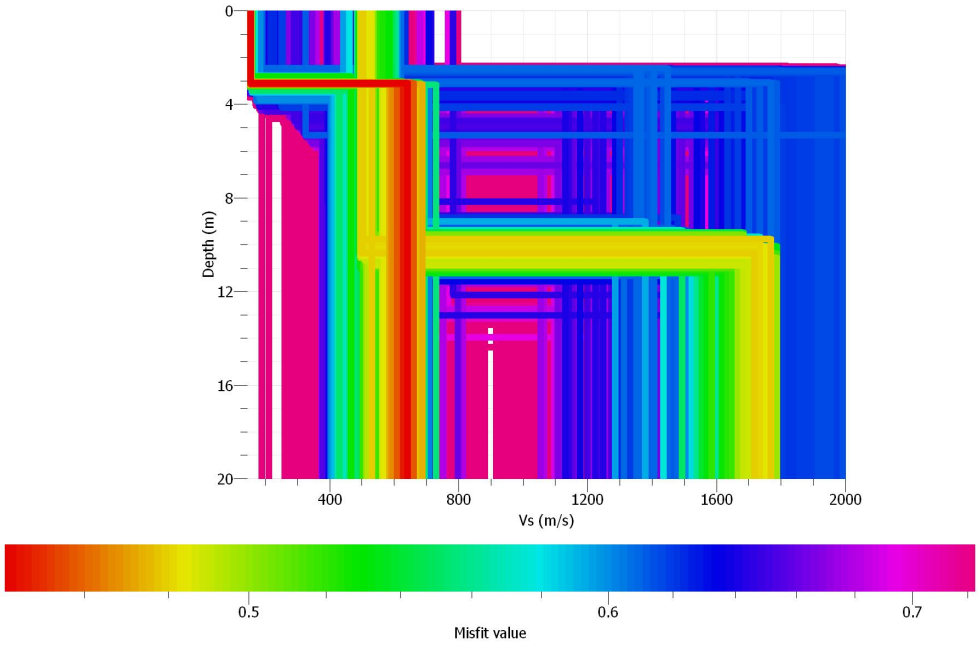

Figure A32. Class C: 40 Marbern Drive Velocity Profile from Rayleigh Wave Ellipticity Inversion. Each 2-layer Vs model is represented by each colored line where the color refers to the misfit value. The red models have the lowest misfit and the pink models have the highest misfit. The lowest misfit models cluster around an interface at ~3 m with an average sediment Vs of ~243 m/s and Vs30 of ~937, Class B.

555 Middle Turnpike East, Manchester, CT

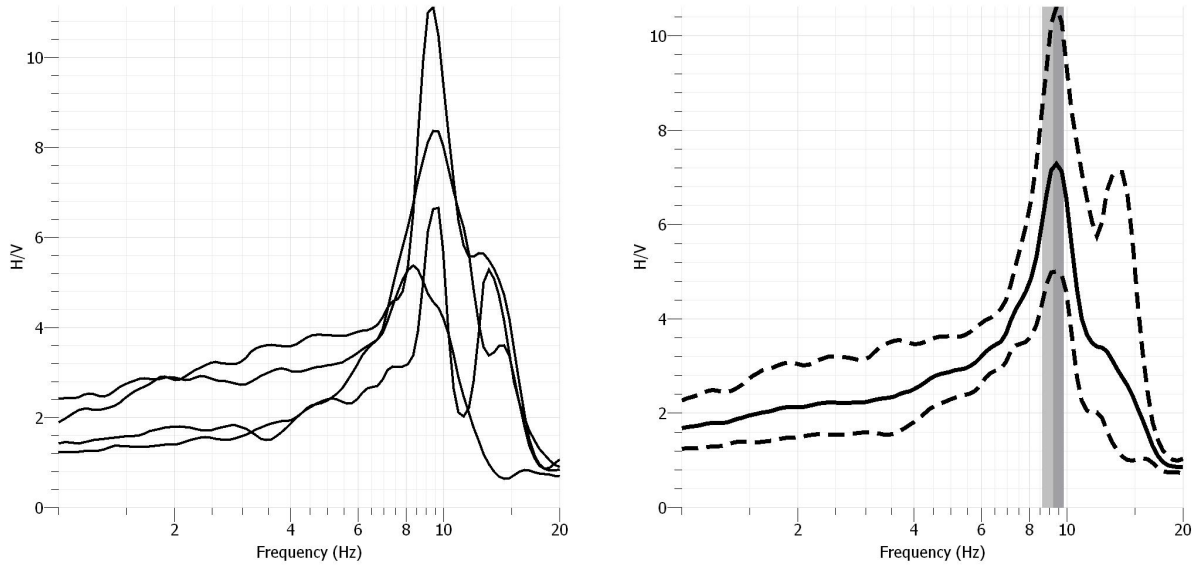

Figure A33. Class C: HVSR Huddle Test from 555 Middle Turnpike East. Four HVSR measurements were taken near the borehole and the resulting HVSR curves and resonance frequencies are displayed in (a). The average resonance frequency at this site was 9.3 Hz as indicated by the vertical gray rectangle in (b) with standard deviation. Based on well information, the depth to bedrock was 7.3 m; therefore the average velocity of the sediments was 272 m/s.

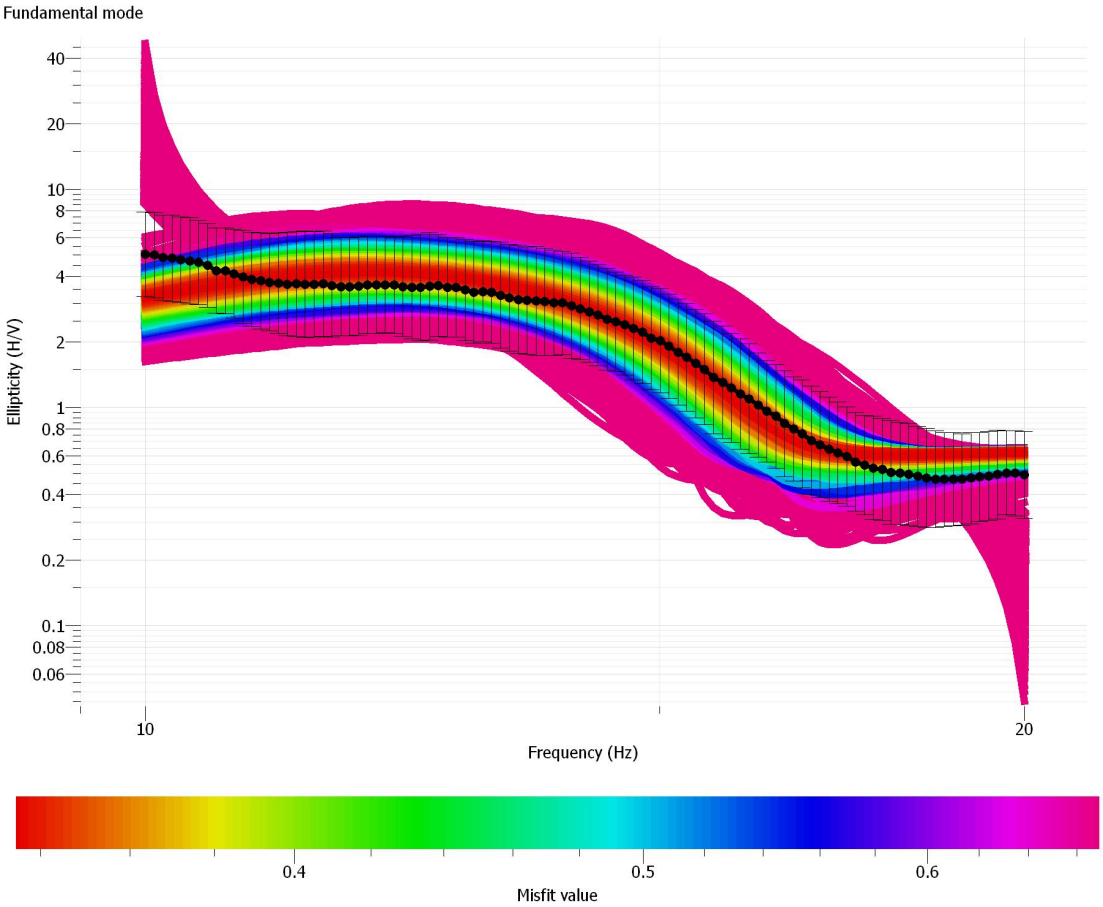

Figure A34. Class C: 555 Middle Turnpike East Rayleigh Wave Ellipticity. The black dotted curve represents the observed ellipticty curve after the TFA with associated error bars. Each colored curve behind the data represents a different model generated by the inversion where red curves have the lowest misfit and the pink have the highest misfit.

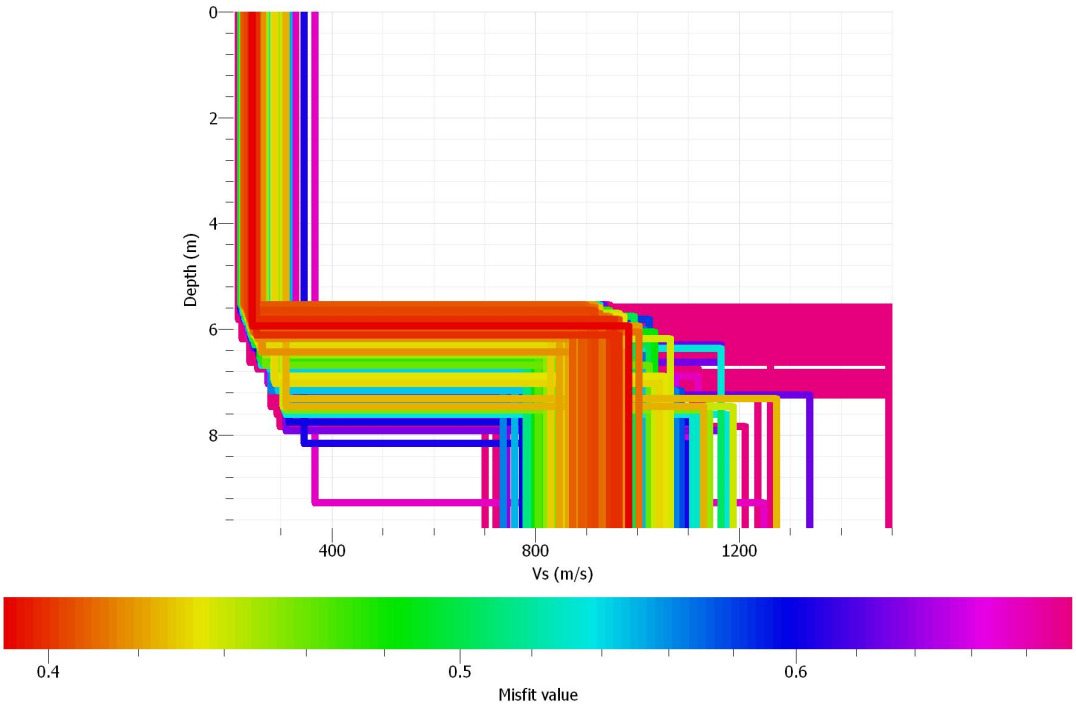

Figure A35. Class C: 555 Middle Turnpike East Velocity Profile from Rayleigh Wave Ellipticity. Each 2-layer Vs model is represented by each colored line where the color refers to the misfit value. The red models have the lowest misfit and the pink models have the highest misfit. The lowest misfit models cluster around an interface at ~6 m with an average sediment Vs of ~250 m/s and Vs30 of 615 m/s, Class C.

Nevers Park, South Windsor, CT

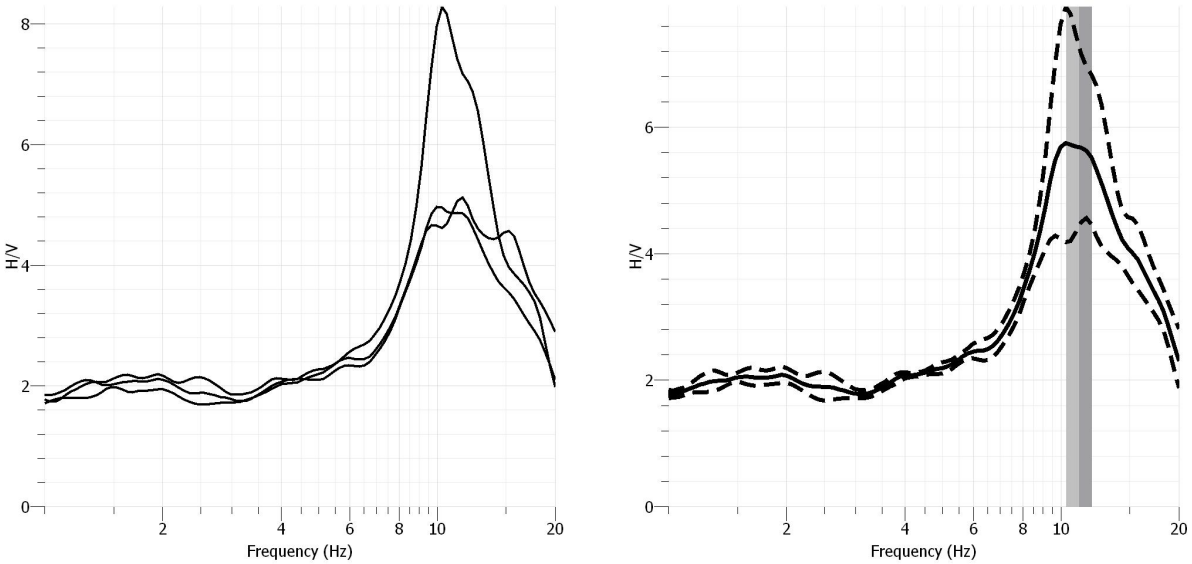

Figure A36. Class D: HVSR taken along MASW Profile at Nevers Park. Three HVSR measurements taken along an MASW profile at Geophone location 1, 12, and 24. Each individual measurement is displayed in (a) and the average resonance frequency and standard deviation are displayed in (b). The average HVSR curve from (a) is displayed as the solid black line with respect to frequency and H/V amplitude. The two dotted lines represent the upper and lower bounds of the standard deviation. The vertical gray line shows the standard deviation of the observed resonance frequencies which range from 10.27-11.6 Hz from Geophone 1-24.

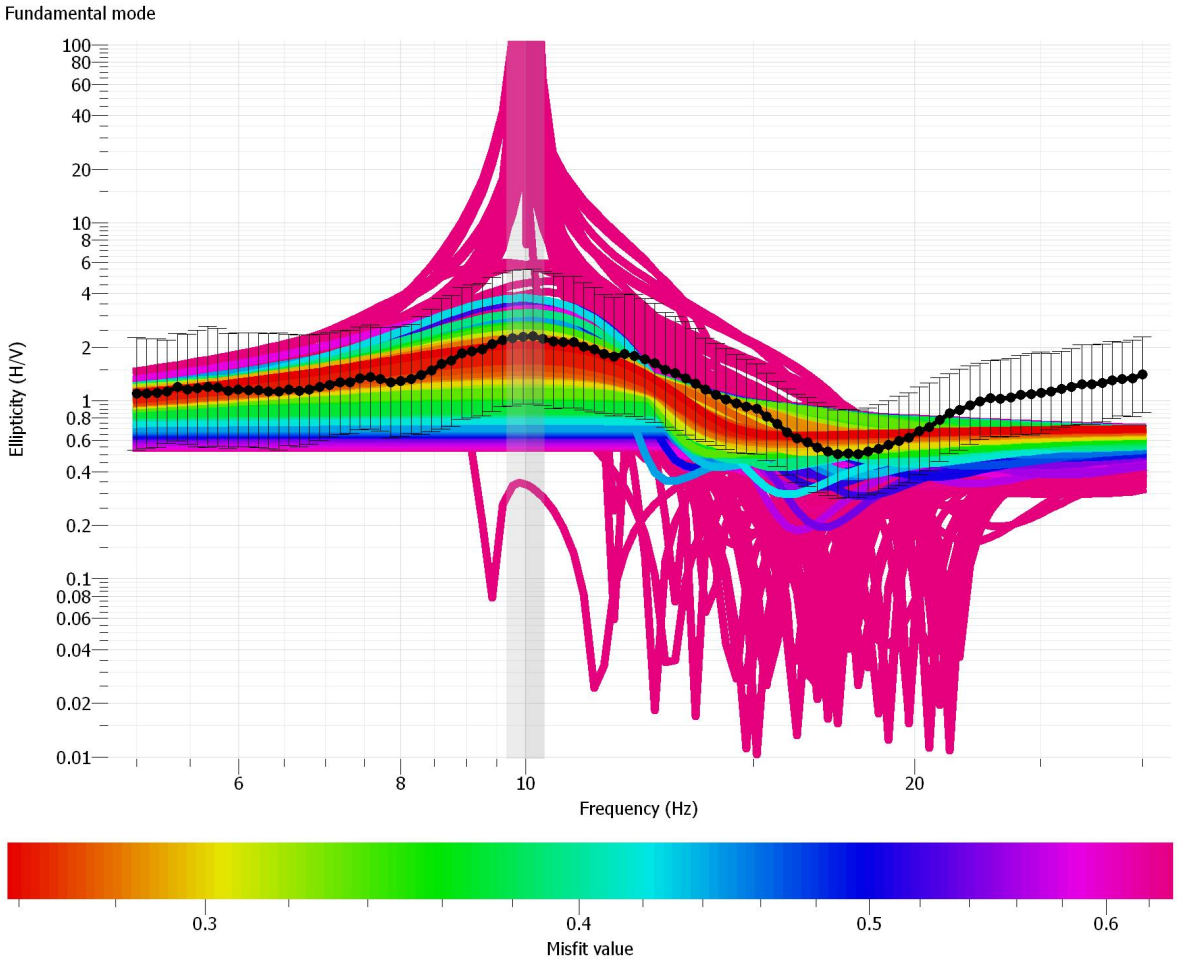

Figure A37: Class D: Nevers Park Rayleigh Wave Ellipticity. The black dotted curve represents the observed ellipticty curve after the TFA with associated error bars. The observed ellipticity curve has a peak at 10 Hz as indicated by the vertical grey rectangle. Each colored curve behind the data represents a different model generated by the inversion where red curves have the lowest misfit and the pink have the highest misfit. The vertical grey rectangle indicates the peak frequency value and standard deviation.

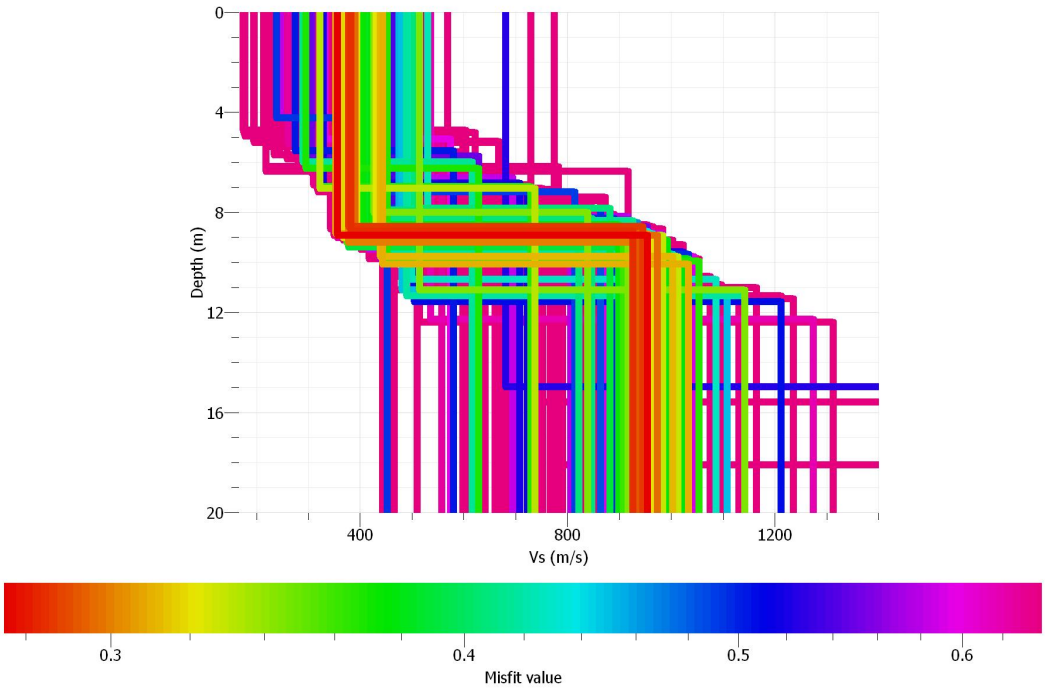

Figure A38. Class D: Nevers Park Velocity Profile from Rayleigh Wave Ellipticity Inversion. Each 2-layer Vs model is represented by each colored line where the color refers to the misfit value. The red models have the lowest misfit and the pink models have the highest misfit. The lowest misfit models cluster around an interface at ~9 m with an average sediment Vs of ~380 m/s and Vs30 of 655 m/s, Class C.

Layer Depth (m)	Vs (m/s)
1.1	484
2.5	604
4.2	662
6.3	650
9	614
12.3	423
16.5	463
21.7	912
28.2	1237
Half Space	1818
Vs sediments	661.7
Vs30	688.0
Surficial Class	D
Vs30 Site Class	C

Table A4. Class D: Active MASW Results from Nevers Park. A 10-layer model was generated from the dispersion curve in A36. A summary of the depth and shear-wave velocity information is listed here. This site was initially assigned hazard class D by the surficial materials data and then assigned hazard class C by the geophysical field data and Vs30. The gray colored boxes indicate the assumed bedrock interface based on the inversion.

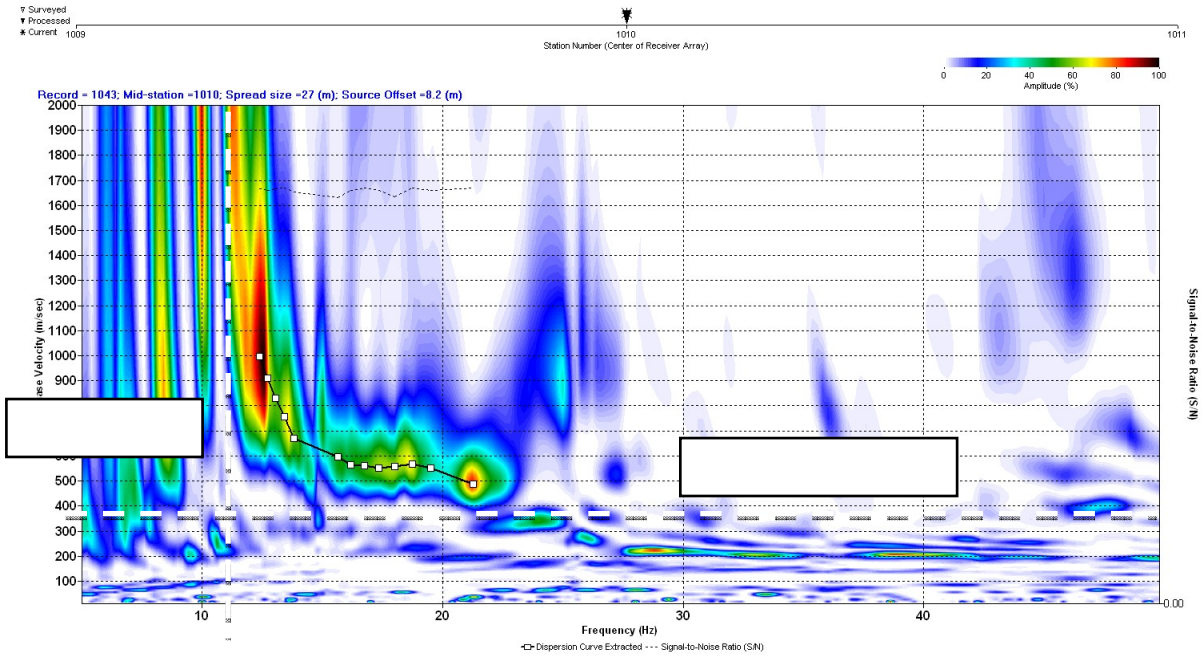

Figure A39. Class D: Nevers Park Dispersion Curve. The picked dispersion curve is represented by the white boxes connected by a black line with respect to frequency and phase velocity. The vertical white, dashed line indicates the average resonance frequency, 10.3 Hz, observed at the field site using HVSR, which is relative to the dispersion curve's observed higher frequencies; these high frequencies are indicative of the bedrock interface. The white horizontal dashed line indicates the average shear-wave velocity of the sediments, 380 m/s, based on the observed resonance frequency. This line coincides with the dispersion curve's observed higher frequencies, which are relative to the underlying sediments.

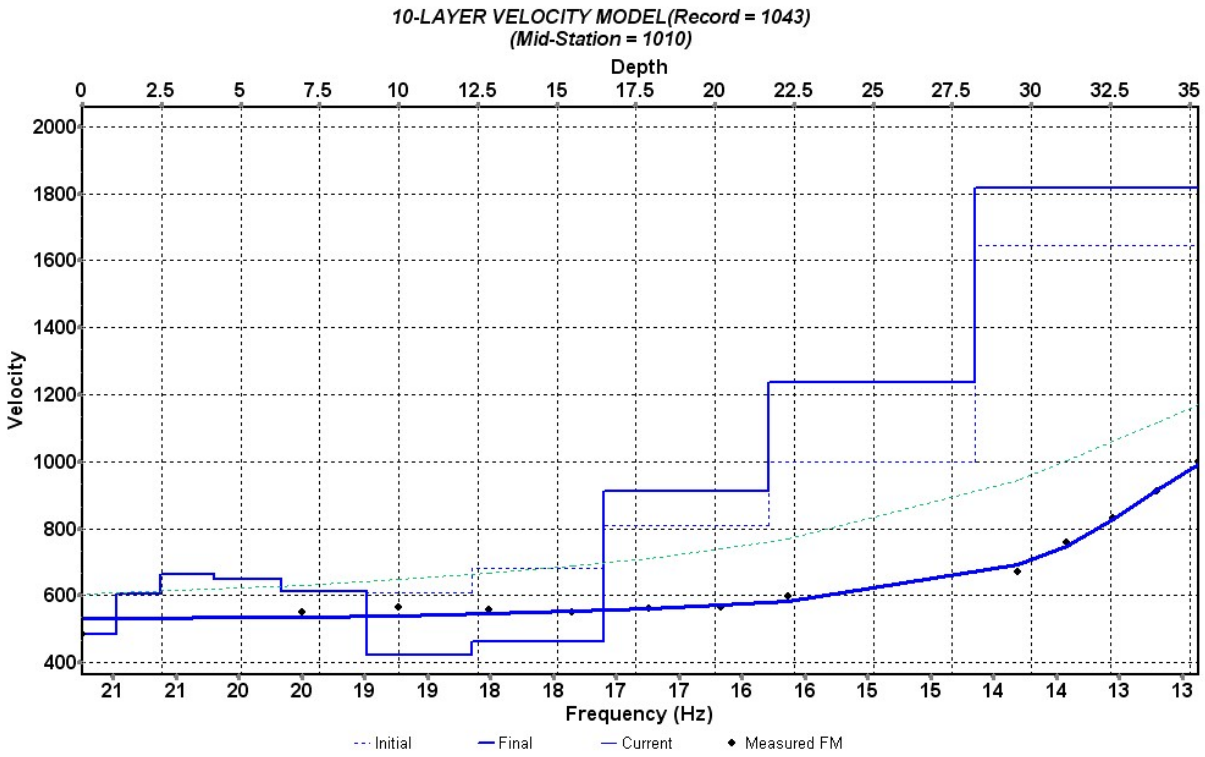

Figure A40 Class D: Nevers Park Velocity Profile from Inversion. A 10-layer model was generated using the dispersion curve in Figure A36. The black dotted curve is the extracted dispersion curve and the blue solid curve is the model's theoretical curve. Based on this profile, the bedrock surface was observed at 28.2 m, the average sediment velocity was 662 m/s and the Vs30 was 688 m/s, Class C.

580 Mountain Road, West Hartford, CT

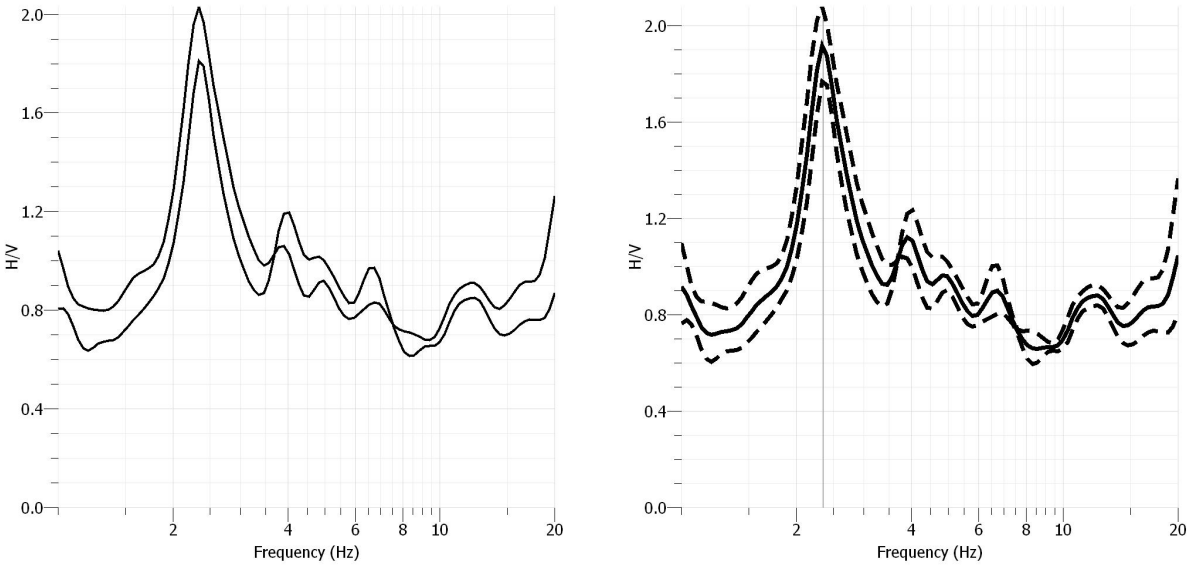

Figure A41. Class D: HVSR Huddle Test from 580 Mountain Road. Two HVSR measurements were taken around the borehole and the resulting HVSR curves and resonance frequencies are displayed in (a). The average resonance frequency at this site was 2.3 Hz as indicated by the vertical gray rectangle in (b) with standard deviation. Based on well information, the depth to bedrock was 14.9 m; therefore the average velocity of the sediments was 218 m/s.

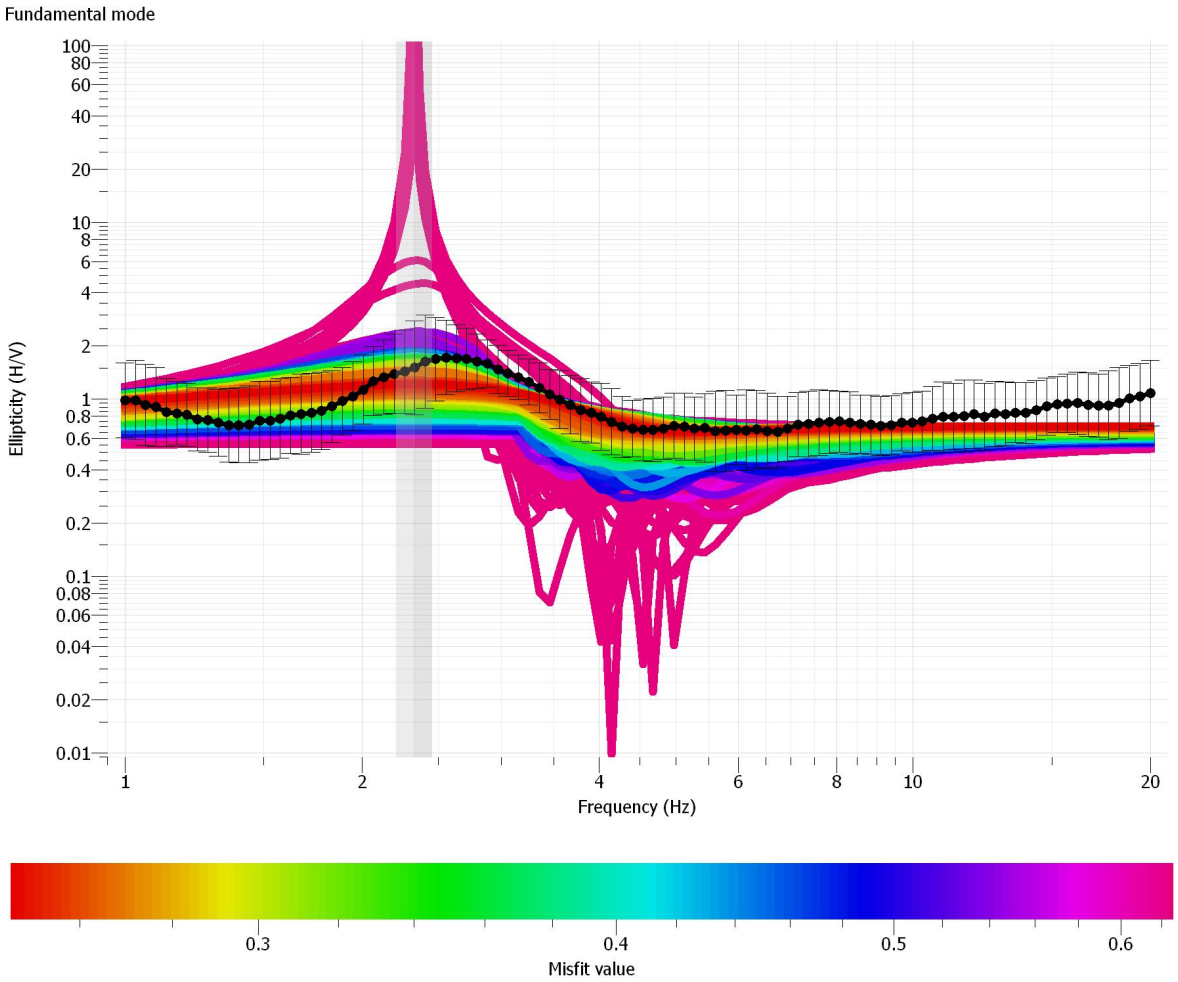

Figure A42. Class D: 580 Mountain Rd. Rayleigh Wave Ellipticity. The black dotted curve represents the observed ellipticty curve after the TFA with associated error bars. The observed ellipticity curve has a peak at 2.3 Hz as indicated by the vertical purple rectangle. Each colored curve behind the data represents a different model generated by the inversion where red curves have the lowest misfit and the pink have the highest misfit. The vertical purple rectangle indicates the peak frequency value and standard deviation.

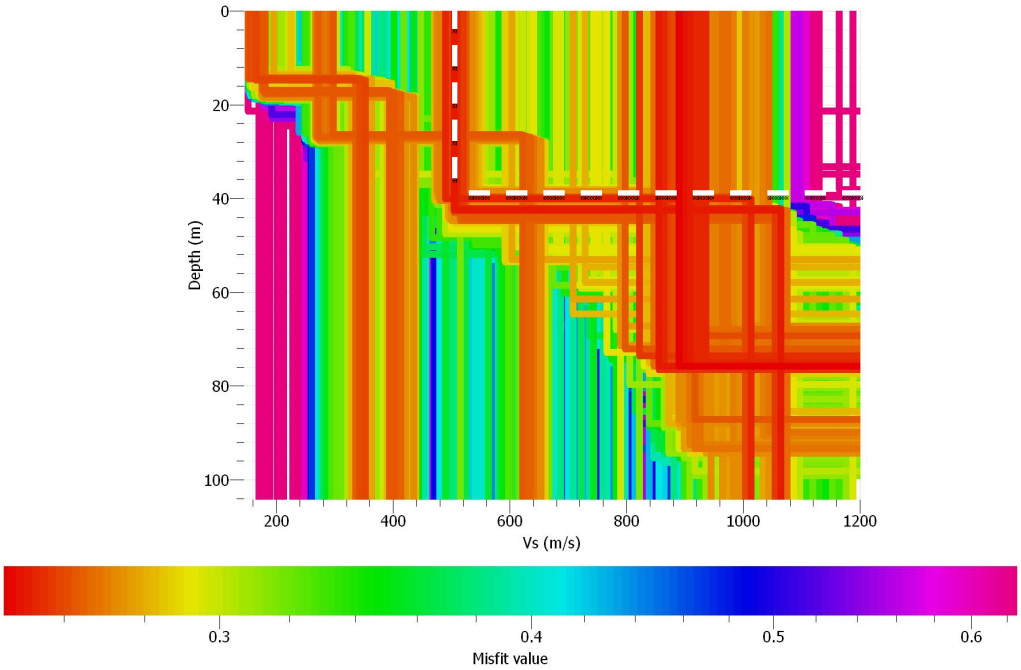

Figure A43. Class D: 580 Mountain Rd. Velocity Profile from Rayleigh Wave Ellipticity Inversion. Each 2-layer Vs model is represented by each colored line where the color refers to the misfit value. The red models have the lowest misfit and the pink models have the highest misfit. The lowest misfit models, indicated by the white dotted line, cluster around an interface at ~39 m with an average sediment Vs of ~510 m/s and Vs30 of 510 m/s, Class C. Based on the low resonance frequency observed, the recorded 14.9 m depth in the well log is too shallow. Therefore, the deeper interface and low velocity sediment velocity better account for the given site.

1046 Tolland Turnpike, Manchester, CT

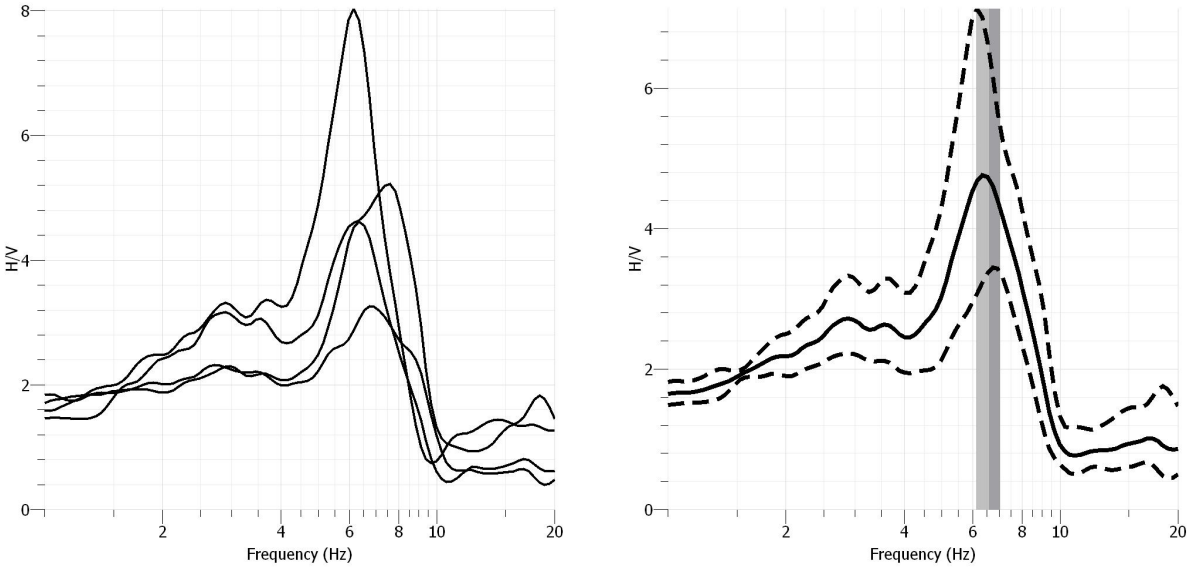

Figure A44. Class D: HVSR Huddle Test from 1046 Tolland Turnpike. Four HVSR measurements were taken near the borehole and the resulting HVSR curves and resonance frequencies are displayed in (a). The average resonance frequency at this site was 6.1 Hz as indicated by the vertical gray rectangle in (b) with standard deviation. Based on well information, the depth to bedrock was 13.7 m; therefore the average velocity of the sediments was 334 m/s.

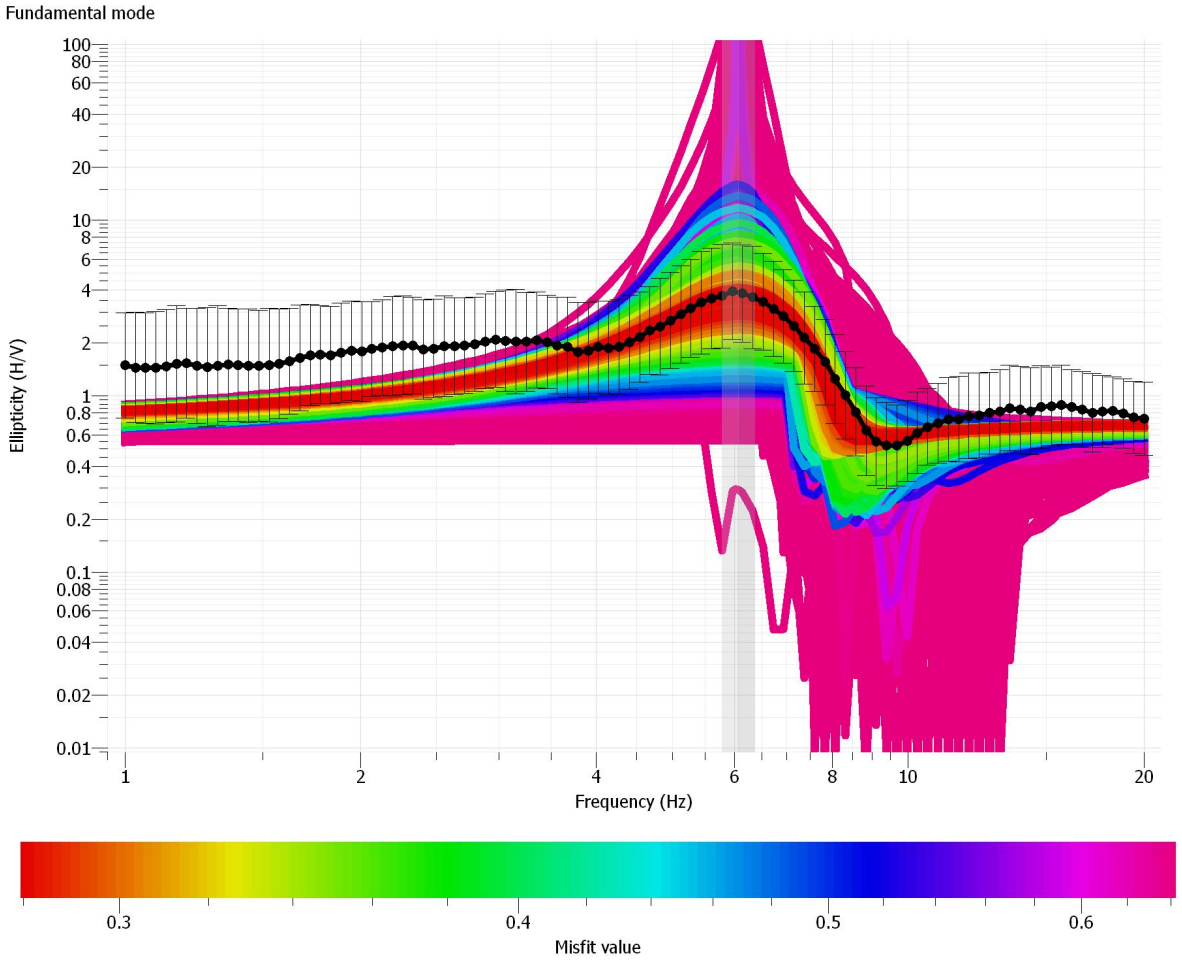

Figure A45. Class D: 1046 Tolland Turnpike Rayleigh Wave Ellipticity. The black dotted curve represents the observed ellipticty curve after the TFA with associated error bars. The observed ellipticity curve has a peak at 6.1 Hz as indicated by the vertical purple rectangle. Each colored curve behind the data represents a different model generated by the inversion where red curves have the lowest misfit and the pink have the highest misfit. The vertical purple rectangle indicates the peak frequency value and standard deviation.

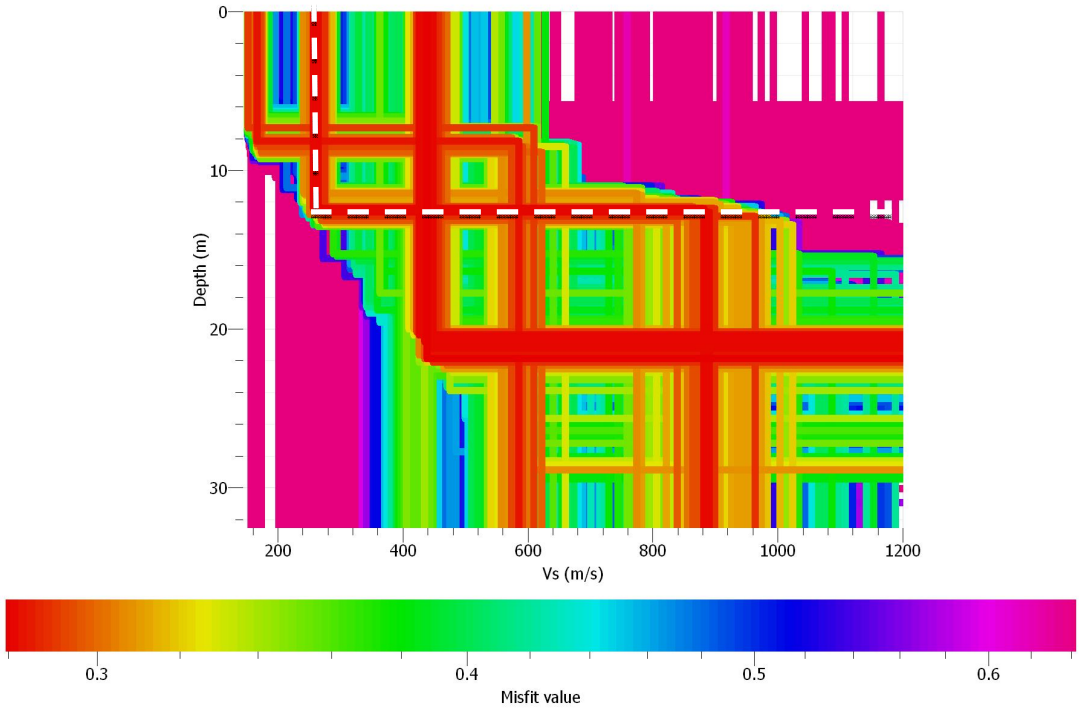

Figure A46. Class D: 1046 Tolland Turnpike Velocity Profile from Rayleigh Wave Ellipticity Inversion. Each 2-layer Vs model is represented by each colored line where the color refers to the misfit value. The red models have the lowest misfit and the pink models have the highest misfit. The lowest misfit models, indicated by the white dotted line, cluster around an interface at ~12.5 m with an average sediment Vs of ~272 m/s.

2279 Mount Vernon Road, Southington, CT

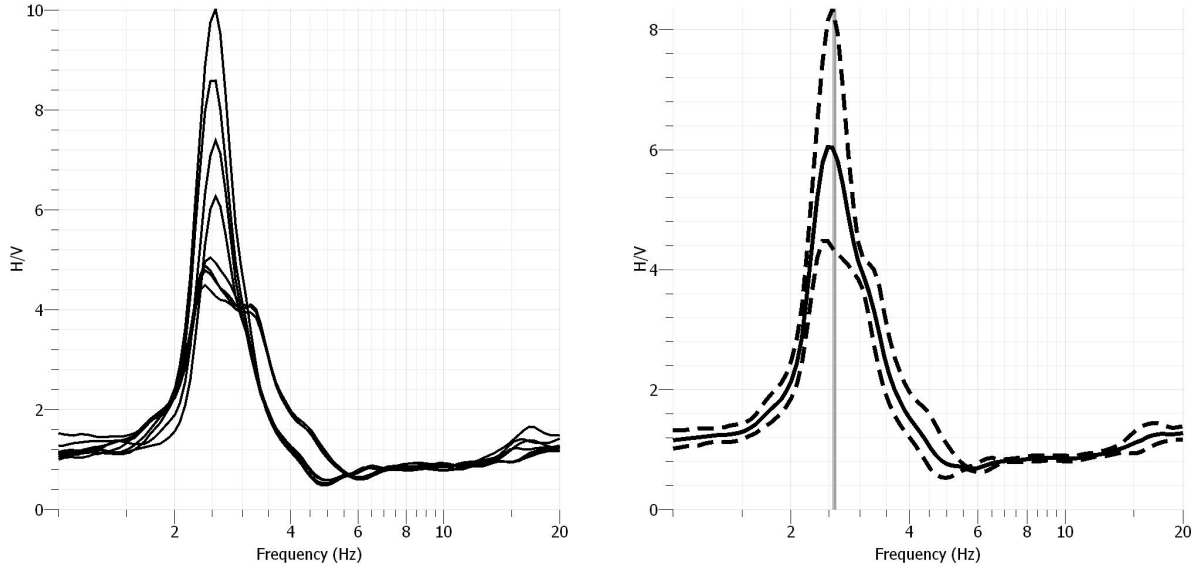

Figure A47. Class D: HVSR Huddle Tests from 2279 Mount Vernon Road. A total of six HVSR measurements were taken near two boreholes and the resulting HVSR curves and resonance frequencies are displayed in (a). The average resonance frequency at this site was 2.6 Hz as indicated by the vertical gray rectangle in (b) with standard deviation. Based on well information, the depth to bedrock was 46 m; therefore the average velocity of the sediments was 450 m/s.

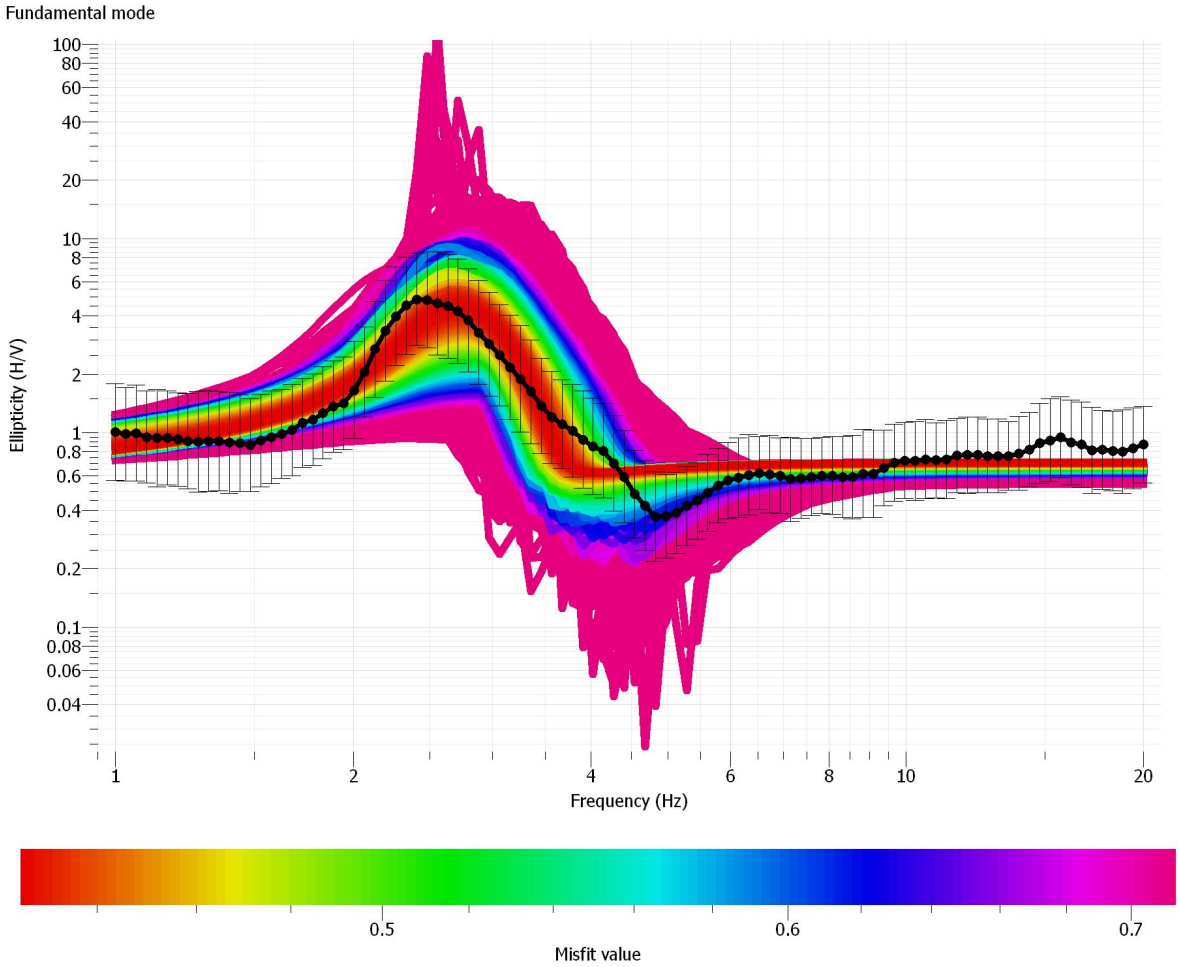

Figure A48. Class D: 2279 Mount Vernon Rd. Rayleigh Wave Ellipticity. The black dotted curve represents the observed ellipticty curve after the TFA with associated error bars. The observed ellipticity curve has a peak at 2.6 Hz as indicated by the vertical purple rectangle. Each colored curve behind the data represents a different model generated by the inversion where red curves have the lowest misfit and the pink have the highest misfit. The vertical purple rectangle indicates the peak frequency value and standard deviation.

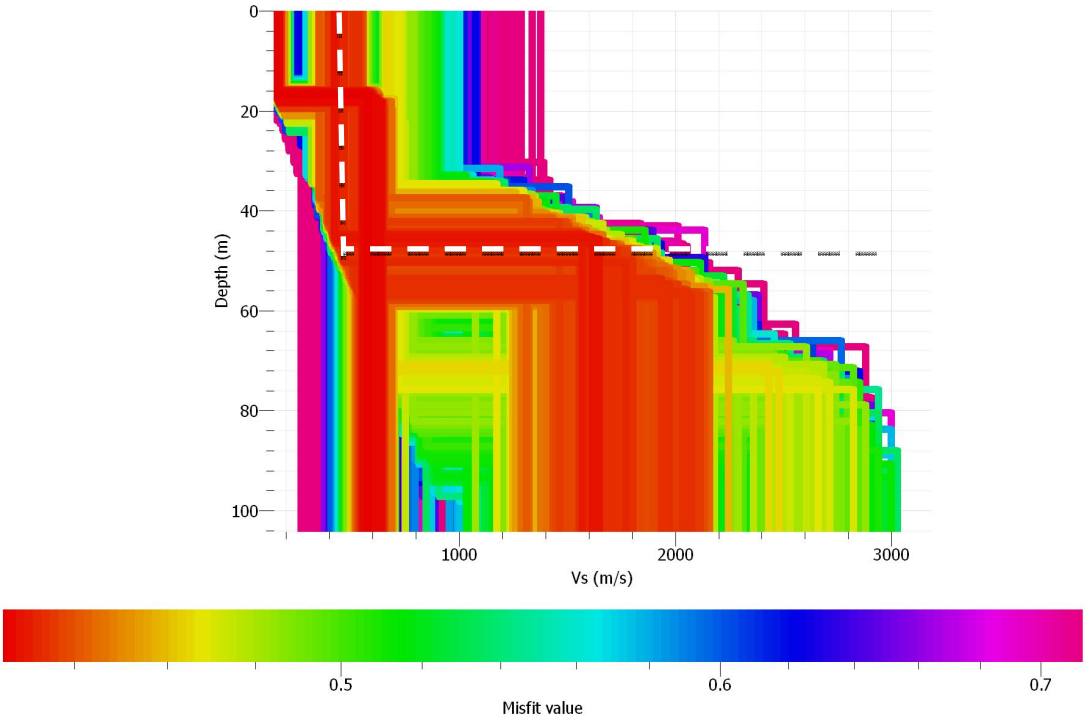

Figure A49. Class D: 2279 Mount Vernon Rd. Velocity Profile from Rayleigh Wave Ellipticity Inversion. Each 2-layer Vs model is represented by each colored line where the color refers to the misfit value. The red models have the lowest misfit and the pink models have the highest misfit. Based on the well information and the lowest misfit models at ~46 m, the average sediment Vs is ~450 m/s; these models are indicated by the white dotted line.

Goodwin Park, Hartford, CT

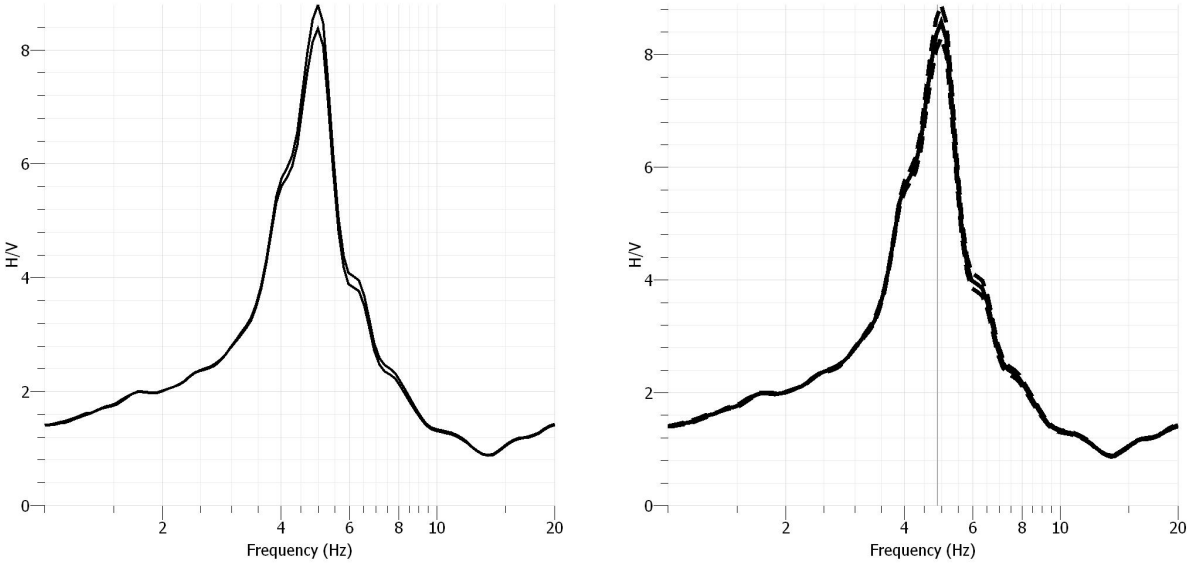

Figure A50. Class E: HVSR Huddle Test from Goodwin Park. Two HVSR measurements were taken near the borehole and the resulting HVSR curves and resonance frequencies are displayed in (a). The average resonance frequency at this site was 4.8 Hz as indicated by the vertical gray rectangle in (b) with standard deviation. Based on well information, the depth to bedrock was 15.2 m; therefore the average velocity of the sediments was 292 m/s.

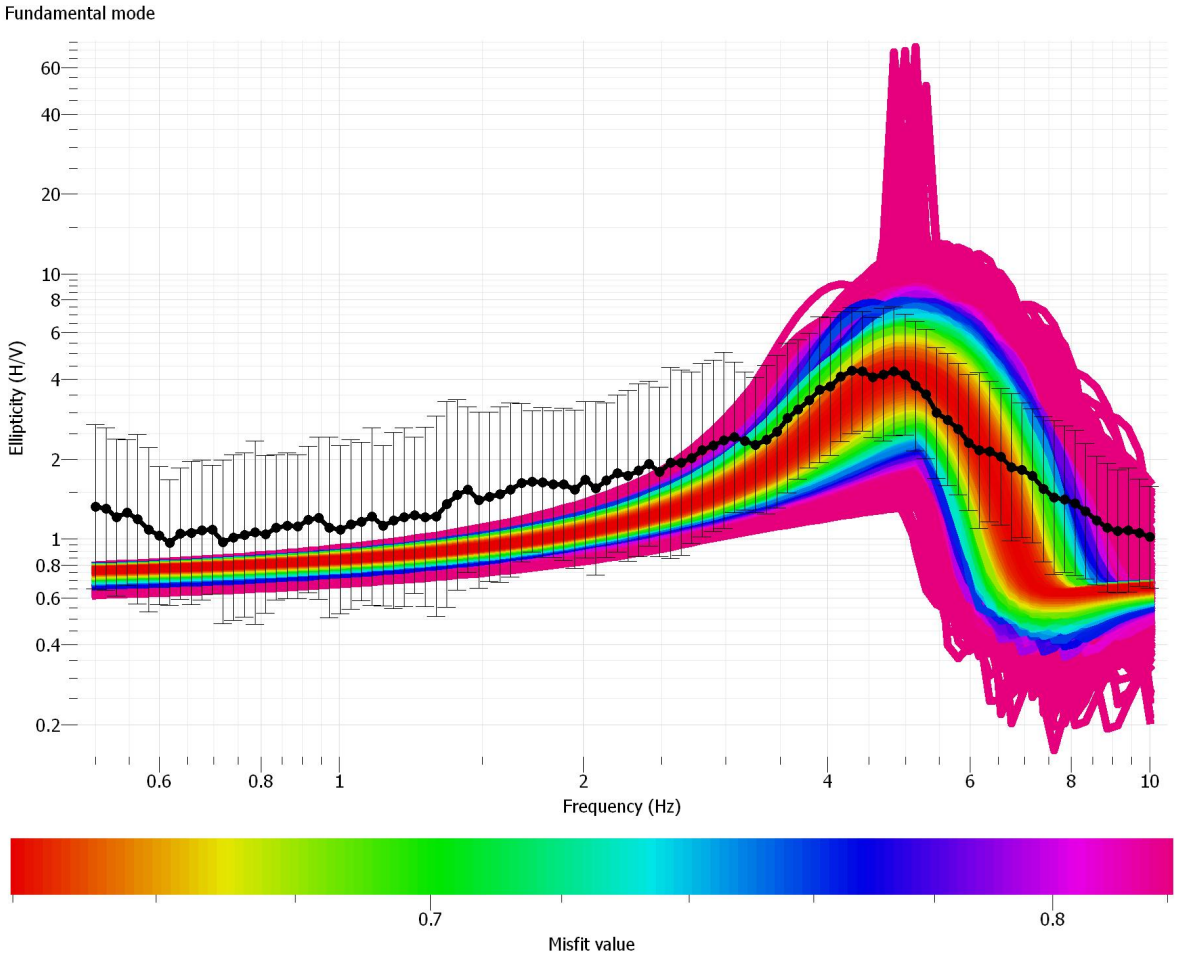

Figure A51. Class E: Goodwin Park Rayleigh Wave Ellipticity. The black dotted curve represents the observed ellipticty curve after the TFA with associated error bars. The observed ellipticity curve has a peak at 5 Hz. Each colored curve behind the data represents a different model generated by the inversion where red curves have the lowest misfit and the pink have the highest misfit.

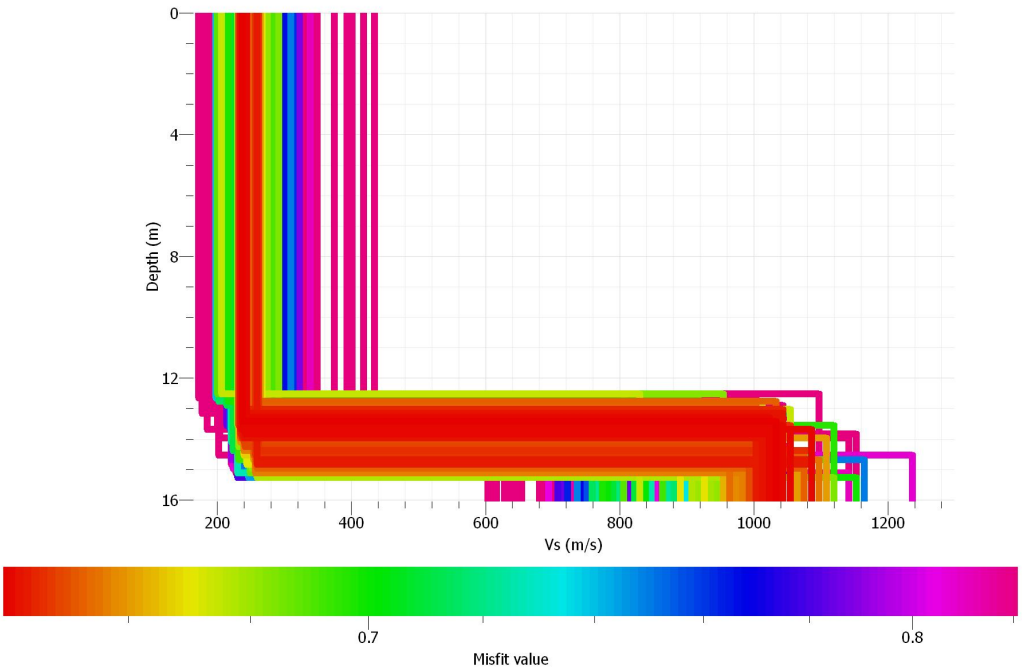

Figure A52. Class E: Goodwin Park Velocity Profile from Rayleigh Wave Ellipticity Inversion. Each 2-layer Vs model is represented by each colored line where the color refers to the misfit value. The red models have the lowest misfit and the pink models have the highest misfit. Based on the well information and the lowest misfit models from ~14-15 m, the average sediment Vs is ~292 m/s and the Vs30 is 377 m/s, Class C.

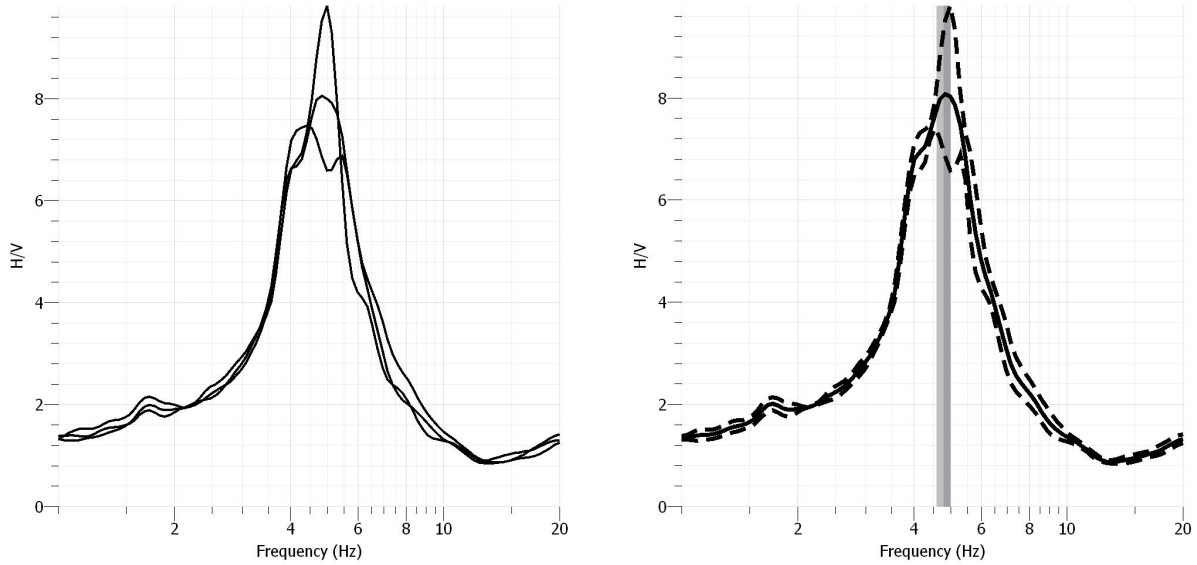

Figure A53. Class E: Average HVSR taken along MASW Profile at Goodwin Park. Three HVSR measurements taken along an MASW profile at Geophone location 1, 12, and 24. Each individual measurement is displayed in (a) and the average resonance frequency and standard deviation are displayed in (b). The average HVSR curve from (a) is displayed as the solid black line with respect to frequency and H/V amplitude. The two dotted lines represent the upper and lower bounds of the standard deviation. The vertical gray line shows the standard deviation of the observed resonance frequencies which range from 4.4-4.9 Hz from Geophone 1-24.

Layer Depth (m)	Vs (m/s)
1.1	92
2.4	167
4.	282
6.1	179
8.7	309
12	433
16.	235
21.1	339
27.40	577
Half Space	683
Vs sediments	247.5
Vs30	284.9
Surficial Class	E
Vs Site Class	D

Table A5. Class E: Active MASW Results for Goodwin Park. A 10-layer model was generated from the dispersion curves in A48. A summary of the depth and shear-wave velocity information is listed here. This site was initially assigned hazard class E by the surficial materials data and then assigned hazard class D by the geophysical field data and Vs30. The gray colored boxes indicate the assumed bedrock interface based on the inversion.

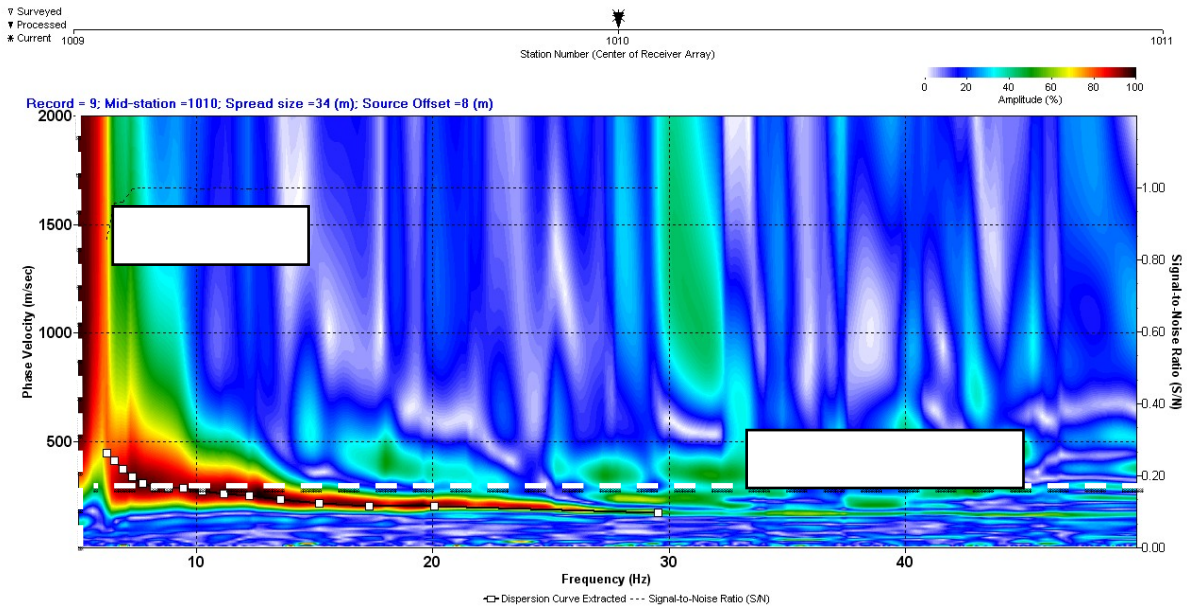

Figure A54. Class E: Goodwin Park Dispersion Curve. The picked dispersion curve is represented by the white boxes connected by a black line with respect to frequency and phase velocity. The vertical white, dashed line indicates the average resonance frequency observed at the field site, which is relative to the dispersion curve's observed higher frequencies; these high frequencies are indicative of the bedrock interface. The white horizontal dashed line indicates the average shear-wave velocity of the sediments based on the resonance frequency. This line coincides with the dispersion curve's observed higher frequencies, which are relative to the underlying sediments.

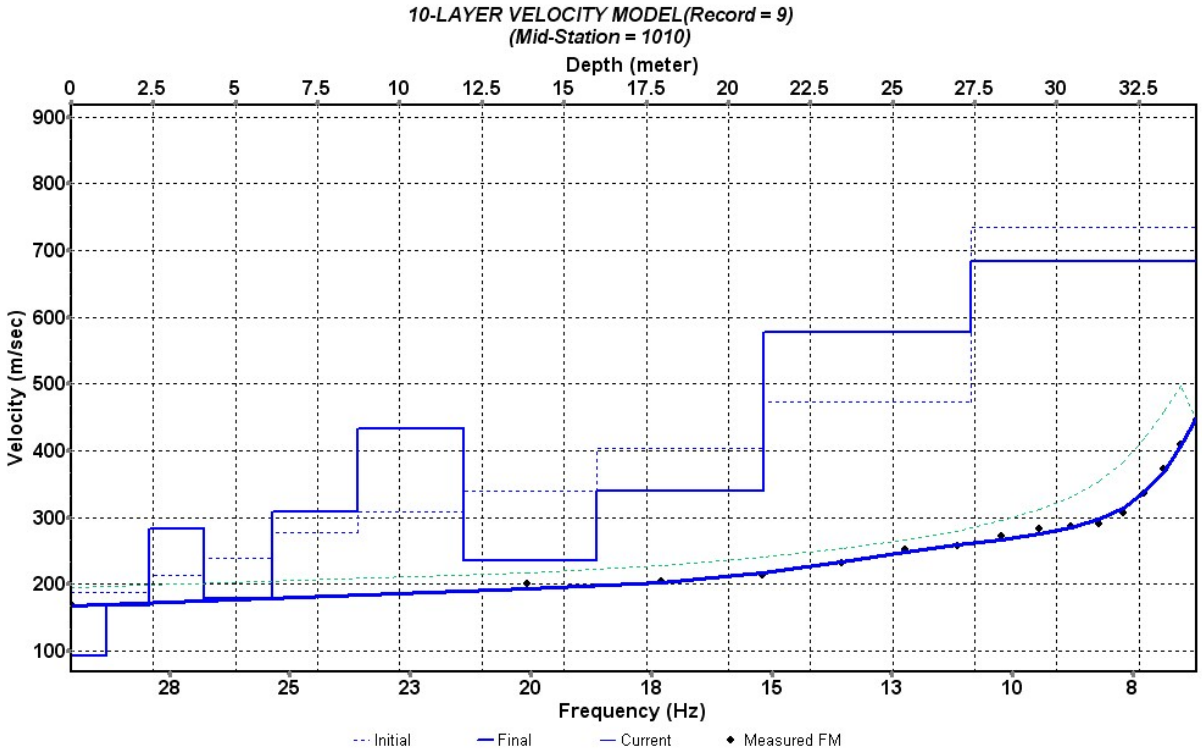

Figure A55. Class E: Goodwin Park Velocity Profile from Inversion. A 10-layer model was generated using the dispersion curve in Figure A48. The black dotted curve is the extracted dispersion curve and the blue solid curve is the model's theoretical curve. Based on this profile, the bedrock surface was observed at 28.2 m, the average sediment velocity was 297.2 m/s and the Vs30 was 315.9 m/s.

Keney Park, Hartford, CT

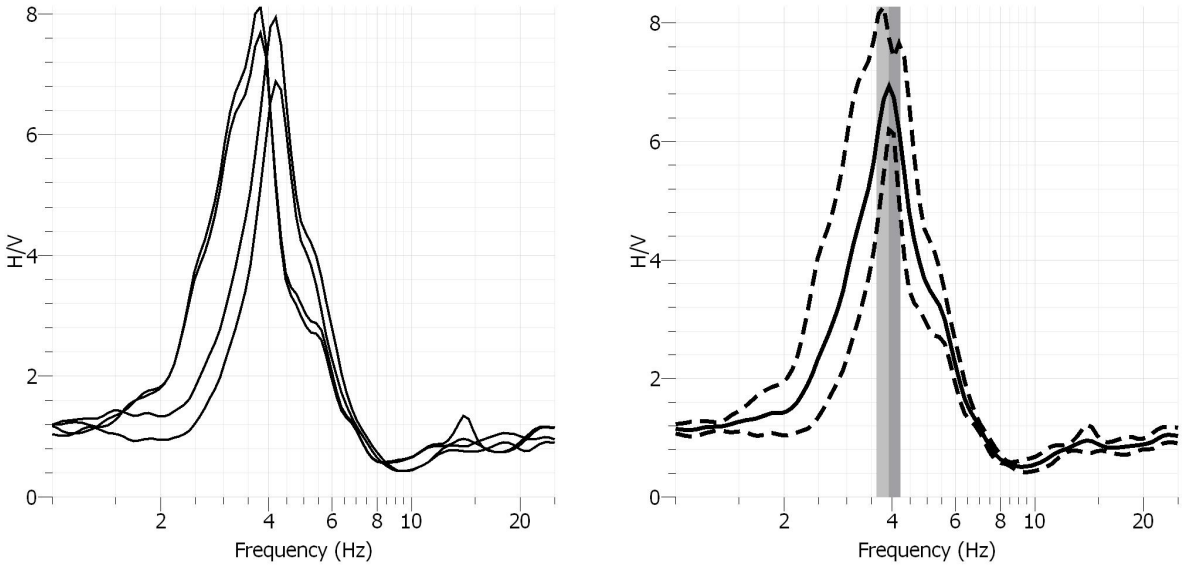

Figure A56. Class E: HVSR Huddle Test from Keney Park. Four HVSR measurements were taken around the borehole and the resulting HVSR curves and resonance frequencies are displayed in (a). The average resonance frequency at this site was 3.9 Hz as indicated by the vertical gray rectangle in (b) with standard deviation. Based on well information, the depth to bedrock was 15.2 m; therefore the average velocity of the sediments was 292 m/s.

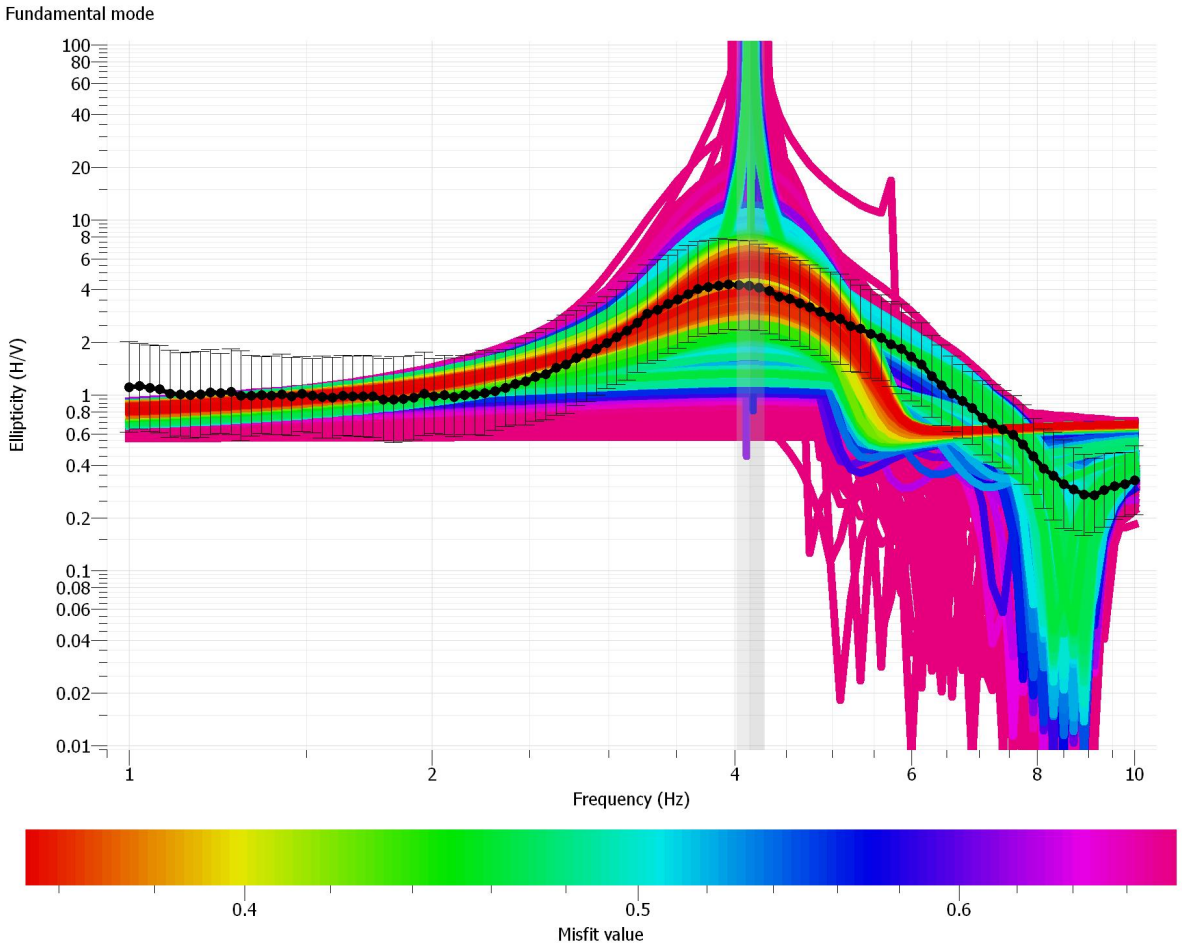

Figure A57. Rayleigh wave ellipticity of Keney Park. The black dotted curve represents the observed ellipticty curve after the TFA with associated error bars. The observed ellipticity curve has a peak at 4.2 Hz as indicated by the vertical purple rectangle. Each colored curve behind the data represents a different model generated by the inversion where red curves have the lowest misfit and the pink have the highest misfit. The vertical purple rectangle indicates the peak frequency value and standard deviation.

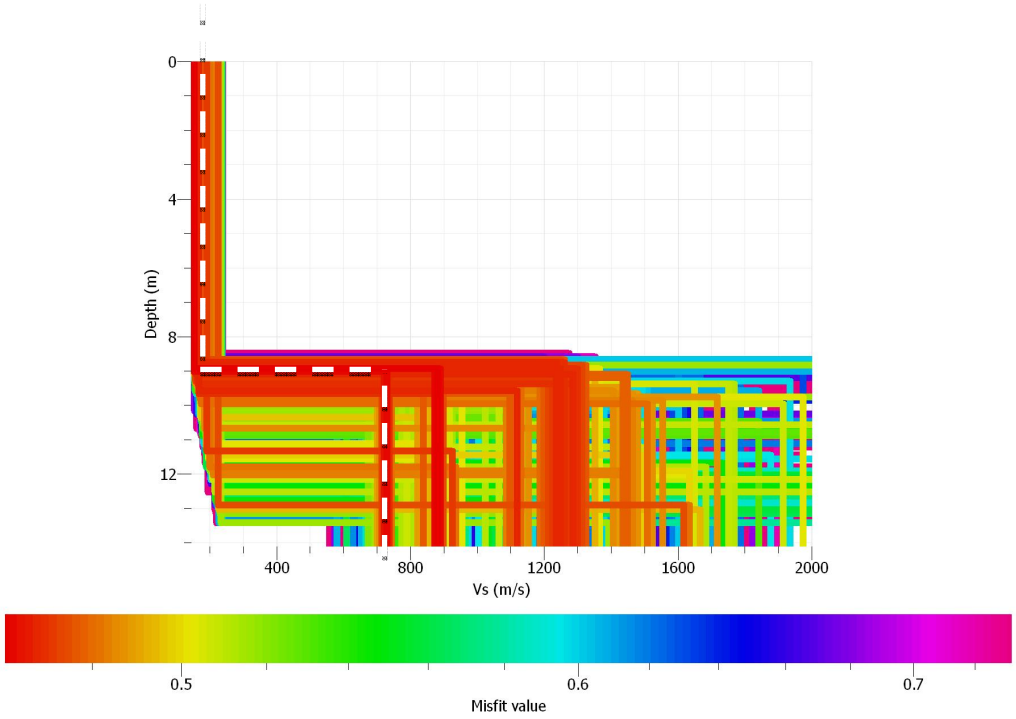

Figure A58. Velocity Profile from Rayleigh Wave Ellipticity of Keney Park. Each 2-layer Vs model is represented by each colored line where the color refers to the misfit value. The red models have the lowest misfit and the pink models have the highest misfit. Based on lowest misfit models at ~9 m, the average sediment Vs is ~237 m/s; these models are indicated by the white dotted line. The Vs30 is 435 m/s.

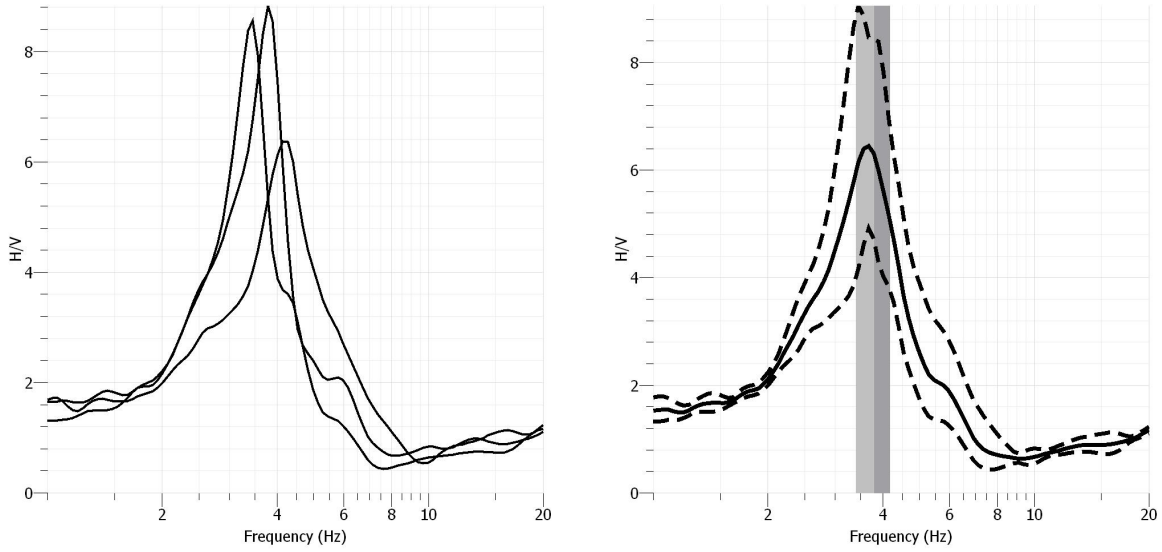

Figure A59. Class E: Average HVSR taken along MASW Profile at Keney Park. Three HVSR measurements taken along an MASW profile at Geophone location 1, 12, and 24. Each individual measurement is displayed in (a) and the average resonance frequency and standard deviation are displayed in (b). The average HVSR curve from (a) is displayed as the solid black line with respect to frequency and H/V amplitude. The two dotted lines represent the upper and lower bounds of the standard deviation. The vertical gray line shows the standard deviation of the observed resonance frequencies which range from 3.4-4.2 Hz from Geophone 1-24.

Layer Depth (m)	Vs (m/s)
0.58	154.50
1.31	171.72
2.23	172.72
3.37	148.68
4.79	109.16
6.57	152.85
8.80	220.86
11.59	270.64
15.07	316.39
Half Space	556.00
Vs sediments	195.6
Vs30	288.7
Surficial Class	E
Vs30 Site Class	D

Table A6. Class E: Active MASW Results from Keney Park. A 10-layer model was generated from the dispersion curves in A60. A summary of the depth and shear-wave velocity information is listed here. This site was initially assigned hazard class E by the surficial materials data and then assigned hazard class D by the geophysical field data and Vs30. The gray colored boxes indicate the assumed bedrock interface based on the inversion.

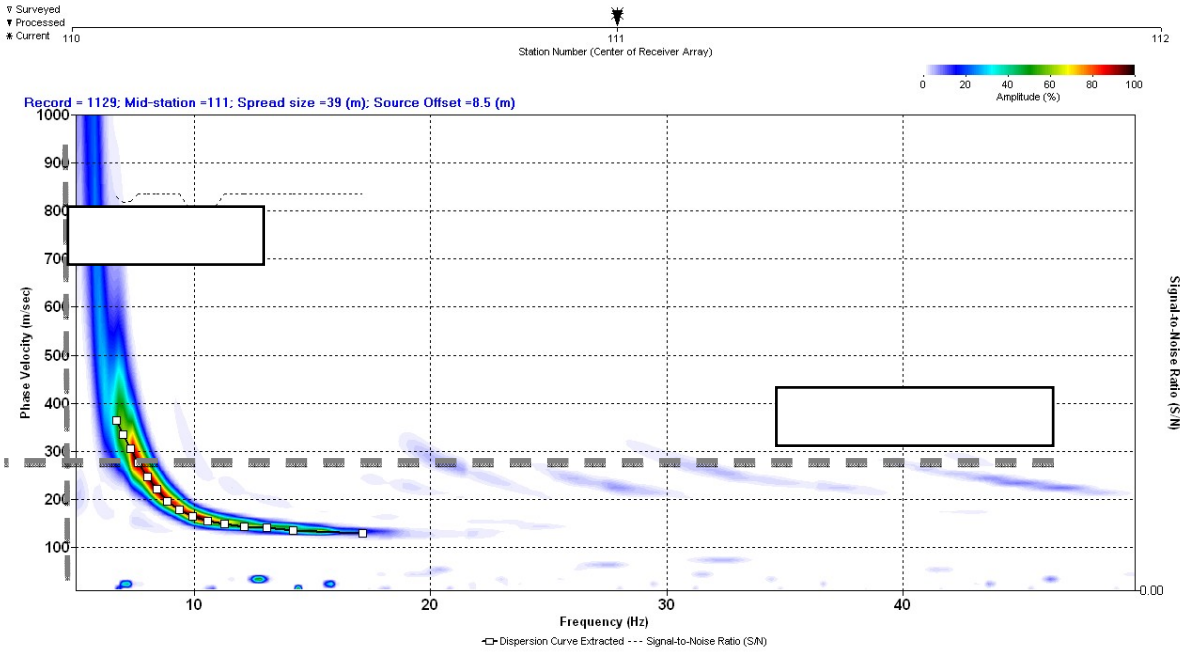

Figure A60. Class E: Keney Park Dispersion Curve. The picked dispersion curve is represented by the white boxes connected by a black line with respect to frequency and phase velocity. The vertical grey, dashed line indicates the average resonance frequency observed at the field site, which is relative to the dispersion curve's observed higher frequencies; these high frequencies are indicative of the bedrock interface. The grey horizontal dashed line indicates the average shear-wave velocity of the sediments based on the resonance frequency. This line coincides with the dispersion curve's observed higher frequencies, which are relative to the underlying sediments.

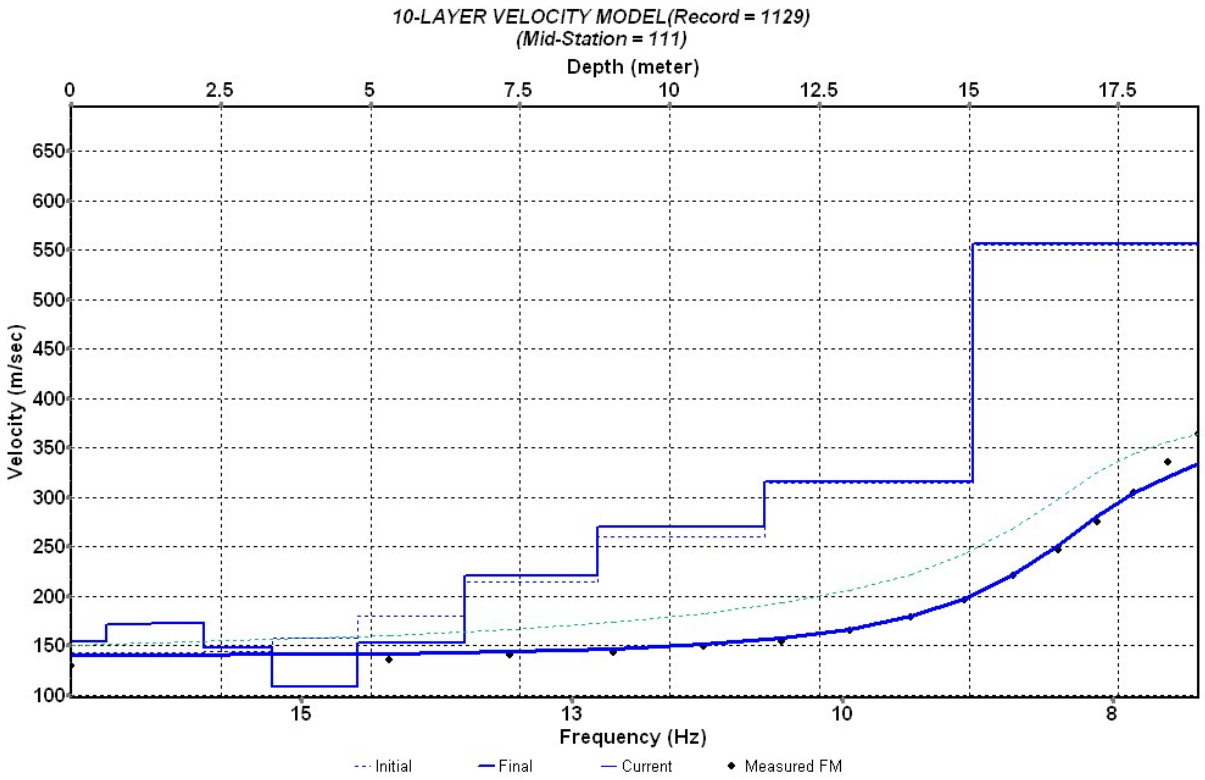

Figure A61. Class E: Keney Park Velocity profile from Inversion. A 10-layer model was generated using the dispersion curve in Figure A60. The black dotted curve is the extracted dispersion curve and the blue solid curve is the model's theoretical curve. Based on this profile, the bedrock surface was observed at ~15 m, the average sediment velocity was 195.6 m/s and the Vs30 was 288.7 m/s.

Pope Park, Hartford, CT

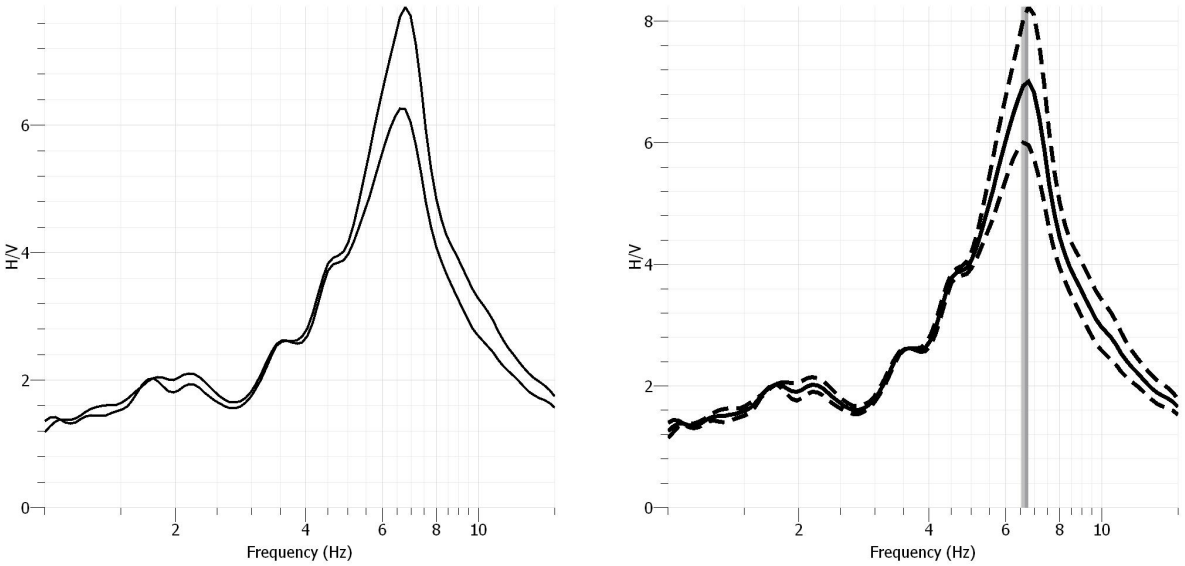

Figure A62. Class E: HVSR Huddle Test from Pope Park. Two HVSR measurements were taken around the borehole and the resulting HVSR curves and resonance frequencies are displayed in (a). The average resonance frequency at this site was 6.6 Hz as indicated by the vertical gray rectangle in (b) with standard deviation. Based on well information, the depth to bedrock was 19.8 m; therefore the average velocity of the sediments was 432 m/s.

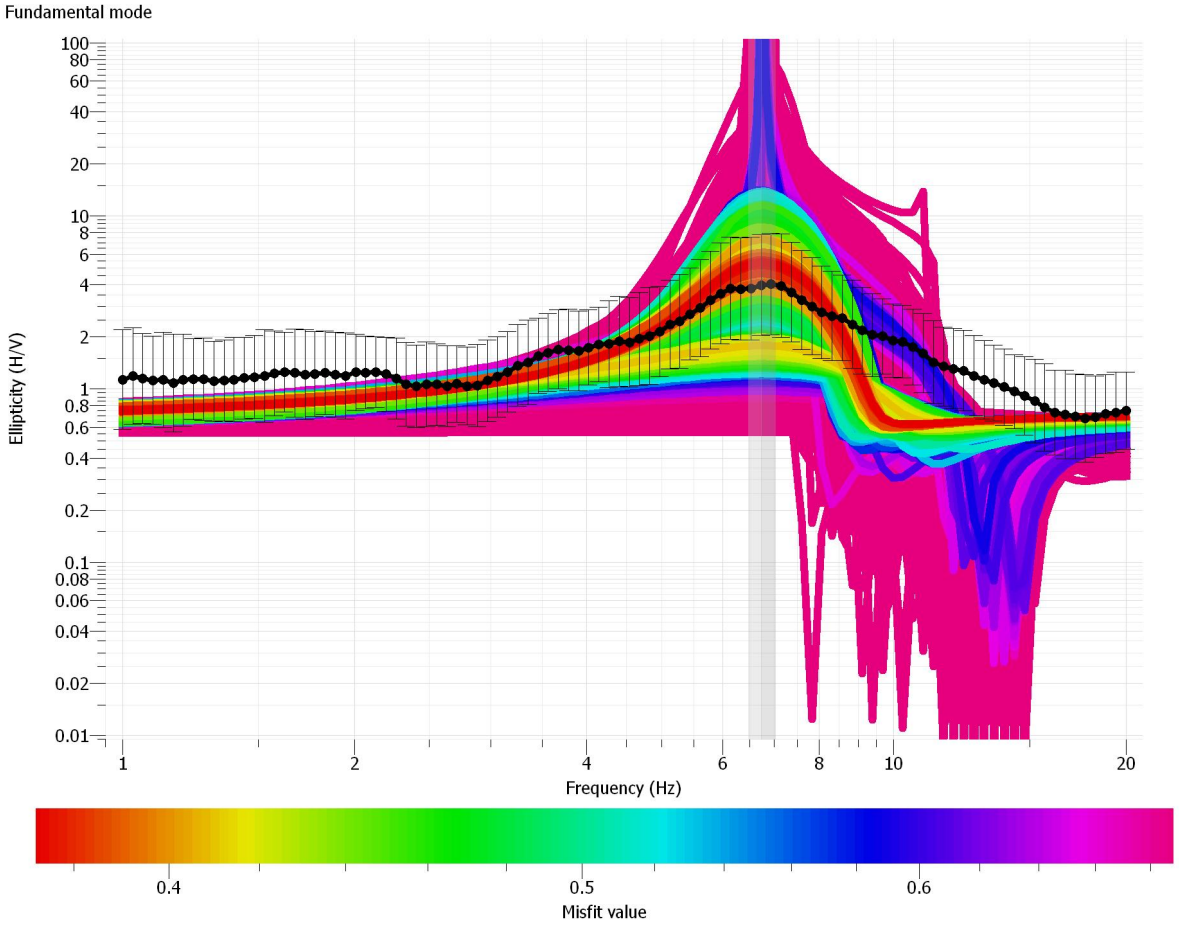

Figure A63. Class E: Pope Park Rayleigh Wave Ellipticity. The black dotted curve represents the observed ellipticty curve after the TFA with associated error bars. The observed ellipticity curve has a peak at 6.6 Hz as indicated by the vertical purple rectangle. Each colored curve behind the data represents a different model generated by the inversion where red curves have the lowest misfit and the pink have the highest misfit. The vertical purple rectangle indicates the peak frequency value and standard deviation.

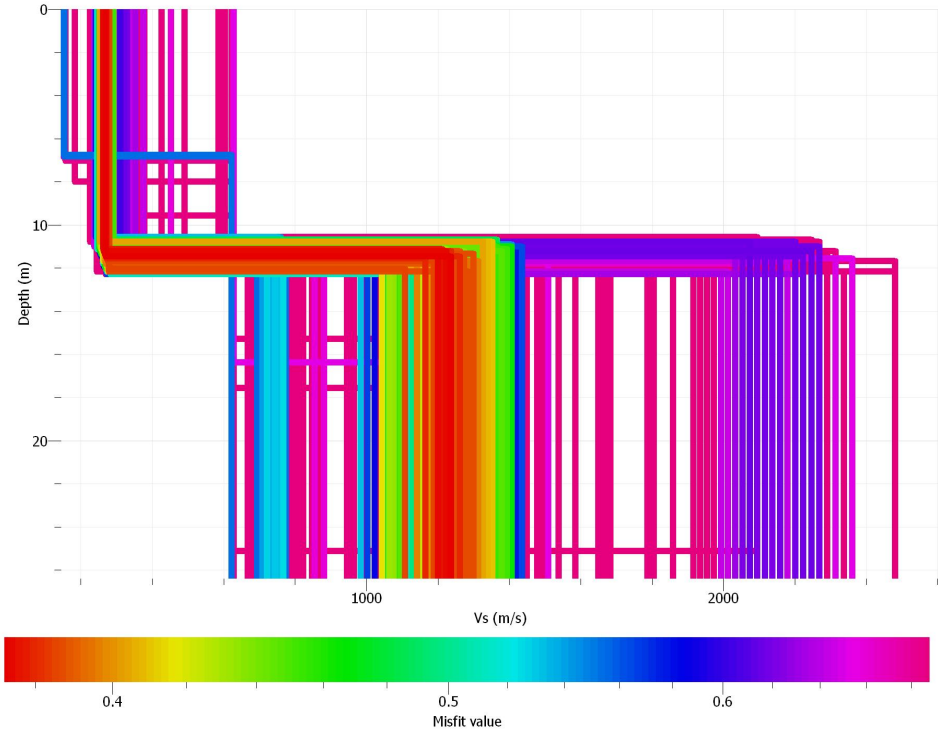

Figure A64. Class E: Pope Park Velocity Profile from Rayleigh Wave Ellipticity Inversion. Each 2-layer Vs model is represented by each colored line where the color refers to the misfit value. The red models have the lowest misfit and the pink models have the highest misfit. Based on lowest misfit models at ~11 m, the average sediment Vs is ~263 m/s. The calculated Vs30 is 520 m/s, Class C.

Layer Depth (m)	Vs (m/s)
0.41	107.26
0.93	104.42
1.57	124.18
2.37	120.60
3.37	135.81
4.63	203.90
6.20	263.95
8.16	304.05
10.61	327.75
Half Space	433.77
Vs sediments	303.9
Vs30	303.9
Surficial Class	E
Vs30 Site Class	D

Table A7. Class E: Active MASW Results for Pope Park. A 10-layer model was generated from the dispersion curves in A65. A summary of the depth and shear-wave velocity information is listed here. This site was initially assigned hazard class E by the surficial materials data and then assigned hazard class D by the geophysical field data and Vs30. The gray colored boxes indicate the assumed bedrock interface based on the inversion.

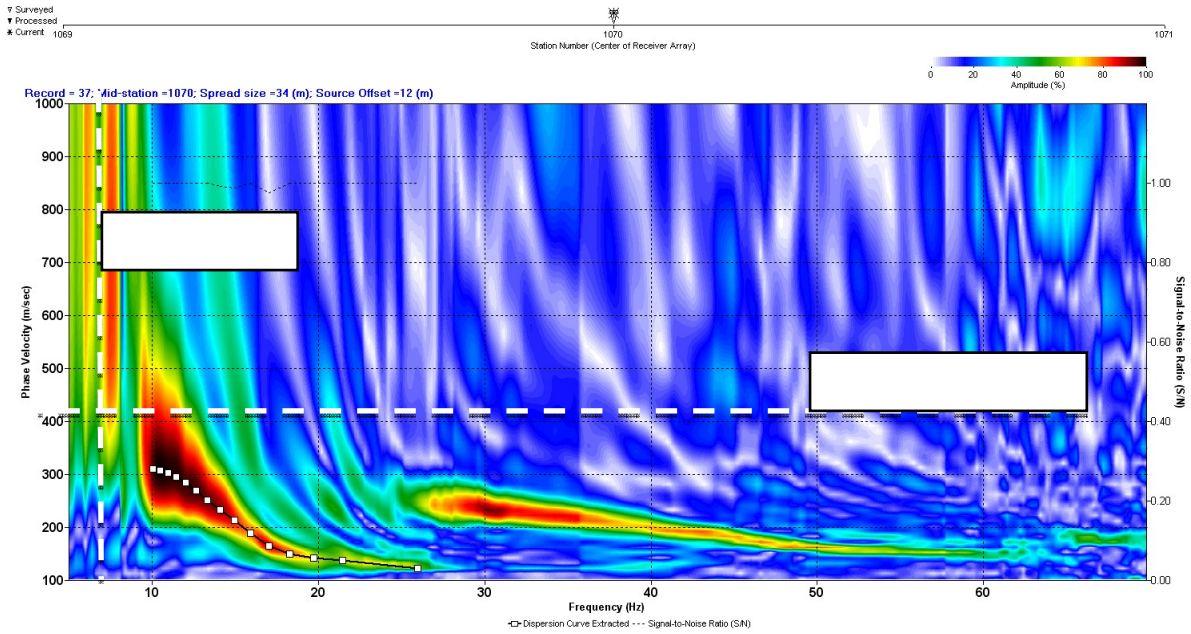

Figure A65. Class E: Pope Park Dispersion Curve. The picked dispersion curve is represented by the white boxes connected by a black line with respect to frequency and phase velocity. The vertical white, dashed line indicates the average resonance frequency observed at the field site, which is relative to the dispersion curve's observed higher frequencies; these high frequencies are indicative of the bedrock interface. The white horizontal dashed line indicates the average shear-wave velocity of the sediments based on the resonance frequency. This line coincides with the dispersion curve's observed higher frequencies, which are relative to the underlying sediments.

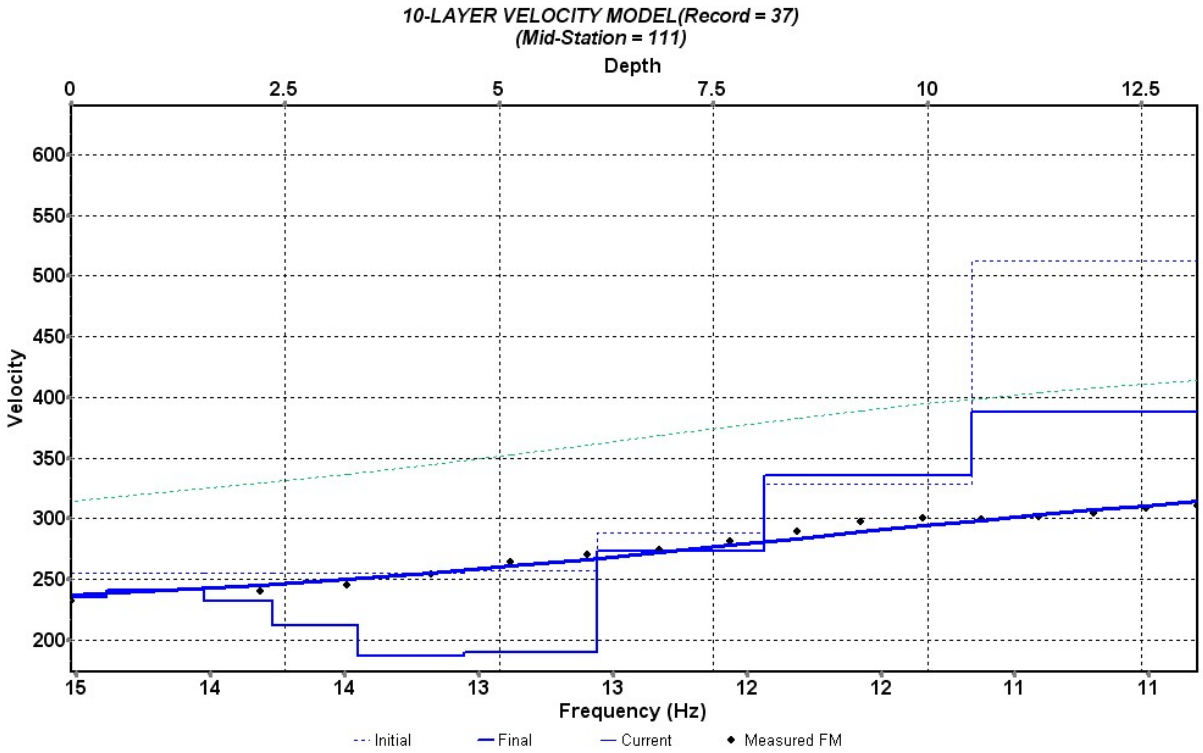

Figure A66. Class E: Pope Park Velocity profile from Inversion. A 10-layer model was generated using the dispersion curve in Figure A65. The black dotted curve is the extracted dispersion curve and the blue solid curve is the model's theoretical curve. Based on this profile, the half space was observed at ~10.6 m, the average sediment velocity was 303.9 m/s and the Vs30 was 303.9 m/s, Class D.

269 Main Street, Windsor Locks, CT

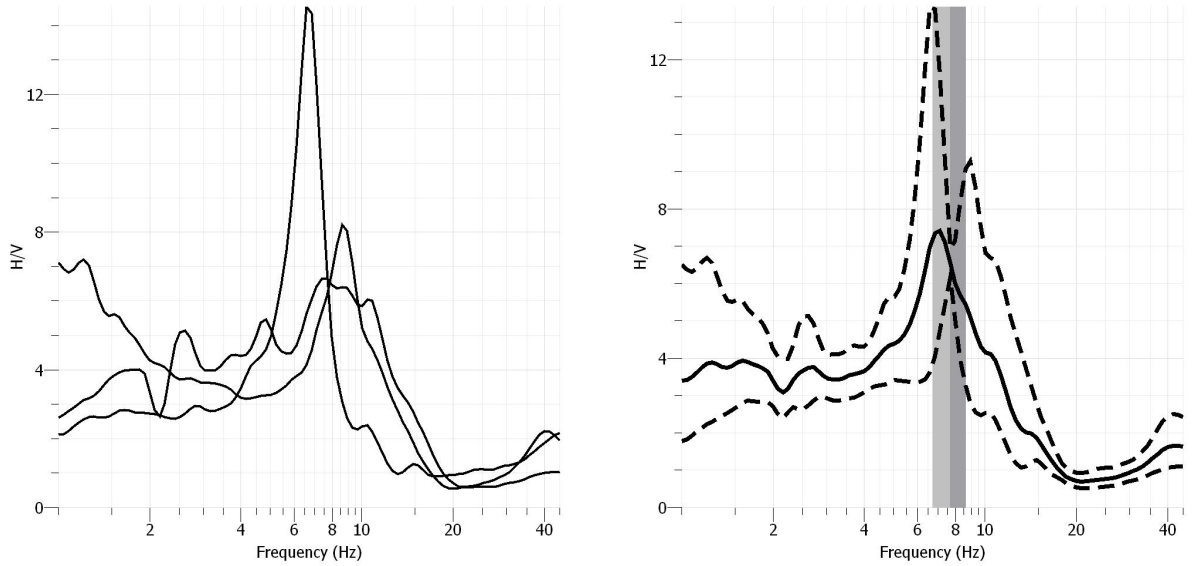

Figure A67. Class E: HVSR Huddle Test from 269 Main Street. Three HVSR measurements were taken near the borehole at a gas station and the resulting HVSR curves and resonance frequencies are displayed in (a). The average resonance frequency at this site was 6.4 Hz as indicated by the vertical gray rectangle in (b) with standard deviation. Based on well information, the depth to bedrock was 6.1 m; therefore the average velocity of the sediments was 468 m/s.

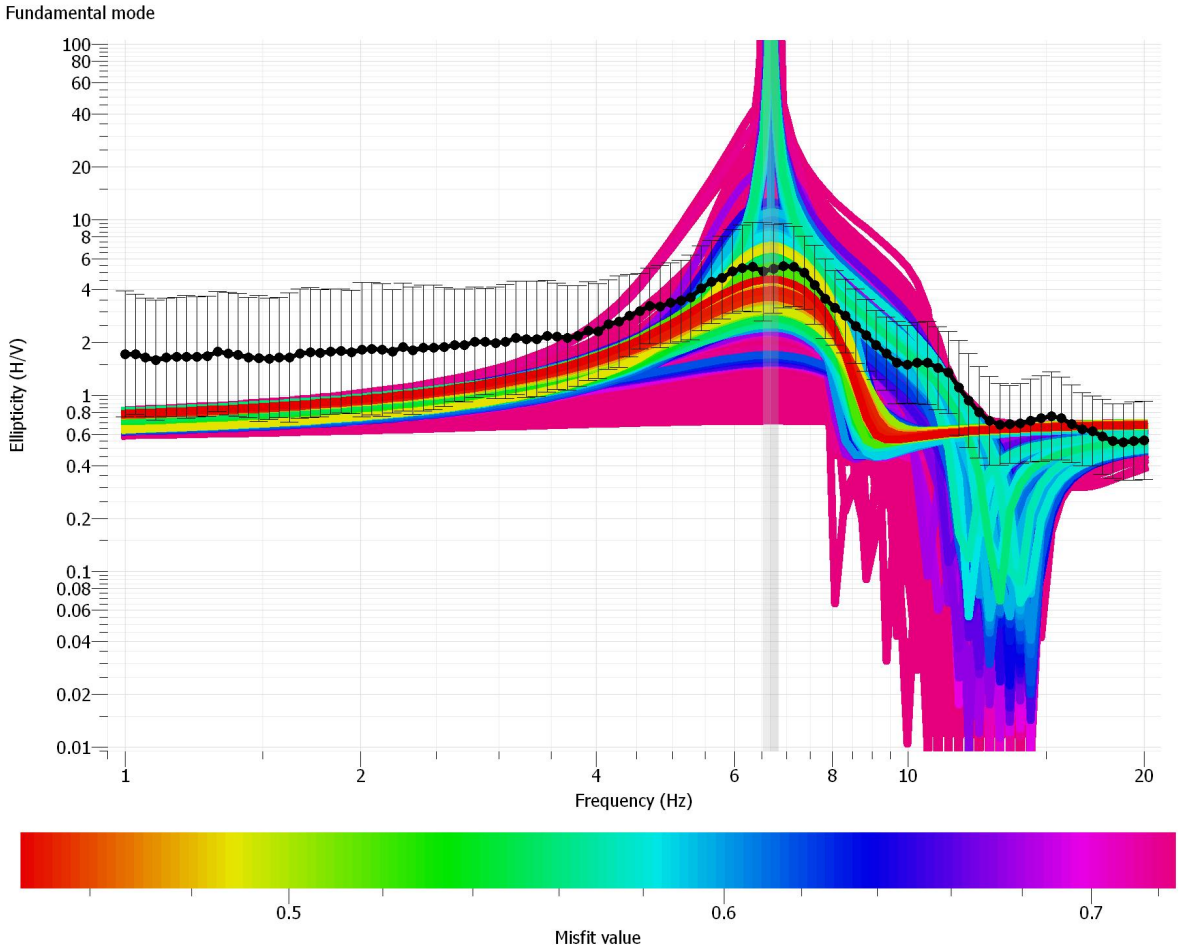

Figure A68. Class E: 269 Main St. Rayleigh Wave Ellipticity. The black dotted curve represents the observed ellipticty curve after the TFA with associated error bars. The observed ellipticity curve has a peak at 6.6 Hz as indicated by the vertical purple rectangle. Each colored curve behind the data represents a different model generated by the inversion where red curves have the lowest misfit and the pink have the highest misfit. The vertical purple rectangle indicates the peak frequency value and standard deviation.

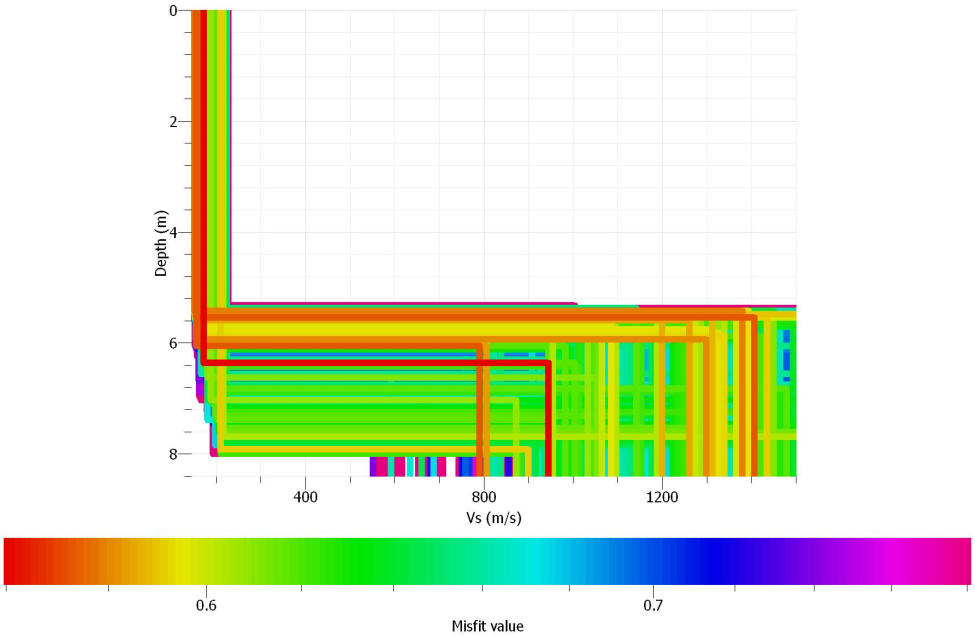

Figure A69. Class E: 269 Main St. Velocity Profile from Rayleigh Wave Ellipticity Inversion. Each 2-layer Vs model is represented by each colored line where the color refers to the misfit value. The red models have the lowest misfit and the pink models have the highest misfit. Based on lowest misfit models at ~6.3 m, the average sediment Vs is ~167 m/s. The calculated Vs30 is 477 m/s, Class C.

Bushnell Park, Hartford, CT

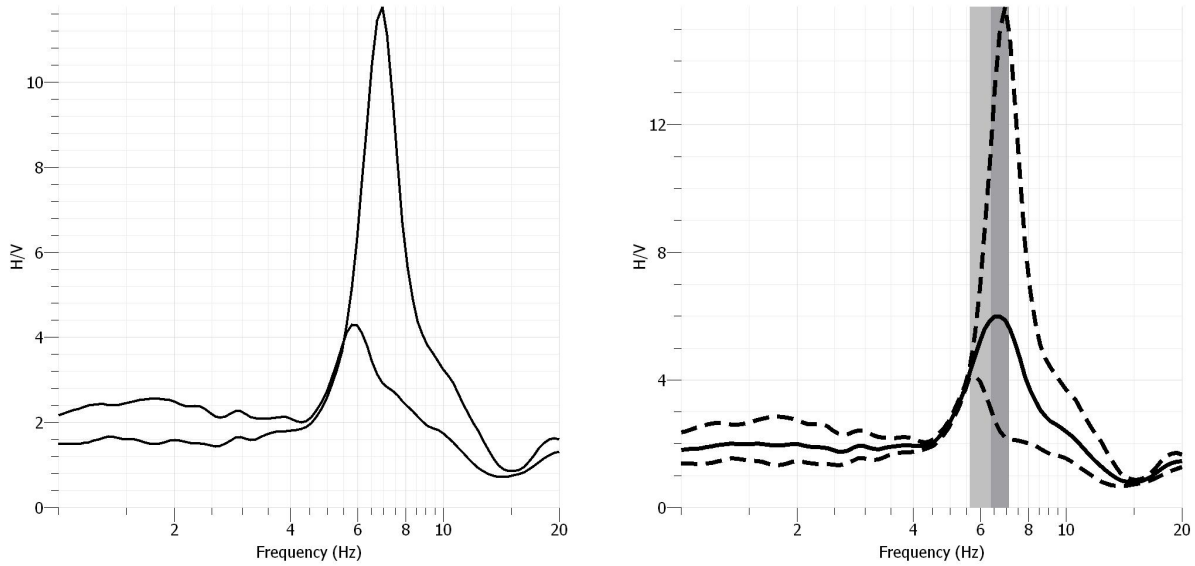

Figure A70. Class E: HVSR measurements from Bushnell Park. Two HVSR measurements were taken near the borehole and the resulting HVSR curves and resonance frequencies are displayed in (a). The average resonance frequency at this site was 6.4 Hz as indicated by the vertical gray rectangle in (b) with standard deviation. Based on well information, the depth to bedrock was 12.5 m; therefore the average velocity of the sediments was 319 m/s.

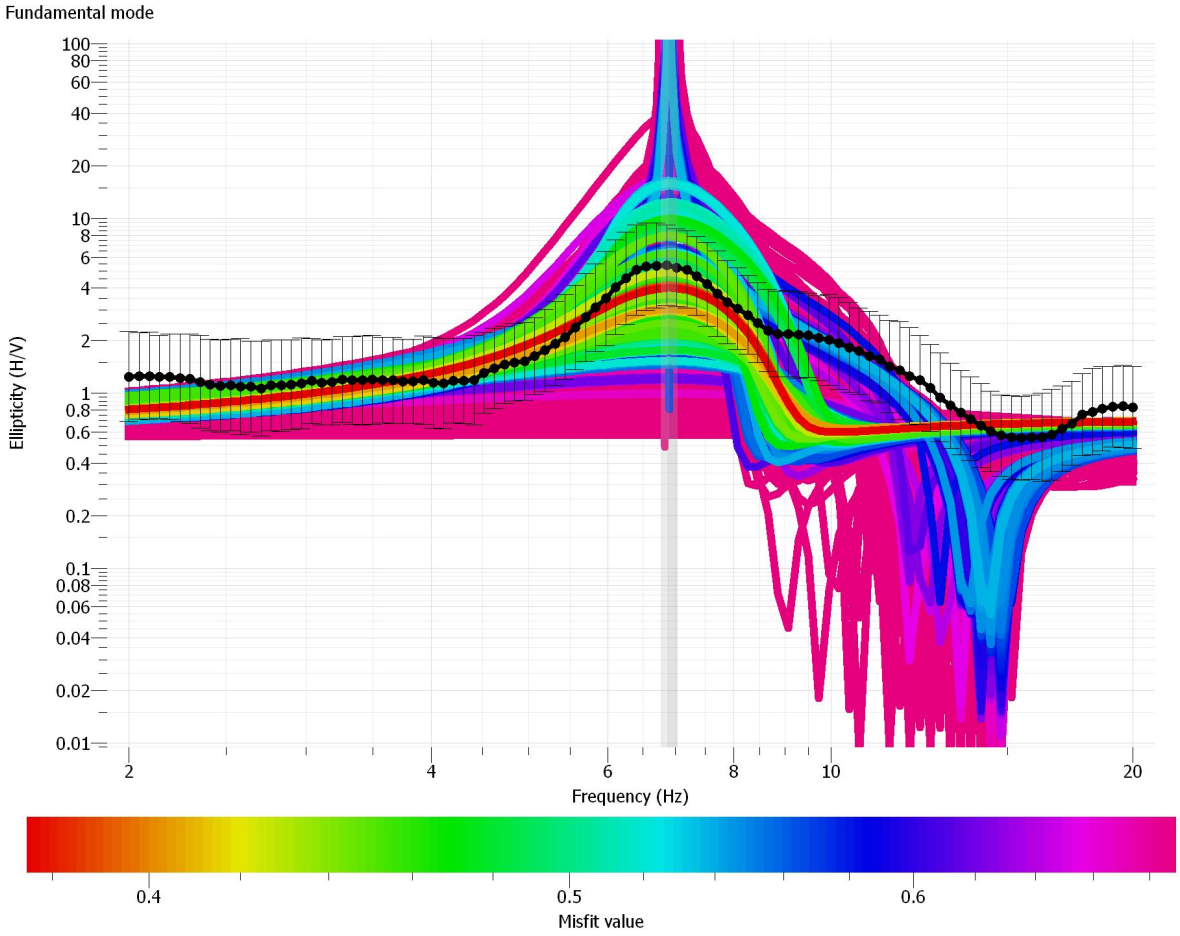

Figure A71. Class E: Pope Park Rayleigh Wave Ellipticity. The black dotted curve represents the observed ellipticty curve after the TFA with associated error bars. The observed ellipticity curve has a peak at 6.9 Hz as indicated by the vertical purple rectangle. Each colored curve behind the data represents a different model generated by the inversion where red curves have the lowest misfit and the pink have the highest misfit. The vertical purple rectangle indicates the peak frequency value and standard deviation.

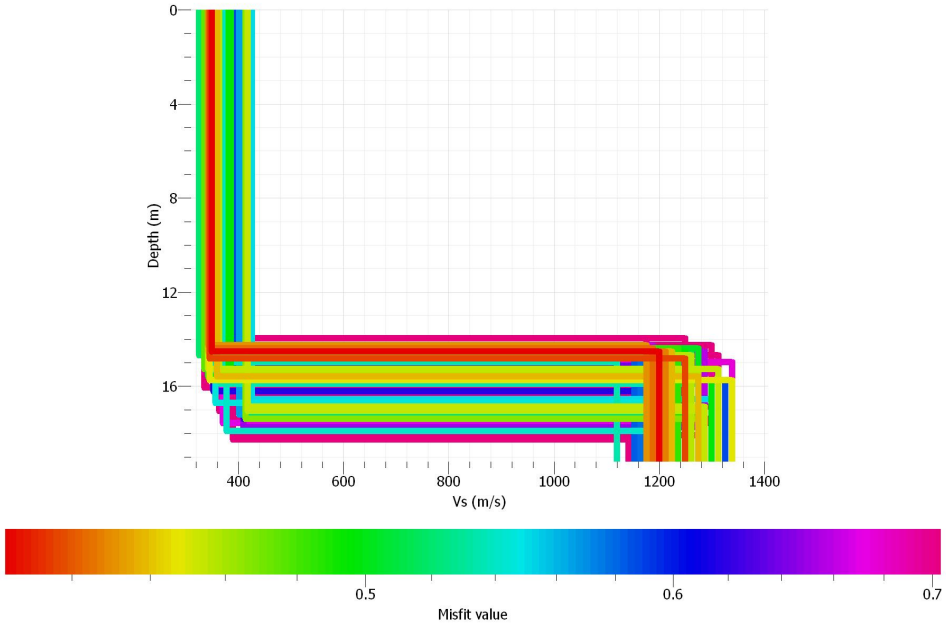

Figure A72. Class E: Bushnell Park Velocity Profile from Rayleigh Wave Ellipticity Inversion. Each 2-layer Vs model is represented by each colored line where the color refers to the misfit value. The red models have the lowest misfit and the pink models have the highest misfit. Based on lowest misfit models at ~14.4 m, the average sediment Vs is ~436 m/s. The calculated Vs30 is 549 m/s, Class C.

Mark Twain House, Hartford, CT

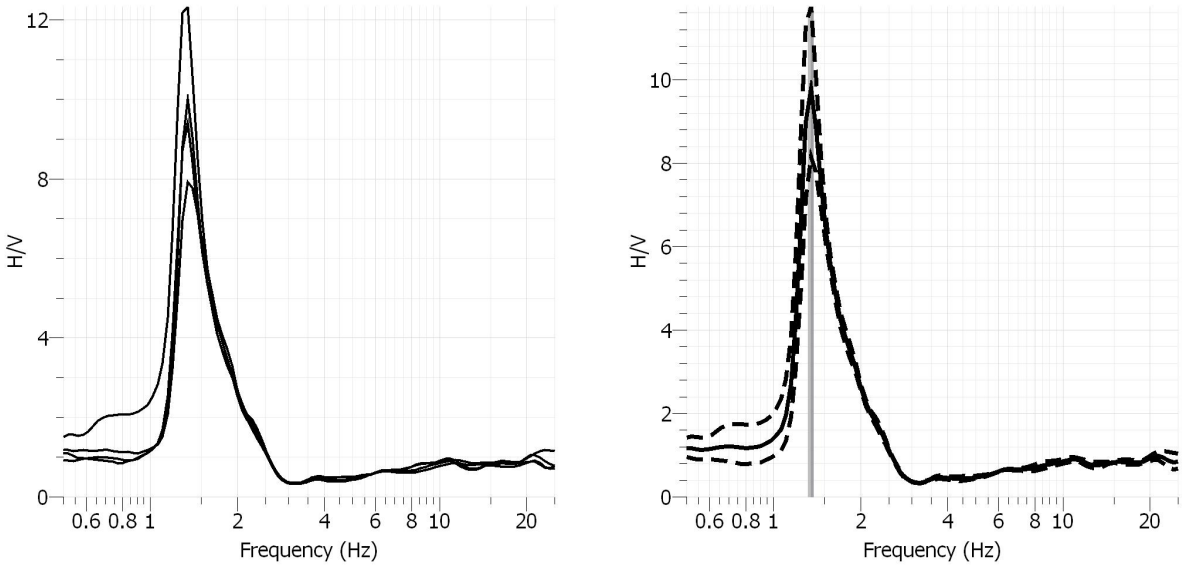

Figure A73. Class E: HVSR Huddle Test from Mark Twain House. Three HVSR measurements were taken around the borehole and the resulting HVSR curves and resonance frequencies are displayed in (a). The average resonance frequency at this site was 1.3 Hz as indicated by the vertical gray rectangle in (b) with standard deviation. Based on well information, the depth to bedrock was 38 m; therefore the average velocity of the sediments was 204 m/s.

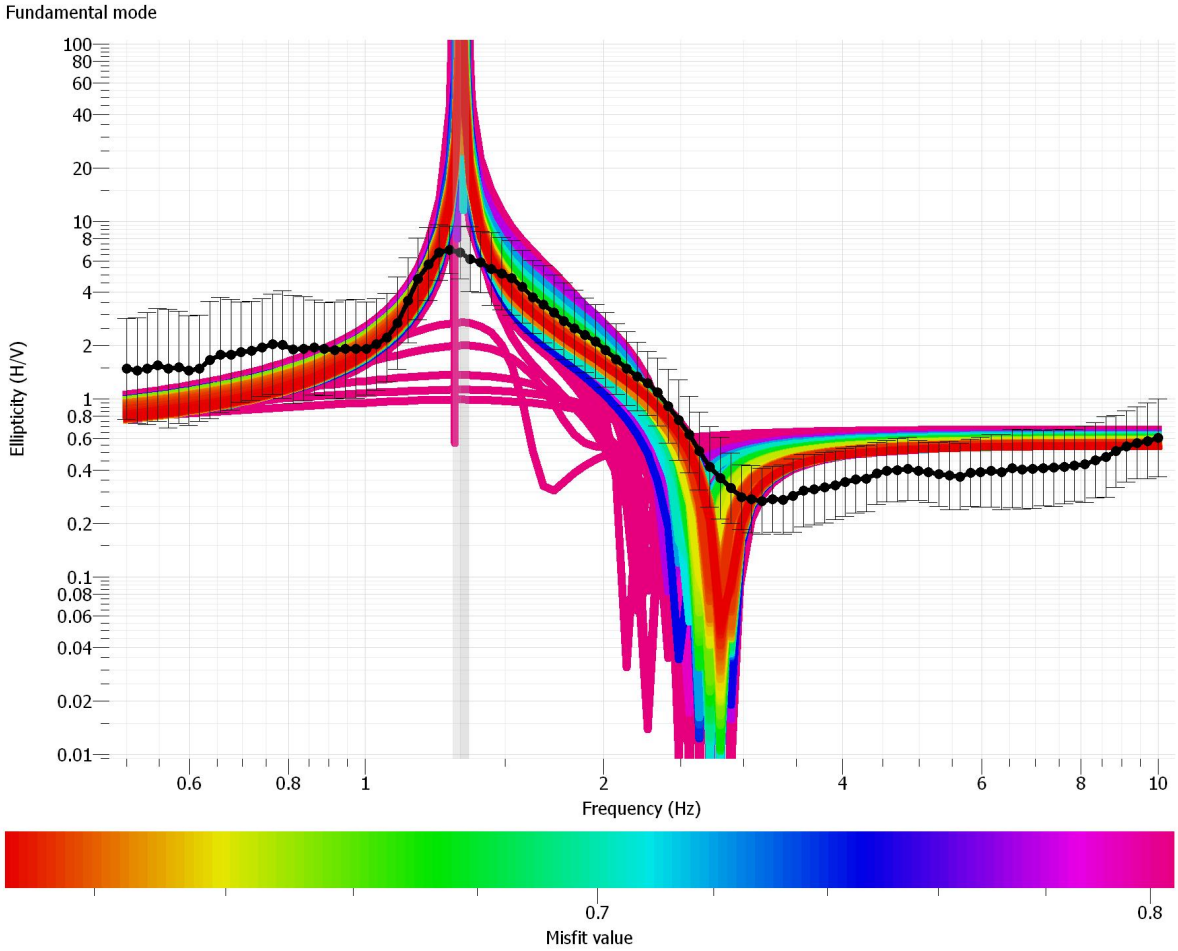

Figure A74. Class E: Mark Twain House Rayleigh Wave Ellipticity. The black dotted curve represents the observed ellipticty curve after the TFA with associated error bars. The observed ellipticity curve has a peak at 1.3 Hz as indicated by the vertical purple rectangle. Each colored curve behind the data represents a different model generated by the inversion where red curves have the lowest misfit and the pink have the highest misfit. The vertical purple rectangle indicates the peak frequency value and standard deviation.

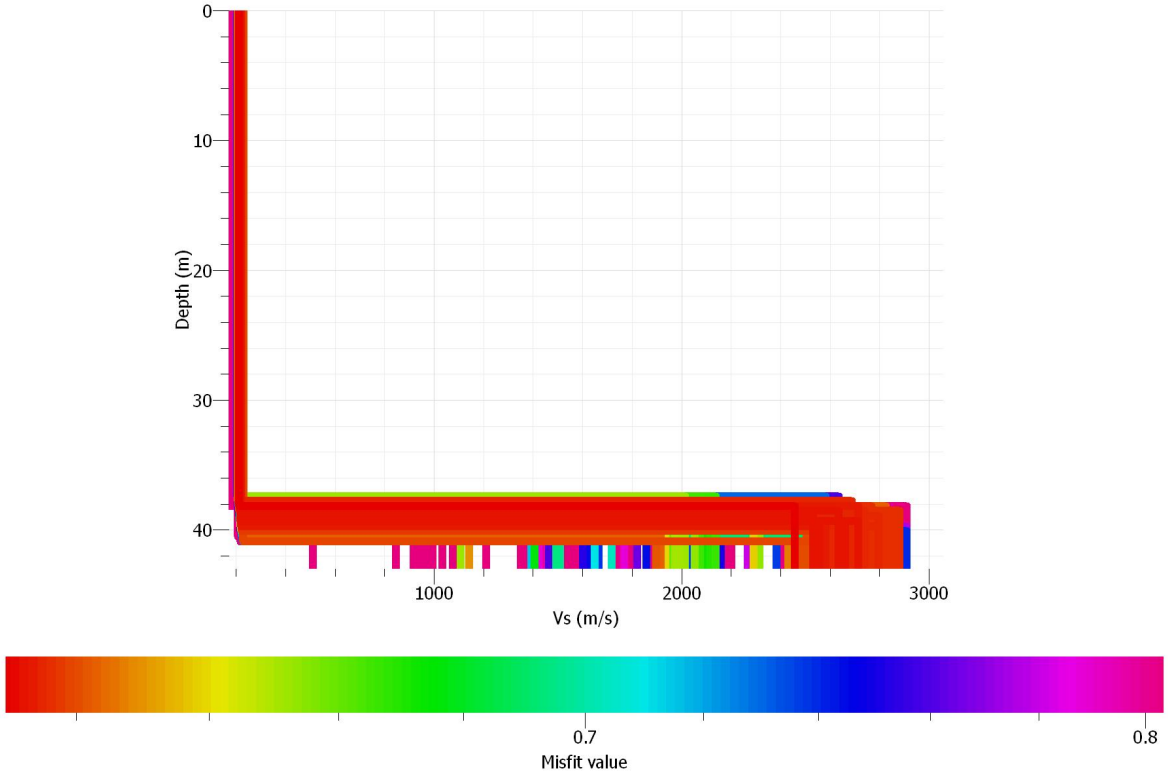

Figure A75. Class E: Mark Twain House Velocity Profile from Rayleigh Wave Ellipticity Inversion. Each 2-layer Vs model is represented by each colored line where the color refers to the misfit value. The red models have the lowest misfit and the pink models have the highest misfit. Based on lowest misfit models at ~38 m, the average sediment Vs is ~210 m/s. The calculated Vs30 is 210 m/s, Class D.

Rentschler Field, East Hartford, CT

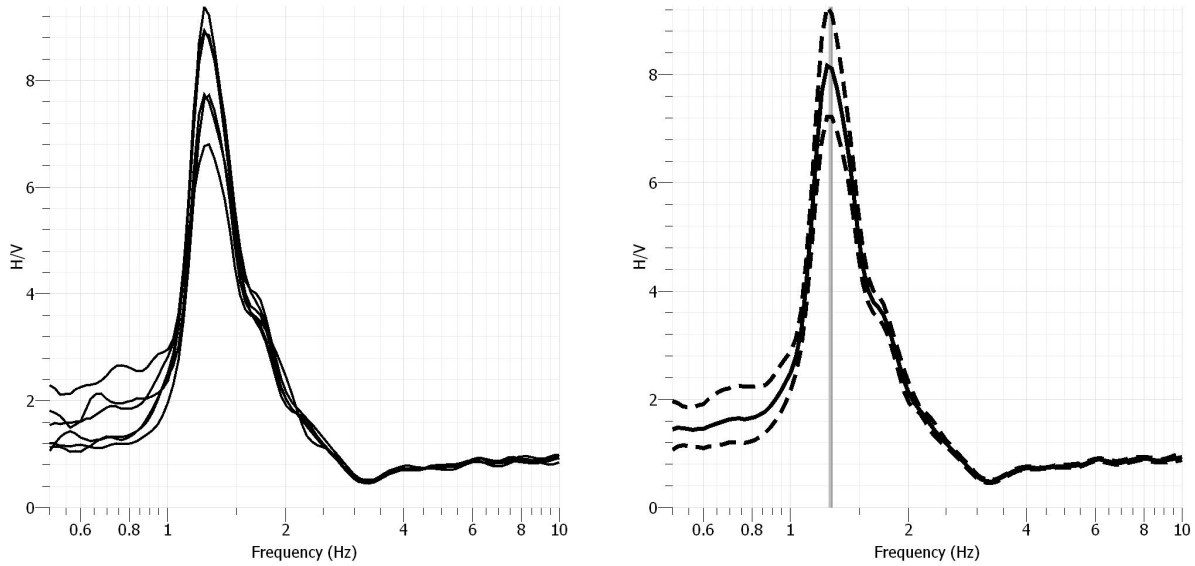

Figure A75. Class E: HVSR measurements from Rentschler Field. Six HVSR measurements were taken outside the Rentschler Field football stadium and the resulting HVSR curves and resonance frequencies are displayed in (a). The average resonance frequency at this site was 1.3 Hz as indicated by the vertical gray rectangle in (b) with standard deviation. The nearest well to this site is over 100 m from this site, which had a depth to bedrock of 35 m, this was not used to calculate shear-wave velocity.

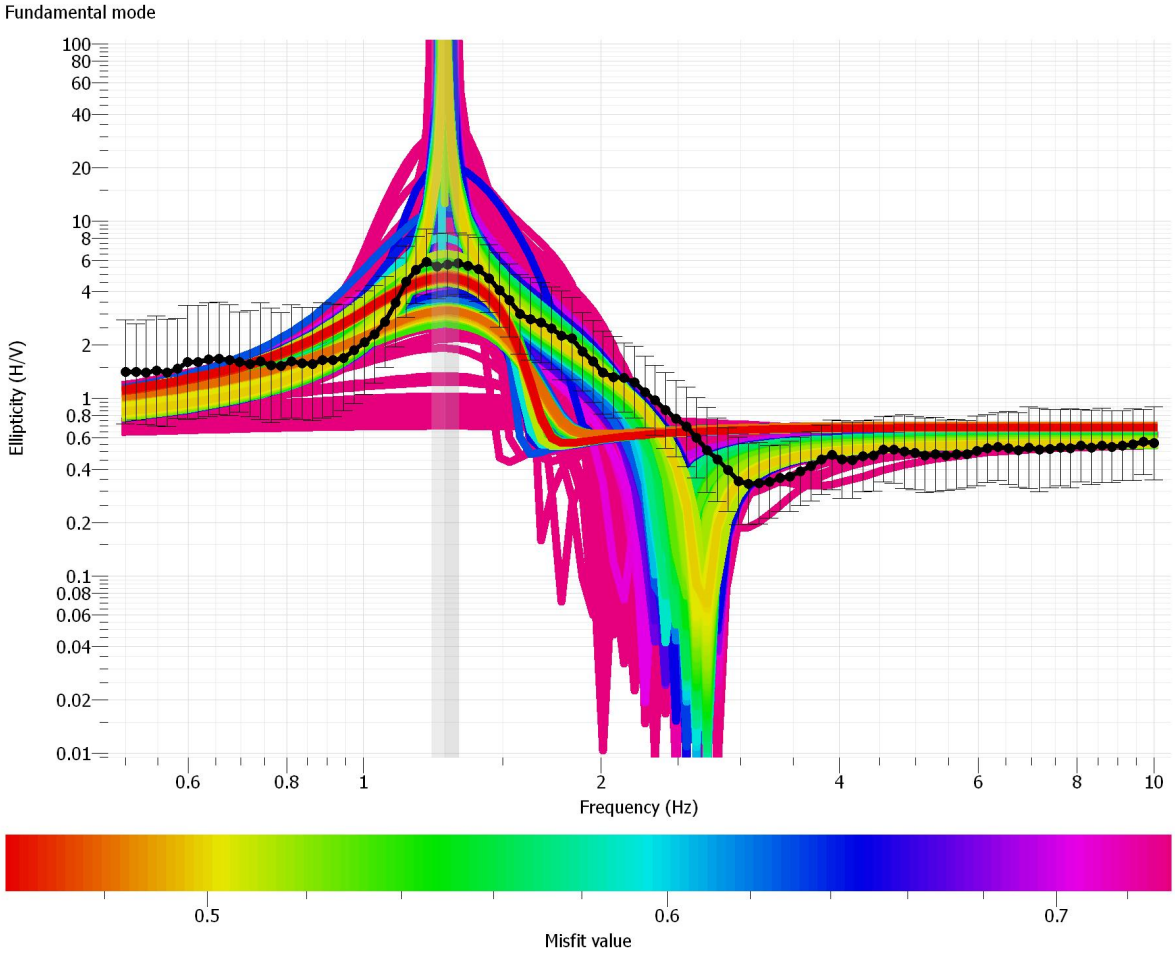

Figure A76. Class E: Rentschler Field Rayleigh Wave Ellipticity. The black dotted curve represents the observed ellipticty curve after the TFA with associated error bars. The observed ellipticity curve has a peak at 1.26 Hz as indicated by the vertical purple rectangle. Each colored curve behind the data represents a different model generated by the inversion where red curves have the lowest misfit and the pink have the highest misfit. The vertical purple rectangle indicates the peak frequency value and standard deviation.

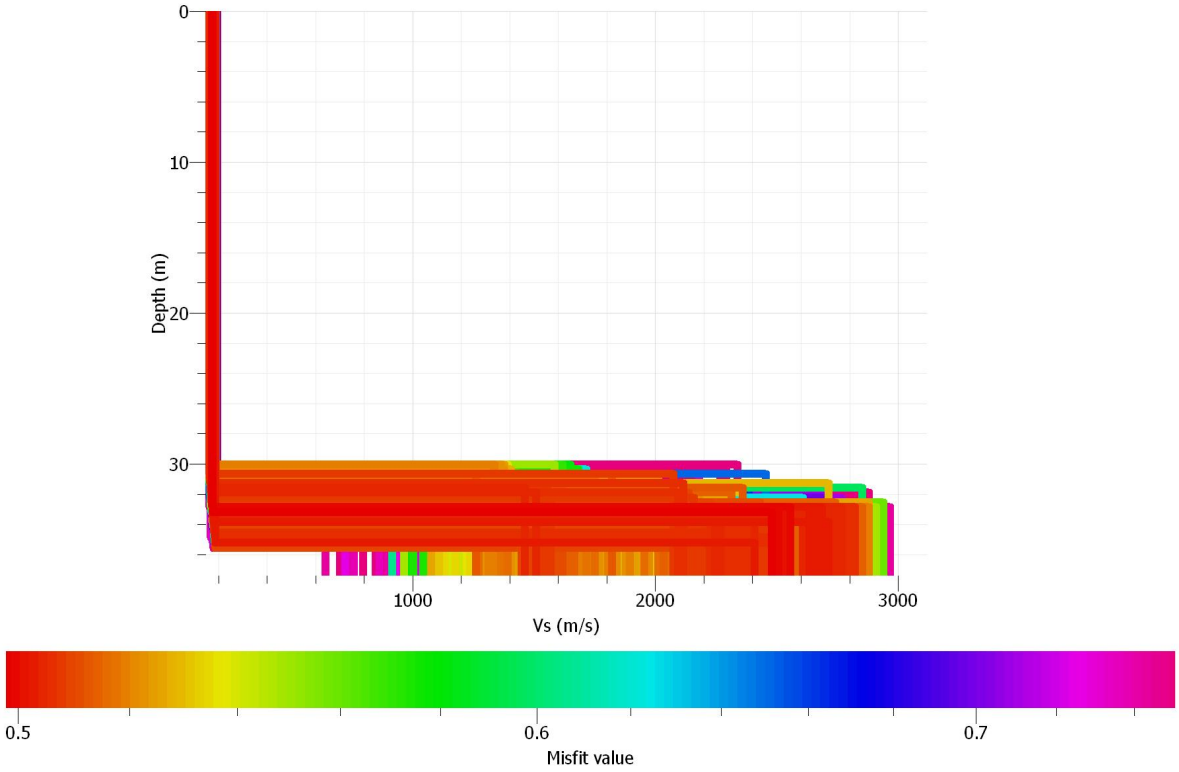

Figure A77. Class E: Rentschler Field Velocity Profile from Rayleigh Wave Ellipticity Inversion. Each 2-layer Vs model is represented by each colored line where the color refers to the misfit value. The red models have the lowest misfit and the pink models have the highest misfit. Based on lowest misfit models from 30.5-36m, the average sediment Vs is ~180 m/s. The calculated Vs30 is 180 m/s, Class E.

Riverside Park, Hartford, CT

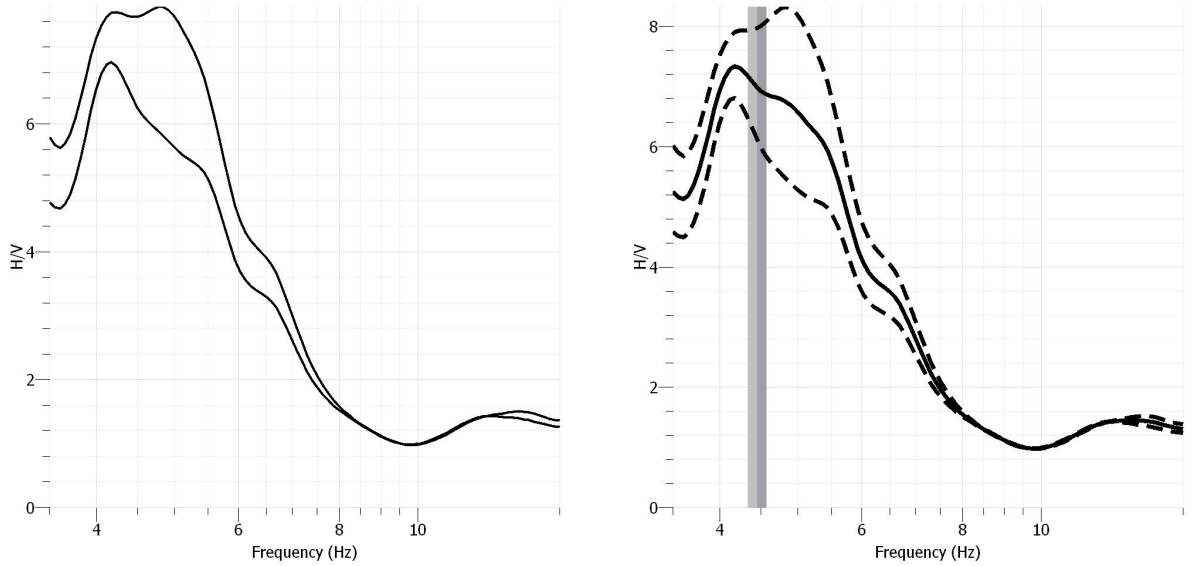

Figure A78. Class E: HVSR Huddle Test from Riverside Park. Four HVSR measurements were taken near the borehole and the resulting HVSR curves and resonance frequencies are displayed in (a). The average resonance frequency at this site was 4.4 Hz as indicated by the vertical gray rectangle in (b) with standard deviation. Based on well information, the depth to bedrock was 17.4 m; therefore the average velocity of the sediments was 305 m/s.

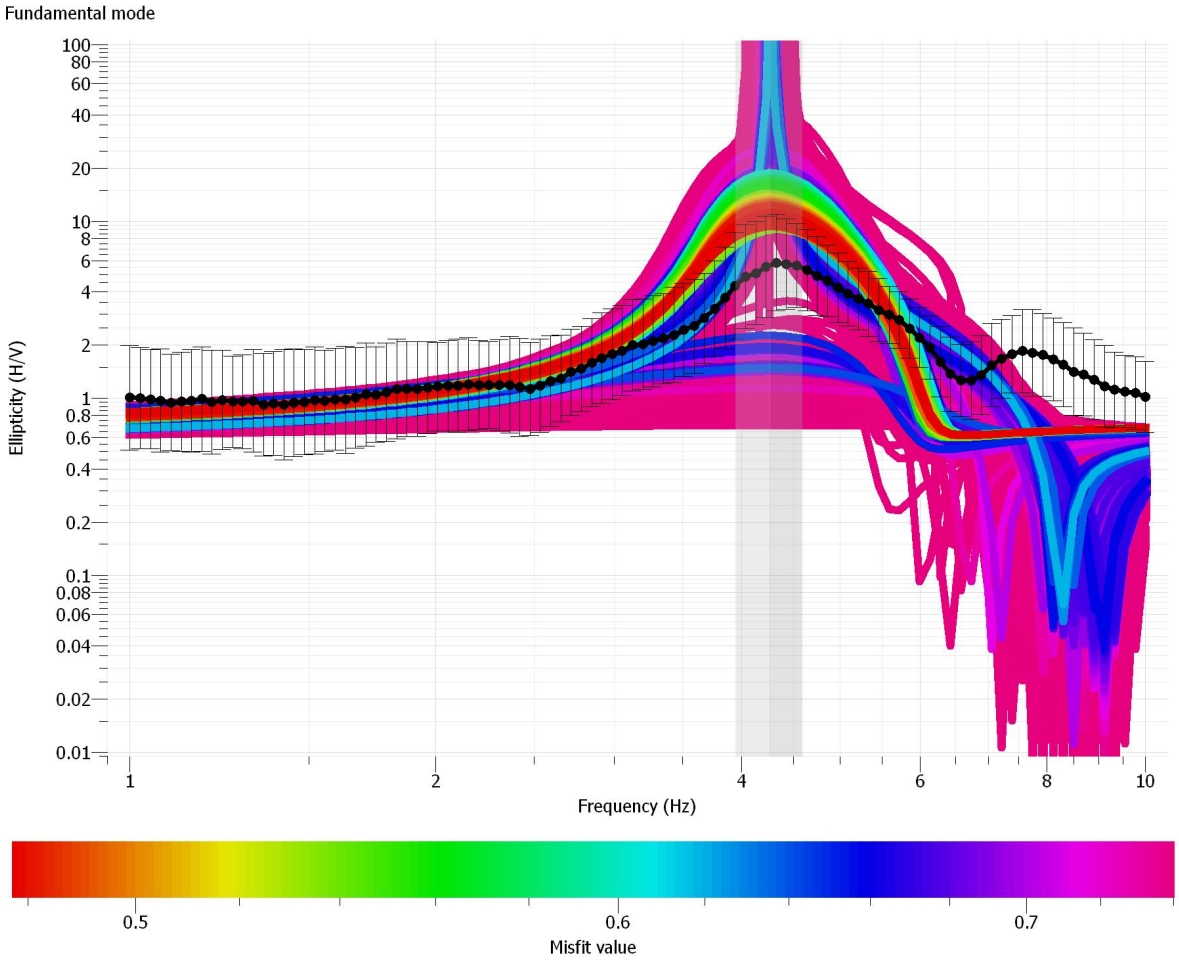

Figure A79. Class E: Riverside Park Rayleigh Wave Ellipticity. The black dotted curve represents the observed ellipticty curve after the TFA with associated error bars. The observed ellipticity curve has a peak at 4.4 Hz as indicated by the vertical purple rectangle. Each colored curve behind the data represents a different model generated by the inversion where red curves have the lowest misfit and the pink have the highest misfit. The vertical purple rectangle indicates the peak frequency value and standard deviation.

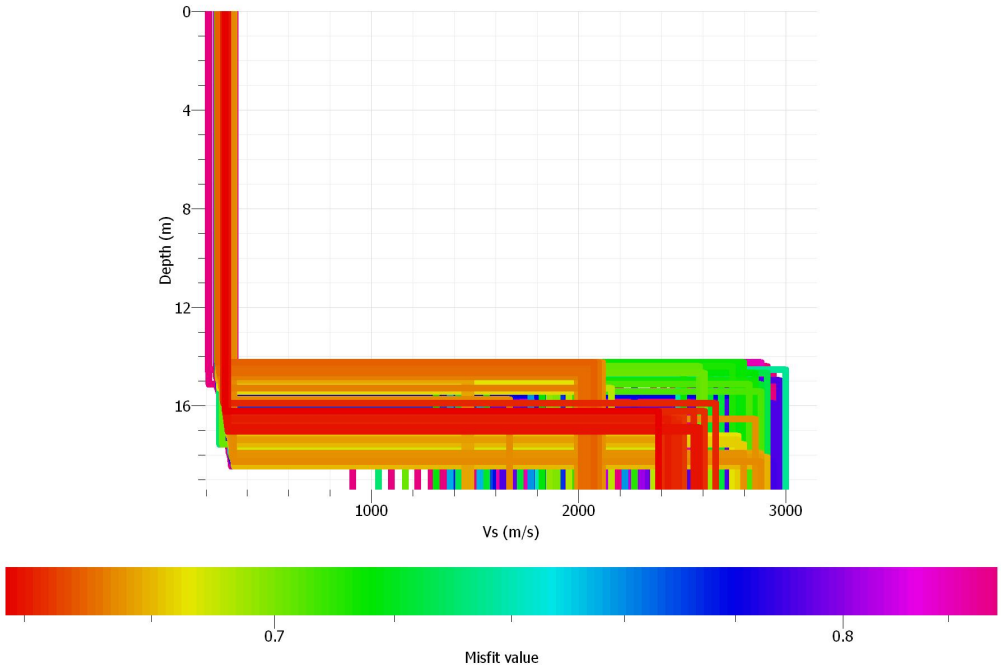

Figure A80. Class E: Riverside Park Velocity Profile from Rayleigh Wave Ellipticity Inversion. Each 2-layer Vs model is represented by each colored line where the color refers to the misfit value. The red models have the lowest misfit and the pink models have the highest misfit. Based on lowest misfit models at 16.5m, the average sediment Vs is ~288 m/s. The calculated Vs30 is 419 m/s, Class C.